5-14-2016

AN INVESTIGATION OF HYDROGEOLOGIC, STRATIGRAPHIC, AND STRUCTURAL CONTROLS ON ACER GRANDIDENTATUM COMMUNITIES IN A KARST LANDSCAPE, OWL MOUNTAIN PROVINCE, FORT HOOD MILITARY INSTALLATION, TEXAS

Melinda S. Faulkner
Stephen F Austin State University, mgshaw@sfasu.edu

AN INVESTIGATION OF HYDROGEOLOGIC, STRATIGRAPHIC, AND STRUCTURAL CONTROLS ON ACER GRANDIDENTATUM COMMUNITIES IN A KARST LANDSCAPE, OWL MOUNTAIN PROVINCE, FORT HOOD MILITARY INSTALLATION, TEXAS

AN INVESTIGATION OF HYDROGEOLOGIC, STRATIGRAPHIC, AND STRUCTURAL CONTROLS ON *ACER GRANDIDENTATUM* COMMUNITIES IN A KARST LANDSCAPE, OWL MOUNTAIN PROVINCE, FORT HOOD MILITARY INSTALLATION, TEXAS

By

MELINDA SHAW FAULKNER, B.S., M.S.

Presented to the Faculty of the Graduate School of

Stephen F. Austin State University

In Partial Fulfillment

Of the Requirements

For the Degree of

Doctor of Philosophy in Forestry

STEPHEN F. AUSTIN STATE UNIVERSITY

May 2016

AN INVESTIGATION OF HYDROGEOLOGIC, STRATIGRAPHIC, AND STRUCTURAL CONTROLS ON *ACER GRANDIDENTATUM* COMMUNITIES IN A KARST LANDSCAPE, OWL MOUNTAIN PROVINCE, FORT HOOD MILITARY INSTALLATION, TEXAS

By

MELINDA SHAW FAULKNER, B.S., M.S.

APPROVED:

_____
Dr. Matthew W. McBroom, Dissertation Director

_____
Dr. Kenneth W. Farrish, Committee Member

_____
Dr. Yanli Zhang, Committee Member

_____
Dr. Alyx S. Frantzen, Committee Member

_____
Dr. Kevin W. Stafford, Committee Member

_____
Dr. Joseph A. Musser, Committee Member

_____
Dr. Richard Berry, D.M.A.
Dean of the Graduate School

For Marley, Vivienne, Carli, Cypress, Kira, Fern
and those yet to be:

The story of Earth is written in the rocks,
the rivers, and the forests.

I can't wait to share it with you.

ABSTRACT

The Owl Mountain Province is located within the Fort Hood Military Installation, an approximately 880 km^2 installation established in the 1940s in Bell and Coryell counties, Texas, which has undergone extensive land use changes associated with military training, maintaining much of the vegetation in early succession. This study investigates the lithologic, stratigraphic, and structural controls on the hydrologic, hydrogeologic, and geomorphologic evolution of the Owl Mountain Province as expressed by mesic vegetation communities, including Pleistocene relicts (*Acer grandidentatum*), within karst terrains. These systems exhibit complexly overprinted speleogenetic evolutions within a dynamic groundwater regime resulting from regional climate shifts throughout the Neogene that have been complicated by extensive anthropogenic modifications as a result of urbanization, agriculture, and expanding populations in the region. Landscape evolution and the resulting vegetation patterns, examined through the prism of hydrologic and geologic principles, are investigated throughout the inter-disciplinary nature of this study and used as the foundation for the explanation of the floristic phenomena observed within the Owl Mountain Province.

ACKNOWLEDGEMENTS

Much of science research today is done in collaboration, and this work is no exception. While the research is my own, I had many willing (and some not as willing) field partners and am very grateful for their help.

First, I would like to recognize Charles Pekins, the Wildlife Biologist at the Fort Hood Natural Resources Management Branch for acting as my liaison and allowing me to conduct my research on the military installation. He provided maps, initial tours of areas that might be of scientific interest, field passes, housing, and the all-important code to the ice machine. His guidance and support were instrumental during field data collection.

My committee has been very supportive as I shifted my educational focus from geology to forestry to complete this research. Dr. Matthew McBroom, my dissertation advisor, was willing to take on the challenge of navigating a geologist through the forest; he is a wonderful mentor, a challenging advisor, a curator of cryptic musical lyrics, and I treasure his friendship. Dr. Kevin Stafford was my introduction into the world of karst science, unique cave music, and some the culinary wonders found under gas station heat lamps. Dr. McBroom and Dr. Stafford spent many hours helping me tailor this project to highlight my unique set of research skills and without their guidance this project would not have come to completion. Dr. Kenneth Farrish was also very helpful in the evolution

of this project and his wise counsel and direction were often sought. Dr. Yanli Zhang and Dr. Alyx Frantzen were instrumental in offering helpful advice and I look forward to working with all of my committee members in the future. I would also like to mention Dr. Dean Coble and Dr. Brian Oswald, both of whom supplied timely advice and direction regarding this project, and Dr. Montague Whiting and Dr. Michael Fountain, with whom I began my forestry education many years ago.

I would also like to express my gratitude to the Arthur Temple College of Forestry and Agriculture and the Division of Environmental Science for allowing me use of a vehicle and boat to complete parts of my research. Mr. Wayne Weatherford in the SFA Soil, Plant, and Water Analysis Laboratory assisted with soil samples and water analyses. The Department of Geology was also very supportive, providing transportation and "quiet time" when needed. A special thank you is also extended to Dr. Joseph Musser who stepped in at the last minute to serve as the Graduate School representative on this committee.

Field assistance was provided by Brandon Tate, Aaron Bryant, Kevin Stafford, William Welles, JaHoward Hutchins, Asa Vermeulen, and my very patient and loving husband Joel. Laboratory assistance was provided by Kyle Altimore, Cassie Jay Barron and Lillian O'Shay. I am very grateful for all who helped me with this project, your assistance was invaluable.

My parents also deserve recognition and have waited a very long time for this moment, particularly my mother who endured my teenage rebellious nature. When I

decided to return to school in 1999, none of us could imagine that this is where my educational path might lead. To my children Jillian, Asa, Chris, Caiti, and Emily: thank you for all the love and support you extended to me when I decided to return to school (again). To my beautiful, perfect granddaughters, thank you for your patience.

Finally, I would like to thank my husband Joel for his enduring love and support. He spent many hours reading my papers, driving the boat, collecting rock samples in the middle of summer, looking for maples in densely vegetated canyons, collecting water samples, cutting billets for thin sections, camping in inclement weather, and driving on questionable roads so that I could conduct my research. If love is indeed an action word, he proved it every day. Without his help, this dissertation would not have happened, and I will never be able to fully express my gratitude.

TABLE OF CONTENTS

LIST OF FIGURES

LIST OF TABLES

CHAPTER I:
INTRODUCTION

The Fort Hood Military Installation is located within the Lampasas Cut Plain and encompasses approximately 880 km^2 in Bell and Coryell counties (Hammer 2011; Figure I.1). Named for Confederate General John Bell Hood, the installation was established in 1942, with most of the land appropriated from rural land owners under authority of eminent domain after the United States entered World War II (Pugsley 1992). Before the establishment of the military base, the area consisted of rural farms and homesteads and in January of 1942, the War Department relocated approximately 300 families living in the area to create the original installation, Camp Hood. As partial compensation for relocation, the U.S. Army agreed to allow land to continue to be grazed for a nominal fee, an agreement that still continues today (Freeman et al. 2001).

Today, the installation is the largest active duty armored post in the U.S. Armed Services. It is home to two full divisions, 1st Cavalry Division and 4th Infantry Division, supports 12 additional units, and is home to approximately 41,000 soldiers and their families (Hayden *et al.* 2001). The administrative section of the installation is located in the south-central portion, surrounded by training areas used by the U.S. Army for dismounted and wheeled exercises, and tracked vehicle training (Hammer 2011; Figure I.2). Training lands on the installation are divided into three major areas; West Fort Hood

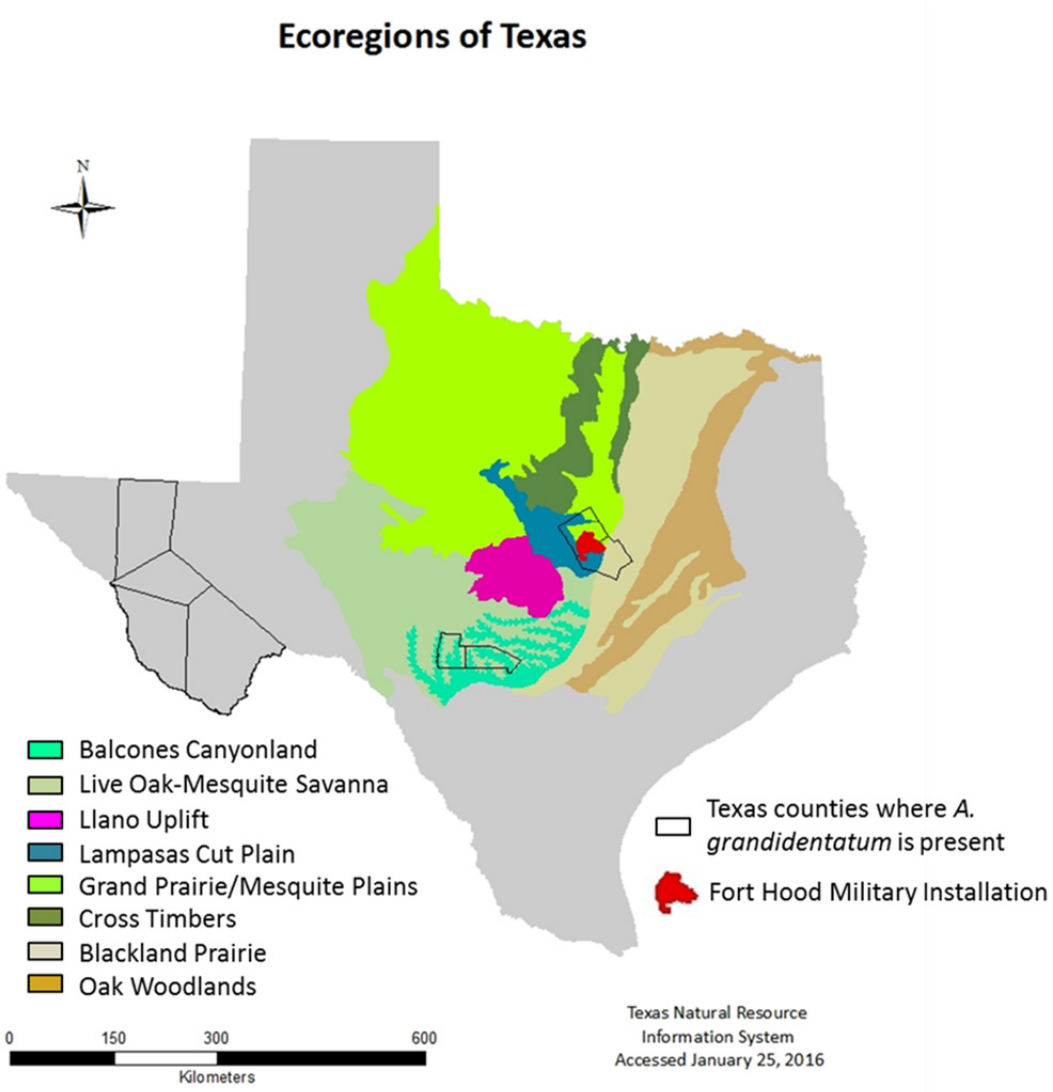

Figure I.1. Ecoregions of Texas. The Fort Hood Military Installation is uniquely situated between the Edwards Plateau and the Crosstimbers and Prairie ecoregions, resulting in providing ecological diversity and high quality habitat for wildlife and endangered avian species.

is primarily used for heavy mechanical (tracked and wheeled) maneuver training; the terrain is rolling and isolated mesas are present. The Live Fire Impact Range is located in the center of the installation and is used for pyrotechnic training. East Fort Hood is used primarily for dismounted and wheeled exercises, and some small-scale tracked vehicle training. Here, the terrain is more rugged than other areas with steep scarps and canyons (Hammer 2011; Hayden *et al*. 2001). The installation also functions as an isolated island of high quality habitat for many threatened and endangered species. Land use surrounding the installation has greatly modified and degraded many such habitats through urbanization, infrastructure support for the burgeoning population, and agriculture.

The study area, the Owl Mountain Province, is located in the northeastern section of the installation and is approximately 90 km^2 bounded by Owl Creek to the north, Belton Lake to the east, Cowhouse Creek to the south and the Live Fire Impact Range to the west (Figure I.2). The province is a multi-use facility and is utilized by the U.S. Army for troop maneuvers with the southern and western sections having been extensively modified by road construction and military training infrastructure. The terrain is rugged and dominated by xeric, plateaued drainage divides hosting thick, scattered clusters of Ashe juniper (*Juniperus ashei*), Texas ash (*Fraxinus texensis*), and Texas red oak (*Quercus buckleyi*) (Hammer 2011; Teague and Reemts 2007). Where the landscape has been partially denuded, cacti and shrubs such as prairie sumac (*Rhus lanceolate*) and false willow (*Baccharis neglecta*) grow in small sinks and fractures where meteoric water

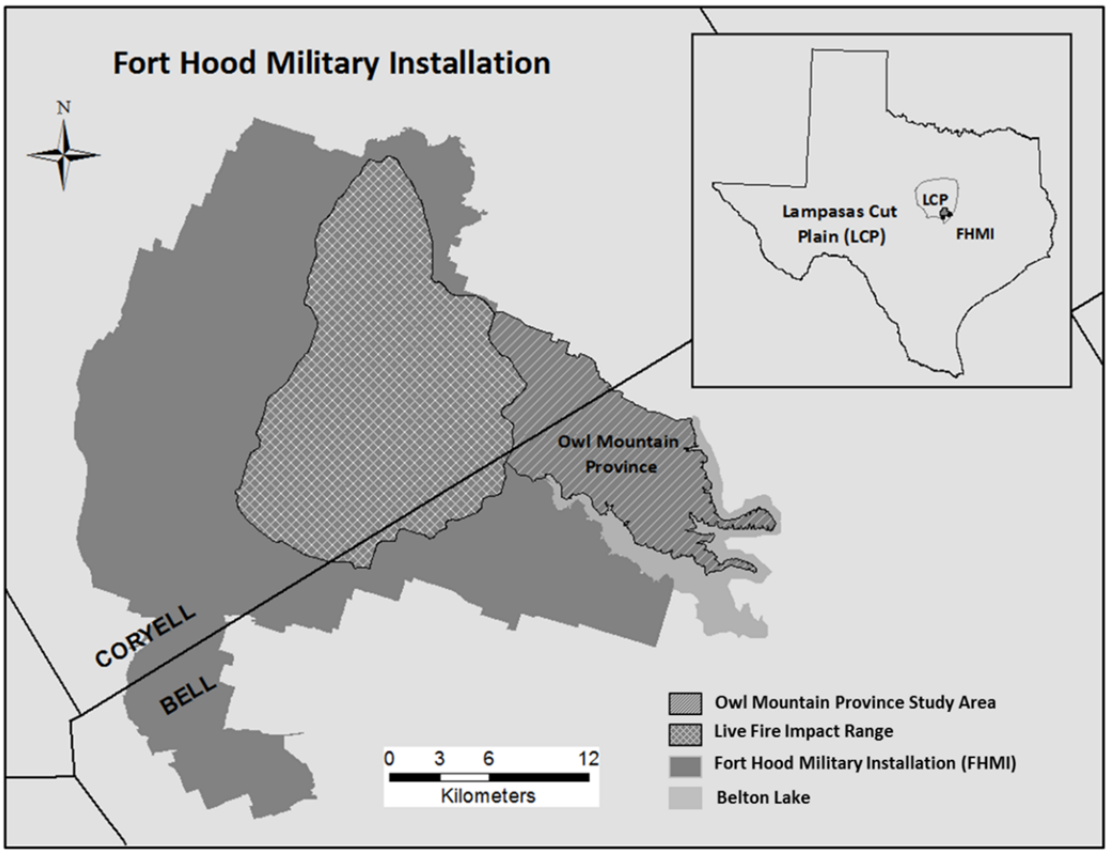

Figure I.2. The Fort Hood Military Installation is within the Lampasas Cut Plain in Central Texas. The western and eastern areas, including the Owl Mountain Province, are used for troop maneuvers and training. The Owl Mountain Province also has acreage set aside for grazing and endangered species habitat.

resources are focused. The northern and eastern sections are more remote with acreage set aside as grazing land and wildlife habitat (Pekins 2012; Hammer 2011; Hayden *et al*. 2001). This area is also home to several protected avian species such as Golden-cheeked Warbler (*Dendroica chrysoparia*) and Black-capped Vireo (*Vireo atricapilla*); and much of the eastern section of the province is left mostly undisturbed by military activities as endangered species habitat (Picinich 2011). The plateaus are bordered by steep scarps

and incised canyons along the edges of the plateaus hosting mesic woodland species such as pecan (*C. illoinensis*), Texas cedar elm (*Ulmus crassifolia* Nutt.), Chinkapin oak (*Quercus muehlenbergii*), sugarberry (*Celtis laevigata*), Edwards Plateau Sedge (*Carex edwardsiana*), and bigtooth maple (*A. grandidentatum*) (Hammer 2011; Teague and Reemts 2007; Figure I.3).

Regional Geology

The Lampasas Cut Plain is a karst landscape located in North-Central Texas and is characterized by exposures of Lower Cretaceous Comanchean Series carbonates of the Trinity, Fredericksburg, and Washita Groups. The geomorphic evolution of the Cut Plain is the result of varying geologic, hydrogeologic and biologic processes that have influenced the region over the past 350 million years. Beginning in the late Mississippian and continuing into the Pennsylvanian Period, the Ouachita Orogeny, one of the major structural features influencing the Lampasas Cut Plain, occurred along the southern Laurentian margin (Culotta et al. 1992; Caran et al. 1982; Figure I.4) initiating the eventual formation of Pangaea at the end of the Paleozoic (Garrison 2005). Today, most geologic evidence lies in the subsurface as part of the Ouachita fold-thrust belt extending from the subsurface of Mississippi to the Marathon region of West Texas (Caran et al. 1982). This tectonic boundary has remained structurally active through most of the Phanerozoic, influencing deposition and structural deformation along most of the southern margin of the continental craton (Caran et al. 1982).

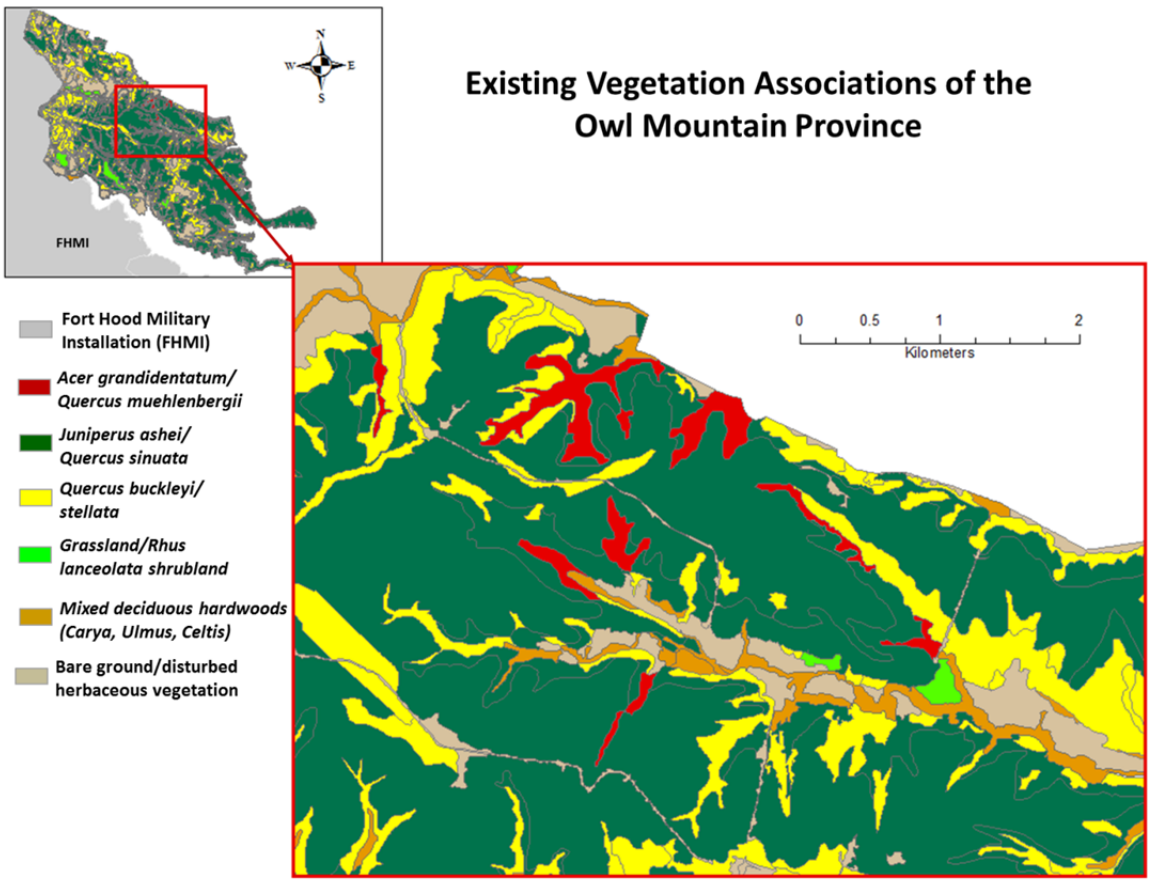

Figure I.3. Vegetation associations found in the Owl Mountain Province (modified from Pekins 2012 and Hammer 2011).

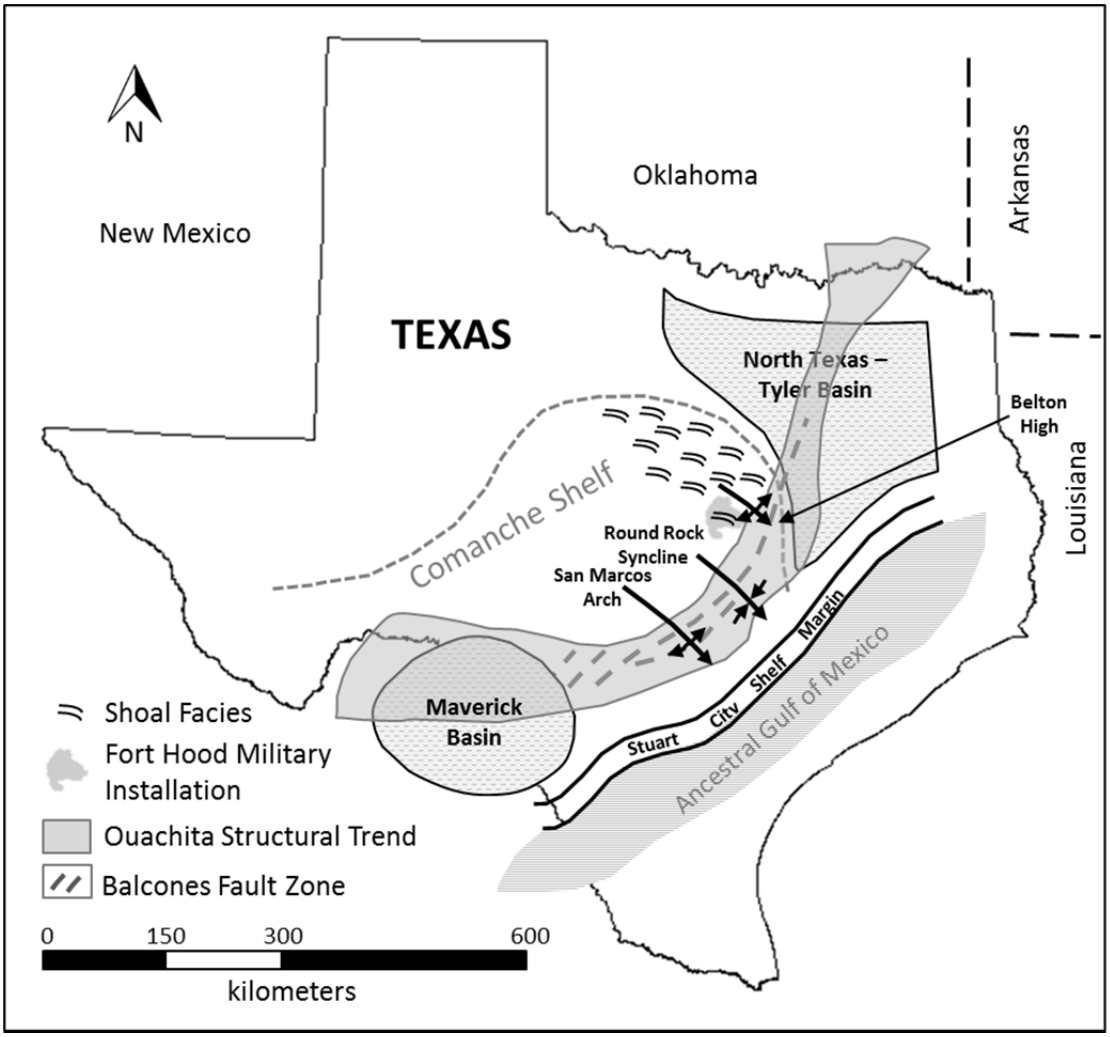

Figure I.4. Location map showing the major structural trends influencing strata in the Central Texas region. Shoal facies such as the Owl Mountain Province were formed on the topographic high between the North Texas-Tyler Basin across the axis of the Belton High (modified from Anaya and Jones 2009; Walker 1979; Fisher and Rodda 1969).

The Ouachita orogenic belt began to subside in Mesozoic time, coincident with the Zuni and Tejas transgression that controlled deposition during the Cretaceous Period (McCann 2012; Rose 1972) when thick sequences of sedimentary rock were deposited across the Comanche Shelf, including the Trinity (Glen Rose), Fredericksburg (Comanche Peak and Edwards), and Washita (Georgetown) Groups (Figure I.5). By the end of the Cretaceous, a thick marine carbonate sequence covered most of the Ouachita System in Central Texas and the initial Gulf of Mexico basin existed to the southeast (Figure I.4). The final shaping of the Gulf of Mexico occurred during the Laramide orogeny, as peninsular Mexico was transported eastward forming the Sierra Madres and constricting circulation in the Gulf (Caran et al. 1982). Uplift in the region provided clastic sediments from the interior of Texas for the extending Gulf Coastal plain (Hayward et al. 1990), resulted in exposure and partial erosion of Edwards sediments, increased secondary porosity, and tilted the strata to the southeast. As a result of the uplift and aerial exposure in the Paleogene, the rivers flowing across the Central Texas region began to erode the softer rocks and sediments of the Upper Cretaceous and early Tertiary, sending massive sediment influxes to the east toward the widening Gulf of Mexico.

In the late Miocene, the buried Lower Cretaceous Texas coastline provided sufficient crustal weakness for the uplifting of the Central Texas region along the trend of the former Ouachita deformation zone, creating the Balcones Fault Zone and defining the Edwards Plateau and Balcones Escarpment (Faulkner and Bryant 2015; Ferrill and Morris 2008; Caran et al. 1982; Figure I.4). The Balcones (also the Luling, Mexia, and

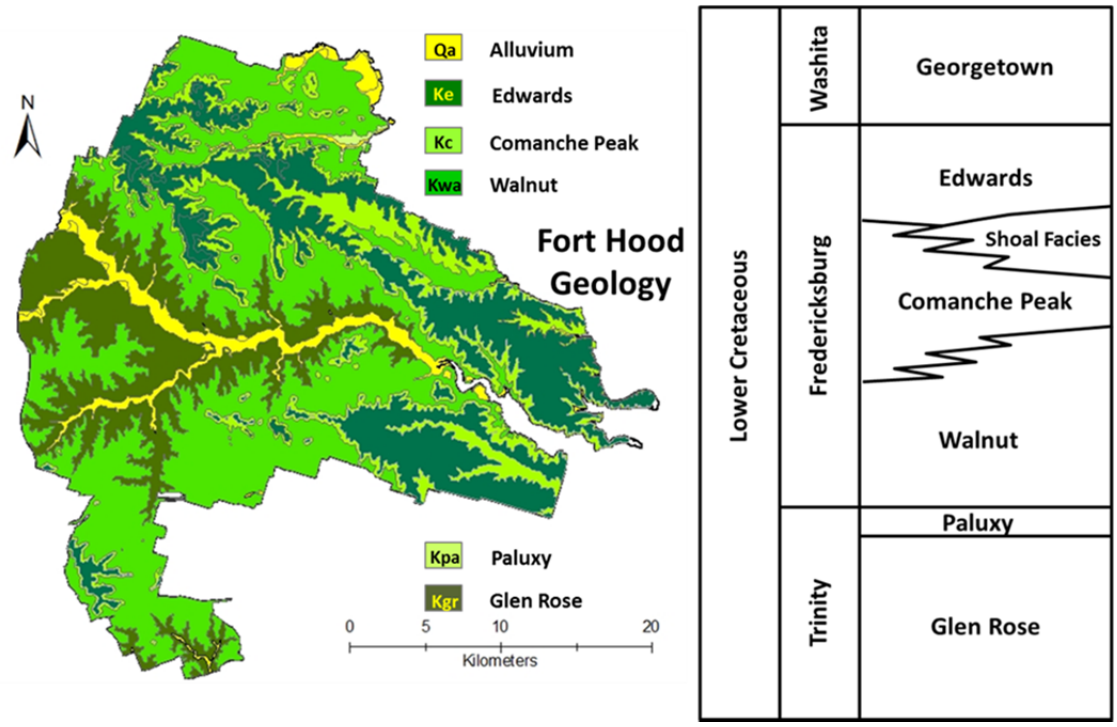

Figure I.5. Geology and stratigraphic column of the Lower Cretaceous Trinity and Fredericksburg Groups for the Fort Hood Military Installation (stratigraphic column modified from Amsbury et al. 1984).

Talco) fault zones extend as an arcuate belt of *en echelon* normal faults from Del Rio to Dallas with the Mexia/Talco fault zone extending into eastern Texas, displacing the Mesozoic to lower Paleogene section and dissecting the Lower Cretaceous strata (Caran et al. 1982). Buried Ouachita structures acted as a hinge for downwarping into the ancestral Gulf of Mexico (Caran et al 1982) and this downwarping, along with upward flexing of the continental interior west, continued throughout the Cenozoic. This uplift would eventually influence early human settlement and transportation patterns along the Balcones Escarpment.

Structural deformation transverse to the Ouachita/Balcones trend appears to coincide with structural features known primarily from subsurface data such as platforms, anticlines, and synclines. The San Marcos Arch, Round Rock Syncline, and Belton High-Moffatt Mound trend are three such features that represent undulation and thickening in Cretaceous lithofacies (Culotta et al. 1992; Caran et al. 1982; Figure I.4). Moffatt Mound and the shoal facies of the Owl Mountain Province are northwesterly trending areas on the flank of the Belton High in which the Edwards exhibits increased thickness and lithology changes; these areas indicate local, high-energy shoaling adjacent to a shallow marine shelf sequence (Faulkner et al. 2016; Bryant 2012; Amsbury et al. 1984; Brown 1975; Figure I.6).

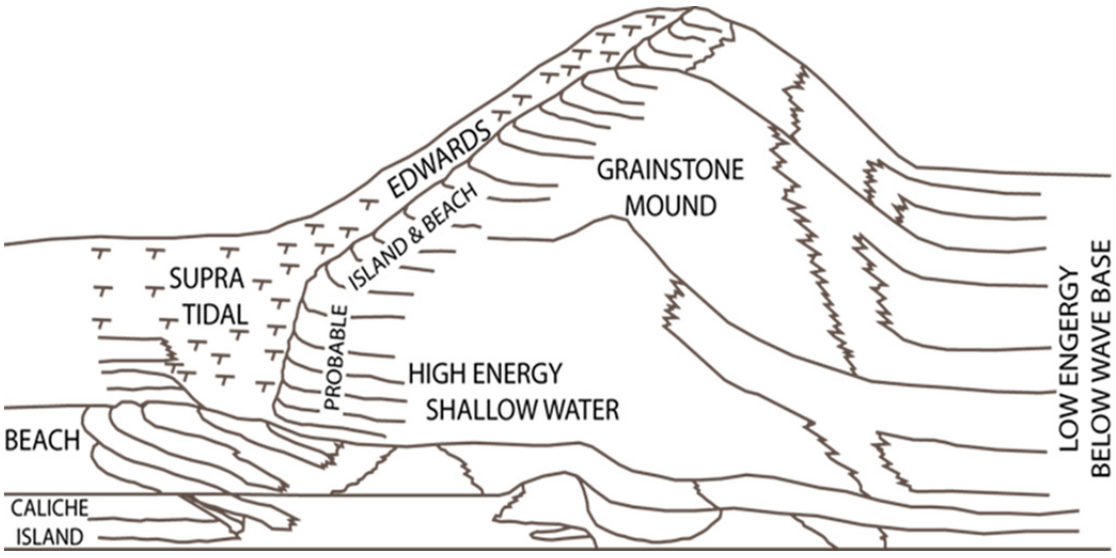

Figure I.6. Idealized drawing of shoal facies (modified from Amsbury *et al.*1984; Bryant 2012).

Regional Stratigraphy

Early geologic mapping by Barnes (1970) shows the undivided Edwards conformably overlying the Comanche Peak limestone, with the Edwards thinning to the north and gradually inter-fingering with the Comanche Peak. Within the Lampasas Cut Plain, the Edwards can be quite variable; thicknesses range from approximately two to fifty meters. In this region, Cannata and Yelderman (1987) described the Edwards as a massive rudist reef limestone with elongate reef front circular bioherms. Deposition of these bioherms began approximately 110 mya on the Comanche Shelf, behind the main structure of the Stuart City Shelf Margin complex (Nelson, 1973; Figure I.4). The Comanche Shelf was bounded on the east and south by a relatively deep-water oceanic basin, the ancestral Gulf of Mexico, and on the north and west by an extensive shallow-water open marine basin, the North Texas-Tyler basin (Fisher and Rodda 1969; Figure I.4). Major stratigraphic groups (Figure I.5) found in the study area are listed below.

Trinity Group

In the study area, the Trinity Group is represented by the Glen Rose and Paluxy Sand. These units comprise much of the Lower Cretaceous and consist of limestones, marls, shales and sandstone. Outcrops are confined to the lower elevation in the western section of Fort Hood and along developed drainage with varying thicknesses. Alternating sequences between depositional environments within the Glen Rose expose resistant

ridges of limestone separated by less resistant ridges of soft marl, creating characteristic stair-step topography commonly found in Glen Rose outcrops.

Fredericksburg Group

The Fredericksburg Group is represented by the Walnut, Comanche Peak, and Edwards Limestone. The Walnut consists of varying thicknesses of marl and crystalline limestone exposed at lower elevations near the shores of Belton Lake and along developed drainage. The Comanche Peak is a nodular limestone and marl sequence exhibiting transitional contacts with the underlying Walnut and the overlying Edwards (Senger et al., 1990). The Edwards Limestone is a series of transgressive facies characterized by varying textures of massive to thin bedded limestones with isolated high energy shoals formed on the northern extent of the Comanche Shelf. Parts of the Owl Mountain Province have been interpreted as one of these shoals, following the model presented for Moffatt Mound (Amsbury et al. 1984; Brown 1975; Figure I.6)

Washita Group

The Washita Group is represented by the Georgetown Formation and consists of fossiliferous limestone, argillaceous limestone and minor marl that have wackestone, packstone and grainstone facies (Collins, 2005). Pelecypods are diagnostic features of the Georgetown Formation, as well as vuggy porosity present in some of the facies. In the study area, the Georgetown is generally not divided south of the Lampasas River; in the

northern section of the Lampasas Cut Plain, the Georgetown thickens and is locally divided into seven members (Barnes, 1970).

Regional Ecology

The Lampasas Cut Plain is located between the Edwards Plateau Ecoregion (TNC 2004) and Crosstimbers and Prairie Ecoregion (Diggs et al. 1999; Griffith et al. 2004; USDA 2007) and shares affinities with both (Figure I.1). The area owes its ecological diversity partly to its location at the intersection of these two ecoregions; and these plant communities owe much of their origin to the Sierra Madre Oriental and its outliers, and by floristic contributions from the eastern deciduous forests, including tall-grass prairie species (Riskind and Diamond 1986).

The vegetation communities present today in Central Texas have been heavily influenced by the fluctuating climate of the past two million years. In North America, the ice sheets reached their maximum growth around 20,000 years ago; resulting in the presence of plant species that occur in more mesic sites and cooler environments (Van Devender and Spaulding 1979). The mesic climate encouraged existing forests; the spruce, juniper, Douglas fir, and pine forests of the West Texas Mountains expanded downward to lower altitudes and spread out onto the mountain flanks, where they mixed with grasslands to form parklands and savannas (Mecke 1996; Nordt *et al.* 1994). As the ice age came to an end, the climate in the central and southwestern regions of the United States fluctuated but gradually warmed to its present day trend toward the semi-arid to

arid environment found across the region. This trend continues today; therefore, some of the current vegetation of Texas may have developed under a previous set of climatic conditions characterized by cooler, more mesic conditions than exist today (Smeins *et al*. 1997; Riskind and Diamond 1986).

The vegetation of the Lampasas Cut Plain responded to the change in climate by a shift in vegetation dominance of piñon and juniper to a dominance of scrub oak and Ashe juniper (Fuhlendorf and Smeins 1996). East of the Balcones Escarpment, the forests lost some of their cool-loving species while others did not disappear entirely but were reduced to minor components in the new deciduous forests (Diggs *et al*. 1999). Over time, as moister climates shifted to the east, relict populations of Pleistocene vegetation contracted to mesic slot canyons in Central and West Texas associated with springs and seeps where consistent moisture was more readily available.

Today, many of the mesa-like drainage divides within the Lampasas Cut Plain are more xeric and open and are strongly influenced by the Great Plains grasslands to the north (Diggs *et al*. 1999). Juniper-oak woodlands are widespread on limestone terraces across uplands in the Lampasas Cut Plain, usually over karstic features or Quaternary terrace deposits (Huxman *et al*. 2005; Diamond, 1997). On the more xeric rolling hills to the west, the semi-desert grasslands are biotic contributions from the dry plateaus and massifs of northern Mexico and Trans-Pecos Texas (Riskind and Diamond 1986).

Presently, the climate of the Lampasas Cut Plain is sub-humid and becomes increasingly arid to the west and cooler to the north. Prevailing winds are generally from

the south and the general decrease in moisture content of air from the Gulf of Mexico as it flows north-westward across the plain is the controlling factor responsible for this difference in moisture regime (Bradley and Malstaff, 2004). Mean annual precipitation decreases from east to west, ranging from about 85 cm/yr on the eastern edge to 35 cm/yr on the western edge. Summer average highs and lows do not vary significantly and average about 35° C and 22°C, respectively. The average minimum January temperatures decrease northward, ranging from approximately 4°C to 0°C.

Soil Series of the Owl Mountain Province

Variations in substrate and a generally hilly landscape have led to the development of a number of different soil types in the Owl Mountain Province. The soils in the study area were developed over Lower Cretaceous carbonate rocks, namely the Walnut Clay, Comanche Peak, and Edwards Limestone. These units were deposited on a carbonate platform on the lee side of the Stuart City Reef trend as the Gulf of Mexico was beginning to open. Today, the landscape preserves former isolated carbonate mound structures as dissected plateaus with steep scarps and widened stream valleys. Alternating sequences of limestone, dolomite, chert, and marl crop out at the surface and provide the parent material for soil development. The lower valleys along established drainage are covered by deeper, alluvial soils and vegetative cover; shallow, less developed soils mantle the plateaus. Most of the soils are dark colored, calcareous, and moderately alkaline. The textures vary from loamy to clayey, depending on the substrate and profile

development. Soil descriptions of the prominent soil series present in the study area are below; all soil descriptions are from the United States Department of Agriculture Natural Resources Conservation Service Soil Resource Report for Bell and Coryell counties, Texas.

Topsey Series

The Topsey Series (BtC2) consists of moderately deep over densic material, well drained, moderately slowly permeable soils that formed in shaly and marly sediments over the Walnut Clay and the shale member of the Paluxy Sand Formations. These soils are on gently sloping to moderately sloping erosional uplands. Surfaces are plane to concave, and slopes range from 1 to 8 percent.

TAXONOMIC CLASS: Fine-loamy, carbonatic, thermic Udic Calciustolls;
TYPICAL PEDON: Topsey clay loam, on a concave 3 percent slope in rangeland. Elevation ranges from 200 to 450 meters above sea level.

A: 0 to 20 cm; dark grayish brown (10 YR 4/2) clay loam; very dark grayish brown (10 YR 3/2) moist; moderate very fine granular and subangular blocky structure; slightly hard, friable; common very fine, fine, and few medium roots; common fine pores; few wormcasts; calcareous; moderately alkaline; clear, smooth boundary.

Bw1: 20 to 36 cm; grayish brown (2.5 Y 5/2) clay loam; dark grayish brown (2.5 Y 4/2) moist; moderate very fine granular and subangular blocky structure; hard, friable; common fine and few medium roots; common fine pores; dark stains on some ped surface; few very fine concretions and soft masses of calcium carbonate; about 2 percent fossil shells; calcareous; moderately alkaline; clear smooth boundary.

Bw2: 36 to 48 cm (14 to 19 in); light yellowish brown (2.5 Y 6/4) gravelly loam; light olive brown 2.5 Y 5/4) moist; moderate medium subangular blocky structure; hard, friable; common fine and few medium roots; common fine pores; few very fine concretions, threads, and soft masses of calcium carbonate; about 30 percent fossil shells; few grayish shale fragments; calcareous; moderately alkaline; clear smooth boundary.

Bk: 48 to 71 cm; light yellowish brown (2.5 Y 6/4) silt loam; light olive brown (2.5 Y 5/4) moist; few fine faint yellowish brown and pale yellow mottles; weak medium and coarse subangular blocky structure parting to moderate very fine subangular blocky; hard, friable; few fine roots; common fine pores; common soft fine and medium and few coarse masses of calcium carbonate; about 3 to 5 percent fossil shells; few thin grayish shale fragments; calcareous; moderately alkaline; gradual smooth boundary.

2Cd: 71 to 170 cm; pale yellow (2.5 Y 7/4) marl with silty clay loam texture; light yellow brown (2.5 Y 6/4) moist; interbedded with yellowish brown (10 YR 5/8) and light gray

(10 YR 7/2) thin discontinuous shaly strata; massive; very hard, firm; few fine roots; few fine and medium soft masses of calcium carbonate; about 2 percent fossil shells; calcareous; moderately alkaline.

Additional Information: The Topsey clay loam is located in the lower elevations of the study area on low hillsides along established drainage; uses include pasture and range land. The soil is well drained, with medium surface runoff and moderately slow permeability. Native vegetation includes mid and tall grass prairie.

Denton Series

The Denton Series (DeB) consist of deep, well drained, slowly permeable soils that formed in clayey material over residuum weathered from limestone bedrock. In the study area, these soils are formed over the Walnut Clay and Comanche Peak Limestone. These nearly level or gently sloping soils are on uplands and have slopes ranging from 0 to 5 percent.

TAXONOMIC CLASS: Fine-silty, carbonatic, thermic Udic Calciustolls

TYPICAL PEDON: Denton silty clay-cropland. Elevation ranges from 200 to 450 meters above sea level.

Ap: 0 to 15 cm; dark brown (7.5 YR 4/2) silty clay; dark brown (7.5 YR 3/2) moist; moderate fine and very fine granular structure; soft, very friable, sticky and plastic; few fine and medium roots; few fine pitted concretions of calcium carbonate; strongly effervescent; moderately alkaline; clear, smooth boundary.

A: 15 to 33 cm; dark brown (7.5 YR 4/2) silty clay; dark brown (7.5 YR 3/2) moist; moderate fine and very fine subangular blocky structure; very hard, firm, sticky and plastic; few fine roots; many pressure faces; few small slickensides less than 1 inch across forming wedge-shaped peds; few fine pitted concretions of calcium carbonate; strongly effervescent; moderately alkaline; clear, gradual, wavy boundary.

Bw: 33 to 48 cm; reddish brown (5YR 4/4) silty clay; dark reddish brown (5YR 3/4) moist; moderate fine and very fine angular blocky structure; very hard, firm, sticky and plastic; few fine roots; many pressure faces forming wedge-shaped peds; few fine pitted concretions of calcium carbonate; strongly effervescent; moderately alkaline; gradual wavy boundary.

2Bk: 48 to 91 cm; reddish yellow (7.5 YR 7/6) silt loam; reddish yellow (7.5 YR 6/6) moist; common medium masses of strong brown (7.5 YR 5/6); weak medium and fine subangular blocky structure; hard, firm, sticky and plastic; few fine roots; about 20

percent fine and medium concretions and soft masses of calcium carbonate; violently effervescent; moderately alkaline; clear irregular boundary.

2CBk: 91 to 132 cm; strong brown (7.5 YR 5/6) marly soil materials, massive; with about 5 percent reddish yellow (7.5 YR 6/6) Bk material along root channels and fracture planes; few fine roots; 10 percent by volume limestone fragments 2.5 to 20 cm across and 5 to 10 cm thick; fragments form a discontinuous line mainly in the upper part of layer; about 25 percent coarse and very coarse soft masses and thin discontinuous strata of calcium carbonate; violently effervescent; moderately alkaline; abrupt wavy boundary.

2R: 132 to 178 cm; indurated, slightly weathered, limestone bedrock; interbedded with marl or chalky limestone at vertical intervals of 15 to 30 cm; bedrock has tight fractures spaced about 20 to 60 cm apart and cannot be excavated with backhoe machine.

Additional Information: The Denton silty clay is located in the lower elevations of the study area on nearly level to gently sloping uplands; uses include cropland, pasture, and range land. The soil is well drained, with medium surface runoff and slow permeability. Native grasses include bluestems, sideoats grama, indiangrass, and Texas wintergrass with a few live oak and bois'd arc trees.

Real-Rock Series

The Real-Rock Series (REF) consists of gravelly, clay loam formed on 12 to 40 percent convex slopes within incised canyons on side slopes of the dissected plateau uplands in the study area. The soils are well drained and formed in residuum from weathered limestone, chalk and marl from the Comanche Peak Limestone. These soils have a very low available water capacity (<3.5cm) and the depth to the water table is more than 200cm.

TAXONOMIC CLASS: Loamy-skeletal, carbonatic, thermic, shallow Typic Calciustolls.
TYPICAL PEDON: Real gravelly clay loam in rangeland.

A: 0 to 15 cm; dark grayish brown (10YR 4/2) gravelly clay loam, very dark grayish brown (10YR 3/2) moist; weak medium subangular blocky structure parting to moderate fine granular; hard, friable; many very fine and fine roots; 15 percent weakly cemented limestone and caliche gravel; 1 percent limestone cobbles and stones; violently effervescent; moderately alkaline; abrupt wavy boundary.

Ak: 15 to 33 cm; dark grayish brown (10YR 4/2) extremely gravelly clay loam, very dark grayish brown (10YR 3/2) moist; weak medium subangular blocky structure parting to moderate fine granular; hard, friable; many very fine and fine roots; 75 percent weakly

cemented limestone and caliche gravel; 1 percent limestone cobbles and stones; violently effervescent; moderately alkaline; abrupt wavy boundary.

Cr: 33 to 91 cm; 80 percent white (10YR 8/1), 10 percent brownish yellow (10YR 6/6), and 10 percent light yellowish brown (2.5Y 6/3) moist weakly cemented limestone bedrock that is moderately cemented in the upper 2.5 cm.

Additional Information: Real-Rock outcrop is generally in long and narrow horizontal bands, along the edges of escarpments and abrupt slope breaks. Some areas include large boulders that have broken away from escarpments and fallen downslope. Many areas have a layer of soil less than 10cm thick overlying bedrock; rock outcrops are generally strongly cemented carbonates and/or indurated marls. The climax plant community is a tall grass and mid grass, oak savannah. The dominant grass is little bluestem, and woody plants include live oak, Texas oak, and sumac. Overgrazing of these areas, and/or disturbance would produce a plant population of Ashe juniper, scrub oak, and mesquite. Within the study area, mesic riparian corridors of oaks and elms dominate canyon vegetation.

Eckrant Series

The Eckrant Series (ErB) consists of soils that are very shallow and shallow to indurated limestone bedrock and interbedded cryptocrystalline quartz, chert, marl, and chalk of the

Edwards Limestone. These well drained soils formed in residuum derived from limestone. These nearly level to very steep soils are on summits, shoulders, and backslopes of ridges on dissected plateaus. Slope ranges from 1 to 60 percent.

TAXONOMIC CLASS: Clayey-skeletal, smectitic, thermic Lithic Haplustolls.

TYPICAL PEDON: Eckrant very cobbly clay in rangeland.

A1: 0 to 10 cm; very dark gray (10 YR 3/1) very cobbly clay; black (10 YR 2/1) moist; moderate fine subangular blocky structure and moderate fine granular; very hard, firm; common fine roots; common fine pores; 20 percent limestone gravel; 15 percent limestone cobbles; very slightly effervescent; moderately alkaline; clear irregular boundary.

A2: 10 to 30 cm (4 to 12 in); very dark gray (10 YR 3/1) very cobbly clay; black (10 YR 2/1) moist; moderate fine subangular blocky and fine granular structure; very hard, firm; common fine roots; common fine pores; 20 percent limestone gravels; 35 percent limestone cobbles; very slightly effervescent; moderately alkaline; abrupt wavy boundary.

R: 30 to 76 cm (12 to 30 in); coarsely fractured indurated limestone bedrock.

Additional Information: The Eckrant series located in the upper elevations of the study area on dissected plateaus; uses include rangeland, military training exercises, and wildlife habitat. The soil is well drained and permeability is moderately slow. Runoff is very low on 1 to 3 percent slopes; low on 3 to 5 percent slopes; medium on 5 to 20 percent slopes; and high on 20 to 60 percent slopes. The climax plant community is a tall grass savannah with live oak and ashe juniper throughout the landscape. The dominant grasses are little bluestem and sideoats grama. Woody plants include shin oak, evergreen sumac, hackberry, elbowbush, redbud, mesquite, ash juniper, and white honeysuckle.

Vegetation Communities of the Owl Mountain Province

Pre-settlement vegetation on Fort Hood was characterized by tallgrass and midgrass prairies dominated by little bluestem (*Schizachyrium scoparium*) and Texas wintergrass (*Nassella leucotricha*) among other grasses, and forests, woodlands and shrublands variously dominated by Texas red oak (*Quercus buckleyi*), shin oak (*Quercus sinuata* var. *breviloba*), Ashe juniper (*Juniperus ashei*), Texas live oak (*Quercus fusiformis*) and post oak (*Quercus stellata*) (Van Devender and Spaulding 1979). Historically, fire, climate, native grazing and edaphic factors all played a role in maintaining an open structure in flat to rolling uplands of the Fort Hood landscape (Fuhlendorf and Smeins 1996; Sullivan 1993; Smeins 1980). Denser forests of deciduous trees and Ashe juniper were likely restricted to side slopes and canyons (Diamond 1997). Succession after land-clearing and loss of these natural processes resulted in a shift

toward a more closed canopy, with an increase in woody species such as Ashe juniper and decrease in native grass cover (Smeins 1980).

Since the establishment of Fort Hood in the 1940s, the area has undergone extensive land use changes associated with military training (Freeman et al. 2001). Vegetation communities on the installation are heterogeneous and patchy, often intergrading abruptly amongst different types. Woody vegetation is characterized by contiguous, closed-canopy, Ashe juniper-oak (*J. ashei-Quercus* spp.) forests on mesa slopes, tops, and canyons, with some post oak/blackjack oak (*Q. stellata/Quercus marilandica*) forests (Teague and Reemts 2007). Shin oak (*Q. sinuata* var. *breviloba*) shrubland/grassland matrices are found where wildfire has occurred. Expansive, open grasslands occur on some valleys and rolling uplands, and in small patches near and amongst mesa forest/shrubland stands (Hammer 2011). Grassland/plateau live oak (Q. fusiformis) savannas occur on some rolling uplands. Riparian corridors are characterized by juniper-oak forests and forest belts of southern pecan (*Carya illinoinensis*), walnut (*Juglans* spp.), American sycamore (*Platanus occidentalis*), eastern cottonwood (*Populus deltoides*), bur oak (*Q. macrocarpa*), black willow (*Salix nigra*), and red elm (*Ulmus rubra*) trees (Teague and Reemts 2007; Figure I.3). Within the Owl Mountain Province, mesic canyons host disjunct populations of bigtooth maple (*Acer grandidentatum*) as Pleistocene relicts, isolated from larger populations by several hundred miles (Riskind and Diamond 1986; Gehlbach and Gardner 1983; Figure I.3).

Vegetation and soil disturbance resulting from military activities also maintains much of the vegetation in early succession, particularly evident in the training areas in West Fort Hood, the Live Fire Impact Range, and parts of East Fort Hood (Hammer 2011; Teague and Reemts 2007). More remote areas of the eastern side typically support later successional vegetation, with disturbance in these areas associated with the cutting of vegetation, construction of individual fighting positions ("foxholes"), road maintenance, and other activities associated with dismounted training (Teague and Reemts 2007). Many of these training areas are multi-use facilities with areas that are set aside as endangered species habitat and recreational areas for military families. The Army also allows other non-military uses of Fort Hood lands such as fishing, hunting, and grazing. These uses, together with military training, affect the soil, water, vegetation and animals that occur on the installation (Hayden et al. 2001).

Training on Fort Hood is the primary cause of wildfires on the installation, particularly in the Live Fire Impact Range. Tracers, incendiary devices, smoke generators, and other pyrotechnic devices provide a year round source of ignition (Hayden et al. 2001). Under certain conditions, training related wildfires can occur almost daily in the Live Fire area, which serves to maintain large expanses of grassland and fire-adapted vegetation in this area. Areas historically dominated by grassland in the training areas of East and West Fort Hood have fewer, less intense fires because of the effects of vehicle traffic and grazing on reducing fuels (Hammer 2011). These areas either remain in early successional vegetation (annual forbs and grasses) due to frequent

disturbance or are invaded by Ashe juniper in areas where disturbance is less frequent or intense (Teague and Reemts 2007).

Overview

The following chapters investigate the lithologic, stratigraphic, and structural controls on the hydrologic, hydrogeologic, and morphologic evolution of the Owl Mountain Province as expressed by mesic vegetation communities, including Pleistocene relicts, within karst terrains that exhibit complexly overprinted speleogenetic evolutions within a dynamic groundwater regime resulting from regional climate shifts throughout the Neogene that have been complicated by extensive anthropogenic modifications as a result of urbanization, agriculture, and expanding populations in the region. In these chapters, landscape evolution and the resulting vegetation patterns, examined through the prism of hydrologic and geologic principles, are investigated throughout the inter-disciplinary nature of this study and are used as the foundation for the explanation of the floristic phenomena observed within the Owl Mountain Province.

Chapter II is an overview of hypogene karst within the Lampasas Cut Plain, emphasizing the Fort Hood Military Installation. Chapter III is a study of the geochemistry of subaerial springs within the Owl Mountain and Nolan Creek provinces and the spatial delineation of potential subaqueous springs along the shoreline of Belton Lake. Chapter IV investigates the relationship between regional deformation events and lineament analyses of joints, stream segments, cave features and vegetation patterns as an

indicator of the structural control on surface hydrology and subsurface hydrogeology and its relationship to mesic vegetation communities. Chapter V is a detailed study on the ecohydrology, stand dynamics, and spatial delineation of *Acer grandidentatum* within the Owl Mountain Province, utilizing traditional vegetation mapping and a remote sensing model to locate existing but as yet undocumented *A. grandidentatum* habitat in the study area. Chapter VI is the summary of this research and implications for future geologic, hydrologic, and vegetation studies.

The appendices contain the background data tables used to produce the results found in Chapters 3 – 5. Appendices 1 – 3 are associated with Chapter 3; the data tables in Appendix 1 are the field measurements and laboratory analyses for the subaerial springs, Appendix 2 contains all Piper diagrams for subaerial springs, and Appendix 3 contains maps of the individual physicochemical parameters measured for each sonde sampling period. Appendices 4-7 are individual data tables of lineament orientations for surface joints, stream segments, caves, and mesic vegetation habitats associated with Chapter 4. Appendices 8 – 10 are associated with Chapter 5; Appendix 8 contains the soil and site parameters, Appendix 9 contains the trees per hectare (TPH), basal area per hectare (BAPH), and stems per hectare (SPH) for the individual plots in established and modeled maple habitat, and Appendix 10 contains the results from the independent-samples T-tests conducted to determine the differences between stand dynamics in the Owl and Bear Creek watersheds.

CHAPTER II:
HYPOGENE KARST OF THE LAMPASAS CUT PLAIN

Abstract

The Lampasas Cut Plain is associated with the northern extent of the Edwards Plateau and is characterized by exposures of Lower Cretaceous Comanchean Series carbonates of the Trinity, Fredericksburg, and Washita Groups. In the eastern section, the topography is dominated by plateaued drainage divides capped by resistant limestones with steep slopes and scarps exposing the inter-fingering Edwards and Comanche Peak limestones. Exposures along these scarps reveal significant karst development near the Comanche Peak and Edwards boundaries, including caves, shelters, grottos, vugs, and tafoni. Surficial karst features associated with these plateaus include sinks and caves with upward stoping and collapse structures, including significant overprinting by epigenic processes.

Permeability varies greatly over the boundaries of the Comanche Peak and Edwards; the inter-fingered formations have likely created a semi-confined aquifer system where deeper seated fluids migrate upwards through low permeability strata along preferential flow paths and communicate with meteoric waters near the ground surface. Geochemical analyses of springs within the Fort Hood Military Installation and the inter-

fingering nature of the Comanche Peak and Edwards limestone occurring within these high energy shoals indicates a mixed fluid system where deeper seated phreatic or semi-confined hypogenic waters migrated upwards to maintain base flow as the landscape evolved. Since there are many conduits at the surface for direct recharge of both the Trinity and Edwards aquifers, the possibility of the Trinity Aquifer providing potentiometric pressure for ascending fluids is a possible potential driver for hypogenic speleogenesis within the Lampasas Cut Plain.

Introduction

The Lampasas Cut Plain region can be defined as the southern extension of the Great Plains of North America and/or the northwestern extension of the Edwards Plateau; and is located in North Central Texas. While both definitions would be correct in a larger sense, the Lampasas Cut Plain is distinctly different from these neighboring regions, both as a physiographic province and a karst region. Although there are similarities between the Lampasas Cut Plain and the Edwards Plateau, the genesis, geomorphic evolution, and karst development of the area does not favor inclusion with the Edwards Plateau, but rather deserves an independent explanation of the complex development of the region.

According to the Texas Speleological Survey (2014), the Lampasas Cut Plain is defined as an area bounded to the north by the Brazos River, to the south by the Colorado River, and to the east by the Balcones Fault System (Figure II.1). The landscape and its

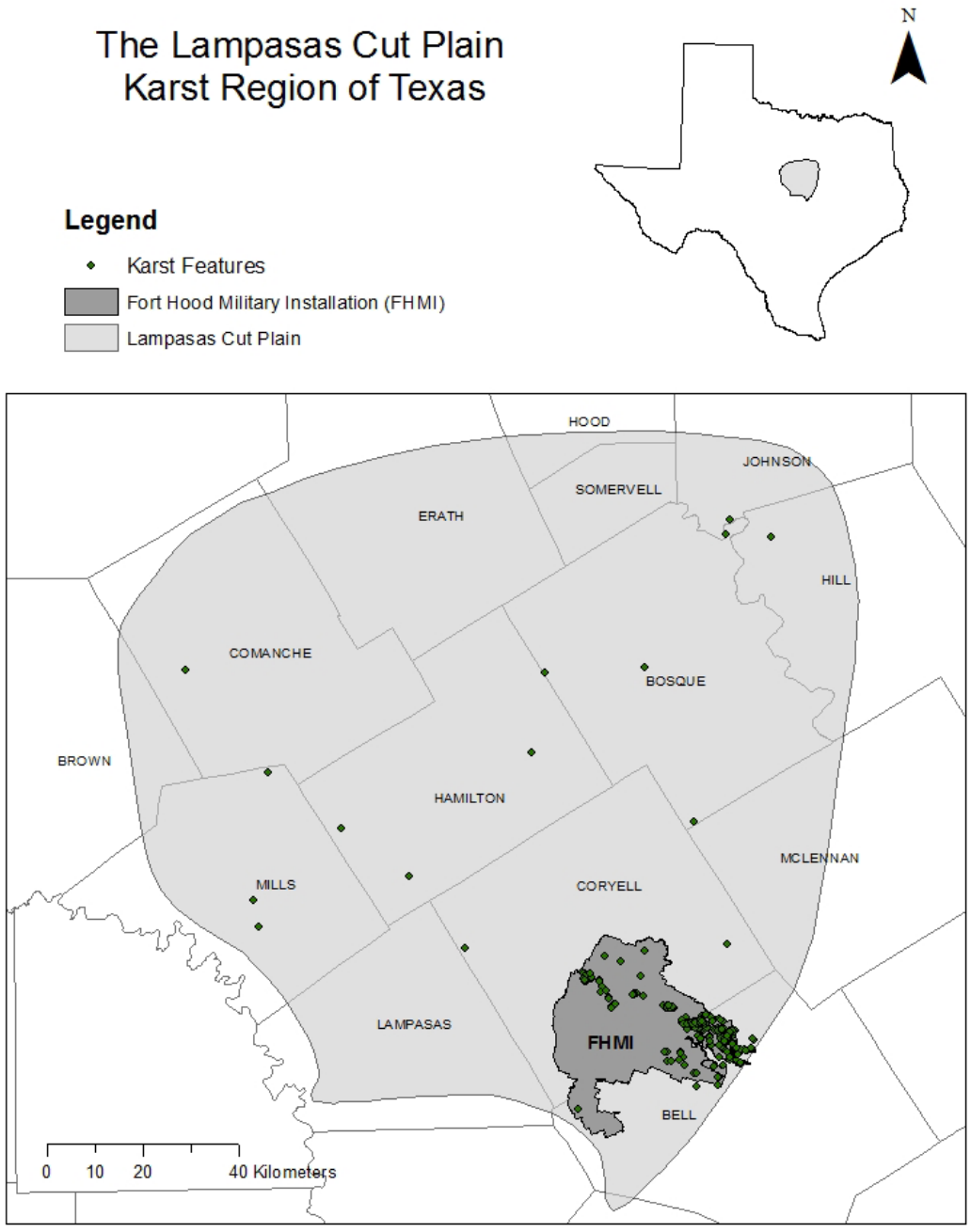

Figure II.1. The karst region of the Lampasas Cut Plain, data sourced from Texas Speleological Survey, 2014.

topography are largely controlled by the erosional behavior of the Edwards limestones and marls; with downcutting of major rivers and streams dissecting the mostly flat mesa-like drainage divides by the Brazos River and its tributaries (Hayward). The topography becomes rolling in areas proximal to streams, exposing Lower Cretaceous carbonates from the Fredericksburg and Trinity Groups. Soil development is minimal on the divides with better developed soils at the base over the Comanche Peak and Walnut Clay units that dominate the valleys (Riskind and Diamond, 1986). The Lampasas Cut Plain covers over 18,000 km^2, including part or all of Bell, Lampasas, Coryell, Mills, Brown, Comanche, Hamilton, Erath, Hood, Somervell, Johnson, Bosque, Hill, and McLennan counties (Figure II.1).

The climate of the Lampasas Cut Plain is sub-humid and becomes increasingly arid to the west and cooler to the north. Due to the Gulf Stream, prevailing winds are generally from the south and the general decrease in moisture content of air from the Gulf of Mexico as it flows northwestward across the plain is the controlling factor responsible for this difference in moisture regime (Bradley and Malstaff, 2004). Mean annual precipitation decreases from east to west, ranging from about 85 cm/yr on the eastern edge to 35 cm/yr on the western edge. Summer average highs and lows do not vary significantly and average about 35° C and 22°C, respectively. The average minimum January temperatures decrease northward, ranging from approximately 4°C to 0°C.

Although the area is dominated by cave forming carbonates, until recently, the Lampasas Cut Plain has not been extensively explored by local or regional caving groups (Reddell, 2001). The first recorded visits to any of the caves in this region were made in the 1940s and recounted in Bulletin 10 of the National Speleological Society (White, 1948). Grottos from the University of Texas, led by David McKenzie, began exploring caves in Bell and Coryell County in the 1960s. Their data was published by the Texas Speleological Survey (McKenzie and Reddell, 1964); this work attracted other groups such as the HUACO Cavers of Waco, the Coryell County Cavers in Temple, the University of Texas Speleological Survey, the Dallas-Fort Worth Grotto, and the Maverick Grotto in Arlington to the area.

To date, surface mapping and LiDAR analyses by Reddell et al. (2011), Bryant (2012), and Faulkner (2013a) across the Fort Hood Military Installation have identified over 300 caves, 80 springs, 667 sinks and 491 shelter caves. Outside the boundaries of Fort Hood, few caves have been documented within the Lampasas Cut Plain (Figure II.1). Much of the land and cave access in this area is owned and controlled by private individuals or is located within the Fort Hood Military Installation, making public access problematic. In recent years, the Fort Hood Natural Resources Division has contracted with environmental consulting firms and research partners to inventory and document the natural resources including caves, rock shelters, sinkholes, and springs located on the base to facilitate land use planning and document environmentally sensitive areas. These

inventories, as well as research projects conducted by karst geoscientists and hydrologists, have greatly improved the understanding of karst systems within the Lampasas Cut Plain.

Geologic Setting

The Lampasas Cut Plain is dominated by exposed carbonates, mostly thick sequences of Lower Cretaceous Comanchean Series limestone and dolostone, known traditionally and informally as the "Edwards." The Lampasas Cut Plain, which represents a generally more mature landscape than the main portion of the Edwards Plateau to the south and west, is composed of strata from the Trinity (Glen Rose), Fredericksburg (Edwards), and Washita (Georgetown) Groups (Figure II.2). Patches of limestone, dolomite, chert and marl alternately crop out at the surface across the area. (Rose, 1972; Amsbury et al. 1984; Adkins and Arick, 1930).

This area has been characterized as a dissected dip plain, with the rocks to the west of the Balcones Fault Zone gently dipping to the east at less than one degree; east of the fault zone, the dip increases to about one degree. The erosional dissection of the Lampasas Cut Plain has been done by first and second order streams; with first order streams such as the Brazos, Leon, Lampasas, and North Bosque River flowing at angles to the regional dip and dissecting the Lampasas Cut Plain along previously established flow routes. Second order streams such as the Middle Bosque River, Hog Creek, and

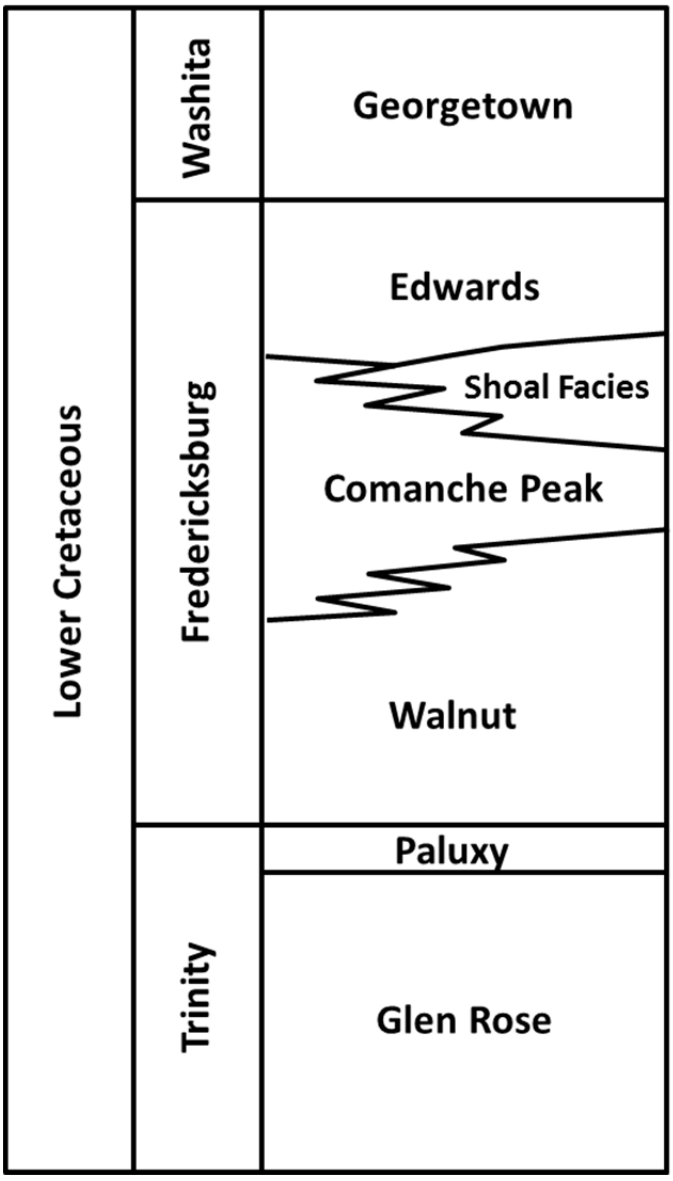

Figure II.2. Stratigraphic column of the Lower Cretaceous Trinity, Fredericksburg, and Washita Groups for the prominent lithologies of the Lampasas Cut Plain (modified from Amsbury et al., 1984).

Coryell Creek flow to the east in the general dip direction. These streams, with their tributaries, are responsible for most of the slope retreat and incision that has created the unique topography of the Lampasas Cut Plain. As streams have cut down through the more easily eroded Georgetown Formation and have further eroded into the more resistant Edwards Group, the interaction between surface water and groundwater within the aquifers below have characterized the erosional forces and topographic expression that define the area. In the southern extent of the Lampasas Cut Plain, the drainage divides are capped by the resistant Edwards and characterized by steep slopes and scarps with interbedded exposures of the Edwards and Comanche Peak Formations. These scarps are common in areas where first order streams have significantly widened stream valleys. The northern extent of the Lampasas Cut Plain is characterized by exposures of the Georgetown Formation, most noticeable in areas where second order streams have not completely removed the more easily eroded material.

Geologic History

The tectonic history of the Lampasas Cut Plain began in the Precambrian as thick sequences of sediments were deposited into a shallow sea along the Laurentian margin (Walker, 1979). As sea level fluctuated in the early to mid-Paleozoic, transgressing seas deposited Ordovician carbonates and clastics of the Ellenburger Group in the south-western section of the Lampasas Cut Plain near Lampasas and San Saba counties. During

the Pennsylvanian Period, the Ouachita Orogeny occurred along the southern Laurentian margin; the resulting deformation caused crustal downwarping to the west and the eventual uplift of the Concho Arch, an elongated topographic positive structure that extended along a NNW trend to the west of the Lampasas Cut Plain. Continued deformation initiated the development of the Concho Shelf and Bend Flexure to the north, and the Eastern Shelf along the western flank of the Concho Arch (Anaya and Jones, 2009; Figure II.3). As the Paleozoic Period came to a close and the Laurentian continent was assimilated into the Pangaean supercontinent, the Central Texas region began to tilt to the northwest along the Ouachita orogenic front and sediment from the surrounding uplands filled the western basins as organically-rich sediments, reef structures, and coastal deposits were covered, buried, and compressed (Walker, 1979; Talbert and Atchley, 2000).

At the beginning of the Mesozoic, Pangaea began to break apart and the remains of the Ouachita mountain range began eroding into the newly opened Gulf of Mexico (Anaya and Jones, 2009). Mesozoic transgressive sequences, the Zuni and the Tejas, deposited large packages of sedimentary rock over Paleozoic erosive surfaces. In the Central Texas region, these rocks are the Glen Rose Formation, the Fredericksburg Group (including the Edwards) and the Washita Group (Talbert and Atchley, 2000; Figure II.2). In the late Cretaceous and into the early Tertiary, this area was influenced by the

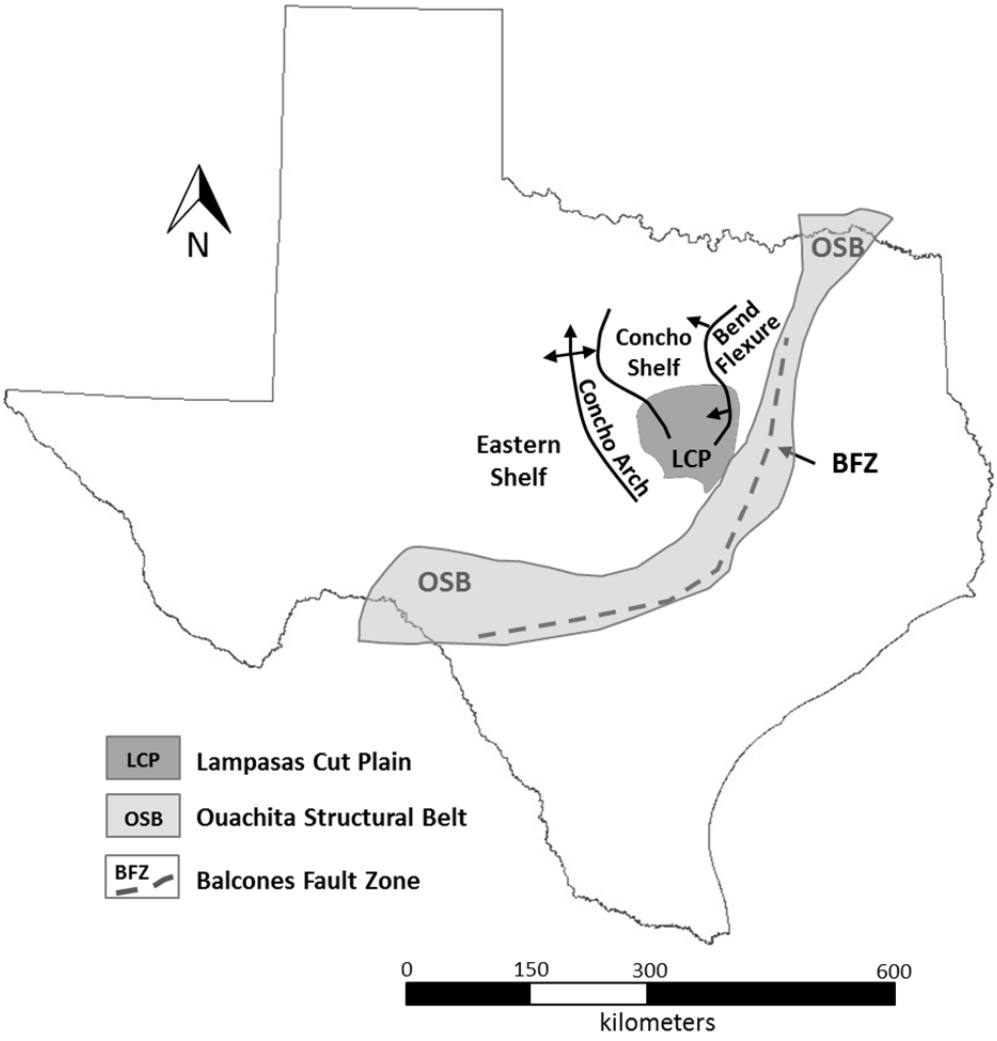

Figure II.3. Late Paleozoic deformation associated with the Ouachita Orogeny created several structural positives in the future Lampasas Cut Plain region. Paleogene deformation associated with the Balcones Fault Zone follows the trend of the Ouachita Structural Belt (adapted from Walker, 1979).

Laramide orogeny; the regional uplift of the Edwards Group resulted in the exposure and partial erosion of Edwards sediments, which increased secondary porosity and tilted the strata to the southeast (Elliott and Veni, 1994).

As a result of the uplift and aerial exposure in the Tertiary, the rivers flowing across this Central Texas region began to erode the softer rocks and sediments of the Upper Cretaceous and early Tertiary, sending massive sediment influxes to the east toward the widening Gulf of Mexico. The harder, more resistant Edwards Limestone formed a broad, flat plateau that was dissected by the erosive force of the major river systems. In the late Miocene, the buried Lower Cretaceous Texas coastline provided sufficient crustal weakness for the uplifting of the Central Texas region along the trend of the former Ouachita deformation zone, creating the Balcones Fault Zone and defining the Edwards Plateau (Bloom, 1998; Figure 3).

In the Quaternary, substantial climatic changes helped redefine the topography in the Central Texas region. Wind-blown loess deposits built the foundations for soil accumulation across the prairies and increasing available moisture from melting glaciers helped build the major watersheds of the Trinity and the Brazos rivers. Over time, the Brazos and Trinity watersheds eroded the north/south trending Balcones escarpment from its original location to the present location nearly 320 kilometers to the west (Woodruff and Abbott, 1979).

Structural Controls on Karst Development

The Balcones Fault Zone is the major structural feature influencing the geology of the Edwards Plateau and Lampasas Cut Plain. It extends as an arcuate belt of *en echelon* normal faults from Del Rio to Dallas with recent faulting (between 24 and 5 mya) initiating the uplift and subsequent dissection of the Lower Cretaceous strata (Figure II.3). Most of the displacement along the faults is believed to have occurred in the late Oligocene or early Miocene as evidenced by the abundance of reworked Cretaceous fossils and limestone fragments in the fluvial sandstones created down-dip of the major fault trends (Adkins and Arick, 1930; Ferrill and Morris, 2008) There is some evidence for both earlier movement along faults within this zone during the late Cretaceous and perhaps later movement during the Pliocene, but the evidence is inconclusive at the present time.

These major normal faults generally strike N/NE and dip from 40^0 to 80^0 (Ferrill and Morris, 2008). The net throw across the fault zone is down toward the east, although faults dip both to the east and west (Senger et al., 1990). There are some faults that have been mapped sub-perpendicular to the major Balcones faults, but they are not well exposed in the northern segment of the Edwards Plateau and Lampasas Cut Plain and could be related to the reactivation of basement deformation associated with Paleozoic rocks and the Ouachita Orogeny (Ferrill and Morris, 2008). In the southern part of the Balcones Fault System, the fault curves around to the west and juxtaposes the older Glen

Rose Formation against the younger Edwards Group. These western trending faults in the northern segment could be sub-parallel to this major trend in the south, but more evidence would be needed (Anaya and Jones, 2009; Cannata and Yelderman, 1987).

Displacement along the main fault-line scarp varies, and decreases from east to west. This fault bound exposure of limestone has resulted in a compartmentalization of the Edwards Aquifer into a narrow belt that includes most of the recharge and discharge areas within the eastern basins (Cannata and Yelderman, 1987; Eckhardt, 2012; Figure II.4). Breccia zones, nearly vertical dipping strata, and abundant minor faults and joints occur adjacent to the major faults as well as gentle monoclinal and anticlinal flexures that occur near these major faults. The activation of this fault system and the subsequent deformation was probably caused by a number of contributing factors such as the migration of Jurassic salts in the off-ramp basin, the southeastern extension of the Gulf of Mexico associated with Basin and Range tectonism, and tensional stress along the Ouachita fold and thrust belt precipitated by the accumulation of sediments in the Gulf of Mexico (Rose, 1972; Ferrill and Morris, 2008).

Stratigraphy

Within the Lampasas Cut Plain, the majority of known caves are found within the Edwards and Georgetown Formations, with the Edwards being the most important cave forming unit in the region. A few caves have been documented in the upper Cretaceous

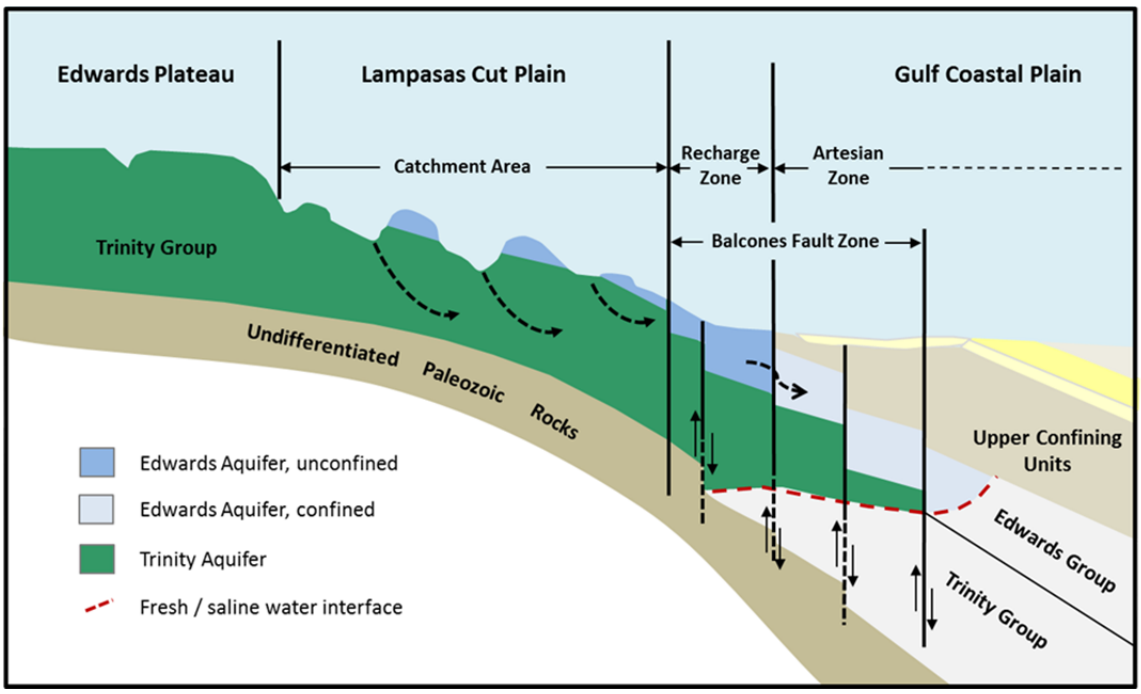

Figure II.4.Within the Lampasas Cut Plain, the Edwards and Trinity Aquifers both receive direct recharge from the surface. Communication between the Trinity and Edwards Aquifer could serve as a potentiometric driver for continuous discharge along the edges of the plateaus. Modified from Blome and others, 2015.

Austin Chalk and in the lower Cretaceous Comanche Peak, but these are the exceptions. Cave forming strata are mostly exposed in the eastern section of the study area (Figure II.5), where the Edwards provides a resistant cap over broad drainage divides and steep scarps. The lower valleys along creeks and rivers are covered by deeper soils and vegetative cover with few prominent exposures of Lower Cretaceous rocks. The Comanche Peak outcrops are exposed along the base of the plateaus, interfingering with exposures of the Edwards Group. Across the top of the plateaus, the Edwards Group forms the cap rock and varies from rudistid-rich limestone to vuggy, porous

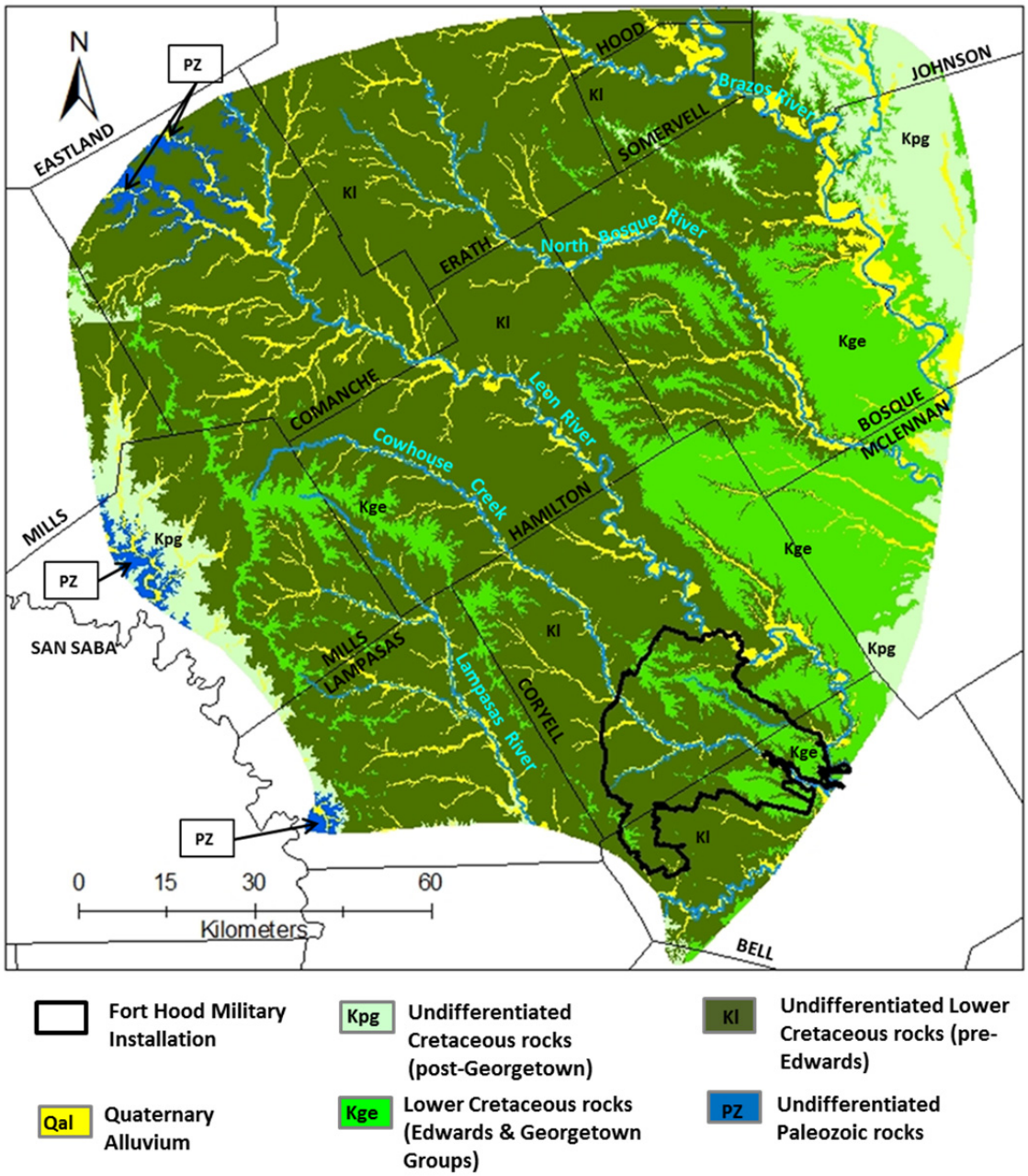

Figure II.5. The geology of the Lampasas Cut Plain is dominated by Lower Cretaceous carbonates from the Trinity, Fredericksburg, and Washita Groups.

outcrops (Amsbury, et al. 1984; Cannata and Yelderman, 1987).

Early geologic mapping by Barnes (1970) shows the undivided Edwards Group conformably overlying the Comanche Peak limestone, with the Edwards thinning to the north and gradually interfingering with the Comanche Peak (Figure II.2). Within the Lampasas Cut Plain, the Edwards can be quite variable; thicknesses range from approximately two to fifty meters, with an average of ten to twenty-five meters. In this region, Cannata and Yelderman (1987) described the Edwards as a massive rudist reef limestone with elongate reef front circular bioherms. Deposition of these bioherms began approximately 110 mya on the Comanche platform, which was constructed on the tectonically positive Llano and Devils River uplifts in Texas behind the main structure of the Stuart City Shelf Margin complex (Nelson, 1973). The Comanche Shelf was bounded on the east and south by a relatively deep-water oceanic basin, the ancestral Gulf of Mexico, and on the north and west by an extensive shallow-water open marine basin, the North Texas-Tyler basin (Fisher and Rodda, 1969; Figure II.6).

Although there are many geologic formations that crop out within the region, for ease of discussion, the lithologies have been grouped into larger packages (Figure II.5). Within the Lampasas Cut Plain, the following lithologies are recognized:

Lower Cretaceous Units (pre-Edwards) – The Glen Rose, Paluxy Sand, and Walnut Clay. These units comprise much of the Lower Cretaceous and consist of

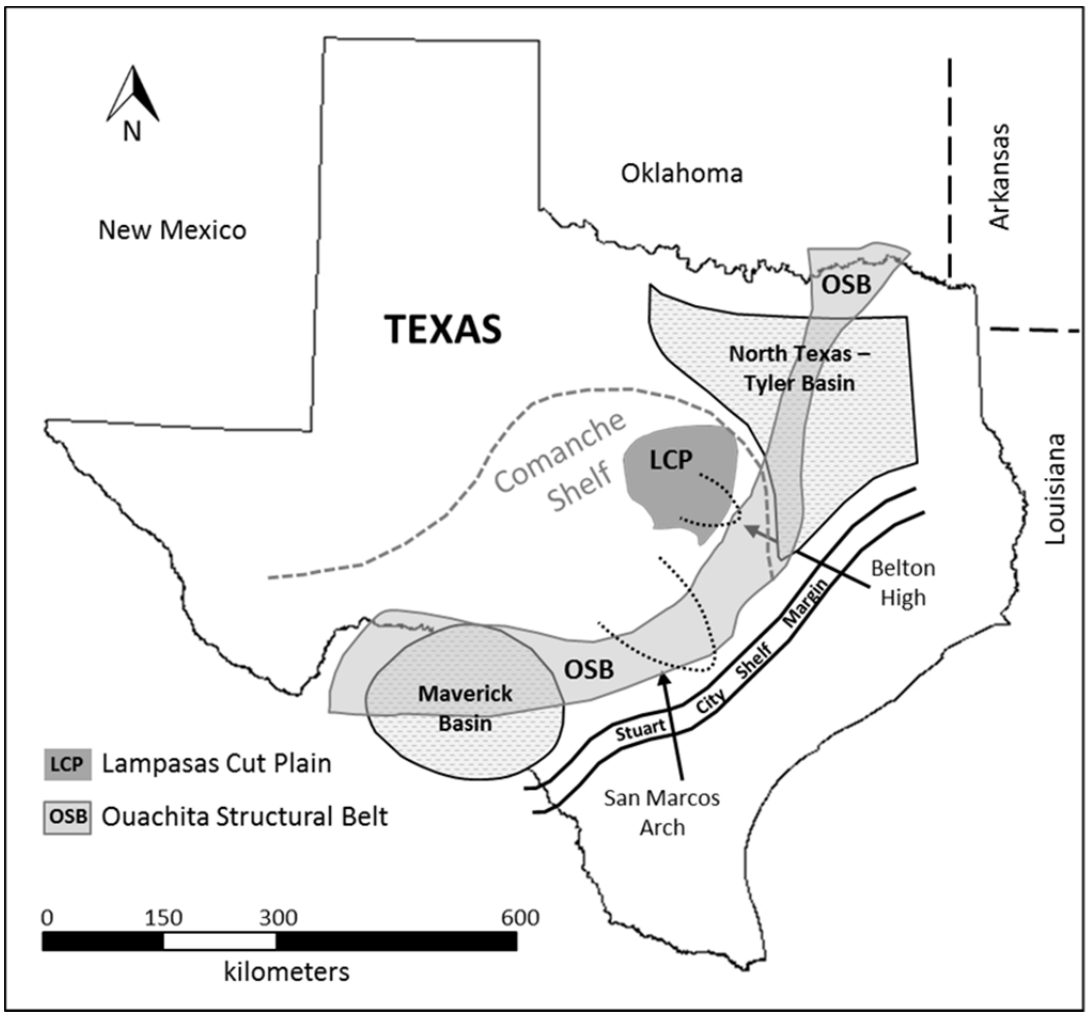

Figure II.6. Location map showing regional features which influenced the depositional environment for the Trinity, Fredericksburg, and Washita Groups on the Comanche Shelf behind the Stuart City Shelf Margin trend (modified from Anaya and Jones, 2009).

limestones, clays, marls, shales and sandstone. Outcrops are confined to the lower elevation and along developed drainage with varying thicknesses. Alternating sequences between depositional environments within the Glen Rose expose resistant ridges of limestone separated by less resistant ridges of soft marl, creating characteristic stair-step topography commonly found in Glen Rose outcrops.

Comanche Peak Limestone (Kc) – The Comanche Peak Formation is a nodular limestone and marl sequence with a maximum thickness in Bell County of approximately 21 m, thinning to the south in Williamson County. This unit has transitional contacts with the underlying Walnut Formation and the overlying Edwards Group (Senger et al., 1990). Most of this formation consists of chalky or firm limestone nodules imbedded in a subordinate amount of limey marl matrix. These limestones contain transmissive zones, although permeabilities in Comanche Peak strata within the wackestone and packstone facies are considerably less than those in the overlying Edwards Group. Most of the Comanche Peak is not distinctly bedded, distinguishing it from the overlying Edwards (Adkins and Arick, 1930).

Edwards Group (Ked) – The Edwards Group has been described as a transgressive facies representing a reef lagoon complex (Collins, 2005). It is informally divided into four members based on lithology: (1) a lower interval of massive, rudistid bearing, porous limestone and dolostone with abundant chert nodules, (2) a unit of interbedded, varying thickness of cherty limestone containing rudists, foraminifera and thin-bedded flaggy limestone; (3) a unit of nodular, fossiliferous, burrowed, argillaceous limestone and marl; (4) an upper interval of varying thickness limestone, dolomitic limestone and dolostone (Barnes, 1970;). Although these informal designations have been described and named, most mapping and descriptions of the northern outcrops of the Edwards Group do not differentiate based on these informal divisions. The Edwards Group is characterized by honeycomb textures, voids in collapse breccias, cave systems and local transmissive zones (Senger et al., 1990). Within the Edwards, several higher energy shoals have been described. The trend of these shoals, formed across the axis of the Belton High, follow the model presented for Moffatt Mound (Amsbury et al., 1984; Brown, 1975). The Moffatt Mound area consists of thicker, more well-defined outcrops of Edwards Group strata that are lithologically distinct from the main Edwards reef trend. Recent research by Bryant (2012) and Shaw (2012) have described two additional shoals within the Fort Hood Military Installation, the Nolan Creek Province and the Owl Mountain

Province. The strata in these provinces formed to the west of the Belton High in more restricted circulation waters and the minor differences in water depth due to the spatial distribution across the Belton High are the main control for differences in lithology of outcrops between Moffatt Mound and the Nolan Creek and Owl Mountain provinces (Bryant, 2012; Brown, 1975).

Georgetown Formation (Kgt) – The Georgetown Formation, a unit within the Washita Group, consists of fossiliferous limestone, argillaceous limestone and minor marl that have wackestone, packstone and grainstone facies (Collins, 2005). Pelecypods are diagnostic features of the Georgetown Formation, as well as vuggy porosity present in some of the facies. In the study area, the Georgetown is generally not divided south of the Lampasas River; in the northern section, the Georgetown thickens and is locally divided into seven members (Barnes, 1970).

Lower and Upper Cretaceous Units (post-Georgetown) – Most of these units consist of soft marls and limestones, with interbedded shales and sands. The Austin Chalk consists of interbedded chalk and marl, with thickness between fifty and one hundred meters (Collins, 2005). Exposures of these units are mostly limited to the eastern and western segments of the Lampasas Cut Plain.

Hydrogeology

There are two primary aquifers within the Lampasas Cut Plain; the Trinity Aquifer containing the lower Cretaceous units stratigraphically below the Edwards Group (namely the Glen Rose Formation) and the Edwards Aquifer, primarily composed of the Edwards and Georgetown limestones (Figure II.4). Both of these aquifers crop out within the Lampasas Cut Plain and are instrumental in providing base flow for perennial and intermittent streams, as well as numerous springs and seeps associated with the area (Jones, 2003). The communication between the Trinity and Edwards Aquifers and the surface are also a potentiometric driver for solutional widening of fractures and eventual cave formation (Ferrill et al., 2008).

Within the Lampasas Cut Plain, the shoal facies function as outliers to the north and west of the Northern Segment of the Edwards Aquifer and exhibit distinct differences due to their unique depositional environment. Karst development within the Lampasas Cut Plain is concentrated in areas where these positive topographic features are directly coupled to the atmosphere (Amsbury et al., 1984; Bryant, 2012). Precipitation is either directed into short stream segments and drainage basins or directly into the subsurface through fractures, sinkholes and smaller conduits (Jones, 2003; George Veni and Associates, 2005). This water will travel vertically and/or sub-vertically until it reaches a lower permeability unit; it will then travel laterally to form one of the numerous springs and seeps on the outer edges of the uplands. While epigenic karsting processes are

responsible for solutional widening of surficial conduits, geochemical analyses of springs within the Fort Hood Military Installation and the inter-fingering nature of the Comanche Peak and Edwards limestone occurring within these high energy shoals indicates a mixed fluid system where deeper seated phreatic or semi-confined hypogenic waters migrate upwards to maintain base flow as the landscape evolves (Shaw and Stafford, 2014; Figure II.7).

The Trinity Aquifer is composed of older Lower Cretaceous rocks, including the Glen Rose Limestone, and crops out in the western part of the Lampasas Cut Plain. In the subsurface, the Trinity consists of layers of limestone, calcareous sands and silts, and conglomerate. These sediments were originally eroded from the higher elevation Llano Uplift and provided much of the clastic sedimentation found in these rock layers. In much of the Lampasas Cut Plain, the Trinity Aquifer underlies the Edwards, and there could be some sub-surface connectivity between the aquifers that contribute to the hydrologic activity, but that has not been confirmed (Ferrill et al., 2008).

Karst of the Lampasas Cut Plain

The Lampasas Cut Plain is an evolving karst landscape, with Cretaceous aged carbonates exposed at the surface over most of the area. All of the known karst features that occur are coupled to the surface and heavily overprinted by epigenic processes; many exhibit solutional widening as a result of the interaction between surface and groundwater

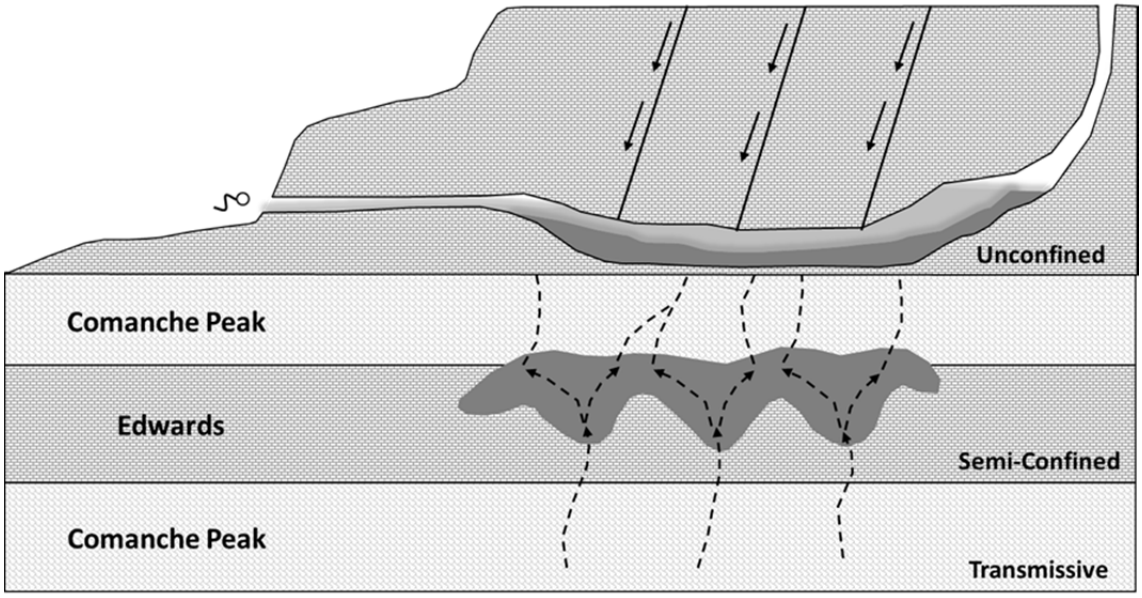

Figure II.7. Within the Lampasas Cut Plain, the Comanche Peak and Edwards are interbedded with permeable transmissive zones occurring between and within the units. (modified from Bryant, 2012).

(Elliott and Veni, 1994; George Veni and Associates, 2005; Reddell, 2001). Many of the sub-surface karst features are fracture controlled, with both local and regional trends (McCann, 2012). Some karst development is controlled by bedding planes with springs, seeps, and rock shelters developing along the interface of lithologic contacts between the Comanche Peak and Edwards formations (Elliott and Veni, 1994; Reddell 2001; Reddell, et al. 2011). Cave development is truncated by the abrupt eroded edges of the plateaus and most of the extensive caves and cave remnants are small-diameter conduits.

During the Miocene, faulting and subsequent uplift along the Balcones initiated rapid downcutting of existing drainage systems; as stream segments incised exposed rock, the intersection of fracture conduits with stream base level helped widen cavities and develop spring discharge outlets. As downcutting continued and base level dropped, some caves began to develop multiple levels in response to stream incision (Elliott and Veni 1994). As erosion continued, these cave systems would eventually breach the surface and be altered by meteoric waters.

Hypogene Karst of the Lampasas Cut Plain

Modern interpretations of hypogene karst systems can be complicated by epigenic overprinting; as landscape evolution causes hypogenic karst systems to lose confinement from uplift and denudation, the suite of features indicative of hypogene karsting are directly modified by mixing hydrologic systems related to phreatic and epigenic hydrologic conduits (Klimchouk, 2007). Initial development and flow of hypogenic systems are predominantly vertical, although considerable lateral components can develop as a result of noncompetitive flow in confined conditions. Karst development within the Lampasas Cut Plain is controlled primarily by lithology; almost all known caves within the Lampasas Cut Plain are found in the Edwards and Georgetown units, the exceptions are a few caves within the Comanche Peak Formation and Upper Cretaceous Austin Chalk, formed along bedding planes or transmissive zones. Overall, the Edwards

Limestone is the most important cave-forming unit in the Lampasas Cut Plain (Reddell, 2001).

Speleogenesis in the study area reflects a long and complex porosity evolution; where hypogene features may have developed at permeability boundaries in the past, today they are being actively overprinted by recent epigene processes and continue to develop additional new pore networks, both through channelized conduit and matrix flow. Geochemical analyses of springs within the Fort Hood Military Installation and the inter-fingering nature of the Comanche Peak and Edwards limestone occurring within high energy shoals indicates a mixed fluid system where deeper seated phreatic or semi-confined hypogenic waters migrate upwards to maintain base flow in area springs during periodic droughts, while meteoric, vadose waters recharge and mix with deeper seated phreatic or hypogene waters during precipitation events (Bryant, 2012, Shaw and Stafford, 2014). Within the Lampasas Cut Plain, both the Trinity and Edwards aquifers receive direct recharge from surficial processes; therefore, the possibility exists for the Trinity Aquifer to provide potentiometric pressure for ascending fluids is a potential driver for hypogenic speleogenesis (Ferrill et al., 2008). The evolving nature of this open karst system and the complex inter-fingering of the lithologies make it difficult to differentiate between features associated with deeper phreatic circulation and semi-confined hypogenic fluid.

Today, most of the karst features within the Lampasas Cut Plain are predominantly surficial expressions of collapse features or features resulting from vadose entrenchment, creating windows into karst conduits. Sinkholes and cave entrances are often small and associated drainage basins generally covering less than one hundred square meters in area. In the Lampasas Cut Plain, many sinkholes and cave entrances appear to have formed as upward stoping collapse structures and/or features that have been breached by surficial denudation (Bryant, 2012, Faulkner et al., 2013b). Some of the caves within the Lampasas Cut Plain exhibit well-defined cupolas and ceiling notches that may be characteristic of ascending fluid migration; indicating that at least part of the diagenetic history of those cave systems may have originated by pressurized fluids from below, with later subsequent overprinting by meteoric waters.

Hypogenic Cave Features

Most of the known caves that occur in the Lampasas Cut Plain are within the boundaries of the Fort Hood Military Installation. Many of the possible hypogenic features described have a complex genetic history and could have been formed through hypogenic and/or phreatic processes, making the discussion of true hypogene features in this setting difficult at best. Some of the caves exhibit cupolas, bedrock partitions, ceiling pendants, solutional widening and ceiling notches that may have been created by pressurized ascending fluids; however, these structures are generally found in relatively

shallow caves today that have been breached by surface denudation and upward stoping associated with vadose waters.

Many of the caves in this area formed along conjugate joint sets in a semi-confined environment, both laterally and vertically. Some of these joint sets follow major regional trends (E/W and N/S; NE/SW and NW/SE) that would have provided a planar surface for ascending fluids with solutional widening along these fractures initiating cave development along transmissive zones or bedding planes. Eleven caves have been chosen for discussion purposes that exhibit possible hypogenic speleogenesis and have been divided into three basic morphologies: maze, ramiform, and linear.

Maze Caves

Maze Caves form as a network of interconnecting and mainly contemporaneous passage loops in bedded, fractured rock where dissolution occurs along multiple paths – and sometimes multiple levels – at similar rates. Maze caves can form in epigenic or hypogenic settings where high discharge rates as fluid migrates into fractured rock, maintaining flow along many alternate routes over a significant amount of time, or by local production of aggressive conditions in the soluble rock by mixing waters of varying chemistry (Palmer, 2007). As surface erosion occurs above the developing conduits, sediment transport facilitates the opening of pre-solutional fractures. Tensional stresses associated with faulting and focused along the axes of folds can have a similar effect by

opening multiple conduits such that fluid migration is dispersed along various pathways as dissolution commences along the fracture planes (Palmer, 1991). The following caves show gradational levels of maze development and are found in areas where fracture density is greatest (Figure II.8).

Mixmaster Cave developed along a NW/SE trend with shorter passages developed along a NE/SW trend. Near the entrance, a maze-like network of passages with notched ceilings lead to the main passage and entrance to an area called Domes City Maze, a complex area approximately 18 m long with wide smooth passages and large numbers of 1.5 m to 3 m high domes. Within the Domes City Maze and along the remainder of the passage, numerous small crawlways exist to the NE and SW but quickly become too narrow for further exploration. The main passage opens into a larger clay-floored chamber with notched ceilings. At the end of the main passage, there is a pit that connects to a lower level but the passage is too small to follow (Texas Speleological Survey, 2014).

Triple J Cave exhibits two levels of linear passages developed along a dominant NW/SE trend and shorter, truncated passages developed along a secondary N/S trend. Most of the passages trending N/S quickly become too constricted for further exploration, although the Highland Crawl has notched ceilings and exhibits solutional widening along less resistant bedding planes. The ceiling of the eastern section of the main passage

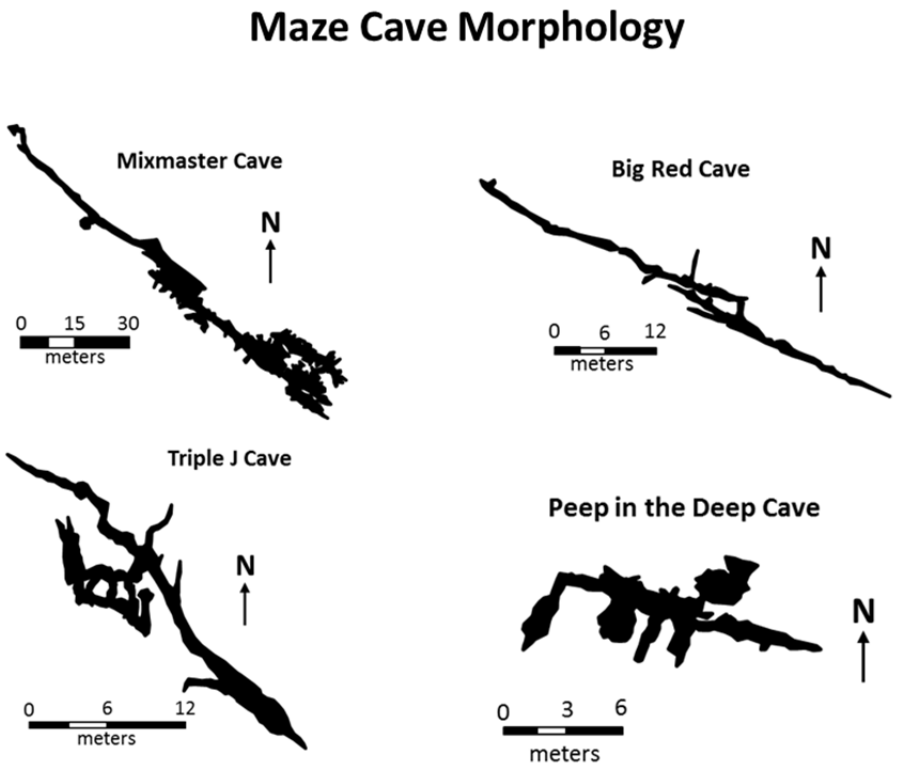

Figure II.8. Maze caves within the Lampasas Cut Plain are associated with conjugate joint sets and tend to develop in areas where fracture density is the greatest. Cave drawings were simplified from cave maps obtained from the Texas Speleological Survey proprietary database, 2014.

contains several large cupolas and the passage eventually opens into Triple J Hall where larger domes exist with numerous speleothems. A drop on the south side of Triple J Hall leads to the lower level with notched ceilings and Chimney Dome (Texas Speleological Survey, 2014).

Big Red Cave formed in the basal Edwards unit near the contact of the Comanche Peak Limestone. Over time the cave has developed linear passages and multiple levels along a dominant NW/SE joint trend with secondary passages extending N/S. The main cave passages trend to the east and west, following the dominant joint pattern. The upper level, the East Crevice Room passage, extends southeast about 15 m and then quickly narrows to prevent further exploration. Undulations in the ceiling and floor of this passage may indicate differential erosion along preferential flow paths. Lower in the cave, the main passage trends to the northwest with several small drains (pits); one of which descends to the Comanche Peak/Edwards contact. Most of the passages in the cave are low crawlways along fissure like voids that follow the joint trends; these passages quickly constrict and become too narrow and low for continued exploration, often ending abruptly. Along the main passage, three well-developed cupolas (each over 4 m tall) show variation in cave morphology and indicate the possibility upwelling of fluids during cave formation. The northwestern passage continues into a low crawlway, the Treasure Hunters Gallery, which continues for another 23 m before becoming too narrow for further exploration. Cave development along the short passages extending N/S may be due to rising fluids from the interface of the Comanche Peak and Edwards Limestone contact (Texas Speleological Survey, 2014).

Peep in the Deep Cave developed along a dominant NW/SE trend with shorter passages developed along a secondary NE/SW trend. The cave exhibits one cupola at the

end of one of the secondary passages, and notched ceilings in the Turn Around Room. Many of the passages end abruptly, with some containing breakdown fill from vadose entrenchment (Texas Speleological Survey, 2014).

Ramiform Caves

Ramiform caves consist of irregular room and chambers in a three dimensional pattern extending outward from the main areas of development. These caves tend to form isolated chambers in thicker bedded rocks in zones of lower fracture density; cave development tends to be isolated but often occurs as clusters within a region (Figure II.9). This cave morphology is most commonly produced in hypogene systems by sulfuric acid from the oxidation of rising hydrogen sulfide; the resulting cave morphology often exhibits no relationship to recharge through the overlying surface. Ramiform caves can be formed in phreatic and epigenic systems by chemical variations in mixing waters, although this tends to be less common (Palmer, 1991). Passage profiles and cross-sections are highly irregular and show abrupt changes over short distances. The outward branches usually form as sequential outlets for groundwater at different times and at different elevations.

Camp 6 Cave No. 1 exhibits globular chambers along a dominant NW/SE trend with secondary development along the NE/SW trend. The main passage has two major

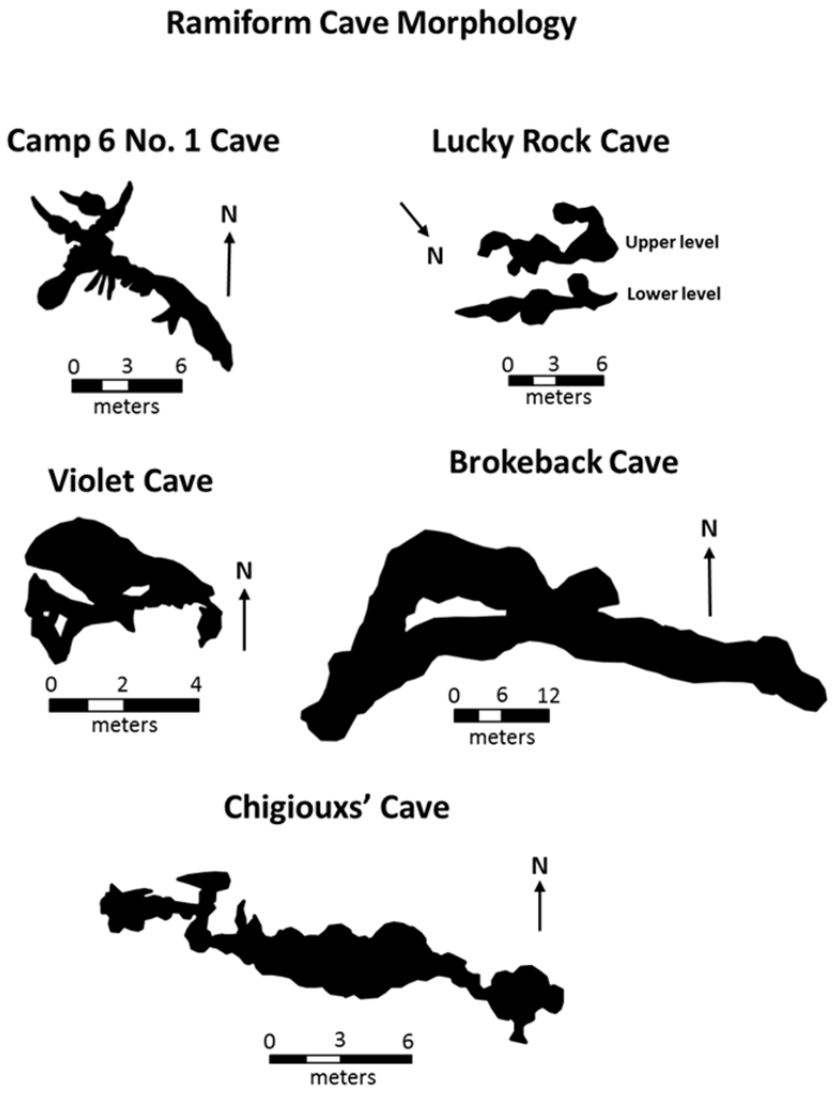

Figure II.9. Ramiform caves tend to form isolated chambers in thick bedded rocks, concentrated in areas where fracture density is not as prevalent. Cave drawings were simplified from cave maps obtained from the Texas Speleological Survey proprietary database, 2014.

cupolas, one 3. 7m tall and the other 3 m. Several alcoves exist along the main passage, most of which are filled with breakdown debris. Blind passages trend NE/SW from the main passage, but quickly become too low and narrow for further exploration (Texas Speleological Survey, 2014).

Lucky Rock Cave exhibits multiple levels of globular chambers with large cupolas on the first and second level. The first level dome is 2.4 m high, the second level domes are much larger, one is 6 m and the other over 9 m high, reaching up to the height of the first level (Texas Speleological Survey, 2014). Violet Cave exhibits globular chambers developed on two levels. The lower level has no known passages extending from this area. The upper level contains several cupolas along the passage (Texas Speleological Survey, 2014).

Brokeback Cave formed along a general WNW/ESE trend with secondary development along a NE/SW trend. Multiple collapse features have been mapped along the trend of the passages. The most accessible entrance is one of these collapse features; a 3 m natural bridge spanning the width of the cave exists near the main entrance. From the main entrance, the cave trends along three passages; one passage extends to the ESE approximately 9.1 meters before ending abruptly, one passage extends to the WSW approximately 18 meters, and the other loops around a vertical partition to the northwest before connecting back to the WSW passage. The ceiling of the third passage contains four cupolas. The abrupt ending of the ESE passage and sloping entrance through a

collapse feature might be indicative of additional passages that extend from the main cave, but that is unknown at this time (Texas Speleological Survey, 2014).

Chigiouxs' Cave exhibits globular chambers developed along a major E/W trend with secondary development along the N/S trend. The cave is developed in two main levels, with the chamber passages forming along an E/W trend. The western passage opens into a small chamber and the floor is covered in debris; primarily breakdown from ceiling collapse and vadose entrenchment. The main passage, Crystal Walk Hallway, extends to the east with multiple chambers and small alcoves that trend N/S. The easternmost chamber, Last Chance Lounge Room, formed along the N/S trend and the cave terminates with blind passages to the south and east filled with debris. The cave ceiling in the Crystal Walk Hallway exhibits several cupolas, indicating a sluggish flow regime associated with ascending fluids. The domed cave ceiling in the Last Chance Lounge Room also has ceiling notches, another indication that ascending fluids might have been responsible for present day cave morphology (Texas Speleological Survey, 2014).

Linear Caves

For these purposes, a linear cave would be one whose morphology follows a linear trend, either as stream caves fed by sinking surface streams or as a remnant of what were once more extensive passages of a network of a larger cave (Figure II.10). These caves could

be formed by epigenic processes such as sinking streams and sinkhole recharge, or as preferential dissolution by aggressive fluids in hypogene systems (Palmer, 2007). Viper Den Cave has been connected to Tumble Down Sink by voice and smoke contact, but today is mapped as a linear feature due to sediment infill. There are passages to the east and west in the cave but the sediment load in the cave prevents further exploration. Viper Den Cave exhibits a linear E/W trend with notched ceilings and solutionally widened passages. The cave contains extensive ceiling channels, cupolas, and bedrock partitions, indicative of hypogenic or phreatic fluids. To the west of the entrance, the passage extends approximately 4.6 m before becoming too sediment filled. Two domed structures extend into the ceiling for approximately 0.5 m along a central ceiling channel that extends upwards toward the cave entrance. To the east, three cupolas, elliptical in shape, extend into the ceiling in the main room. The eastern portion of the cave splits into two smaller passages with several small domed structures and is divided by a central bedrock column. The passage to the north narrows rapidly as the floor rises; the passage to the south narrows more gradually and eventually becomes too small. A linear series of domed structures follows the trend of the southern passage, and a small dome was observed in the northern passage (Bryant, 2012).

Little Red Cave formed along a NW/SE trend with the entrance separated from the main passage by a vertical partition. The entrance is through a collapse structure and offset from the main passage to the NE. Along the main passage, domed structures and

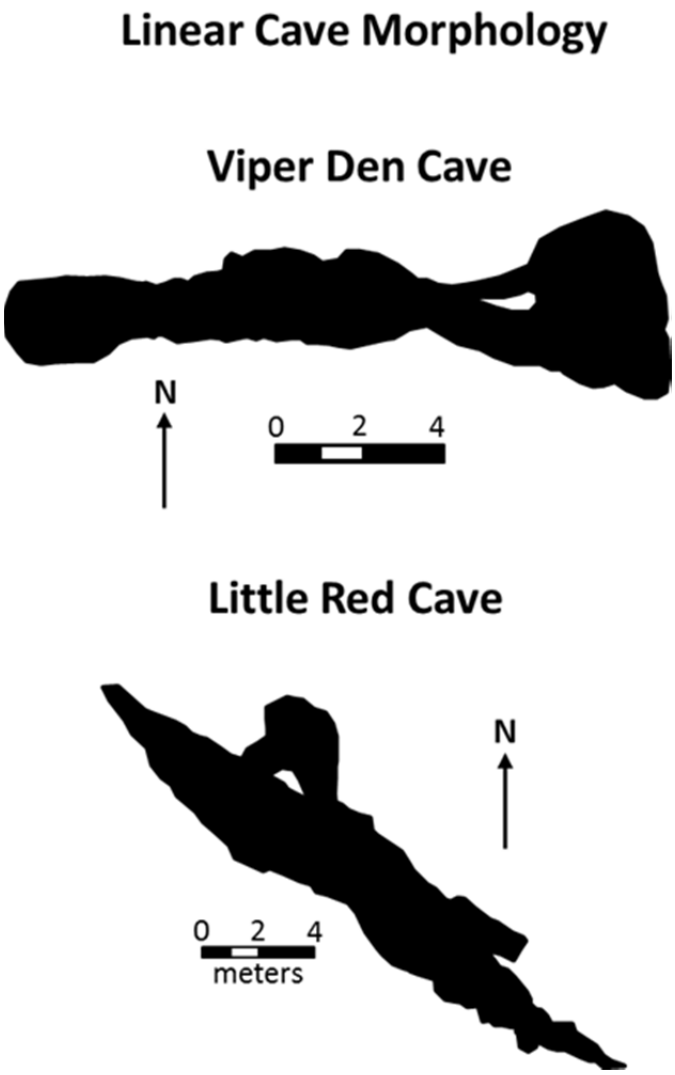

Figure II.10. Linear caves such as Viper Den and Little Red caves have been heavily overprinted by epigenic processes. Cave drawings were simplified from cave maps obtained from the Texas Speleological Survey proprietary database, 2014.

ceiling notches indicate dissolution by sluggish fluids (Texas Speleological Survey, 2014).

With regards to the caves listed, fracture density tends to exert the greatest control on the level of cave development and morphology. In areas where fracture density is greatest and bedding is relatively uniform, the caves tend to develop a maze-like structure in response to solutional widening along conjugate joint sets. Mixmaster Cave shows the greatest level of maze development and Peep in the Deep the least, but surface modifications and sediment infill partially mask the evidence for interconnected passages.

In areas where bedding is thicker and fracture density is not as great, caves tend to develop isolated, irregular chambers. As dissolution continues, many of these chambers can become connected (Camp Caves No. 1 and 2, Violet Cave) but later surface modifications and sediment infill have blocked potential communication between these chambers. Viper Den Cave is in an area where numerous caves and sinks have been described, and voice and smoke contact have been established with area sinks, but sediment infill has masked the visual connection (Figure II.11).

If features in these cave passages are interpreted as hypogenic, the overlying clays within the Georgetown Formation and/or Tertiary carbonates and clastics could have provided a seal over the Edwards. Late Cretaceous and early Tertiary deformation associated with the Laramide, Basin and Range, and/or Balcones could have exhumed the

layers as the Lampasas Cut Plain was undergoing active uplift. Removal of the overlying sediments occurred as the landscape was eroded by major rivers and their tributaries, depositing sediments to the east into the Gulf of Mexico; eventually exposing the Edwards to surficial processes. Conversely, if these features are interpreted as phreatic, the joint sets could have been formed as a result of later (Balcones) regional deformation with meteoric waters traveling along less permeable bedding planes working in concert with vadose piping to breach the surface. Once breached, the sink became a focal point for fluids, washing soil and debris into the cave and overprinting the phreatic features (Figure II.11).

Most of these caves exist in areas that support military functions such as training exercises and transportation; therefore they have been heavily overprinted by anthropogenic modifications to the surface. Military exercises have been ongoing for the last 70 years, cave surveys and mapping have been conducted in this area for over 50 years, but many of the caves were used by ranchers and early inhabitants long before. Today, the cave floors are filled with soil and insoluble material, with horizontal passages that taper to blind passages, drains, and conduits filled with debris. Varying degrees of epigenic overprinting have occurred, including significant speleothem development in some caves (Figure II.11); making true hypogene features difficult to discern. Since these caves are located within the Fort Hood boundary, extensive excavation enabling further exploration is not permitted at this time.

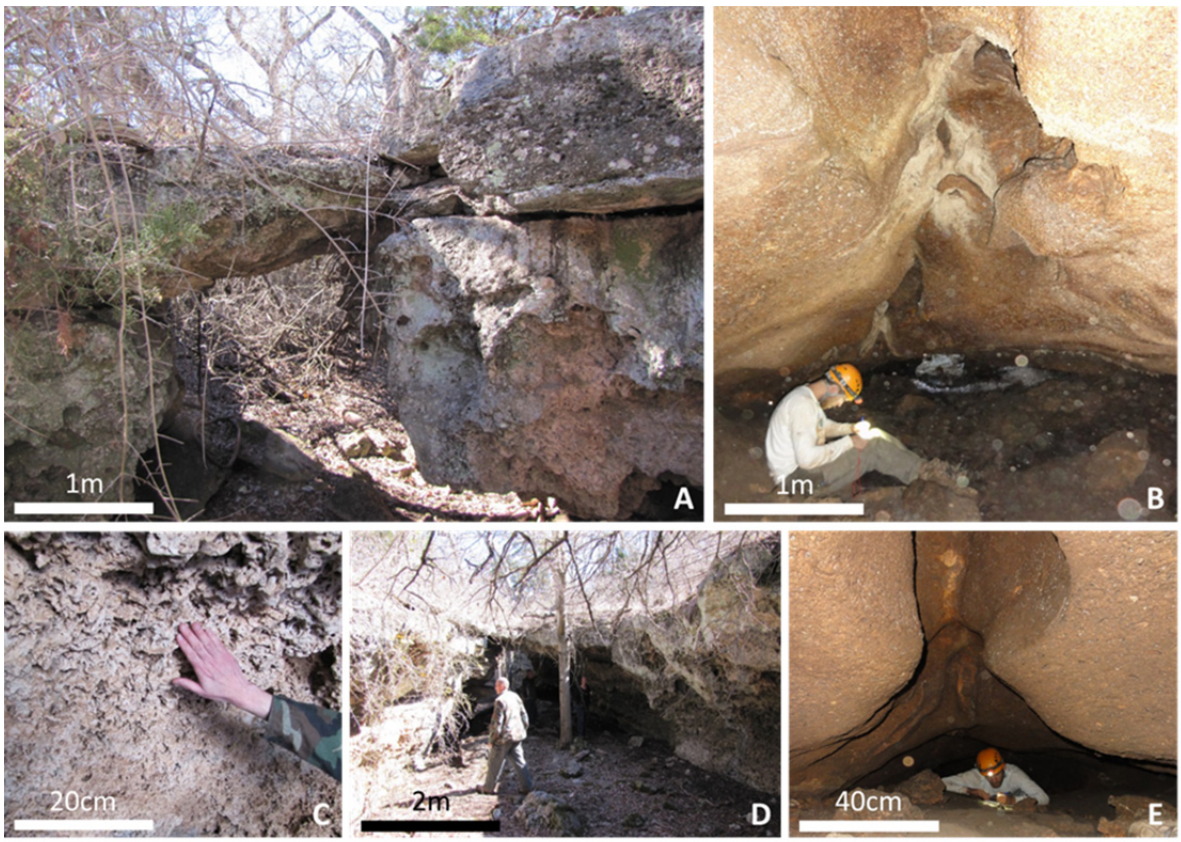

Figure II.11. The main entrance to Brokeback Cave (A) via one of the major sinks associated with the cave structure. Speleothem development (C) and spongework along the interior walls of Brokeback Cave indicate fluid transport. The natural bridge (D) spans the width of the main passage inside Brokeback Cave. Although Viper Den Cave has been heavily overprinted by surficial processes, notched ceilings (B) and cupolas (E) are indicators that ascending fluids may have been part of the speleogenetic history of this cave.

Relict Hypogene Karst Features

Many of the possible hypogene caves previously described formed as a result of solutional widening along conjugate joint sets. The extent of maze development in cave morphologies can be correlated to fracture density as these fracture planes were focal points for ascending fluids into a semi-confined environment. As the Lampasas Cut Plain evolved, surface denudation and river incision removed overlying rocks and sediments, exposing the resistant Edwards to surface processes. Once the overlying sediments were removed, the vertical to sub-vertical fracture planes along the edges of the scarp weakened and slope retreat occurred as a result of detachment and rock falls, creating block talus and exposing previously hidden karst features that formed within these voids (Figure II.12). Although many of these karst features were previously interpreted as selective dissolution and weathering after scarp exposure, correlation with cave features and evidence of fluid convection suggests that these features may have formed within the fractures zones as hypogene dissolution commenced (Klimchouk, 2009). Today tall scarps of the Edwards border remnant plateaus within the Lampasas Cut Plain and contain relict features from these karstified zones, particularly in areas near the Comanche Peak and Edwards boundaries (Figure II.13). The Comanche Peak is less resistant than the overlying Edwards, and in many cases will form a concave wall undercutting the Edwards (Figure II.13). In some cases, these undercut slopes will display dissolution morphologies such as niches and domed structures (Figure II.13). In

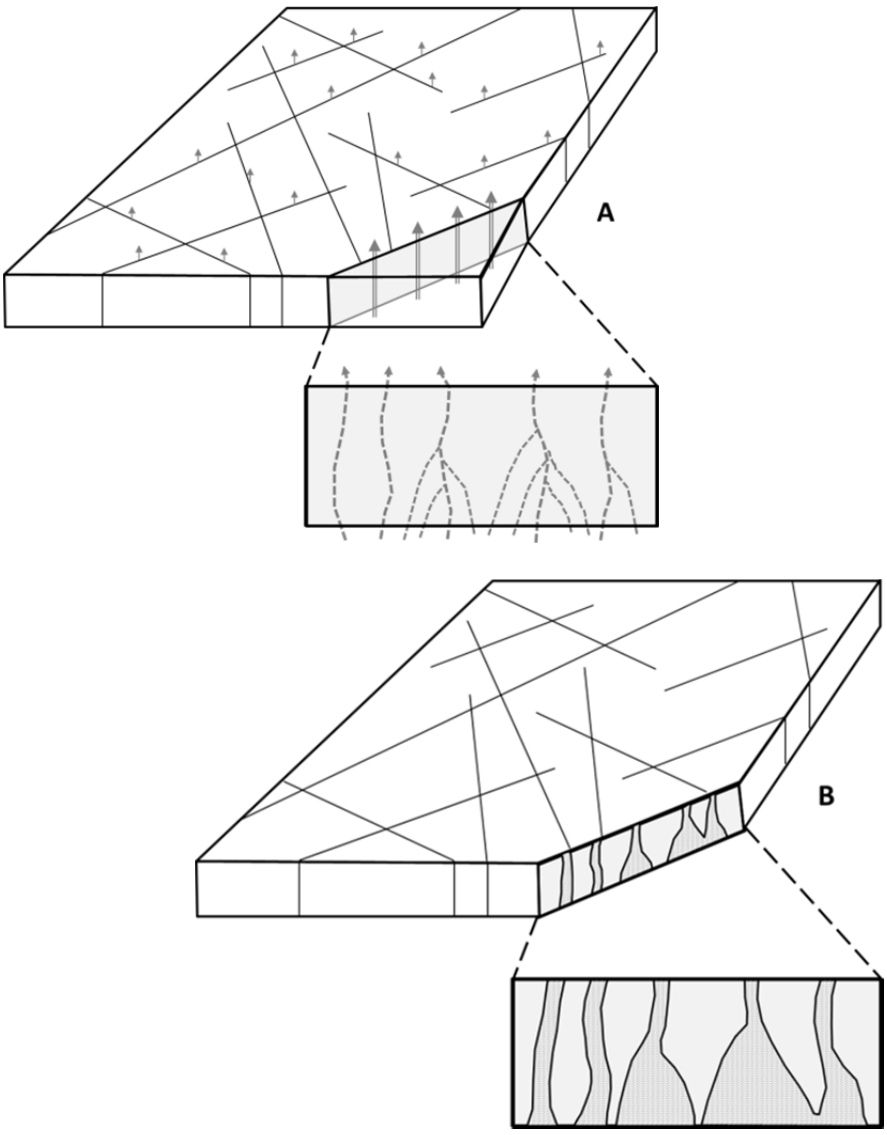

Figure II.12. A conceptual model of hypogenic fluid transport through conjugate joint sets in a confined aquifer (A) and the exposure of hypogenically derived karst features in an escarpment face as a result of block-fall (B). After Klimchouk and Ford, 2009.

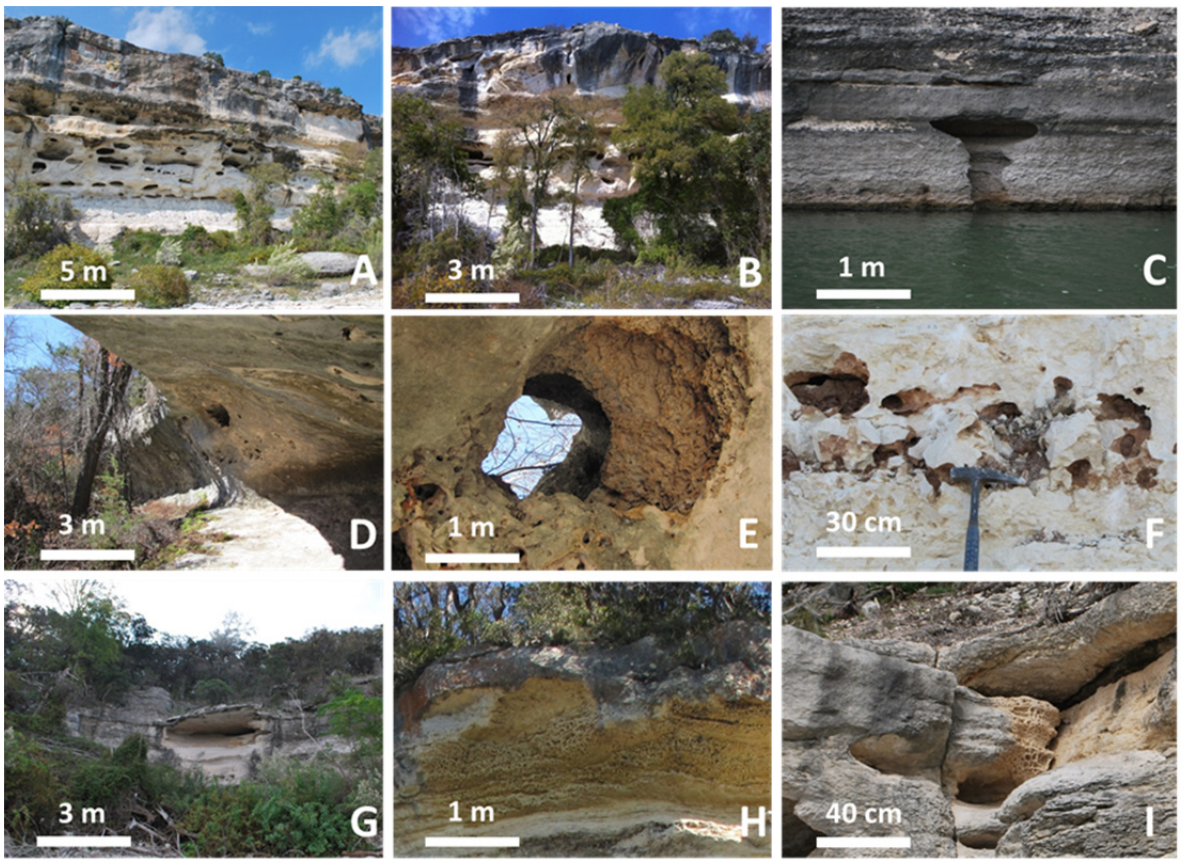

Figure II.13.The steep scarps along the shore of Lake Belton display relict karst features. These scarps are capped by the Edwards Limestone with the Comanche Peak exposed below. Many hollows and vugs (A) form along transmissive zones at the boundaries between the units. Variations in lithofacies can cause over-steepening to occur in areas where the resistant Edwards cap the plateaus (B). Risers within the Comanche Peak (C) are indicators of ascending fluids. Differential weathering of the Comanche Peak has created this overhang (D) with a large open cupola in the ceiling (E). Interstratal transmissive zones (F) occur across permeability boundaries. Grottos and niches (G) may be the remnants of former hypogenic caves; many contain ceiling features indicative of fluid convection. As preferential weathering takes place along conjugate joint sets, exposure can occur as a result of block weathering and slope retreat. Tafoni or spongework structures (H and I) are stratigraphically constrained to the boundary between the Comanche Peak and Edwards; the fragile nature of these structures generally indicates slow moving fluids in a hypogenic environment.

the southern part of the Lampasas Cut Plain, the Comanche Peak and Edwards interfinger; therefore some scarps display several zones of relict karst features. These features include hollows, vugs, niches, grottos, and tafoni; all of which are stratigraphically constrained to the Comanche Peak and Edwards boundaries.

Hollows and Vugs

Hollows and vugs are thought to form by the interaction between rising conduit flow and lateral matrix flow (Klimchouk et al., 2012). Most hollows and vugs do not extend over 2 m into the rock face, but instead form a zone or halo around the conduits along transmissive zones and permeable lenses. These features are commonly associated with vertical fractures, bordering them along certain lithologic intervals, and within the Lampasas Cut Plain, are mostly associated with the interbedded boundaries between the Comanche Peak and Edwards where differences in permeability forced ascending fluid laterally along the contacts. In some cases, transverse, sub-vertical conduits have formed between the units and forced fluid flow between units, connecting ascending fluids with vadose waters (Figure II.12). Many of these features are exposed today along the scarps associated with the Edwards and Comanche Peak, often with several zones of hollows and vugs exposed along these cliff faces with interbedded exposures of these units (Figure II.13).

Grottos and Niches

Grottos and niches, large open hollows in scarp faces, are commonly interpreted as forms of preferential surface weathering at certain places or along the boundary of particular stratigraphic units. In some settings, grottos and niches may be relict hypogene caves exposed in the cliff; particularly when vertical joints are observed perpendicular to the cliff face (Klimchouk et al., 2012). In some cases, grottos and niches may form as a result of the enlargement of exposed hollows or vugs

Within the Lampasas Cut Plain, many grottos and niches are exposed along the steep scarps associated with the Edwards, particularly along the shores of Lake Belton (Figure II.13). Many of these grottos and niches display elements of hypogenic formation and morphology such as ceiling notches and domed structures. Most of the exposed grottos and niches narrow significantly away from the cliff face, making further exploration impossible at this time. These grottos and niches, now exposed, have been heavily overprinted by epigenic processes and will eventually be subject to block removal along joint trends. Many of these scarps have been heavily modified by natural and anthropogenic processes and are subject to further destruction by gravitational forces.

Tafoni

Tafoni is a generally vague term often applied to a wide variety of features formed in different lithologies. It represents characteristic dissolution morphology of

densely packed honeycomb-like cells, typically between 1-5 cm in diameter and depth, separated by sharp or rounded ribs (Klimchouk et al., 2012). In the Lampasas Cut Plain, tafoni is found along the Edwards and Comanche Peak contact, exposed on the high scarps along the eastern shoreline boundary of Lake Belton (Figure II.13). Tafoni structures are poorly understood; the fragile nature of these structures indicates they probably formed in an interior, stable, low-energy environment. Once exposed, these structures are subject to destruction.

Summary and Conclusions

The Lampasas Cut Plain is a karst landscape with Lower Cretaceous carbonates found in outcrop and the sub-surface. The poorly understood, complex interaction of the Edwards and Trinity aquifers within the Lampasas Cut Plain has created a dynamic flow regime whereby ascending fluids could be partially responsible for the suite of features found in the known caves and exposed scarps. Where the Edwards and Comanche Peak limestones are interbedded, varying permeabilities have partially confined hypogene and/or phreatic waters; these confining units have created potentiometric pressures and allowed preferential dissolution along ascending flow paths. Grottos and niches exposed in scarp faces along the trend of major conjugate joint sets could be remnant cave features exposed by block slope retreat. Tafoni and spongework structures could indicate porosity development within sluggish flow regimes in these hypogenic systems.

Analyzed individually, most any single feature could be explained by either epigenic or hypogenic processes. However, when a suite of features are considered, the evidence for possible hypogenic origins of some of the karst features of the Lampasas Cut Plain becomes more compelling. Detailed studies of the Nolan Creek and Owl Mountain Provinces within the Fort Hood Military Installation may provide additional information about flow regimes and the possible connectivity between the Trinity and Edwards aquifers as an indicator of former hypogene flow regimes. Today, many of these caves and karst features have been heavily overprinted by epigenic processes and impacted by anthropogenic surface modifications, therefore the interpretation and discussion of true hypogene features can be problematic. Most of the known karst features are within the boundaries of the Fort Hood Military Installation where access is controlled or on private land. As the population and water requirements within the Lampasas Cut Plain continue to expand, the anthropogenic pressures put on these aquifer systems will likely accelerate the evolution of karst systems. Detailed studies of the poorly understood relationship between the Trinity and Edwards aquifers may help shed light on the complex flow paths of fluid migration within the Lampasas Cut Plain as well as the speleogenetic evolution of the region.

CHAPTER III:
THE HYDROMORPHIC EVOLUTION OF THE OWL MOUNTAIN AND NOLAN CREEK PROVINCES, FORT HOOD MILITARY INSTALLATION, TEXAS

Abstract

The Owl Mountain and Nolan Creek provinces are dissected karst plateaus in the eastern section of the Fort Hood Military Installation. The installation contains surficial exposures of carbonate strata from the Lower Cretaceous Trinity and Fredericksburg groups and is underlain by the Edwards and Trinity aquifers. The Owl Mountain and Nolan Creek provinces are characterized by rugged terrain with steep slopes and incised canyons, and are delineated to the north and south by the installation boundary, the Live Fire Impact Range to the west, and Belton Lake to the east. These provinces are utilized by the United States Army for troop maneuvers and training; some parts have been extensively modified by training exercises and road building, more remote areas are set aside as grazing land, endangered species habitat, and recreational areas for military families.

As part of the U.S. Army's quest to catalog and manage the natural resources in these training areas, the Fort Hood Natural Resources Management Branch requested baseline physicochemical and geochemical data regarding subaerial springs in the Owl Mountain and Nolan Creek provinces as well as subaqueous contributions from the

training areas into Belton Lake. Seven subaerial springs were monitored monthly over a two-year period for physicochemical parameters and ionic concentrations. In order to delineate subaqueous springs discharging into Belton Lake, a multi-parameter sonde was deployed to collect physicochemical data along the shoreline. Spatial analysis was used to interpret the data gathered along the collection route and to delineate potential locations where such springs might exist. These data were used to propose a hydrogeologic model for groundwater migration through varying permeabilities of the inter-fingering Comanche Peak and Edwards carbonates.

Introduction

The Fort Hood Military Installation is located within the Lampasas Cut Plain and currently encompasses approximately 880 km^2 in Bell and Coryell counties (Hammer 2011; Figure III.1). The installation was established in 1942, with most of the land appropriated from rural land owners under authority of eminent domain after the United States entered World War II (Pugsley 2001). The government required that landowners leave fences, well walls and casings, water tanks, and dwellings on each tract of land they acquired so that water sources could be utilized to support troops training in the field and houses could be used for artillery targets. As partial compensation for relocation, the U.S. Army agreed to allow land to continue to be grazed for a nominal fee, an agreement that still continues today (Freeman et al. 2001). Throughout the installation cultural remnants

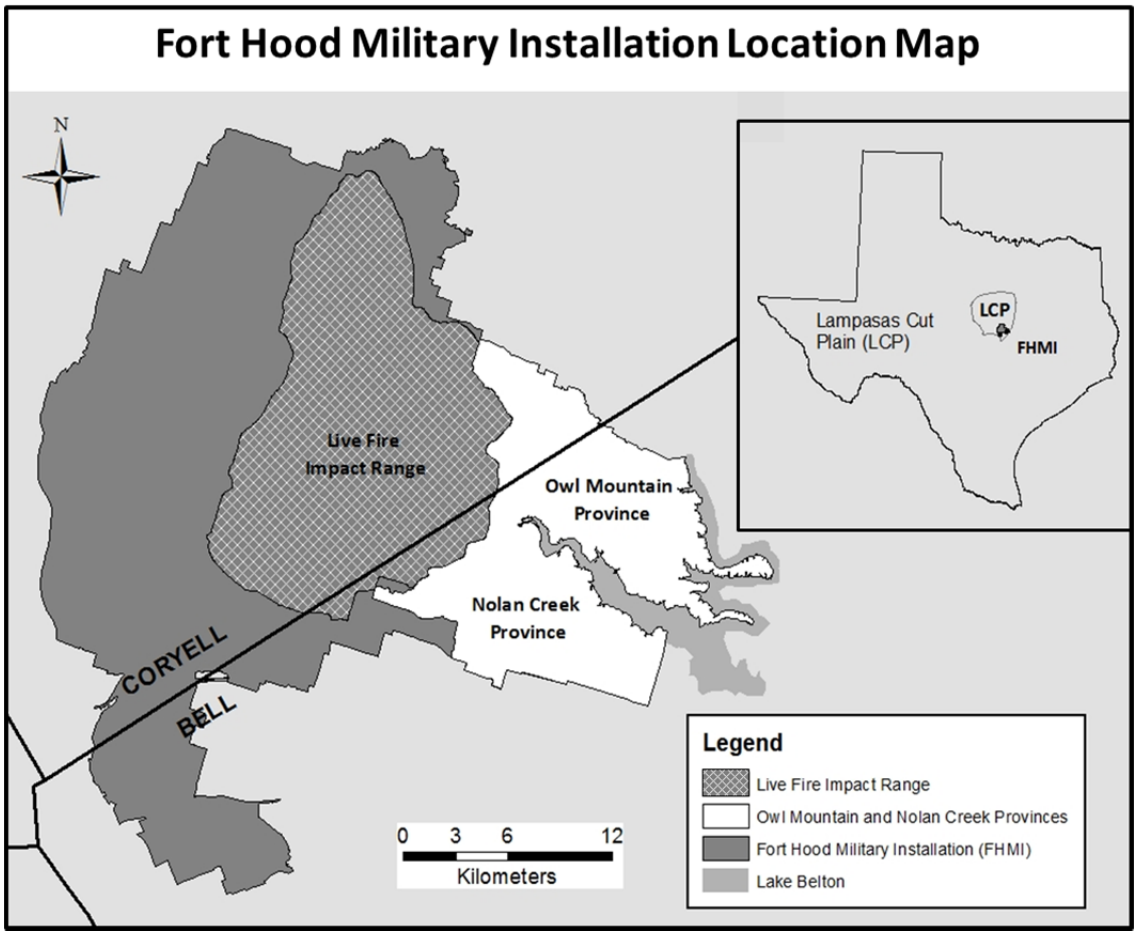

Figure III.1. Location map of the Owl Mountain and Nolan Creek provinces within the Fort Hood Military Installation. The installation is located in the Lampasas Cut Plain physiographic province in Central Texas.

of the previous tenants remain, including anthropogenic modifications associated with springs and wells.

In 1949, as a partial response to the burgeoning population in Central Texas, the U.S. Army Corps of Engineers began construction of Belton Lake reservoir, impounding a portion of the Leon River in Bell and Coryell counties. Construction of the lake and dam began in January 1949 and was completed in 1954, flooding local farmland and creating a reservoir for municipal water supply, flood control, water conservation, fish and wildlife habitat, and recreation. The reservoir impounds 4,980 hectares of water at conservation pool elevation of 186 m above sea level and provides municipal water resources for the cities of Belton, Temple, and the surrounding communities (U.S. Army Corps of Engineers 2007).

Today, the Fort Hood Military Installation is the largest active duty armored post in the U.S. Armed Services. It is home to two full divisions, 1st Cavalry Division and 4th Infantry Division, supports 12 additional units, and is home to approximately 41,000 soldiers and their families (Fort Hood: The Great Place 2013). The administrative section of the installation is located in the south-central portion of the installation and is surrounded by training areas used by the U.S. Army for dismounted and wheeled exercises, and some small-scale tracked vehicle training (Hammer 2011). Many of these training areas are multi-use facilities; some parts have been extensively modified by training exercises and road building, but more remote areas are set aside as grazing land, endangered species habitat, and recreational areas for military families.

Since October of 2011, the Fort Hood Natural Resources Management Branch has been responsible for implementing programs to catalogue and monitor natural resources on the installation and has contracted with civilians, state agencies, and environmental consulting firms to help realize their goals (Pekins 2012; Reddell et al. 2011). The purpose of this study was threefold: to provide baseline physicochemical and geochemical data to the Fort Hood Natural Resources Management Branch regarding karst springs in the training areas, locate potential subaqueous springs along the shoreline of Belton Lake, and to propose a hydrogeologic model for the transmission of water in the subsurface in the Owl Mountain and Nolan Creek provinces (Pekins 2012). This baseline data will help the U.S. Army understand the correlation between surface precipitation events and discharge; understand potential subsurface flow routes; help determine management plans for game and non-game mammals, karst ecosystems, and endangered species; and employ best management practices with regards to water resources and vegetation.

Study Area

The study area is located eastern section of the installation, in training areas known as the Owl Mountain and Nolan Creek provinces (Figure III.1). These provinces are dissected karst plateaus characterized by rugged terrain with steep slopes and incised canyons, and are delineated to the north and south by the installation boundary, the Live Fire Impact Range to the west, and Belton Lake to the east. The climate is sub-humid, with prevailing

winds from the south. Historical mean annual precipitation is approximately 75 cm/yr, but has varied greatly during the sampling period as Central Texas experienced a moderate to severe drought (United States Drought Monitor 2015; Figure III.2). Summer temperature highs and lows do not vary significantly and average about 35°C and 22°C, respectively. The average minimum January temperatures range from approximately 4°C to 0°C (Bradley and Malstaff 2004).

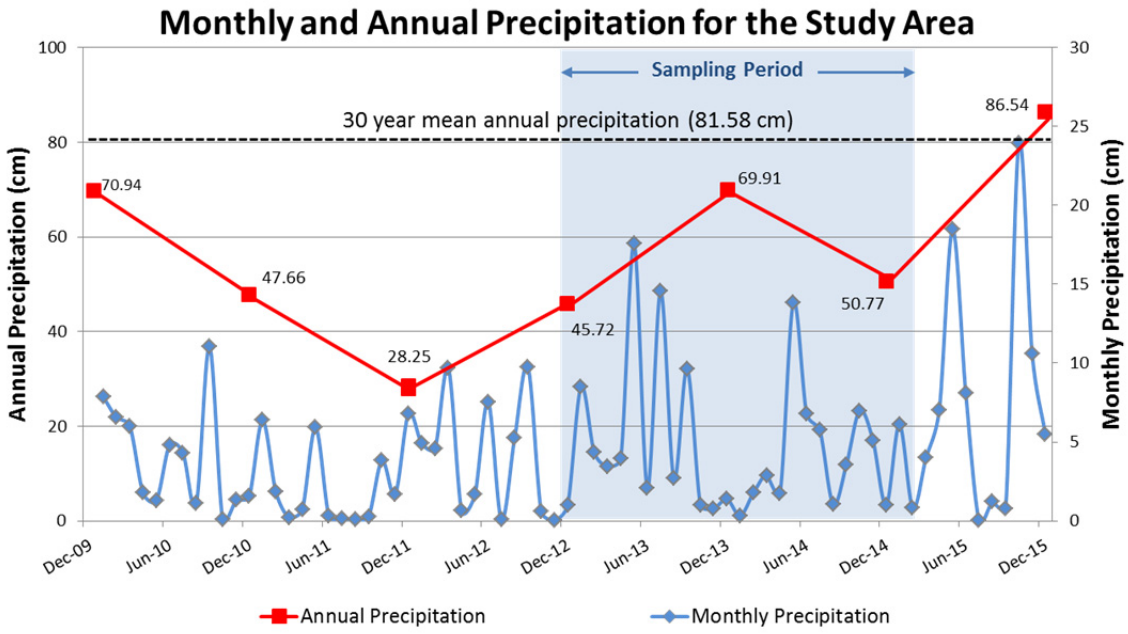

Figure III.2. Historical monthly and annual precipitation for the study area. Precipitation data sourced from Weather Underground for the cities of Belton, Gatesville, Temple, and Killeen, and Fort Hood airfield. Precipitation from these five weather stations was averaged to determine the mean precipitation for the study area. Data accessed on 12/30/2015.

The topography is dominated by plateaued drainage divides capped by resistant limestones and bordered by steep scarps exposing the interfingering relationship of the Lower Cretaceous limestones and marls (Faulkner and Bryant 2015). Surface drainage of the Owl Mountain inland is performed by numerous unnamed ephemeral creeks and streams; larger streams such as Owl and Bear Creeks, Taylor Branch, and Bull Branch flow directly into Belton Lake when sufficient surface water is available. Cowhouse Creek separates Owl Mountain from Nolan Creek Province. Inland drainage of the Nolan Creek Province is performed by North Nolan Creek, Oak Creek, and several smaller unnamed stream segments (Figure III.3). As is common in this type of topography and climate, many of the stream segments will flow intermittently as water transmits between the surface and subsurface.

The western shoreline of Belton Lake varies from accessible beaches to 20-25 m scarps, exposing sequences of the Lower Cretaceous carbonates (Figure III.4). Observable features along the shoreline and scarps of Belton Lake indicate previous conduit and fracture porosity development; however, no evidence exists of surface springs along the shoreline today and few if any of the smaller tributaries were observed contributing surface flow to Belton Lake (Figure III.4).

Geologic Setting

The Owl Mountain and Nolan Creek provinces are dominated by thick sequences of Lower Cretaceous Comanchean Series carbonates, known traditionally and informally as

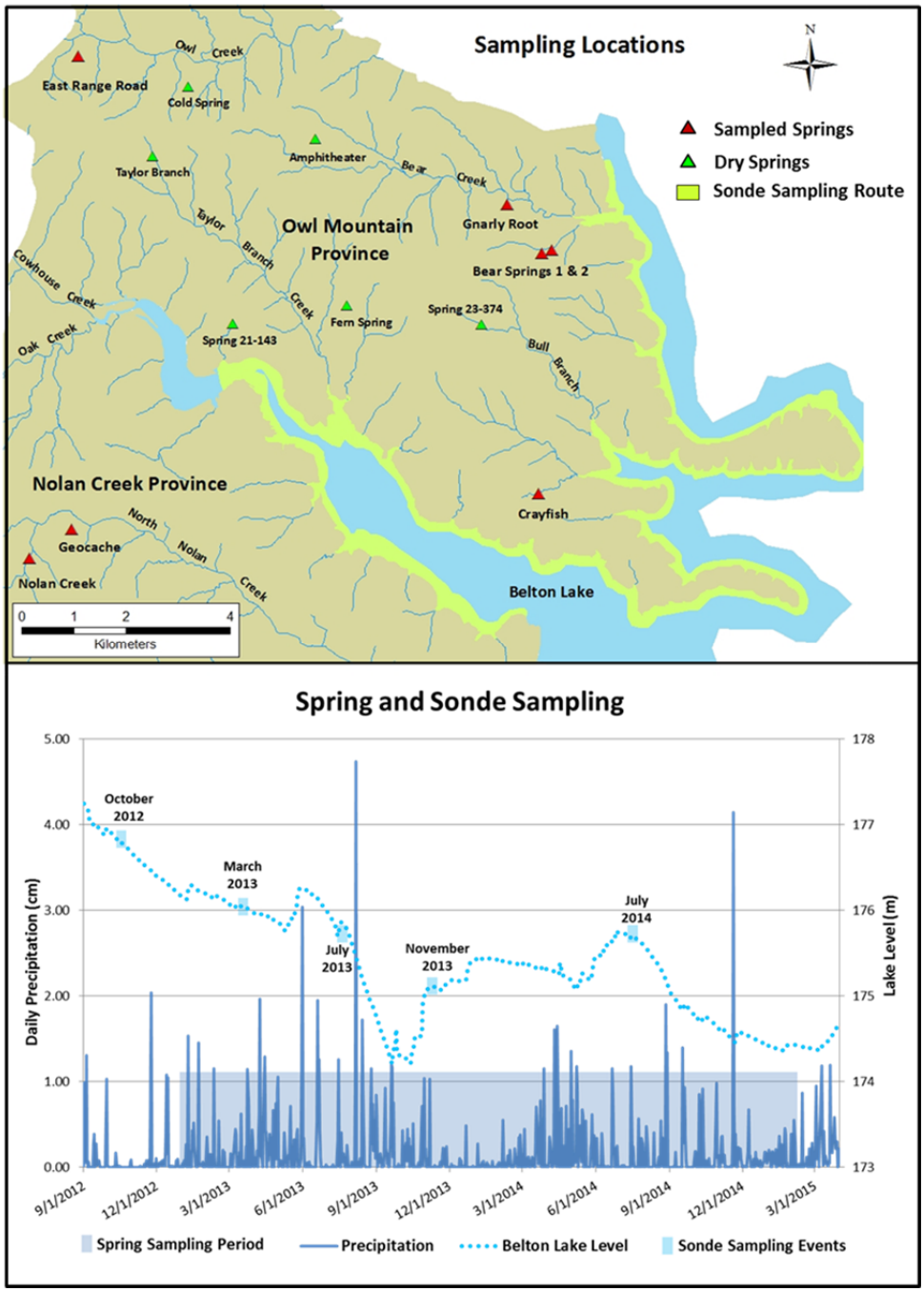

Figure III.3. Above: spring and sonde sampling locations in the Owl Mountain and Nolan Creek provinces. Below: spring and sonde sampling events with respect to daily precipitation and lake levels.

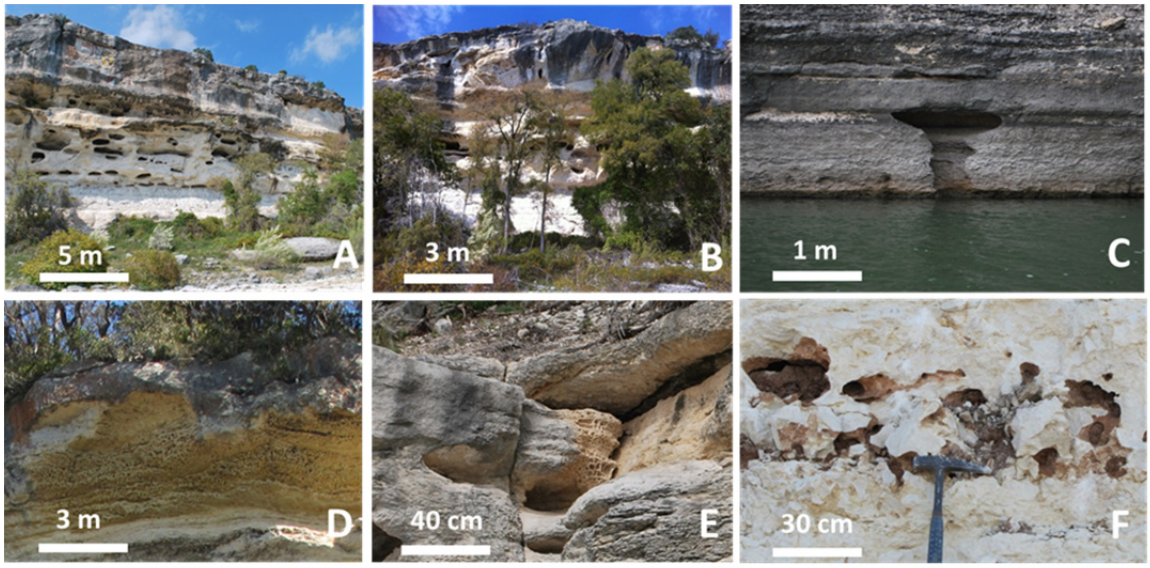

Figure III.4. Relict karst features exposed in the steep scarps along the shore of Belton Lake. These scarps are capped by the Edwards Limestone with the Comanche Peak exposed below. Many of the hollows and vugs (A) form along transmissive zones at the boundaries between the units. Variations in lithofacies can cause over-steepening to occur in areas where the resistant Edwards cap the plateaus (B). Risers within the Comanche Peak (C) are indicators of ascending fluids. Tafoni or spongework structures (D and E) are stratigraphically constrained to the boundary between the Comanche Peak and Edwards; the fragile nature of these structures generally indicates slow moving fluids in a semi-confined environment. Interstratal transmissive zones (F) occur across permeability boundaries.

the “Edwards” (Rose 1972; Adkins and Arick 1930). These lithologies include strata from the Trinity (Glen Rose) and Fredericksburg Groups (Walnut, Comanche Peak, and Edwards) and are composed of limestone, dolostone, chert, and marl (Barnes 1970; Figure III.5). These strata were deposited as part of the major sedimentary sequences during the Zuni and Tejas transgressions, and probably formed as isolated mounds or shoals on the Comanche Platform behind the Stuart City Shelf Margin. The Comanche Platform was bounded on the east and south by a relatively deep-water oceanic basin, the ancestral Gulf of Mexico, and on the north and west by the North Texas-Tyler basin, an extensive marine basin which represents the deeper, backreef marine shelf facies (Nelson 1973; Fisher and Rodda 1969; Figure III.6).

Within the study area, the Walnut, Comanche Peak, and Edwards carbonates crop out at the surface. The lower valleys along creeks and rivers are covered by deeper soils and vegetative cover with few prominent exposures of the Walnut; most are highly weathered and covered by thin veneers of soil. The Comanche Peak outcrops are exposed along the base of the plateaus, inter-fingering with exposures of the Edwards (Bryant 2012; Shaw 2012; Figure III.5). Across the top of the plateaus, the Edwards forms the caprock and varies from rudistid-rich grainstone, oolitic and peloidal packstone, vuggy and porous wackestone, to mudstone outcrops. The strata within these provinces, formed across the western flank of the Belton High, follow the model presented for Moffatt Mound (Faulkner and Bryant 2015; Bryant 2012; Amsbury, Bay

and Lozo 1984; Brown 1975). The Moffatt Mound area and the Owl Mountain and Nolan Creek

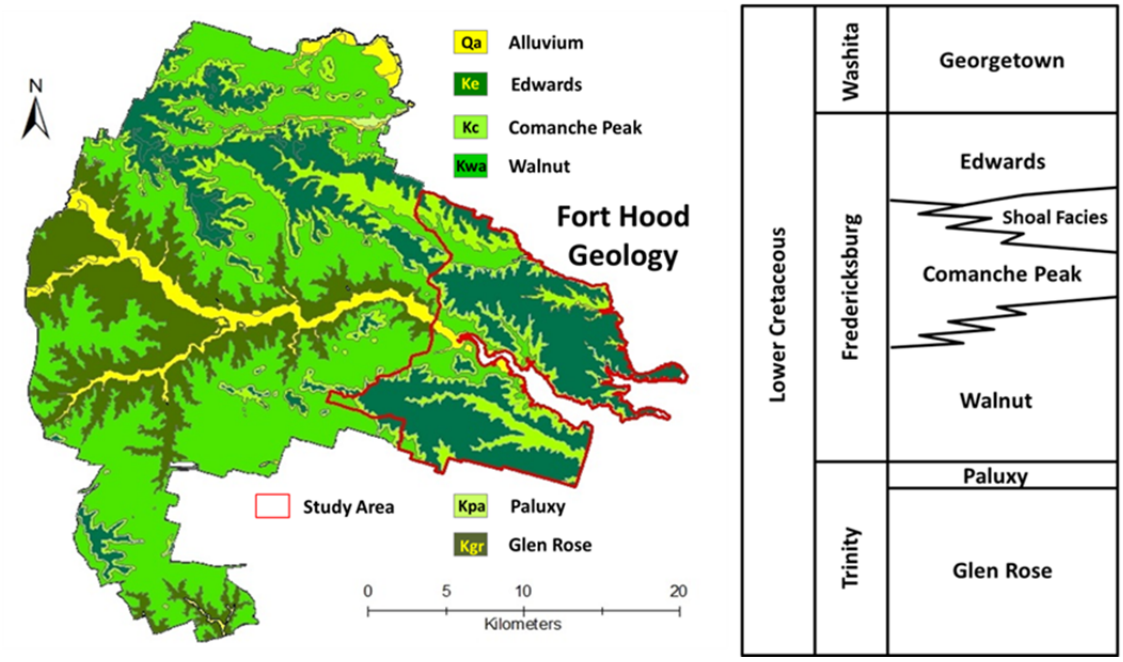

Figure III.5. Geology and stratigraphic column of the Lower Cretaceous Trinity and Fredericksburg Groups for the Owl Mountain and Nolan Creek Provinces (stratigraphic column modified from Amsbury et al. 1984).

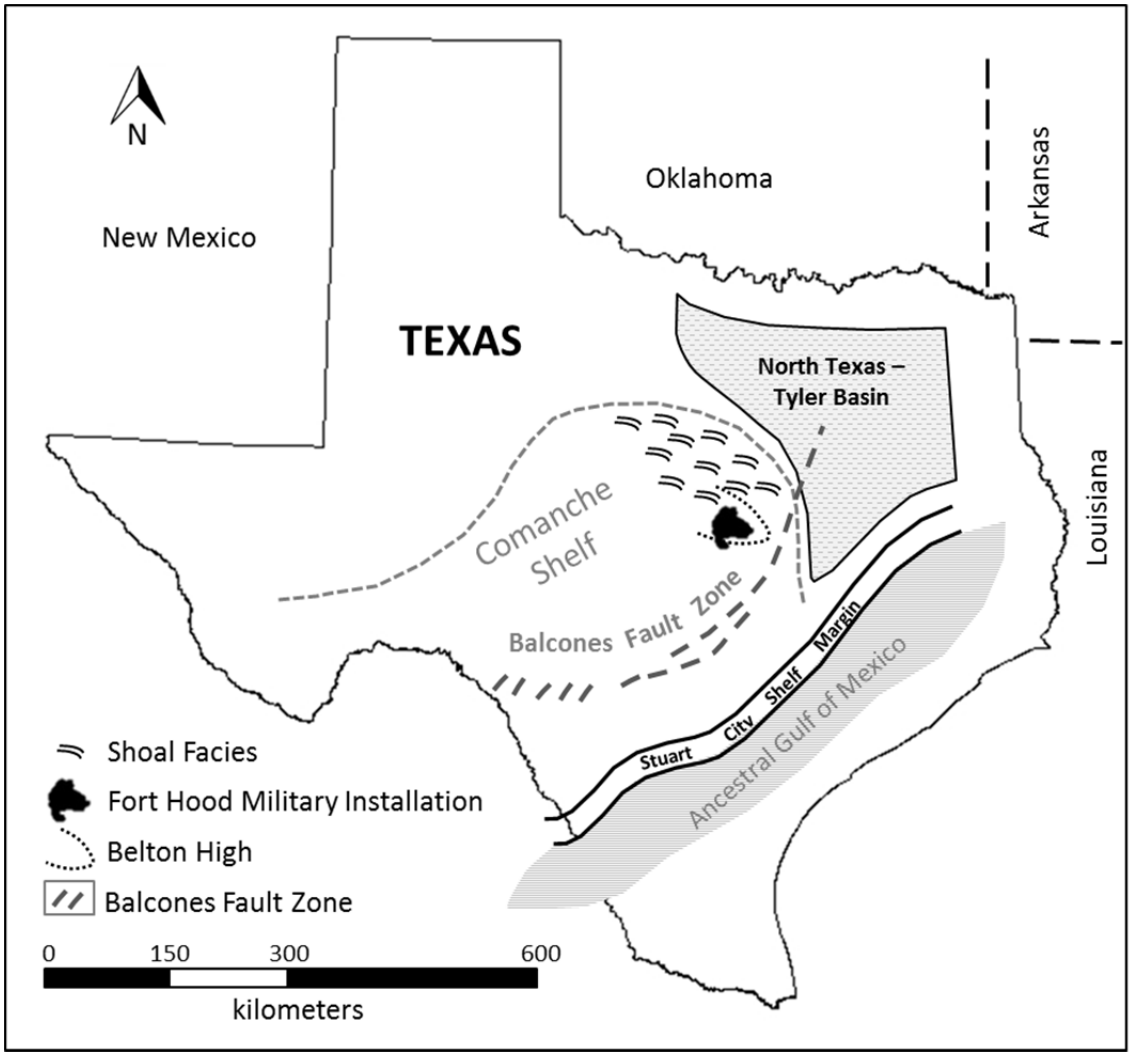

Figure III.6. Shoal facies such as the Owl Mountain and Nolan Creek provinces were formed on the topographic high between the North Texas-Tyler Basin across the axis of the Belton High (modified from Anaya and Jones 2009; Walker 1979; Fisher & Rodda 1969)

provinces consist of thicker, more well-defined outcrops of Edwards Group strata that are lithologically distinct from the main Edwards reef trend. These strata formed in more restricted circulation waters with variations in water depth as the main control for differences in lithology of outcrops (Bryant 2012; Shaw 2012). In the late Cretaceous and into the early Paleogene, this area was influenced by the Laramide Orogeny; the regional uplift of the Edwards Group resulted in the exposure and partial erosion of Edwards sediments, which increased secondary porosity and tilted the strata to the southeast (Woodruff and Abbott 1979; Hayward et al. 1990).

As a result of the uplift and aerial exposure in the Paleocene, the rivers flowing across the Central Texas region began to erode the softer rocks and sediments of the Upper Cretaceous and early Paleogene, sending massive sediment influxes to the east toward the widening Gulf of Mexico (Rose 1972). The harder, more resistant Edwards Limestone formed a broad, flat plateau that was dissected by the erosive force of the major river systems (Woodruff and Abbott 1979). In the late Miocene, the buried Lower Cretaceous Texas coastline provided sufficient crustal weakness for the uplifting of the Central Texas region along the trend of the former Ouachita deformation zone, creating the Balcones Fault Zone and defining the Edwards Plateau (Ferrill and Morris 2008; Figure III.6). Faulting and subsequent uplift along the Balcones initiated rapid downcutting of existing drainage systems; as stream segments incised exposed rock, the intersection of fracture conduits with stream base level helped widen cavities and develop spring discharge outlets. In the Quaternary, substantial climatic changes helped redefine

the topography in the Central Texas region. Wind-blown loess deposits became the soil parent materials across the prairies and increasing available moisture from melting glaciers helped build the watersheds of the Trinity and the Brazos rivers (Woodruff and Abbott 1979).

Hydrogeology

The Fort Hood Military Installation is underlain by the Trinity and Edwards aquifers, with both receiving surficial recharge from meteoric water (Anaya and Jones 2009; Jones 2003; Figure III.7). Aerial exposure of the Glen Rose occurs across the western portion of the installation, where the Trinity Aquifer receives direct recharge from precipitation. The eastern section of the installation, namely the Owl Mountain and Nolan Creek provinces, contains exposures of the Fredericksburg Group that make up the Edwards Aquifer, primarily the Walnut Clay, Comanche Peak and Edwards limestones and marls (Figure III.5). Both aquifers are instrumental in providing base flow for perennial and intermittent streams, as well as springs and seeps in the study area.

The recharge zone of the provinces is not hydrologically connected to the northern segment of the Edwards Aquifer to the southeast, and stands alone as a positive topographic feature directly coupled to the atmosphere (Senger et al. 1990; Cannata and Yelderman 1987). Precipitation is either directed into short stream segments and drainage basins or directly into the subsurface through fractures, sinkholes and smaller conduits (George Veni and Associates 2005). Geochemical analyses of springs within the Fort

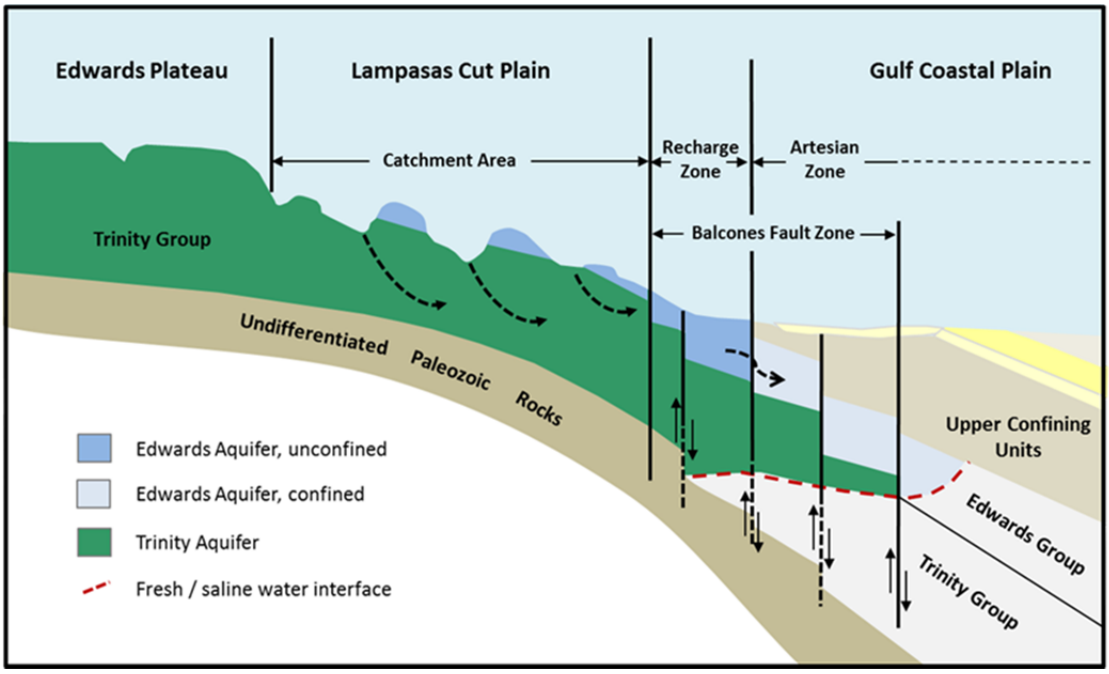

Figure III.7. Hydrogeology of the Edwards and Trinity aquifers within the Fort Hood Military Installation (modified from Blome and others, 2015).

Hood Military Installation and the inter-fingering nature of the Comanche Peak and Edwards limestone occurring within these high energy shoals indicate a vadose fluid system where meteoric water enters the subsurface through karst features and travels vertically and/or subvertically until it reaches a low permeability boundary. The water then travels laterally to form one of the numerous springs and seeps on the outer edges of the uplands. There may be some instances where deeper seated phreatic or semi-confined hypogenic waters migrate upwards to maintain base flow, but the chemical signature of

spring discharge documented during the study period favors an epigenic origin. Varying permeabilities along the scarps control fluid transport, with springs at higher elevations losing flow to those at lower elevations as the water table dropped during the drought (Figure III.8).

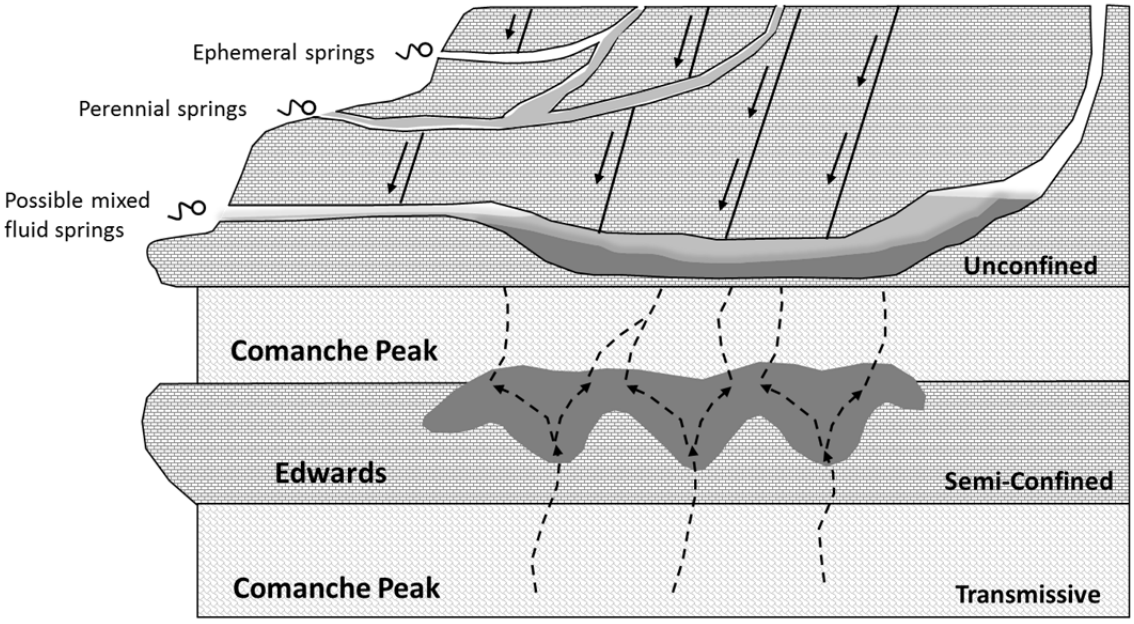

Figure III.8. Proposed hydrogeologic model for the study area (modified from Bryant, 2012).

Methodology

In order to provide an understanding of fluid migration paths and the geochemistry of the natural waters in the subsurface, a suite of thirteen springs were selected from the karst database provided by the Fort Hood Natural Resources Management Branch (Pekins 2012; Reddell et al. 2011). Site visits to these springs were conducted in November and December of 2012 to determine their suitability for continued monitoring (Figure III.3). Six of the springs were dry, with no discernable flow and excluded from the monthly sampling route. The seven remaining springs were monitored monthly from December 2012 to February 2015 (Table III.1; Figure III.9). In the field, physicochemical parameters were measured using an Oakton PCD 650 multi-meter probe to determine conductivity, pH, temperature, and dissolved oxygen (DO %). Flow velocity was measured with a Hach Flow Meter, FH 950. Spring orifices were measured and calculated with flow velocity to determine discharge. In addition to field parameters, spring samples were collected in 500 ml Nalgene bottles and processed by the SFA Soil, Plant, & Water Analysis Lab. Anions were determined using a Dionex 1000 Ion Chromatograph and by titration (total carbonate). Total and dissolved metals were determined using a Thermo Scientific iCAP 7400 ICP Analyzer.

In order to evaluate potential subaqueous contributions to Belton Lake, a multi-parameter YSI 6920 sonde was used to collect five sets of physicochemical data along the shoreline in order to delineate subaqueous spring discharge (Figure III.3).

Table III.1. Mean and standard deviation (SD) values for the physicochemical parameters measured during the study period.

Spring Name	Lithology	Elevation (m)	Mean Values (n=25 samples per spring)				
			Temp (°C)	pH	Cond (µs)	Dissolved Oxygen (%)	Discharge (cm^3 sec^{-1})
Bear Springs 1	Edwards	213	19.4 (0.2)	7.0 (0.5)	648.1 (159.3)	72.6 (9.1)	2713.0 (1551.1)
Bear Springs 2	Edwards	213	19.3 (0.1)	7.0 (0.5)	683.3 (126.6)	67.3 (10.3)	618.8 (428.7)
Crayfish	Edwards	219	19.0 (0.8)	6.9 (0.5)	724.4 (165.2)	77.7 (11.6)	532.8 (468.1)
East Range Road	Terrace Alluvium / Edwards	252	19.9 (1.6)	6.9 (0.4)	624.6 (135.0)	71.8 (12.2)	48.4 (32.1)
Geocache	Edwards	255	19.2 (0.8)	6.9 (0.5)	798.3 (214.7)	72.8 (10.1)	161.9 (138.0)
Gnarly Root	Terrace Alluvium / Walnut Clay	201	18.9 (1.5)	7.1 (0.5)	622.8 (194.9)	74.4 (8.3)	9264.6 (6283.5)
Nolan Creek	Edwards	264	18.99 (1.2)	6.8 (0.5)	671.9 (174.5)	70.9 (9.9)	513.5 (253.2)

Figure III.9. Bear Springs 1 (A) and Bear Springs 2 (B) flow from their source into the collection pool (C). Crayfish (D) has flowed from the bypass feature since March 2013. East Range Road (E and F) emerge from alluvial materials adjacent to the Live Fire Impact Range. Gnarly Root (G) experienced a rise in base level and developed a bypass feature upstream from the original spring orifice. Geocache (H) emerges below Geocache Cave and has an abandoned well near the spring (I). Nolan Creek (J) emerges from Nolan Creek Cave and flows into North Nolan Creek (K).

Physicochemical characteristics such as temperature, dissolved oxygen, pH, turbidity, and conductivity were continually measured with the sonde; during data collection the sampling equipment was coupled with a GPS unit for spatial reference. The pH measurements were recorded with the sonde at a resolution of 0.01 units with an accuracy of ± 0.02 units. Conductivity measurements were recorded at a resolution of 0.001 mS/cm with an accuracy of ± 0.5% of reading. Temperatures were recorded at a resolution of 0.01° C with an accuracy of 0.15° C. Turbidity measurements were recorded at a resolution of 0.1 NTU with an accuracy of ± 2% of the reading. The saturation percent of dissolved oxygen was measured at a resolution of 0.1% air saturation and an accuracy of ± 2% of the reading (YSI, 2009). Data gathered with the sonde were spatially analyzed along the collection route by means of the inverse distance weighted interpolation algorithm.

Spring Sampling Results

Overall results for spring water chemistry show the samples to be fairly uniform during the sampling period and reflective of the lithologies through which they flow (Jones 2006). Five of the seven springs were determined to be flowing from the Edwards or along permeability boundaries between the Edwards and Comanche Peak; East Range Road spring flows through alluvium in close proximity to Edwards outcrops and Gnarly Root originates from terraced alluvium overlying the Walnut Clay (Table III.1). With regard to physicochemical measurements, temperatures for all springs averaged between

18.9°C and 19.9°C, near the average annual temperature for the region (Table III.1). The greatest fluctuation in temperatures occurred at Gnarly Root (4.6°C), Nolan Creek (3.7°C), and East Range Road (3.7°C) in late spring and summer; probably as a result of higher ambient temperatures, thermal heating at the spring orifice, and in the case of Gnarly Root and East Range Road, the transmission of water through shallow alluvial material allowing fluid to be more readily influenced by surface temperatures. Temperatures for all other springs varied less than one degree, suggesting that residence time is sufficiently long for water temperature to equilibrate with rock temperature. Conductivity measurements were relatively consistent throughout the study period for five of the springs (~650 µs/cm); the exceptions were Crayfish and Geocache, both which exhibited an average conductivity of 760 µs/cm (Table III.1).

Gnarly Root and Bear Springs 1 experienced the greatest fluctuation in their discharge rates over the study period. Gnarly Root discharge rates correlated most closely with precipitation events in the study area, possibly as a result of meteoric water recharging a shallow water table in terraced alluvium. The other springs reported varying lag times of three to six months between precipitation events and a spike in discharge, with no discernable patterns emerging from the data. Although each spring was flowing continually during the study period, a noticeable drop in base flow was observed at Geocache, Crayfish, and Bear Springs 1 and 2 (Figure III.9). These springs developed lower bypass features as the water table dropped as a result of prolonged drought. Conversely, Gnarly Root experienced a rise in base flow, developing and maintaining an

upper bypass feature in January 2014 through February 2015 (Figure III.9), although this phenomenon could not be correlated to any specific precipitation event. In the past, Bear Springs 2, Crayfish, and Gnarly Root had spring origins further upstream, but their source has migrated to its present day location in response to a drop in base level.

Calcium and magnesium are enriched in all samples with respect to potassium and sodium; carbonate and bicarbonate are enriched with respect to chloride, fluoride, and sulfate (Figure III.10). Crayfish (4.5:1), Geocache (3:1), and Nolan Creek (3.5:1) springs had higher concentrations of magnesium with respect to calcium (Figure III.10), possibly signifying a longer residence time and/or mixing with deeper seated fluids in contact with dolomitized units in the subsurface. Gnarly Root had lower calcium to magnesium ratio (7:1), but this spring has a larger catchment area and may be receiving fluids from surrounding lithologies as a potentiometric low. Bear Spring 1 (15:1), Bear Springs 2 (13:1) and East Range Road (35:1) had much higher ratios of calcium to magnesium and support the premise that these springs have an epigenic source.

With the exception of sulfur, other metals were not present in significant concentrations in any of the samples (Table III.2). Laboratory results from some of the spring sampling reported concentrations below the detection limit and those were removed from the data set before calculating the mean and standard deviation. Lead concentrations for all samples were less than 20 ppb, with 129 of the 138 reported concentrations less than 15 ppb, the actionable threshold set by the U.S. Environmental Protection Agency (2015) for drinking water. Nine samples with elevated lead

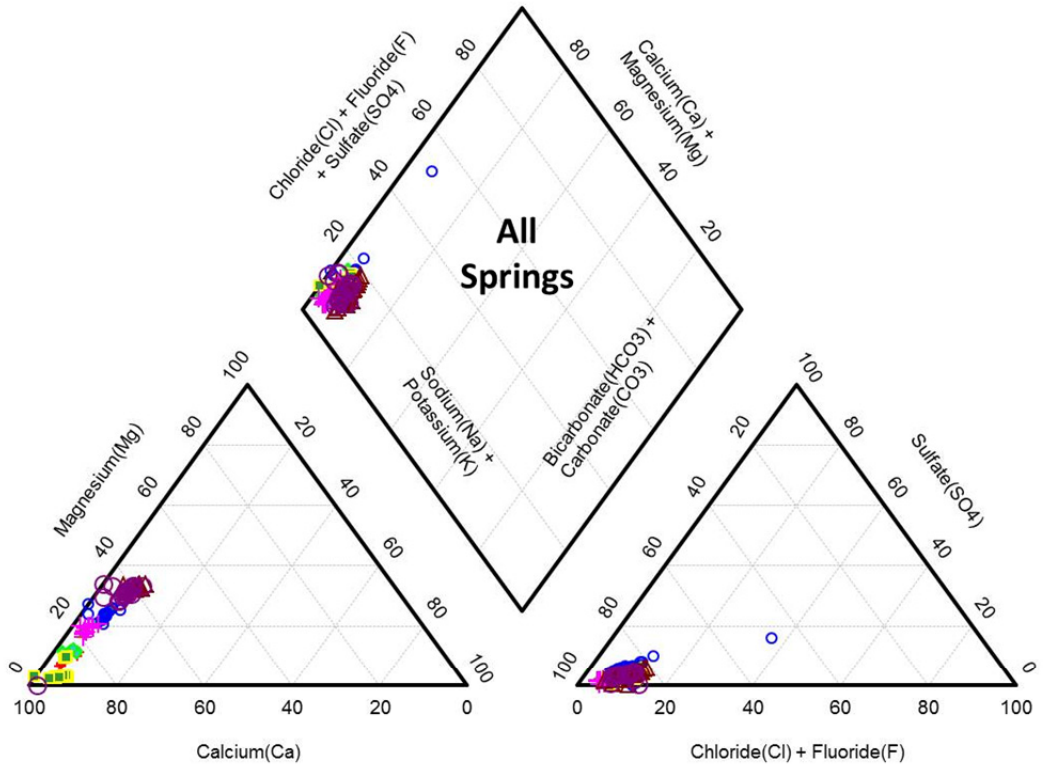

Spring	Cations (ppm)				Anions (ppm)				
	Calcium	Magnesium	Sodium	Potassium	Bicarbonate	Carbonate	Sulfate	Chloride	Fluoride
Bear Springs 1 +	131.8 (15.8)	8.5 (2.6	6.6 (2.3)	0.7 (0.8)	245.4 (42.3)	0 (0.0)	4.8 (1.5)	9.1 (2.1)	0.3 (0.3)
Bear Springs 2 ♦	132.0 (19.5)	10.3 (2.7)	6.2 (3.1)	0.6 (1.0)	248.7 (37.8)	0 (0.0)	5.2 (2.8)	9.3 (2.5)	0.3 (0.2)
Crayfish ○	134.2 (25.7)	30.0 (5.0)	11.8 (4.2)	0.8 (0.7)	258.6 (64.0)	0.9 (3.2)	12.9 (4.7)	14.4 (2.8)	0.5 (0.2)
East Range Road ■	144.3 (42.6)	4.1 (2.7)	9.0 (3.5)	0.6 (0.4)	242.1 (39.9)	0 (0.0)	5.0 (1.7)	12.9 (2.9)	0.2 (0.2)
Geocache △	111.7 (16.7)	37.5 (5.7)	17.1 (3.7)	1.1 (0.6)	298.9 (45.9)	0 (0.0)	8.9 (3.5)	18.3 (3.8)	0.5 (0.2)
Gnarly Root +	119.4 (23.2)	17.6 (3.1)	6.8 (2.4)	0.5 (0.3)	261.9 (39.9)	0.4 (1.8)	4.1 (1.5)	8.9 (2.4)	0.5 (0.3)
Nolan Creek ○	107.3 (23.2)	31.2 (7.8)	11.5 (4.9)	1.3 (0.9)	271.9 (31.9)	0 (0.0)	7.9 (2.6)	14.9 (3.4)	0.2 (0.2)
All Springs	125.8 (26.8)	19.5 (12.6)	9.9 (5.1)	0.8 (0.9)	260.9 (46.8)	0.2 (1.4)	7.0 (4.0)	12.5 (4.4)	0.4 (0.2)

Figure III.10. Above: piper diagrams showing geochemical variations of all springs samples; n=25 for each spring. Below: table reporting the mean and stand deviation (SD) cation and anion concentrations for each spring.

Table III.2. Mean and standard deviation (SD) values of water soluble species for selected cations. Although each spring was sampled 25 times, metal concentrations for some samples were below the detection limit.

Spring Name	Water Soluble Species (ppb)						
	Arsenic	**Copper**	**Iron**	**Manganese**	**Lead**	**Sulfur**	**Zinc**
Bear Springs 1	3.9 (5.2) n=19	5.5 (15.4) n=19	37.7 (31.3) n=4	3.0 (5.7) n=20	4.4 (4.1) n=19	3626.2 (1230.4) n=25	3.4 (2.7) n=19
Bear Springs 2	1.4 (0.9) n=16	2.6 (3.4) n=19	8.4 (10.6) n=8	2.1 (2.3) n=22	4.6 (5.1) n=21	3888.7 (1226.1) n=25	4.2 (2.9) n=20
Crayfish	4.8 (4.0) n=13	6.2 (14.1) n=18	18.6 (28.9) n=6	4.5 (6.8) n=20	4.6 (5.7) n=22	7006.4 (2230.1) n=25	4.6 (5.1) n=21
East Range Road	5.7 (7.8) n=14	13.0 (36.2) n=19	11.1 (8.2) n=2	3.7 (4.7) n=22	4.5 (4.8) n=17	3588.1 (969.5) n=25	6.9 (7.0) n=20
Geocache	5.2 (5.3) n=14	2.9 (3.9) n=17	22.0 (25.2) n=5	3.1 (2.9) n=22	5.4 (5.2) n=20	5080.2 (1417.7) n=25	4.4 (3.2) n=20
Gnarly Root	6.0 (5.6) n=13	3.1 (3.0) n=22	10.8 (16.8) n=3	5.1 (6.9) n=22	5.8 (5.9) n=22	2930.3 (839.7) n=25	4.0 (4.6) n=20
Nolan Creek	4.2 (5.5) n=14	3.6 (8.3) n=17	18.2 (20.3) n=4	0.6 (0.5) n=20	4.0 (6.3) n=17	4487.4 (1183.0) n=25	1.9 (1.7) n=18
All Springs	4.4 (5.3) n=102	5.3 (16.3) n=131	17.7 (21.9) n=32	3.2 (4.9) n=148	4.8 (5.3) n=138	4372.48 (1841.8) n=175	4.3 (4.4) n=138

concentrations presented in springs during two episodes: May–October 2013, and October–November 2014. The first episode of elevated lead concentration in 2013 appeared in May at Gnarly Root and Crayfish; in July at Gnarly Root; and at Nolan Creek in October. The second episode of elevated lead concentration in 2014 appeared in October at East Range Road and Geocache; and at Crayfish and Nolan Creek in November.

All elevated zinc concentrations occurred from January–August, 2013 and only affected the springs in the Owl Mountain province, with seven of the 138 samples reporting zinc concentrations greater than 15 ppb. The U.S. Environmental Protection Agency does not have actionable standards for zinc concentrations, but according to the standard set for surface waters by the Texas Commission on Environmental Quality (2015), a few zinc concentrations may be slightly above the actionable threshold. Elevated zinc concentrations appeared in January and February at East Range Road; in May at East Range Road and Crayfish; in July at Gnarly Root; and in August at East Range Road and Crayfish.

The anomalous concentrations of sulfur throughout the study period are puzzling, and may be the result of laboratory errors or chemical interference rather than verifiable concentrations of sulfur for the sampling period. There appears to be no mineralogical reason for sulfur to be present in such concentrations without a corresponding increase in sulfate concentrations, yet none were reported. Although it would be difficult to state with absolute certainty that the springs all have the same subsurface water source, the

cation and anion content shows they are from very similar sources with varying residence times accounting for the chemical variations present during the study period.

Sonde Sampling Results

Five sonde sampling events were conducted from October 2012 – July 2014 along the shoreline of Belton Lake. During each sampling event, two passes were made along the shoreline; the first followed as close as possible to the shore and the second was approximately 15 m offshore from the previous pass (Figure III.3). Sonde sampling events conducted in October 2012, March 2013, July 2013, November 2013, and July 2014 were used to capture temporal variations and identify potential subaqueous springs (Figure III.3). Due to equipment failure, the March 2013 sonde data collection was excluded in order to provide a more representative geochemical sampling of potential subaqueous springs.

The four remaining data sets were analyzed for each parameter; temperature, pH, conductivity, dissolved oxygen, and turbidity; in order to determine anomalous readings that might indicate potential subaqueous springs. Of the five parameters, dissolved oxygen and conductivity were the most helpful in determining potential locations for subaqueous springs (Faulkner et al. 2015; Figure III.11). Temperature was somewhat helpful, although the seasonal temperature fluctuations were to be expected and temperature anomalies did not correlate well with subaerial springs on the FHMI. Lake

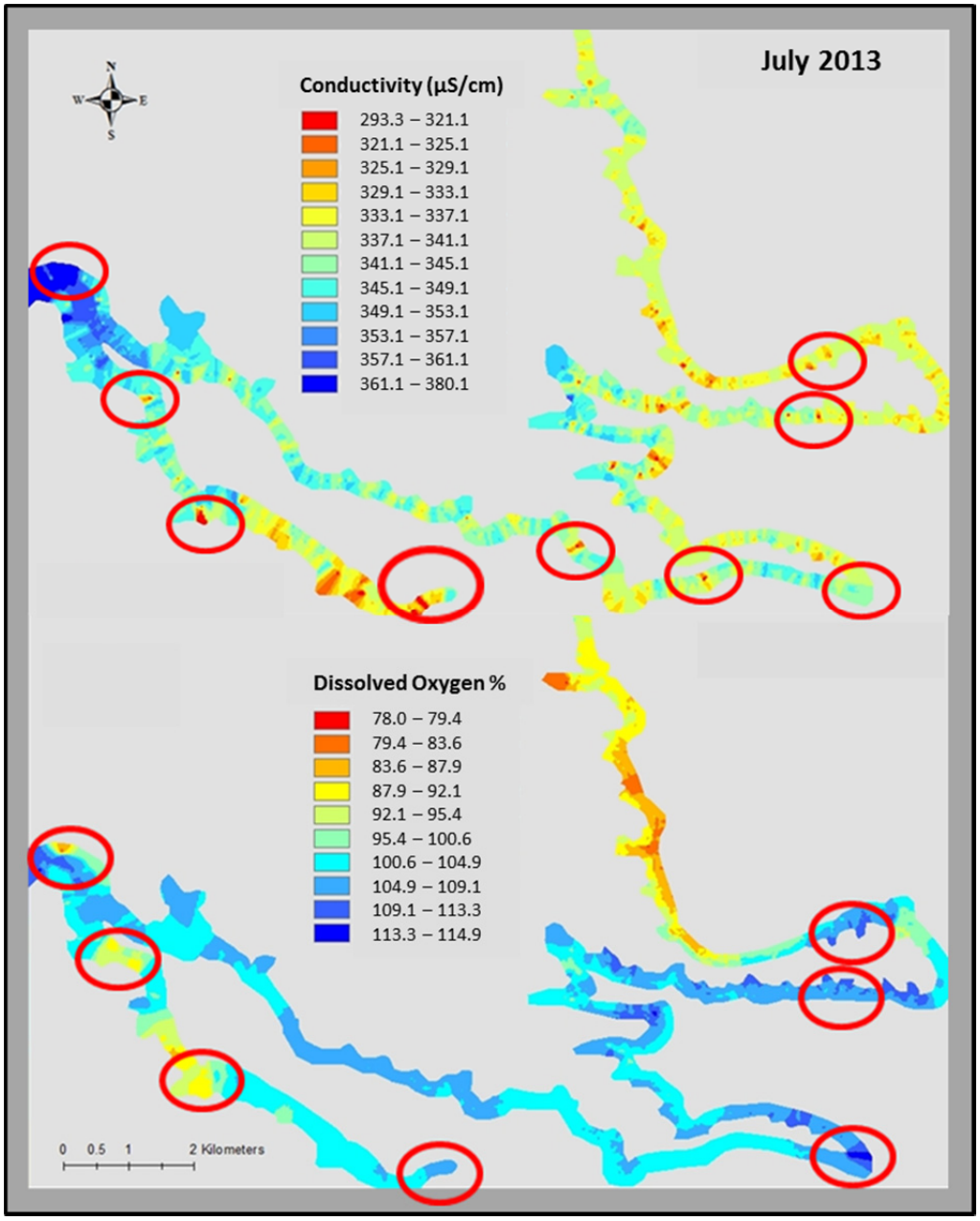

Figure III.11. Comparison of physicochemical parameters for July 2013. Analysis of this sampling identified 7 potential subaqueous spring correlated between conductivity (above) and dissolved oxygen (below).

level fluctuated also (Figure III.3), and many of the anomalies were found within small coves and inlets along the shoreline where there would be variations in water depth and solar radiation. Turbidity and pH were not helpful parameters; pH showed little variations for most sampling events and did not correlate well with pH values for subaerial springs. Turbidity was greatest in shallow coves and inlets where sediments could have easily been disturbed. In the southern portion of the collection route, agitated waters in open lake areas also showed a spike in turbidity but these readings did not correlate well with other parameters. In fluvial environments, temperature and conductivity have been found to be the best indicators of subaqueous discharge, but in this lacustrine environment temperature is more of a function of solar radiation and water depth. Therefore, when determining potential locations of subaqueous springs, temperature, turbidity, and pH anomalies were only considered in conjunction with anomalies associated with dissolved oxygen and conductivity.

After review of all data sets, it was determined that the July 2013 sampling period offered the best results for determining potential subaqueous spring locations (Figure III.11). Using dissolved oxygen and conductivity parameters, seven locations were determined to be potential subaqueous spring locations. Two additional locations were noted on the conductivity map, and these correlate with the turbidity anomalies, but turbidity alone is not very useful, as there were many other anomalies in turbidity.

Hydrogeologic Model

Previous research by Bryant (2012) introduced the initial hydrogeologic model of a semi-confined aquifer resulting from the inter-fingering of the Comanche Peak and Edwards formations. Permeability varies greatly across the study area, reflecting the changes in depositional environments as these high energy shoal facies were accumulating. Relict karst features such as tufa, hollows, vugs, and tafoni in the scarp faces are remnants of previous hydrogeologic conduits that developed as uplift occurred in the Lampasas Cut Plain and stream incision exposed these features as the landscaped adjusted to the falling water table (Faulkner and Bryant 2015; Klimchouk et al. 2012). As stream segments incised exposed rock, the intersection of fracture conduits with stream base level helped widen cavities and develop spring discharge outlets. While many of these features are not currently transmitting water, they are remnants of the previous hydrogeologic system and provide exposed surfaces to help interpret subsurface transmissive zones and conduits (Faulkner et al. 2013; McCann 2012; Figure III.4).

Many of these relict karst features are commonly associated with vertical fractures (Klimchouk and Ford 2009), bordering them along certain lithologic intervals, and within the study area, are mostly associated with the interbedded boundaries between Comanche Peak and Edwards strata where differences in permeability forced ascending fluid laterally along the contacts (Figure III.4). In some cases, transverse, sub-vertical conduits have formed between the units and forced fluid flow between units, connecting ascending fluids with vadose waters (Figure III.8). Many of these features are exposed

today along the scarps associated with the Edwards and Comanche Peak, often with several zones of karst features exposed along these cliff faces with interbedded exposures of these units (Figure III.4).

The proposed hydrogeologic model for the Owl Mountain and Nolan Creek provinces is supported by both geochemical and anecdotal data. The homogeneity of the geochemical signatures determined by spring sampling indicates that most of the water is from a single source, mostly likely meteoric water entering the subsurface during precipitation events. The denudation of the landscape by karst processes and anthropogenic modifications have provided numerous conduits for direct recharge during precipitation. Channel flow in the provinces occurs immediately after precipitation, with most surface water communicated to the subsurface within a short amount of time. This water transmits through karst conduits to the edges of the scarps where it appears as springs. Recently, as the water table has adjusted to drought conditions, springs at lower elevations have maintained their base flow from meteoric inputs (Figure III.8).

Discussion

Within the provinces, archaeological and historical records indicate this area has supported many different cultural groups over the past twelve thousand years. Projectile points, often named for the towns or rivers where they were first found, have been given many Central Texas names as Bell, Nolan, Pedernales, and Travis. These and many other types of prehistoric artifacts are found in the rock shelters and river terrace campsites on

and around Fort Hood. These peoples would have been attracted to the springs and rivers that supported their hunter-gatherer lifestyles and provided ready water sources for herds of grazing animals which they followed. As groups moved in and out of the area, their lifestyles changed too; hunter-gatherers gave way to more settled peoples who moved from site to site within an area, following seasonal food sources. To date, over 2,200 archeological sites containing evidence of prehistoric occupations have been identified on Fort Hood lands (Pugsley 1992).

The first land grant in Texas was awarded to Moses Austin in 1821, and immigration into Central Texas soon followed. The Brazos River and the Camino Real became the main conduits for settlement of the interior part of Texas (Pugsley 1992). The land that would eventually become Fort Hood supported rural, agricultural communities with surface and spring water resources for hamlets from as early as 1850 continuing well into the early 20th century (Freeman et al. 2001); today, many of these former hamlets are used for troop maneuvers and training. Three of the springs, Bear Springs 1 and 2 and Geocache, had anthropogenic modifications at the source or along the flow route, indicating they had been used as a water resource by previous inhabitants (Figure III.9). East Range Road Spring had also experienced anthropogenic modification; the spring is located in proximity to the Live Fire Impact Range and alluvial materials had been altered as a result of road building.

Training encampments near Geocache and Nolan Creek are common in the Nolan Creek province and near Cold Spring and East Range Road in the Owl Mountain

province (Hammer 2011). Although these training exercises are located near ephemeral and flowing springs, current geochemical data does not indicate that use of these areas is having any negative impact on sensitive water resources. East Range Road is located near the boundary of the Live Fire Impact Range, but there was little evidence of contamination or communication from activities in that area to springs in the training areas. Bear Springs 1 and 2, Gnarly Root, and Crayfish are located in more remote sections of the training areas with these areas having been set aside as recreational and grazing acreage, and habitat for endangered avian species (Figure III.3). Elevated lead and zinc concentrations in springs during the sampling period could be the result of contamination from the installation or an offsite area, but the elevated concentrations are just above the actionable threshold and represent less than 6% of all samples. More data would be needed to correlate the geochemical signatures with natural sources of these metals.

Many subaerial springs in the study area, once documented as perennial water sources, have now become ephemeral; partly due to the ongoing drought in Central Texas. Amphitheater (elevation 261 m), one of the springs in the Owl Mountain province, flowed almost continually through 2011. An initial site visit indicated this spring would provide geochemical data, but was dry throughout the sampling period. Fern Spring (elevation 246 m), aptly named for the abundance of fern that occupies the slot canyon associated with the spring, had no discernable flow during the sampling period. Spring 23-374 (elevation 237 m) had a small pool of water underneath a small ledge on the

initial site visit, but never maintained enough discharge for sampling. Spring 21-143 (elevation 255 m) and Taylor Branch (elevation 261 m) were both dry on the initial site visit and did not flow during the sampling period. Cold Spring is actually not a spring at all, but functions as a bypass feature for a small unnamed creek that flows adjacent to Owl Creek. In the past when water was plentiful, this bypass feature would provide discharge directly into Owl Creek from the unnamed creek through the channel wall. The original spring source is further upstream but has been dry for many years. With the exception of East Range Road, all flowing springs sampled in the Owl Mountain province are at a lower elevation than the springs listed above.

During the sonde sampling events, drought conditions may have complicated data analyses due to lake level fluctuations. The October 2012, November 2013, and July 2014 sampling occurred after significant precipitation events; these post-drought precipitation events likely caused mixing in the lake affecting the physicochemical analyses. Although no historical documentation exists of smaller springs that might have been flowing before the construction of Belton Lake, there are physicochemical indications of potential subaqueous springs along the shoreline. Belton Lake is also utilized as a local water resource and increased withdrawals for municipalities may have affected results (Faulkner et al. 2015).

The impoundment of Belton Lake in 1954 has had a significant impact on the hydrogeology of the study area. Prior to the construction of Belton Lake, local base level was probably lower than it is today. Cowhouse Creek would have received significant

input from groundwater sources and functioned as a potentiometric low for migrating fluids. As Belton Lake began to fill and permanently raised the potentiometric surface, the direction of groundwater flow in the study area was altered. Over time, the water table has equilibrated to this new base level but in times of severe drought, or when intense precipitation elevates Belton Lake above the water table, the lake can potentially contribute recharge to the groundwater system. Although the lake is managed by the U.S. Army Corps of Engineers and lake levels are controlled by dam releases, lake level can fluctuate significantly throughout the year, particularly during intense precipitation events near the lake and in the Leon River watershed. During these events, lake level can change more rapidly than the water table can respond, potentially creating high hydraulic heads such that groundwater interactions with Belton Lake could temporarily shift from discharge into the lake to recharge from the lake.

Summary and Conclusions

The physico- and geo-chemical properties of subaerial and potential subaqueous springs coupled with the proposed depositional model of high-energy shoals are the basis for developing a conceptual geochemical model for fluid migration. Permeability varies greatly across the study area; regions where Edwards and Comanche Peak formations interfinger typically have lower permeabilities than regions dominated by only Edwards deposition. Geochemical analyses of subaerial springs within the Fort Hood Military Installation indicate most springs are recharged by meteoric water traveling through karst

conduits in the Edwards Limestone. There exists the possibility of a mixed fluid system where deeper seated phreatic or semi-confined hypogenic waters migrate upwards to maintain base flow in area springs during periodic droughts, and may contribute some flow to Nolan Creek, Geocache, and Crayfish. Increased concentrations of magnesium with respect to calcium in these springs indicate a longer residence time with potential mixing of deeper seated phreatic or hypogene waters during precipitation events (Bryant, 2012, Shaw and Stafford, 2014). As the landscape has evolved and the water table has adjusted to drought conditions, preferential conduits in the subsurface transmit fluids to springs at lower elevations during recharge. Occasional precipitation events may cause some of these now dry springs to flow intermittently, but at present they have lost their connectivity to the fluctuating water table (Figure III.8).

Although lake levels fluctuated during the sampling period, geochemical analysis of the data indicates physicochemical anomalies associated with subaqueous karst springs discharging along the sonde route. These subaqueous springs contribute to lake volume through conduits and fractures in sub-surface lithologies and are further evidence of the complex hydrogeology exhibited in this karst system. Drought conditions during the sampling period could have also influenced aquifer recharge, with Belton Lake providing discharge into the Owl Mountain and Nolan Creek Provinces to augment base flow for subaerial springs. The subsurface hydrogeology of this area is quite complex and reflective of the continuing evolution of this karst landscape.

Acknowledgements

This research was partially funded by the Arthur Temple College of Forestry and Agriculture, the Division of Environmental Science, and the Department of Geology at Stephen F. Austin State University. Access to the Fort Hood Military Installation training areas, maps, and initial scouting for springs was provided by Charles Pekins of the Fort Hood Natural Resources Management Branch. Invaluable field assistance was provided by Joel Faulkner, Aaron Bryant, William Welles, and Asa Vermeulen. Lillian O'Shay assisted with laboratory research and Wayne Weatherford of the SFA Soil, Plant & Water Analysis Laboratory processed the spring samples.

CHAPTER IV:
STRUCTURAL CONTROL OF MESIC VEGETATION COMMUNITIES WITHIN THE OWL CREEK AND BEAR CREEK WATERSHEDS, TEXAS

Abstract

The Fort Hood Military Installation is a karst landscape, dominated by thick sequences of Lower Cretaceous Comanchean Series carbonates of the Trinity and Fredericksburg groups. These strata were deposited as part of the major sedimentary sequences during the Zuni transgression, forming as an isolated mound or shoal on the Comanche Platform behind the Stuart City Shelf Margin. The study area is the eastern peninsula of the military installation known as the Owl Mountain Province, a dissected plateau utilized by the U.S. Army for troop maneuvers and training.

The geomorphic evolution of the Owl Mountain Province has been controlled by the structural development of incised canyons in the Owl Creek and Bear Creek watersheds, following the deformational trend of the Balcones/Ouachita fault system and the transverse Belton High-Moffatt Mound trend. These trends control cave development in the subsurface, joints in outcrop, stream segment orientation, and the transmission of ascending fluids in the study area. While many of the springs in the study area are fed by meteoric waters, these incised canyons also receive fluids from deeper-seated phreatic and/or hypogene fluids which emerge as ephemeral springs and seeps to augment soil

moisture. Traditional vegetation modeling has relied heavily on slope and aspect as a key element of controlling ecological associations and indicators of soil moisture; in karst landscapes permeability and solutional widening of conduits formed by local and regional deformation events exert structural control over the development of mesic vegetation communities.

Introduction

The Owl Creek and Bear Creek watersheds are located within the Owl Mountain Province, the northeastern peninsula of the Fort Hood Military Installation (Figure IV.1). These watersheds drain the uplands in the province and flow into Belton Lake near the confluence of the Leon River. The landscape and its topography are largely controlled by the structural deformation and erosional behavior of the Lower Cretaceous limestones and marls of the Fredericksburg Group, namely the Comanche Peak and Edwards formations (Figure IV.2). The Edwards caps the plateaus while the lower permeability of the Comanche Peak forces ascending fluids to flow laterally and discharge as springs, incising slot canyons into the steep sided scarps. The creeks and their tributaries provide intermittent surface flow responsible for downcutting and incision of the karst plateau, with the Bear Creek watershed creating a solutionally-widened valley that dissects the uplands and the Owl Creek watershed defining the northern extent of the Owl Mountain Province.

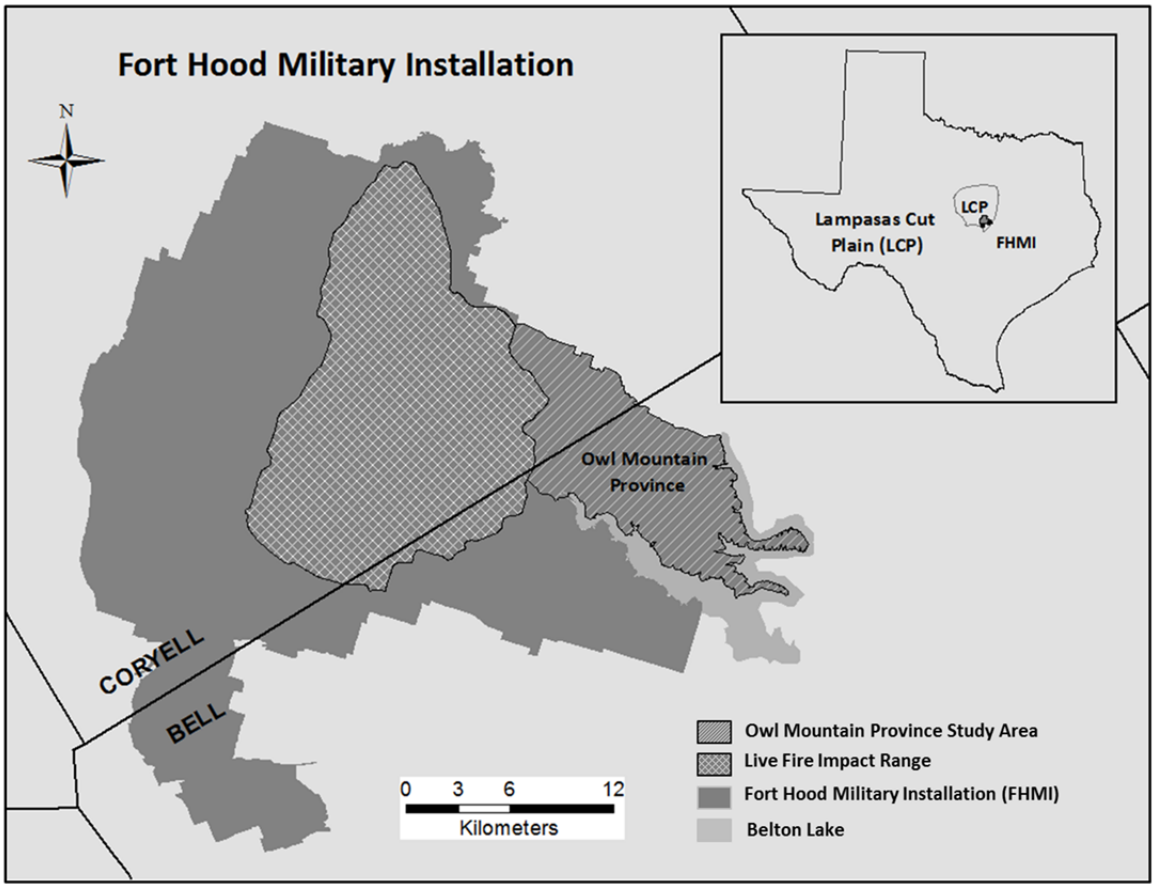

Figure IV.1. The Owl Mountain Province is the northeastern peninsula of the Fort Hood Military Installation. The area is used for troop maneuvers and training, as well as endangered species habitat and grazing acreage.

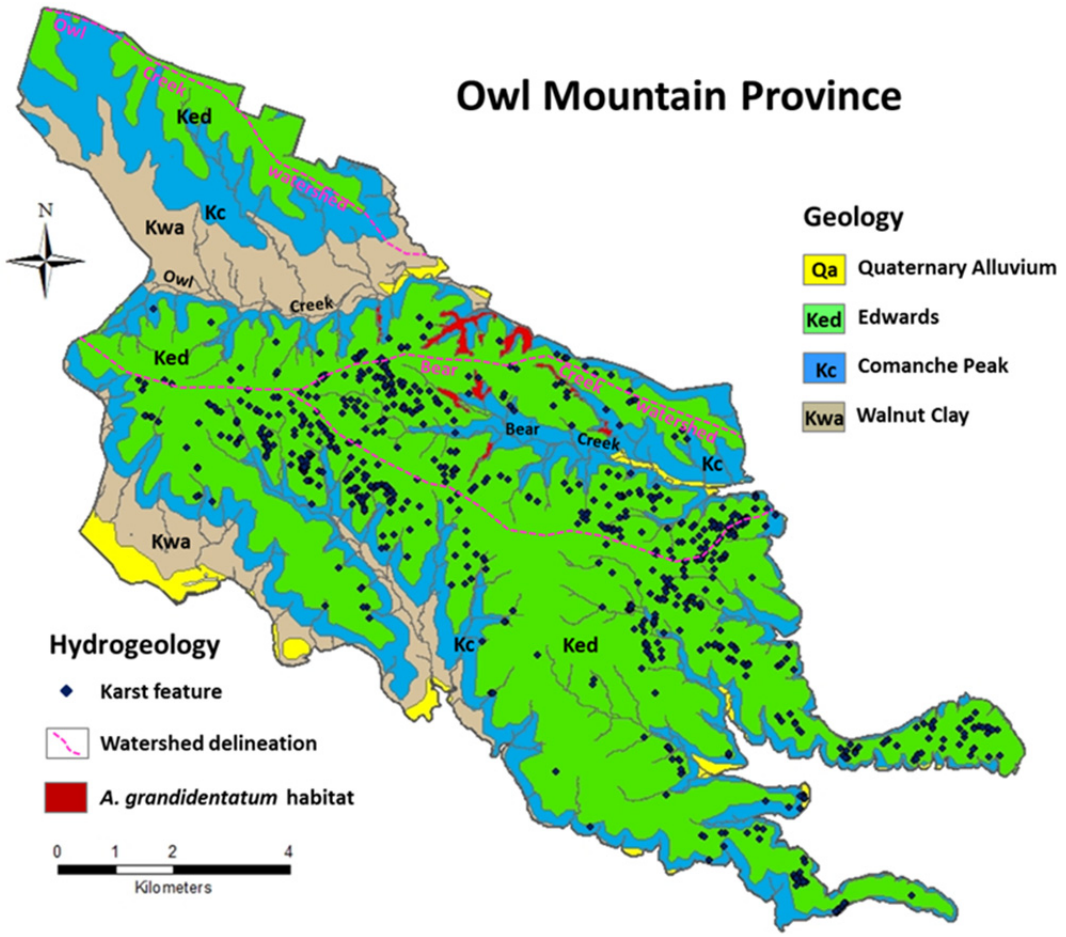

Figure IV.2. Geology and geomorphic features of the Owl Mountain Province. Ongoing geologic mapping and karst inventories provide information about caves, shelters, springs, seeps, and sinkholes (Geology from the Geologic Database of Texas, Texas Natural Resources Information System, accessed January 2016; karst features from Reddell et al. 2011.)

The structural evolution of the Owl Mountain Province has influenced the formation of the slot canyons that host mesic vegetation (Figure IV.2) as they follow the major regional deformational trends from the Ouachita/Balcones lineaments, as well as transverse lineaments from the Belton High- Moffatt Mound trend (Figure IV.3). These lineaments provide conduits for deep-seated fluids to rise along solutionally widened flow paths to augment meteoric waters feeding surface streams and subaerial springs and seeps. Continued erosion along these deformational trends has created mesic slot canyons in varying orientations where forest species that grow best in cool, moist habitats continue to thrive. Today, isolated populations of bigtooth maple, *Acer grandidentatum,* continue to exist as Pleistocene relicts within the Owl Creek and Bear Creek watersheds in Bell and Coryell counties (Figure IV.2).

Traditional vegetation modeling has relied heavily on slope and aspect as a key element of ecological associations and indicators of soil moisture. Within the Owl and Bear Creek watersheds, the geomorphic evolution of the Owl Mountain Province has been controlled by the structural development along the Balcones/Ouachita deformation trend and the transverse Belton High-Moffatt Mound trend (Figure IV.3). These trends control cave development in the subsurface, joints in outcrop, stream segment orientation, and the general transmission of ascending fluids in the study area. While many of the springs in the study area are fed by meteoric waters, these incised canyons also receive fluids from deeper seated phreatic and/or hypogene fluids which emerge as ephemeral springs and seeps to augment soil moisture.

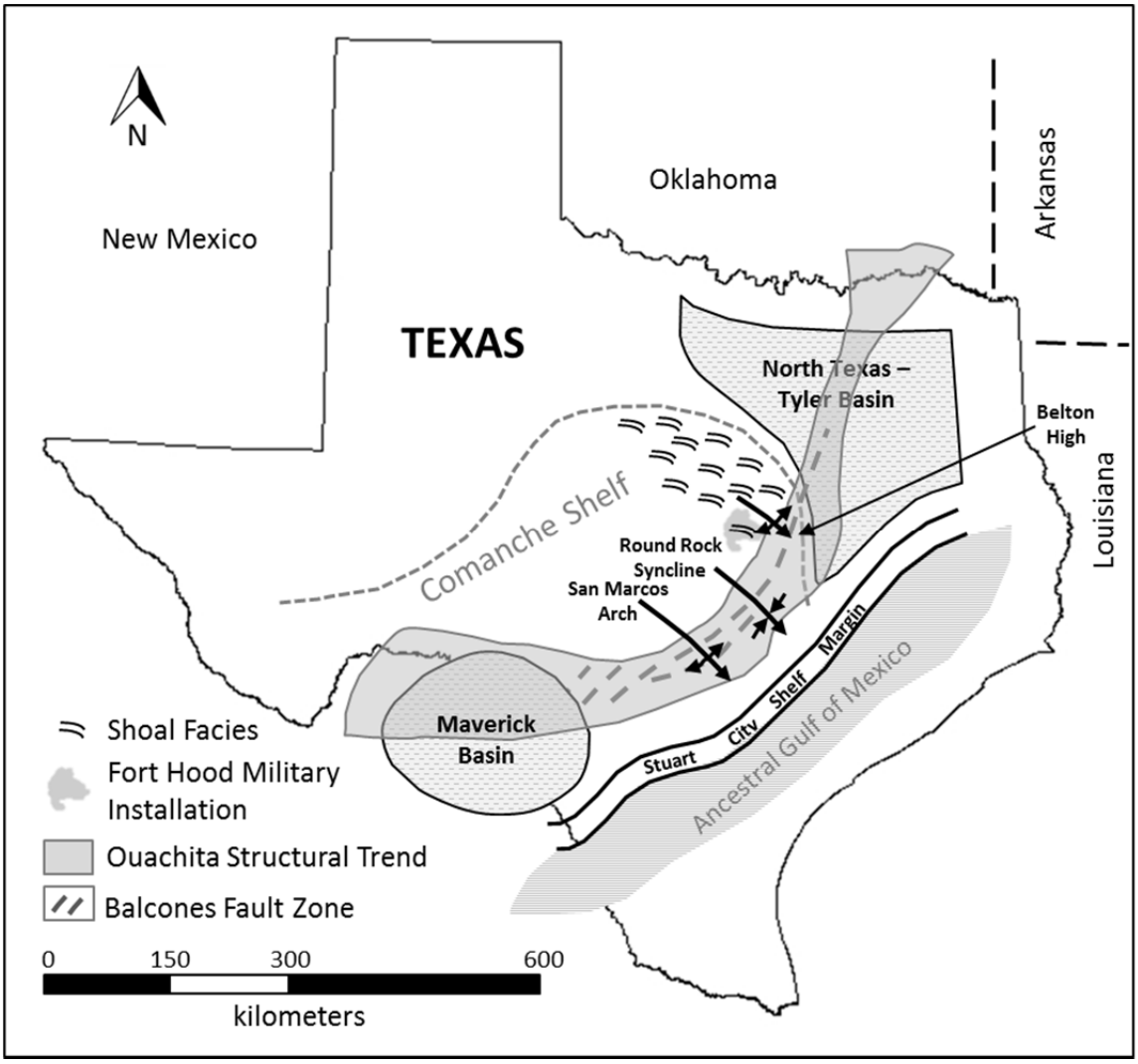

Figure IV.3. Location map showing the major structural trends influencing strata in the Central Texas region. Shoal facies such as the Owl Mountain and Nolan Creek provinces were formed on the topographic high between the North Texas-Tyler Basin across the axis of the Belton High (modified from Anaya and Jones 2009; Walker 1979; Fisher and Rodda 1969).

For the purposes of this paper, a lineament is defined as a surface expression of fracturing represented by alignments of topography and drainage, linear trends in vegetation associations, and the truncation of rock outcrops. Lineaments are often perceived in remotely-sensed images as reliable indicators of geologic structures, with patterns that are linear, continuous, reasonably well expressed, measurable, and related to features of the earth. In karst terrains, lineaments can also be indicative of secondary porosity, with the potential to supply reliable quantities of water from the subsurface in areas where surface water is limited. Lineaments can also be measured in outcrop associated with geologic mapping and in the subsurface by cave mapping.

Study Area

The study area is the eastern peninsula of Fort Hood known as the Owl Mountain Province and is bounded by Owl Creek to the north, Belton Lake to the east, Cowhouse Creek to the south, and the Live Fire Impact Range to the west (Figure IV.1). The province is utilized by the U.S. Army for troop maneuvers and training; some parts have been extensively modified by training exercises and road construction, while more remote areas are set aside as grazing land, endangered species habitat, and recreational areas for military families (Pekins 2012; Hammer 2011; Hayden et al. 2001).

Within the study area, the Walnut, Comanche Peak, and Edwards carbonates crop out at the surface (Barnes 1970; Figure IV.2). The lower valleys along creeks and rivers have deeper soils and more dense vegetation with few prominent exposures of the

Walnut; most are highly weathered and covered by thin veneers of soil (Faulkner and Bryant 2015). The Comanche Peak outcrops are exposed along the base of the plateaus, inter-fingering with exposures of the Edwards (Bryant 2012; Shaw 2012). Across the top of the plateaus, the Edwards forms the caprock and varies from rudistid-rich grainstone, oolitic and peloidal packstone, vuggy and porous wackestone, to mudstone outcrops. These strata, formed across the western flank of the Belton High (Figure IV.3), follow the model presented for Moffatt Mound (Faulkner and Bryant 2015; Bryant 2012; Amsbury et al. 1984; Brown 1975). The Moffatt Mound area and the Owl Mountain Province consist of thicker, more well-defined outcrops of Edwards Group strata that are lithologically distinct from the main Edwards reef trend. These strata formed in more restricted circulation waters with variations in water depth as the main control for differences in lithology of outcrops (Bryant 2012; Shaw 2012).

The vegetation in the study area is characterized as a mix of evergreen savanna, upland deciduous, and lowland riparian plant communities (Riskin and Diamond 1986; Figure IV.4). On the more xeric uplands, vegetation communities contain biotic contributions from the dry plateaus and massifs of northern Mexico and Trans-Pecos Texas (Mecke 1996). In the more open areas where disturbance to the landscape is severe and water potential is limited, *Juniperus ashei* has encroached and dominates the floristic composition (Querejeta et al. 2007; Diamond 1997). Upland soils of the plateau and slopes are shallow (< 30 cm) and have generally developed in place, forming over the limestone bedrock of the Edwards Group (Fowler and Simmons 2008). The habitats of

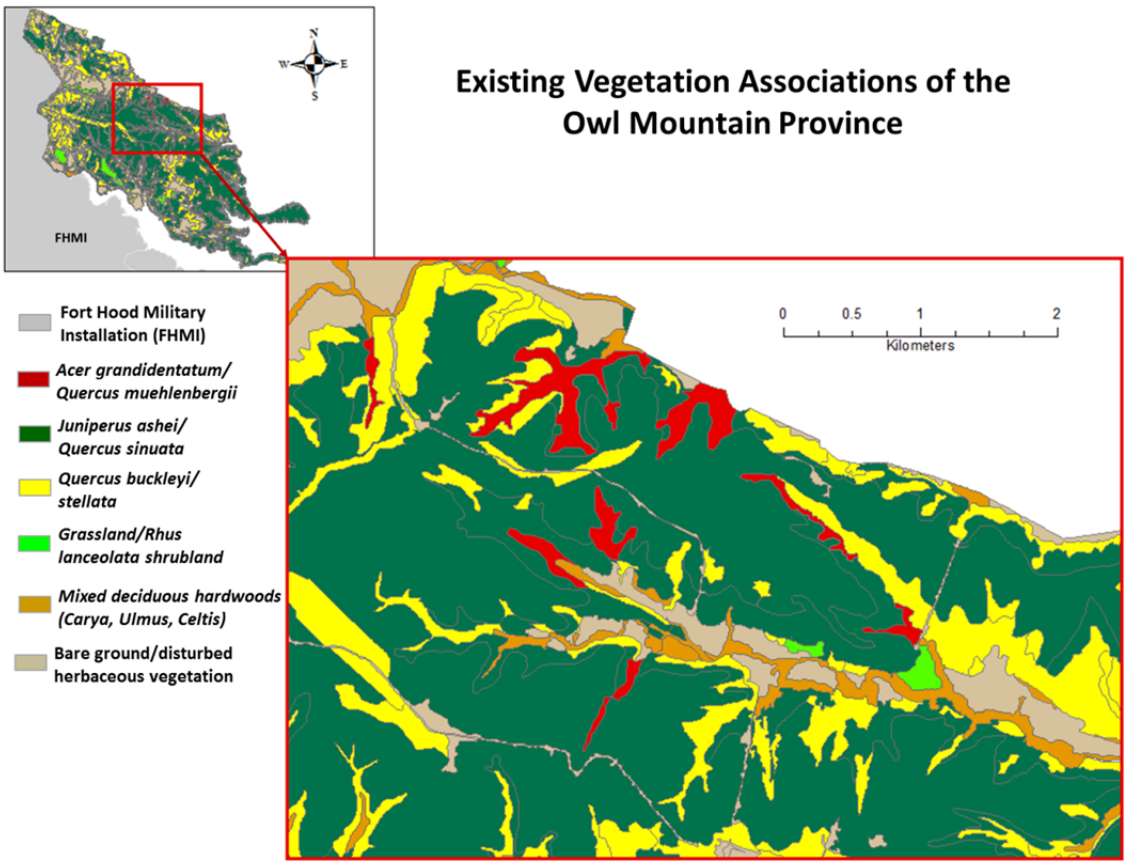

Figure IV.4. Vegetation associations found in the Owl Mountain Province (modified from Pekins 2012 and Hammer 2011).

the mesic, dissected portions of the study area are strongly influenced by floristic contributions from the eastern deciduous forests. The steep slopes of the province support short-stature woodlands which vary from *J. ashei, Quercus sinuate,* and *Quercus buckleyi* on xeric sites to deciduous mixed-oak hardwood woodlands on mesic sites, including isolated populations of *A. grandidentatum* (Ludeke et al. 2005; Gehlbach and Gardner 1983). The alluvial soils of the lower elevations developed over marls and clays, and become thicker proximal to streams and rivers (Picinich 2011). The climate of the Owl Mountain Province is sub-humid to sub-arid and historical precipitation averages fluctuate between 65 and 75 cm per year. Summer temperature highs and lows do not vary significantly and average 35° C and 22°C, respectively. The average minimum January temperatures decrease northward, ranging from approximately 4°C to 0°C (Larkin and Bomar 1983).

Geologic and Structural Evolution of Owl Mountain Province

The Owl Mountain Province is dominated by thick sequences of Lower Cretaceous Comanchean Series carbonates from Fredericksburg Group (Walnut, Comanche Peak, and Edwards, Figure IV.2) deposited as part of the major sedimentary sequences during the Zuni transgression, forming as an isolated mound or shoal on the Comanche Platform behind the Stuart City Shelf Margin (Faulkner et al. 2013; Figure IV.3). The Comanche Platform was bounded on the east and south by a relatively deep-water oceanic basin, the ancestral Gulf of Mexico, and on the north and west by the North

Texas-Tyler basin, an extensive marine basin which represents the deeper, backreef marine shelf facies (Nelson 1973; Fisher and Rodda 1969).

The Ouachita/Balcones structural trend is one of the major features influencing the Owl Mountain Province (Culotta et al. 1992; Caran et al. 1982; Figure IV.3). The Ouachita trend was the result of a major orogenic event as Gondwana and North America collided during Mississippian and Pennsylvanian time, initiating the eventual formation of Pangaea near the end of the Paleozoic (Garrison 2005). Today, most geologic evidence lies in the subsurface as part of the Ouachita fold-thrust belt. The belt is approximately 2100 kilometers and extends from the subsurface of Mississippi to the Marathon region of West Texas (Caran et al. 1982). The result of this collision was a suite of stacked, folded, and imbricated Paleozoic lithofacies that separate the North American craton on the north and west from the downwarping Gulf of Mexico Basin on the south and east (Flawn *et al.*1961). This tectonic boundary has remained structurally active through most of the Phanerozoic, influencing deposition and structural deformation along most of the southern margin of the continental craton (Caran et al. 1982). The Ouachita orogenic belt began to subside in Mesozoic time, coincident with the Zuni transgression that controlled deposition during the Cretaceous Period (McCann 2012; Rose 1972). By the end of the Cretaceous, a thick marine carbonate sequence covered most of the Ouachita System in Central Texas and the initial Gulf of Mexico basin existed to the southeast (Figure IV.3). The final shaping of the Gulf of Mexico occurred during the Laramide orogeny, as peninsular Mexico was transported eastward forming the Sierra Madres and constricting

circulation in the Gulf (Caran et al. 1982). Uplift in the region provided clastic sediments from the interior of Texas for the extending Gulf Coastal plain (Hayward et al. 1990).

By Miocene time, the second principal component of the trend, the Balcones Fault Zone, had been superimposed on the Ouachita deformation zone (Faulkner and Bryant 2015; Ferrill and Morris 2008; Caran et al. 1982; Figure IV.3). The Balcones (also the Luling, Mexia, and Talco) fault zones extend as an arcuate belt of *en echelon* normal faults from Del Rio to Dallas with the Mexia/Talco fault zone extending into eastern Texas, displacing the Mesozoic to lower Paleocene section above the Ouachita System subcrop, with recent faulting (between 24 and 5 mya) initiating the uplift and subsequent dissection of the Lower Cretaceous strata (Caran et al. 1982). Most of the displacement along the faults is believed to have occurred in the late Oligocene or early Miocene as evidenced by the abundance of reworked Cretaceous fossils and limestone fragments in the fluvial sandstones created down-dip of the major fault trends (Adkins and Arick 1930; Ferrill and Morris 2008) There is some evidence for both earlier movement along faults within this zone during the late Cretaceous and perhaps later movement during the Pliocene, but the evidence is inconclusive at the present time. These major normal faults generally strike N/NE parallel to the Ouachita structural grain and dip from 40^0 to 80^0 (Ferrill and Morris 2008). The net throw across the fault zone is down toward the southeast, although faults dip both to the east and west (Senger, Collins and Kreitler 1990). The subsurface Ouachita structures acted as a hinge for downwarping into the ancestral Gulf of Mexico (Caran et al 1982). This downwarping, along with upward

flexing of the continental interior west of the Balcones/Ouachita trend, continued throughout the Cenozoic.

Structural deformation transverse to the Ouachita/Balcones trend appears to coincide with structural features known primarily from subsurface data such as platforms, anticlines, and synclines. The San Marcos Arch, Round Rock Syncline, and Belton High-Moffatt Mound trend are three such features that represent undulation and thickening in Cretaceous lithofacies (Culotta et al. 1992; Caran et al. 1982; Figure IV.3). Moffatt Mound and the shoal facies of the Owl Mountain Province are northwesterly trending areas on the flank of the Belton High in which the Edwards exhibits increased thickness and lithology changes; these areas indicate local, high-energy shoaling adjacent to a shallow marine shelf sequence (Faulkner et al. 2016; Bryant 2012; Amsbury et al. 1984; Brown 1975).

Hydrogeology

The Fort Hood Military Installation is underlain by the Trinity and Edwards aquifers, with both receiving surficial recharge from meteoric water (Anaya and Jones 2009; Jones 2003) within the installation boundary. Aerial exposure of the Glen Rose occurs across the western portion of the base, where the Trinity Aquifer receives direct recharge from precipitation (Faulkner et al 2016; Faulkner and Bryan 2015). In the Owl Mountain Province, exposures of the Fredericksburg Group limestones and marls that make up the Edwards Aquifer, receive direct recharge from meteoric waters via

sinkholes, joints, and other karst features exposed by surface denudation and dissolution (Faulkner and Stafford 2014). Both aquifers are instrumental in providing base flow for perennial and intermittent streams, as well as springs and seeps in the study area.

The topography is dominated by plateaued drainage divides capped by the resistant Edwards limestone and bordered by steep scarps exposing the interfingering relationship of the Comanche Peak and Edwards (Faulkner and Bryant 2015). These sediments were deposited in a restricted environment behind the Edwards reef trend and sheltered by the Moffatt Mound structure to the east (Amsbury et al. 1984; Brown 1975). As a result, permeability varies greatly across the study area with regions where these units interfinger typically having lower permeabilities than areas dominated by only Edwards deposition (Walker 1979; Figure IV.5). Groundwater discharges at the surface where strata of the Edwards Formation crops out or where a gradational facies between Edwards and Comanche Peak formations has sufficient permeability to transmit fluids (Faulkner et al. 2016). Surface drainage of the Owl Mountain inland is performed by numerous unnamed ephemeral creeks and streams; larger streams such as Owl and Bear Creeks flow directly into Belton Lake when sufficient surface water is available (Figure IV.2). As is common in this type of topography and climate, many of the stream segments will flow intermittently as water transmits between the surface and subsurface.

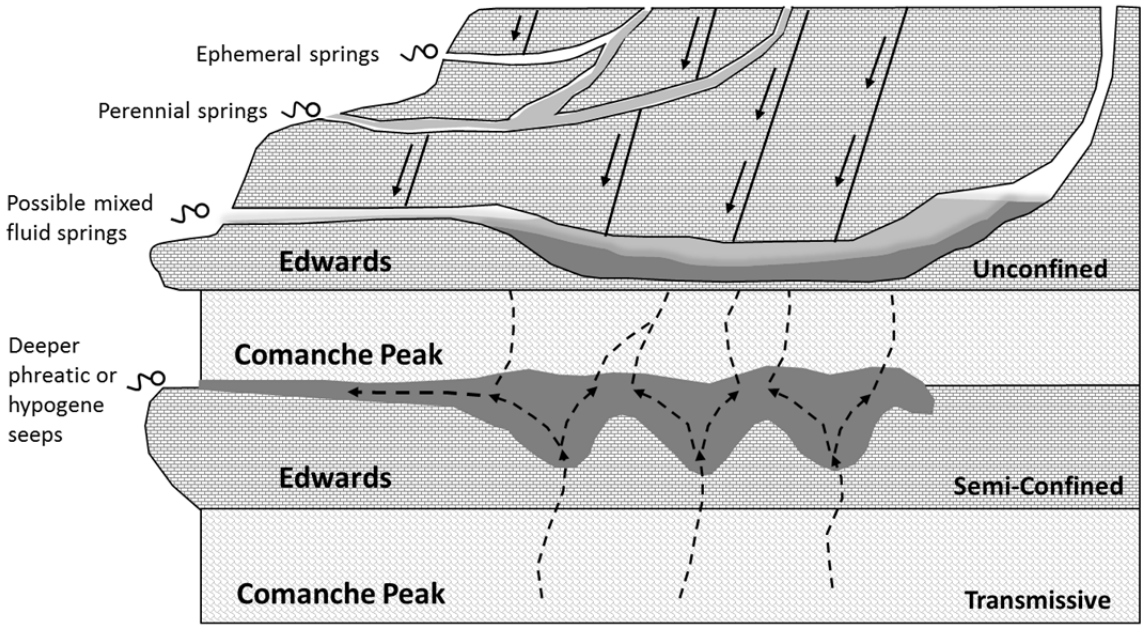

Figure IV.5. Hydrogeologic model of the Owl Mountain Province. Many mesic vegetation sites exhibit no surface flow; these sites are maintained by phreatic and/or hypogenic water resources that maintain soil moisture.

Methodology

For the purposes of this study, a 1m Digital Elevation Model derived from LiDAR data captured in March of 2009 was used as a base map (Pekins 2012). These data, and the color infrared image (Figure IV.6A), were obtained from the Fort Hood Natural Resource Management Branch, and the bare earth LAS files were used to build the Digital Elevation Model (DEM). The DEM was used to derive a hillshade (Figure IV.6B) and slope raster (Figure IV.6C) for lineament analysis. The hillshade raster was derived at azimuth 315 and inclination of 45 degrees above the horizon.

Because the land surface in the Owl Mountain Province has been heavily modified by road building and troop maneuvers, satellite imagery and terrain models are not as useful for determining lineament patterns and trends. In order to augment the lineament trends derived by the digitized surface in the study area, four additional data sets were analyzed: 1) joint trends in outcrop from geologic mapping; 2) joint measurements from Texas Speleological Society cave surveys from Bell and Coryell counties; 3) the orientation of stream segments in the study area; and 4) the orientation of established mesic vegetation communities, using the presence of *A. grandidentatum* as a proxy for subsurface lineaments and potential water resources.

Geologic mapping in the study area yielded 619 joint trends measured in outcrop and along the shoreline of Belton Lake. These measurements were collected from September 2011 through February 2015 during sample collection and facies analyses (Shaw 2012). The Texas Speleological Survey (2014) cave survey data base was mined

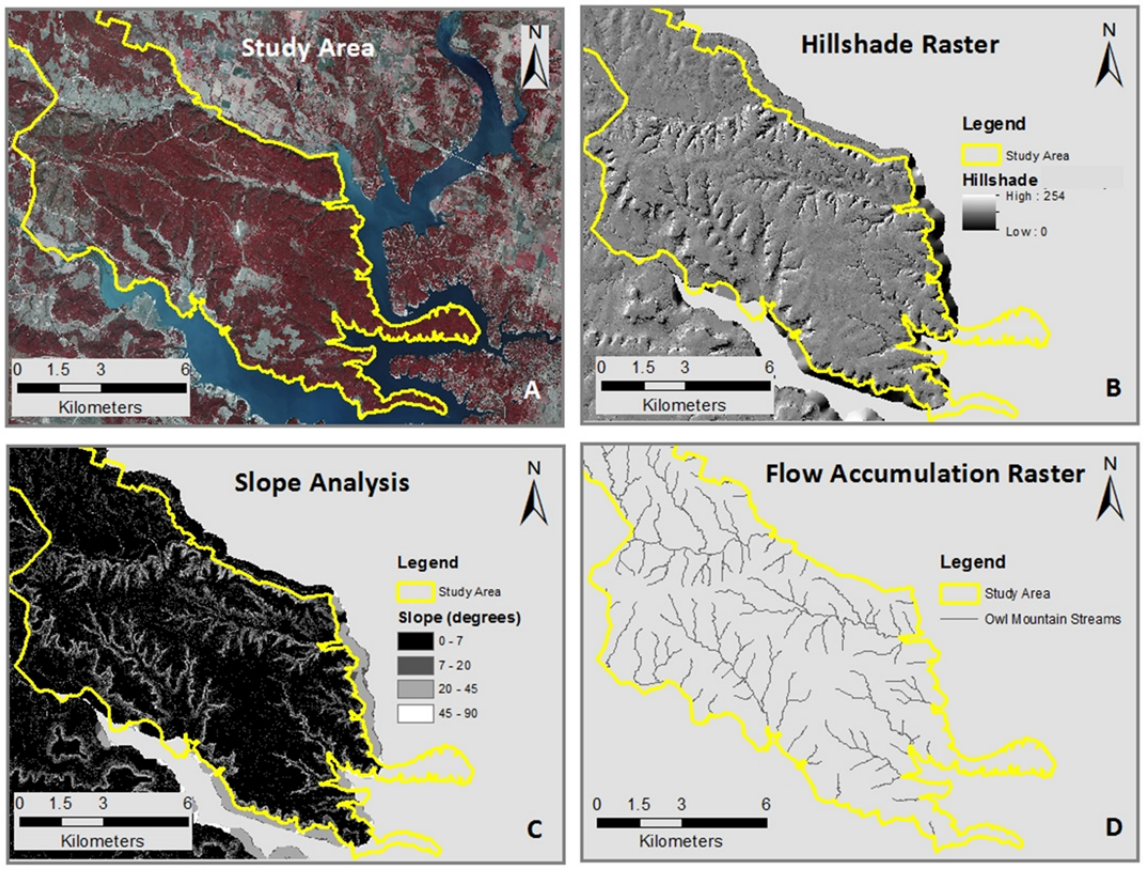

Figure IV.6. ArcGIS models of the study area were processed to determine structural features: the color infrared image (A) was provided by the Fort Hood Natural Resources Division; the 1m DEM derived from LiDAR was used to calculate a hillshade raster (B), slope analysis (C), and flow accumulation raster (D). The landscape has been heavily modified by military activities therefore it was difficult to filter some anthropogenic modifications. The eastern peninsulas of the Owl Mountain Province are in a no-fly zone, therefore no LiDAR data was collected or processed for this area.

for joint trends recorded from cave mapping in Bell and Coryell counties, yielding 1,231 joint measurements. These measurements were weighted according to length in 5m increments, with greater weight being assigned to longer and more well-developed subsurface jointing. Stream segments were delineated for the study area through the creation and classification of a flow accumulation raster in ArcGIS (Figure IV.6D). The zonal geometry tool was used to determine stream segment orientation in 5m increments, yielding 755 measurements. Finally, the vegetation map provided by the Fort Hood Natural Resources Management Branch was used to isolate the vegetation polygons designated as *A. grandidentatum* habitat (Pekins 2012; Hayden et al. 2001). The major orientations of each polygon were measured, yielding 43 measurements. Each of the data sets were plotted on rose diagrams to determine the similarities and differences between lineament orientations in each data set. Finally, the lineament trends were compared to known regional trends from the Ouachita/Balcones and Belton High-Moffatt Mound deformation events.

Results and Discussion

The nearest surficial expression of the Balcones/Ouachita trend occurs seven kilometers east of the study area; at present there are no mapped faults in the Owl Mountain Province. The strike of these normal faults ranges from N0° to N40°E with the general trend of N22°E and net throw to the southeast (McCann 2012; Senger et al. 1990;

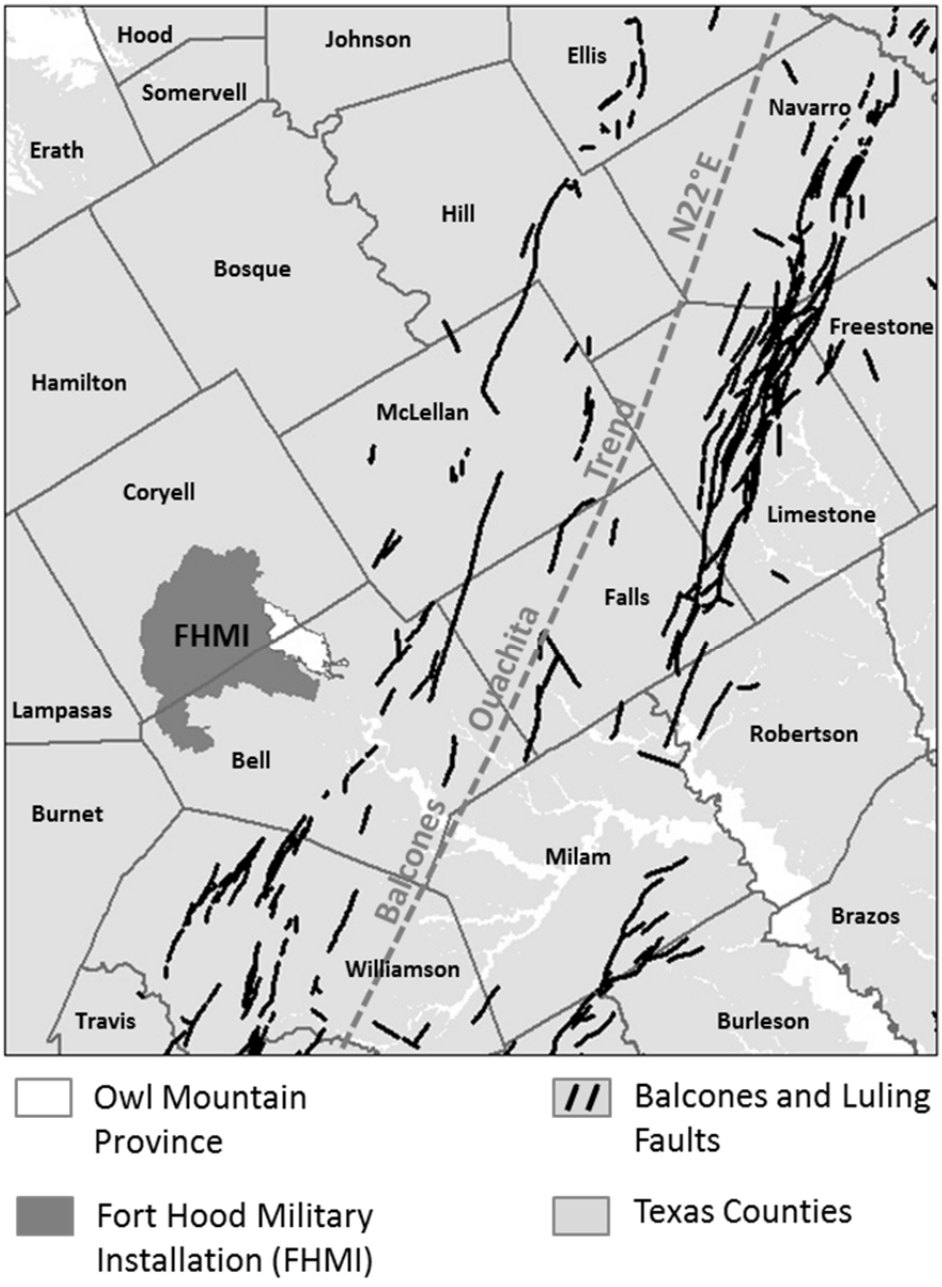

Figure IV.7. Balcones/Ouachita trend in North Central Texas. Balcones and Luling fault data from the Geologic Database of Texas, Texas Natural Resources Information System, accessed January 2016.

Rose 1972; Figure IV.7). The Belton High is a topographic positive that follows the western edge of the North Texas/Tyler basin and separates the basin from the interior of the Comanche Shelf (Figure IV.3). Along this trend, thickened sequences of the Edwards formed isolated shoals of oolitic and peloidal packstones and grainstones indicative of local high energy environments (Bryant 2012; Shaw 2012; Caran et al. 1982). These shoals, such as Moffatt Mound and the Owl Mountain Province, formed adjacent to the shallow shelf environment to the southwest. The Belton High, Round Rock Syncline, and San Marcos Arch are mostly known through subsurface mapping and are thought to be topographic undulations on the Comanche Platform representing a more stable part of the shelf than the adjacent, rapidly subsiding areas of the Fort Worth-Tyler and Marathon basins (Caran et al. 1982). Following the general dip trend of the lithologies in the area, these structures plunge to the southeast.

Within the study area, the development of joint sets in concert with regional deformation events is well documented from outcrop measurements and cave mapping performed as part of the karst inventory of the Fort Hood Military Installation (Reddell et al. 2011). Other research such as sinkhole delineation (Faulkner et al. 2013b) and facies analyses (Bryant 2012; Shaw 2012) have provided a wealth of information about the evolution of the carbonate platform upon which the shoals of the Owl Mountain Province were deposited. Analyses of lineament measurements for each of the data sets revealed two dominant trends; joint measurements and stream channel segments followed a primary northeast/southwest trend concomitant with the regional Balcones/Ouachita trend

(Figure IV.7), and the caves and vegetation polygons followed a northwest/southeast trend associated with the Belton High-Moffatt Mound (Figure IV.3). Each data set also reflected a secondary trend sub-perpendicular to their primary orientation.

Joint measurements in outcrop appear to be more directly influenced by Balcones/Ouachita deformation, exhibiting a 0° to 25° azimuth trend, with a majority trending 22° (Figure IV.8A). Joints can form as a result of tensional movement perpendicular to the resultant fracture plane, or by unloading associated with erosional processes near the surface. As this area was uplifted by the initiation of Balcones faulting, the subsequent removal of Washita Group formations (Georgetown, Austin Chalk) and the extension of the Gulf of Mexico could have created stress along the previously fractured Ouachita sediments, inducing joint creation along the Balcones/Ouachita trend. Even though the study area is to the west of the Balcones/ Ouachita trend (Figure IV.7) and no faults are known in the immediate study area, tensional stresses associated with sediment transport to the southeast and regional stress could have induced fractures in the Edwards and Comanche Peak. Today, these joints are also associated with karst features such as shelter caves, tafoni, tufa, sinks, and springs; indicating they function as a primary mechanism for fluid transport. Since the study area is underlain by both the Trinity and Edwards aquifers, ascending fluid pressure resulting from Balcones deformation could also provide a mechanism for joint trends seen at the surface (Faulkner et al. 2016). Secondary joint development along the Belton High-Moffatt Mound trend

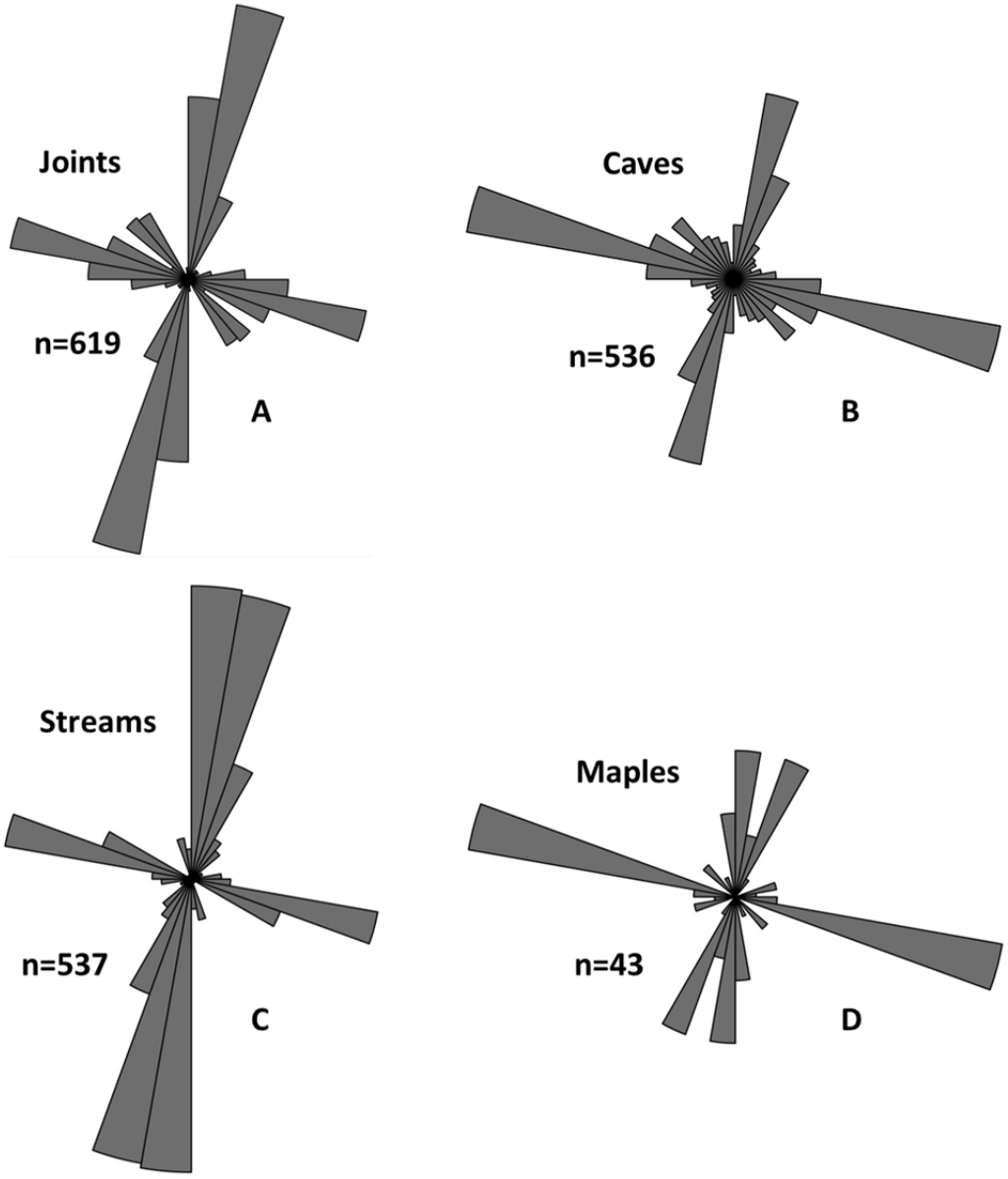

Figure IV.8. Major lineament trends for surface and subsurface deformation in the Owl Mountain Province. Joint measurements (A) were derived from geologic surface mapping; cave measurements (B) from the Texas Speleological Survey data base; stream segment orientation (C) from the flow accumulation raster; and maple habitat orientation (D) from established vegetation maps provided by the Fort Hood Natural Resources Division.

indicates an azimuth trend of 285°, with most measurements falling between 270° and 295° (Figure IV.8A).

Cave measurements were determined to be more influenced by the Belton High-Moffatt Mound trend, with many of cave maps showing a regional lineament trend of 285° (Figure IV.8B). All of the known caves within the Fort Hood Military Installation occur in the Edwards Formation, or along permeability boundaries in the interbedded Comanche Peak and Edwards formations (Faulkner and Bryant 2015). Many of the caves in this area formed along conjugate joint sets in a semi-confined environment, both laterally and vertically. While the northwest lineament trend was dominant, many of the caves exhibited secondary development along the Balcones/Ouachita trend. Joints along this trend would have provided a planar surface for ascending fluids with solutional widening along these fractures continuing cave development along transmissive zones or bedding planes. Tensional stresses associated with faulting and focused along the axes of folds can have a similar effect by opening multiple conduits such that fluid migration is dispersed along various pathways as dissolution commences along the fracture planes (McCann 2012). Today, many of the karst features within the study area are predominantly surficial expressions of collapse features or features resulting from vadose entrenchment, creating windows into karst conduits. Slope retreat along the scarps, stream incision, and surface denudation have exposed karst features formed along dissolution surfaces associated with fluid transmission (Bryant, 2012, Faulkner et al., 2013a; Figure IV.9). Secondary transmissivity along the Belton High-Moffatt Mound

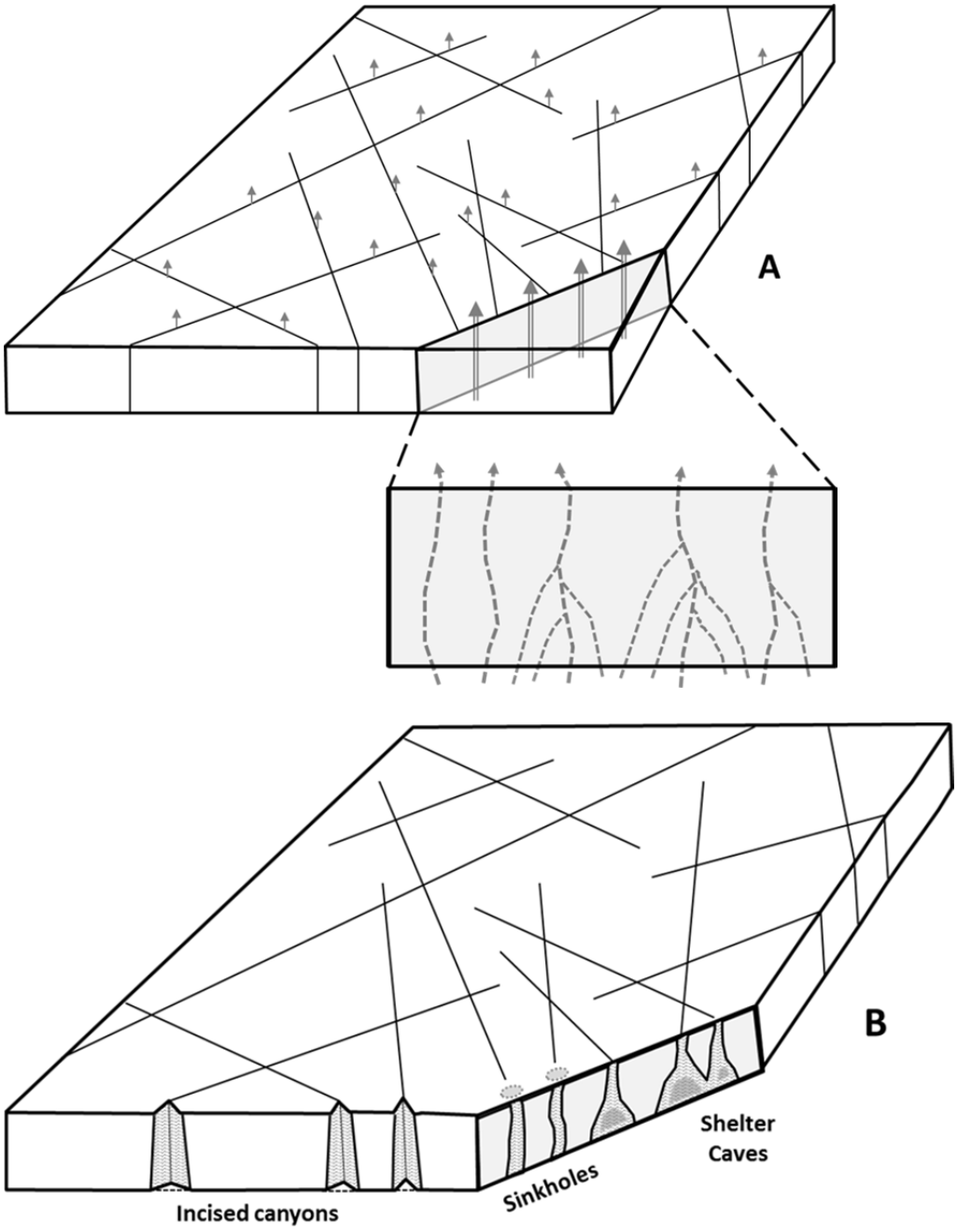

Figure IV.9. A conceptual model of phreatic/hypogenic fluid transport through conjugate joint sets in a semi-confined aquifer. Karst features develop along solutionally-widened conduits, influencing the development of incised canyons for mesic vegetation and surficial karst features (modified from Klimchouk and Ford 2009).

trend probably exists as matrix porosity, particularly within the interbedded Comanche Peak and Edwards carbonates as differences in permeability force ascending fluid laterally along the contacts. As the shoals accumulated along this northwestern trend, restricted circulation along the Comanche Shelf would control facies development. As evidenced in the oolitic and peloidal packstones and wackestones in the interfingering units, transmissivity between facies would be controlled by the shoaling trend to the northwest. This trend would in turn control subsurface porosity in the form of solutionally-widened conduits and cave development.

Analysis of stream segment orientation within the study area shows that Balcones/Oauchita deformation also appears to exert a greater influence on channel orientation (Figure IV.8C), although their orientation may be influenced as much by the topography as regional deformation trends. Within the study area, incised valleys are created to the north and south of the plateaus capped by the resistant Edwards by short stream segments that flow into the Owl and Bear Creek watersheds (Figures IV.2 and IV.6D). These valleys are then drained by larger creeks and streams that flow generally east and southeast, eventually draining into Belton Lake. These streams, with their tributaries, are responsible for most of the slope retreat and incision that has created the unique topography of the Owl Mountain Province. The Owl and Bear Creek watersheds are separated by drainage divides and characterized by steep slopes and scarps with interbedded exposures of the Edwards and Comanche Peak formations. Joints act as focal points for water ascending from below and descending from above, and as slope retreat

intersects with ascending fluids, the joints became solutionally-widened and began to function as ephemeral surface drainage (Klimchouk et al. 2012; Figure IV.9). The communication between the Trinity and Edwards aquifers and the surface are also a potentiometric driver for ascending fluids; geochemical analyses of springs within the Owl Mountain Province indicate that most meteoric water transmits directly to the subsurface and today, many of these stream segments are mostly dry, flowing only for a few hours or days after precipitation events (Faulkner et al. 2016).

Lineament analyses of *A. grandidentatum* vegetation associations determined that the results were mixed. Twenty-one of the 43 lineaments (49%) aligned along the Balcones/Ouachita trend, 30% (13 of 43) were associated with the Belton High-Moffatt Mound trend (Figure IV.8D). Currently, designated maple habitat covers 71 hectares in the Owl Mountain Province, and is found within nine vegetation polygons mapped by the Nature Conservancy and Fort Hood Natural Resources Management Branch. These trees exist in sheltered, incised canyons and along the edges of the scarps in the Owl Creek and Bear Creek watersheds. Within these watersheds, *A. grandidentatum* exists in regions of the installation that have been set aside as environmentally sensitive areas for wildlife habitat and nature preserves. Even though these populations exist within the training areas for military exercises, the terrain is rugged and most of these populations are in remote areas of the base not generally visited by wheeled or tracked vehicles, or used for training exercises.

Some of these canyons are fed by short, ephemeral stream segments flowing north and south off the plateaus, and by ascending fluids along joints following the Balcones/Ouachita trend (Figures IV.5 and IV.10). These fluids migrate through the lower permeability zones of the Comanche Peak and are forced to flow laterally by confining units. Canyons with maple populations are oriented in a variety of aspects: north, northeast, southeast, and south, indicating that canyon aspect cannot be the only determining factor in maple survival. Most of the stream channels in these canyons do not exhibit any base flow, rather they are fed by occasional precipitation events and springs and seeps that provide moisture to maintain these mesic sites. The springs and seeps follow the trend of dominant joint sets, which then exert structural control on the location and continued existence of these maple populations. Access to water in karst landscapes is often controlled by subsurface structural trends, and the Balcones/Ouachita trend appears to be the major conduit by which these mesic vegetation communities gain access to water resources. In some cases, transverse, sub-vertical conduits have formed between the units and forced fluid flow between units, connecting ascending fluids with vadose waters. These features are exposed today along the scarps associated with the Edwards and Comanche Peak, often with several zones of karst features exposed along these cliff faces with interbedded exposures of these units (Figure IV.9).

Vegetation polygons have been mapped with the Comanche Peak as the underlying lithology with no springs or creeks currently flowing within the incised canyons hosting maple vegetation (Figure IV.2). In the study area, the unit consists of

nodular, fossiliferous limestone that has a dull chalky texture; porosity typically ranges from 1 to 8%, much less than the overlying Edwards. The lower permeability of the Comanche Peak supports a deeper phreatic and/or hypogene source for moisture within these incised canyons, as meteoric water that falls on the uplands is directed into the subsurface through karst features and springs out within the Edwards or along the Edwards and Comanche Peak boundary (Faulkner et al. 2016; Figure IV.5). Geochemical analyses of karst springs sampled from December 2012 through February 2015 support this hypothesis, spring chemistry showed a residence time between three and six months with the water in the subsurface long enough to equilibrate with rock temperature. Calcium is enriched with respect to magnesium, indicating a shorter residence time and reflective of the lithology through which the water flows. Permeabilities within the Edwards favor discharge within the unit along the scarps in the Owl Creek and Bear Creek watersheds. Water discharging from the Comanche Peak at lower elevations within the canyons is probably emerging from below along solutionally widened flow paths to augment soil moisture and support mesic vegetation (Figure IV.9).

Summary and Conclusion

This study utilized a variety of methods to determine major structural deformation trends and their influence on the evolution of the topography and mesic vegetation communities in the study area. Within the Owl Creek and Bear Creek watersheds, the geomorphic evolution of the Owl Mountain Province has been controlled by the

structural development of incised canyons along the Balcones/Ouachita deformation trend and the transverse Belton High-Moffatt Mound trend. These trends control cave development in the subsurface, joints in outcrop, stream segment orientation, and the general transmission of ascending fluids in the study area. While many of the springs in the study area are fed by meteoric waters, these incised canyons also receive fluids from deeper seated phreatic and/or hypogene fluids which emerge as ephemeral springs and seeps to augment soil moisture.

Due to the multi-purpose land use of the Owl Mountain Province, the study area has been extensively modified by past and current military use, thus lineaments and other surface features related to military use cover most of the study area and must be taken into consideration when interpreting results. The combination of heavy military use and high resolution elevation data make it extremely difficult to discern between natural and anthropogenic lineaments; therefore models developed from LiDAR analyses at Fort Hood are assumed to have errors, both in the inclusion of anthropogenic lineaments and the exclusion of true structural features.

Acknowledgements

This research was partially funded by the Arthur Temple College of Forestry and Agriculture, the Division of Environmental Science, and the Department of Geology at Stephen F. Austin State University. Access to the Fort Hood Military Installation training areas was provided by Charles Pekins of the Fort Hood Natural Resources Management

Branch. Assistance with digital analyses was provided by Kyle Altimore and invaluable field assistance was provided by Joel Faulkner and Asa Vermeulen.

CHAPTER V:
THE SPATIAL DELINEATION OF *ACER GRANDIDENTATUM* WITHIN THE OWL AND BEAR CREEK WATERSHEDS ON THE FORT HOOD MILITARY INSTALLATION, TEXAS

Abstract

Within mesic, dissected canyons in Central Texas, disjunct populations of bigtooth maple (*Acer grandidentatum)* exist as Pleistocene relicts in several counties within the Edwards Plateau and Lampasas Cut Plain. Several of these isolated populations can be found within the Owl Mountain Province of Fort Hood Military Installation, in Bell and Coryell counties, Texas. The province is the northeastern section of Fort Hood and is used by the Army for dismounted and wheeled exercises, and some small-scale tracked vehicle training. Transect vegetation surveys conducted by the Fort Hood Natural Resources Branch in 1996 and 2011 identified nine distinct areas of *A. grandidentatum* habitat covering 71 hectares within the 9,000 hectare study area.

During spring 2013, fifty-four 78.5m^2 nested vegetation plots were established within known maple habitat, inventorying woody and emergent species. These data were used to create a vegetation model in ERDAS by isolating the spectral intensity of *A. grandidentatum* to determine where additional maple populations may be found within the Owl Mountain Province. Vegetation mapping conducted in January 2016 located an additional 129 hectares of *A. grandidentatum* habitat. Sixty-one nested plots were

established within the newly defined maple habitat and compared with existing vegetation inventories to determine the similarities and differences between modeled and established maple habitat. Independent-samples T-tests were conducted to determine the differences between stand dynamics with regards to *A. grandidentatum* and Ashe juniper (*Juniperus ashei*) in established and modeled vegetation stands within the Owl Creek and Bear Creek watersheds at $\alpha = 0.05$. Statistical analyses for both the established and modeled bigtooth maple habitat reveal that the Owl Creek watershed represents a later successional habitat with maples expressed in near equal proportion in the canopy and understory. The Bear Creek watershed maple habitat is highly segmented with less continuous maple and hardwood habitat; hardwoods are still prominent, but Ashe juniper represents a larger proportion of the vegetation community in the canopy and understory, indicating greater disturbance.

Introduction

The Lampasas Cut Plain region of Central Texas is a species rich, karst terrain that supports a variety of vegetation habitats from mesic canyons to xeric uplands (Riskind and Diamond 1986). The Cut Plain and surrounding areas are considered to be a southern extension of the Great Plains of North America (Hunt 1974) and the Cut Plain is sometimes considered as the northern extension of the Edwards Plateau, but is distinctly different as a physiographic province and ecoregion (Faulkner and Bryant 2015; Texas Natural Resource Information System 2016; Figure V.1). The landscape and topography

are largely controlled by the erosional behavior of the underlying Lower Cretaceous carbonates; with downcutting of major rivers and streams dissecting the mostly flat mesa-like drainage divides by the Brazos River and its tributaries (Hayward *et al.* 1990). The topography becomes rolling in areas proximal to streams, and represents a generally more mature landscape than the Edwards Plateau to the south and west.

The southern portion of the Edwards Plateau and parts of the Lampasas Cut Plain are more highly dissected, with incised, mesic canyons that support forest and woodland vegetation; these plant communities owe much of their origin to the Sierra Madre Oriental and its outliers, and by floristic contributions from the eastern deciduous forests, including tall-grass prairie species (Riskind and Diamond 1986). Many of the mesa-like drainage divides within the Lampasas Cut Plain are more xeric and open and are strongly influenced by the Great Plains grasslands to the north (Diggs *et al*. 1999). Juniper-oak woodlands are widespread on limestone terraces across uplands in the Lampasas Cut Plain, usually over karstic features or Quaternary terrace deposits (Huxman *et al*. 2005; Diamond 1997). On the more xeric rolling hills to the west, the semi-desert grasslands are biotic contributions from the dry plateaus and massifs of northern Mexico and Trans-Pecos Texas (Riskind and Diamond 1986).

Within these dissected canyons in Central Texas, disjunct populations of bigtooth maple (*Acer grandidentatum*), exist as Pleistocene relicts, isolated from larger

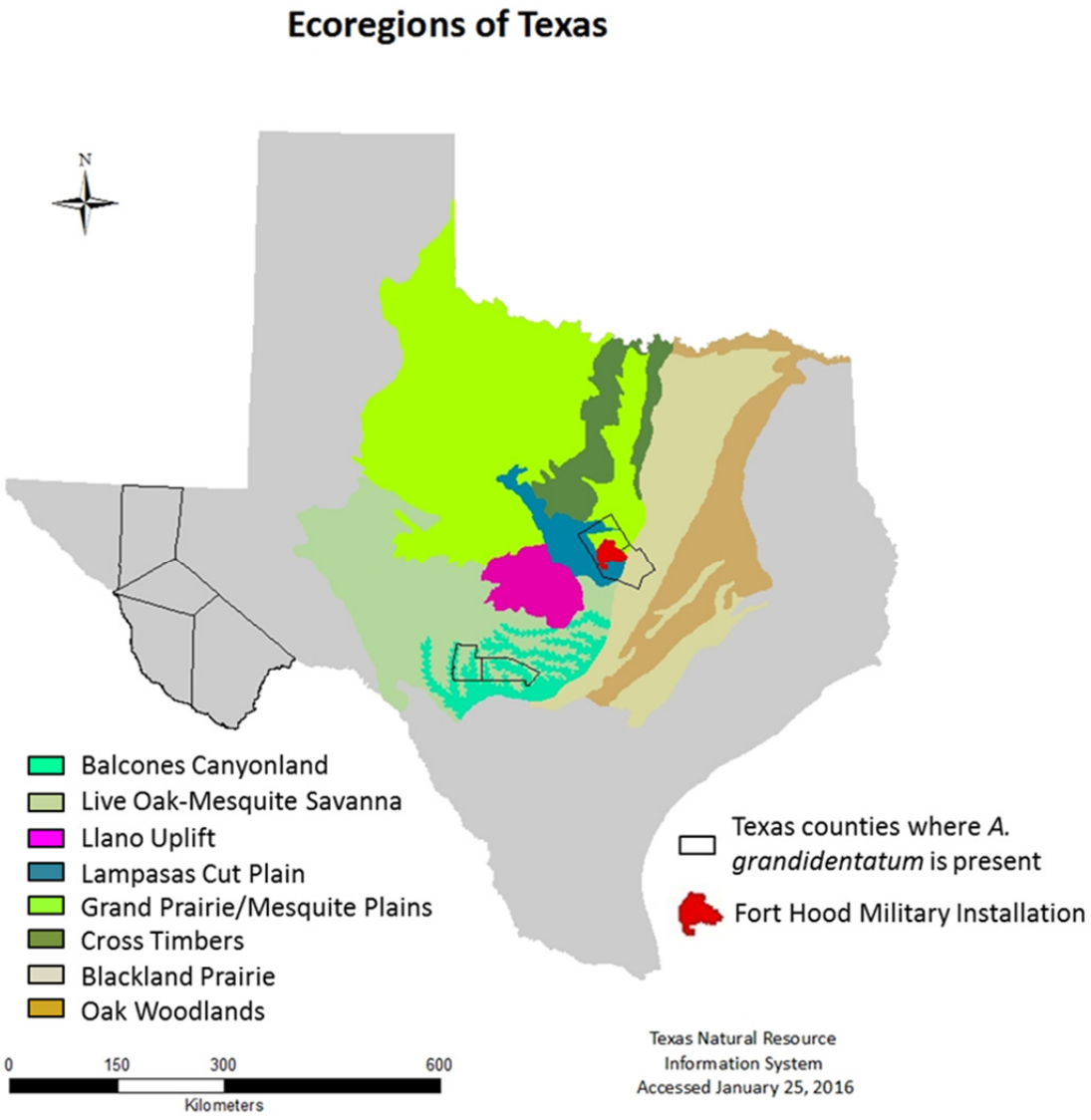

Figure V.1. Ecoregions of Texas. The Fort Hood Military Installation is uniquely situated between the Edwards Plateau ecoregion and the Crosstimbers and Prairie ecoregion, providing high quality habitat for wildlife and endangered avian species.

populations by several hundred miles (Riskind and Diamond 1986). *A. grandidentatum* is a small, deciduous hardwood tree indigenous to North America existing as a continuous population in the intermountain regions of the western United States from southern Idaho through the Wasatch Mountains of Utah (Tollefson 2006). The geographic range spans almost 18° of latitude, varies greatly within elevation limits, and occurs on both xeric and mesic sites. Throughout its continuous range, it is most often located on cool, moist sites in canyons, ravines, along mountain streams, and on lower slopes (Oterdoom 1994). It is relatively tolerant of low soil water potentials, and can grow with oaks on drier, open slopes (Tollefson 2006; Correll and Johnston 1970). Commonly referred to as bigtooth maple, regionally it can be known by other common names including lost maple, canyon maple, Uvalde maple, Sabinal maple, Plateau bigtooth maple, Wasatch maple, Southwestern bigtooth maple, Western sugar maple or Rocky Mountain sugar maple (Dickinson 2011). Although there has been some debate of the phylogenetic grouping of bigtooth maple, most current research refers to it as *A. grandidentatum* (Gehlbach and Gardner 1983; Desmarais 1952).

Smaller, disjunct populations of *A. grandidentatum* can be found at lower latitudes in southwestern Oklahoma, Colorado, New Mexico, Arizona, and into Couhuila, Mexico (Tollefson 2006). Texas has isolated populations located in the Guadalupe and Wichita Mountains in West Texas, and several counties within the Edwards Plateau and Lampasas Cut Plain of Central Texas (Ludeke *et al*. 2005). Over the past 10,000 years, temperatures warmed and water resources became focused along incising canyons across

the Edwards Plateau and Lampasas Cut Plain and populations of *A. grandidentatum* were forced to respond to the changing climate (Larkin and Bomar 1983). Today, isolated populations of *A. grandidentatum* continue to exist in sheltered, incised canyons along the Balcones Escarpment, Edwards Plateau, and Lampasas Cut Plain regions. Several of these isolated populations can be found in Lost Maples State Natural Area in Bandera and Real counties (Dickinson 2011), and within the Owl Mountain Province of the Fort Hood Military Installation in Bell and Coryell counties (Hammer 2011; Ludeke *et al*. 2005; Gehlbach and Gardner 1983).

Since October of 2011, the Fort Hood Natural Resources Management Branch has been responsible for implementing programs to catalogue and monitor natural resources on the installation and has contracted with civilians, state agencies, and environmental consulting firms to help realize their goals (Pekins 2012; Reddell *et al*. 2011). The purpose of this study was fourfold: to document stand dynamics and associated populations within established *A. grandidentatum* habitat, develop a remote sensing based model to determine other suitable locations where bigtooth maple may exist, ground-truth this model to find potential bigtooth maple habitat, and compare dynamics of the bigtooth maple habitat found in Owl Creek and Bear Creek watersheds to determine the similarities and differences between them. This data will help the U.S. Army employ best management practices with regards to training activities, water resources, and environmentally sensitive vegetation habitats.

Evolution of the Edwards Plateau and Lampasas Cut Plain

The genesis of the Edwards Plateau and Lampasas Cut Plain began in the late Paleozoic with the Ouachita orogenic event which brought Gondwana in contact with North America and initiated the eventual formation of Pangaea (Culotta *et al*. 1992). The result of this collision was a curved zone of sub-surface imbricated Paleozoic rocks that extended from the Marathon region of West Texas into Mississippi (Flawn *et al.* 1961). The Ouachita orogenic belt began to subside in Mesozoic time, coincident with the Zuni transgression that controlled deposition during the Cretaceous Period across the Comanche Shelf (McCann 2012, Rose 1972; Figure V.2). By the end of the Cretaceous, a thick marine carbonate sequence covered most of the Ouachita System in Central Texas and the initial Gulf of Mexico basin existed to the southeast (Nelson 1973). The final shaping of the Gulf of Mexico occurred during the Laramide orogeny, as peninsular Mexico was transported eastward forming the Sierra Madres and constricting circulation in the Gulf (Caran *et al*. 1982).

By Miocene time, the Balcones Fault Zone had been superimposed on the Ouachita deformation zone (Faulkner and Bryant 2015; Ferrill and Morris 2008; Caran *et al*. 1982; Figure V.2), displacing the Mesozoic to lower Paleocene section above the Ouachita System subcrop, with recent faulting (between 24 and 5 mya) initiating the uplift and subsequent dissection of the Lower Cretaceous strata (Caran *et al*. 1982) and creating the prominent Balcones Escarpment. Displacement along the faults is believed to have occurred in the late Oligocene or early Miocene (Adkins and Arick 1930; Ferrill and

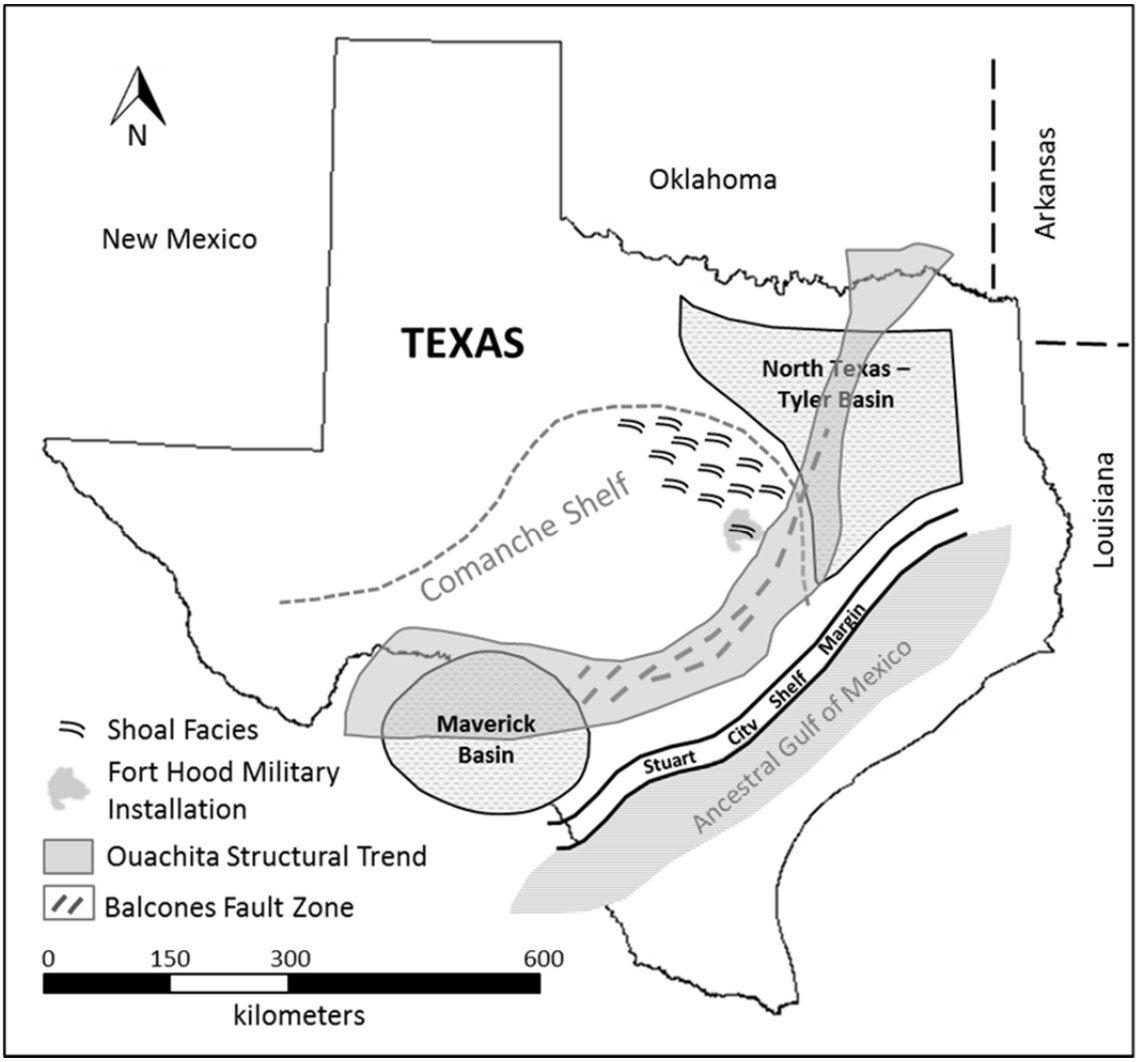

Figure V.2. Location map showing the major structural trends influencing strata in the Central Texas region. Shoal facies such as the Owl Mountain Provinces were formed on the Comanche Shelf during the Zuni transgressive sequence (modified from Anaya and Jones 2009; Walker 1979; Fisher and Rodda 1969).

Morris 2008), with the subsurface Ouachita structures acting as a hinge for downwarping into the ancestral Gulf of Mexico (Caran *et al* 1982). This downwarping, along with upward flexing of the continental interior west of the Balcones/Ouachita trend, continued throughout the Cenozoic.

Uplift in the area altered the base level of many of the first and second order streams and rivers flowing across the region and they began to erode the softer rocks and sediment of the Upper Cretaceous and lower Paleocene, sending massive sediment influxes to the east toward the widening Gulf of Mexico (Hayward *et al*. 1990; Figure V.2). This uplift would eventually influence early human settlement and transportation patterns along the Balcones Escarpment; the escarpment separated early farming communities in the east from the grazing lands to the west. The Austin Chalk, a narrow exposure of carbonate rock paralleling the escarpment from near Sherman in north-central Texas to south of San Antonio, provided serviceable building materials and better drained terrain for oxcarts and wagons than the Blackland Prairie to the east. The change in base level also provided water power to the eventual settlements along the escarpment; by 1861, the town of New Braunfels had a flour mill, four grist mills, and two saw mills, all water-powered (Palmer 1986).

Long Term Climate Fluctuations

The vegetation communities present today in Central Texas have been heavily influenced by the fluctuating climate of the past 2 million years. The Pleistocene Epoch

began approximately 1.8 million years ago and ended with the retreat of the most recent Ice Age about 10,000 years ago. During the most recent glacial episode, between 22,500 and 8,000 B.C., changes in world climates led to the global advance of large continental ice sheets (Musgrove *et al.* 2001). In North America, the ice sheets reached their maximum growth around 20,000 years ago; the climate of Texas became cooler and moisture effectiveness was greater, resulting in the presence of plant species that occur in more mesic sites and cooler environments (Van Devender and Spaulding 1979). The mesic climate encouraged existing forests; the spruce, juniper, Douglas fir, and pine forests of the West Texas Mountains expanded downward to lower altitudes and spread out onto the mountain flanks, where they mixed with grasslands to form parklands and savannahs (Mecke 1996; Nordt *et al.* 1994)). The oak-hickory-pine forests of East Texas did not expand significantly during this period but the dominant species of trees changed somewhat (Riskind and Diamond 1986). Pollen records show that from about 22,500 to 12,000 B.C. the forests were dominated by cooler-weather oak, elm, spruce, maple, hazelnut, alder, and birch (Nordt *et al*. 1994). As the ice age came to an end, climates shifted and warmed and the large glaciers receded. By 8,000 B.C., the ice sheets were gone, bringing a warmer and drier climate to the southwestern U.S. and Texas (Bryant and Shaffer 1977). During the last 10,000 years, the climate in the central and southwestern regions of the United States has fluctuated but gradually warmed to its present day trend toward the semi-arid to arid environment found across the region. This drying trend (on a geologic time scale) continues today; therefore, some of the current

vegetation of Texas may have developed under a previous set of climatic conditions characterized by cooler, more mesic conditions than exist today (Smeins *et al*. 1997; Riskind and Diamond 1986).

The vegetation of the Lampasas Cut Plain responded to the change in climate by a shift in vegetation dominance of piñon and juniper to a dominance of scrub oak and Ashe juniper (Fuhlendorf and Smeins 1996). East of the Balcones Escarpment, the forests lost some of their cool-loving species such as alder, maple, spruce, and hazelnut. Basswood, dogwood, chestnut, and a few other forest species that grow best in cooler, wet habitats did not disappear entirely but were reduced to minor components in the new deciduous forests (Diggs *et al*. 1999). Over time, as moister climates shifted to the east, relict populations of Pleistocene vegetation contracted to mesic slot canyons in Central and West Texas associated with springs and seeps where consistent moisture was more readily available.

Today, the climate of the Lampasas Cut Plain is sub-humid and becomes increasingly arid to the west and cooler to the north. Courtesy of the Gulf Stream, prevailing winds are generally from the south and the general decrease in moisture content of Gulf air as it flows northwestward across the plain is the controlling factor responsible for this difference in moisture regime (Bradley and Malstaff, 2004). Mean annual precipitation decreases from east to west, ranging from about 85 cm/yr on the eastern edge to 35 cm/yr on the western edge. Summer average highs and lows do not vary significantly and average about 35° C and 22°C, respectively. The average

minimum January temperatures decrease northward, ranging from approximately 4°C to 0°C.

Anthropogenic Effects on Central Texas Vegetation Communities

Across the Lampasas Cut Plain, archaeological and historical records indicate this area has supported many different peoples over the past twelve thousand years as indicated by artifacts found in rock shelters and river terrace campsites (Freeman *et al*. 2001; Pugsley 1992; Doughty 1983). These peoples would have been attracted to the springs and rivers that supported their hunter-gatherer lifestyles and provided ready water sources for herds of grazing animals which they followed (Hester 1986). As groups moved in and out of the area, their lifestyles changed too; hunter-gatherers gave way to more settled peoples who moved from site to site within an area, following seasonal food sources. Through selective harvesting and use of various plants and hunting of animals, these early inhabitants influenced local abundances of many species (Doughty 1983). Local encampments produced disturbed patches of altered vegetation. Many of these early inhabitants were also nomadic and served as effective dispersal agents for reproductive propagules of some plant species (Smeins *et al.* 1997).

Through time, these inhabitants exerted more and more influence on their environment by altering the composition and structure of vegetative communities (Smeins 1984). By at least 5,000 years ago, they were using fire to process food as evidenced by widespread occurrences of "burned rock middens" (Hester 1986),

suggesting that fire was a significant tool utilized for food preparation and possibly as a vegetation and wildlife management tool (Smeins 1980). Lightning fires, as well as accidental and intentional fires, likely caused significant long-term impacts on the composition and structure of native vegetation (Fuhlendorf and Smeins 1996). The impact of fire on the vegetation would have been mitigated to some extent by the type of landscape in which it occurred. Heterogeneous landscapes of varying topography, rocky outcrops and patchy surface fuels are affected very differently from areas of level terrain with a continuous cover of fine fuels (Wells 1970).

The first land grant in Texas was awarded to Moses Austin in 1821, and immigration into Central Texas soon followed. The Brazos River and the Camino Real became the main conduits for settlement of the interior part of Texas (Pugsley 1992). Up to the early 1840s the land west of the Balcones Escarpment remained largely free of European influence. Early Anglo settlers had little interest in the shallow soils and when Ferdinand Roemer visited the Hill Country west of New Braunfels in the mid-1840s, he found no Anglo habitation from New Braunfels to Fredericksburg. Ten years later, Frederick Law Olmsted noted in his travel log that the area was dotted with farmsteads (Smeins *et al.* 1997). For a period of time prior to intensive settlement, fires may have become more frequent and were applied to areas that would not have naturally been predisposed to fire (Hester 1986). Clearing the land of woody vegetation to provide more open areas for grazing, improving the growth and quality of grasses, and clearing of areas for growing of crops was commonplace.

The Civil War temporarily halted immigration and the lack of military protection on the frontier impeded settlement, but by the 1870s the pace quickened. The American bison (*Bison bison*), which was abundant and widespread, was hunted to local extinction across most of the state by the 1870s (Doughty 1983, Flores 1991). The introduction of windmills in the 1880s opened the fertile alluvial areas in the more remote regions (Yelderman *et al.* 1987). During the period between 1870 and 1885, before widespread stocking of the ranges by Anglo settlers, the ranges were relatively free of grazing by large herbivores and these lands seemed capable of supplying unlimited amounts of forage for grazing animals (Smeins *et al*. 1997). As a result there was rapid and severe overstocking of the rangelands; originally these animals grazed on free and open range, but with the advent of more settlers, the availability of barbed wire and windmills to provide water, the animals were confined, which led to destructive grazing of many rangelands (Smeins *et al.* 1997). As the more palatable grasses and forbs decreased or even disappeared, many ranchers switched to cattle, sheep, and goat operations, often grazing all three types of livestock to better utilize the now dominant shrubby vegetation. This factor, combined with the exponential increase of white-tailed deer (*Odocoileus virginianus*) populations following the over-hunting that occurred in the 19th and early 20th centuries and free-ranging herds of exotic ungulates, have further deteriorated the landscape and compete with native wildlife and/or livestock for forage.

By 1930, continuous grazing combined with range fencing and the control of wildfire greatly reduced the growth of the more desirable grasses, allowing many trees

and shrubs to invade the uplands. What early explorers once described as a stirrup-high "waving sea of grass" deteriorated into the shortgrass, rock, shrub, cacti, and woody vegetation that currently dominates the landscape (Smeins *et al*. 1997). Soil conservation districts were organized in the 1930s under the supervision of the U.S. Department of Agriculture and after the Second World War, the federal government began to take an active role in encouraging more informed land-management practices (Diamond 1997). Since that time, conservation officers have worked with farmers and ranchers to reintroduce favorable grass species, avoid overgrazing, promote brush control, and prevent soil erosion. Although the uplands of Central Texas were probably never a wide expanse of open grassland, today a grassland-woodland mosaic currently exists on varying soils across extensive portions of the area (Smeins *et al.* 1997; Fowler & Simmons, 2008). Historically, grasslands were more prevalent than today, having been reduced by encroachment of woody species, due in part to the introduction of domestic livestock, agriculture, and ranching; these activities have suppressed the use of fire, and as a result, woody species have and continue to encroach upon grasslands and increase in dominance (Smeins *et al.* 1997; Hammer 2011).

Deterioration of native vegetation communities encourages encroachment, and Ashe juniper (*Juniperus ashei*) is the most widespread and prominent brush invaders (Smeins and Fuhlendorf 1997; Mecke 1996). Every year, the State of Texas devotes millions of dollars to the removal and management of Ashe juniper to combat woody encroachment on grazing lands, help with water availability in streams and aquifers,

increase desirable wildlife forage and habitat, stimulate species diversity, and erosion control (Lyons *et al.* 1998). Because of fire suppression across the plateau and overgrazing, Ashe juniper has increased in dominance and encroached upon former open grasslands and savannas (Smeins *et al*. 1997). As encroaching species spread and utilize water and nutrient resources, competition significantly reduces the production and diversity of associated plant species (Huxman *et al.* 2005). Overgrazing by livestock, which reduces herbaceous plant competition for establishing juniper seedlings, is frequently considered a factor in the increased population and encroachment of Ashe juniper (Nelle 1997).

Vegetation Communities on the Fort Hood Military Installation

The Fort Hood Military Installation is located in the southeastern section of the Lampasas Cut Plain near the city of Killeen, Texas, and currently encompasses approximately 880 km^2 in Bell and Coryell counties (Hammer 2011; Figure V.3). The Lampasas Cut Plain is located between the Edwards Plateau Ecoregion (TNC 2004) and Crosstimbers and Prairie Ecoregion (Diggs *et al*. 1999; Griffith *et al*. 2004; USDA 2007) and shares affinities with both (Figure V.1). Fort Hood owes its ecological diversity partly to its location at the intersection of these two ecoregions. This location, coupled with the installation's topographic, geological, and edaphic diversity, provides an isolated island of high quality habitat for many threatened and endangered species. Land use surrounding the installation has greatly modified and degraded many such habitats

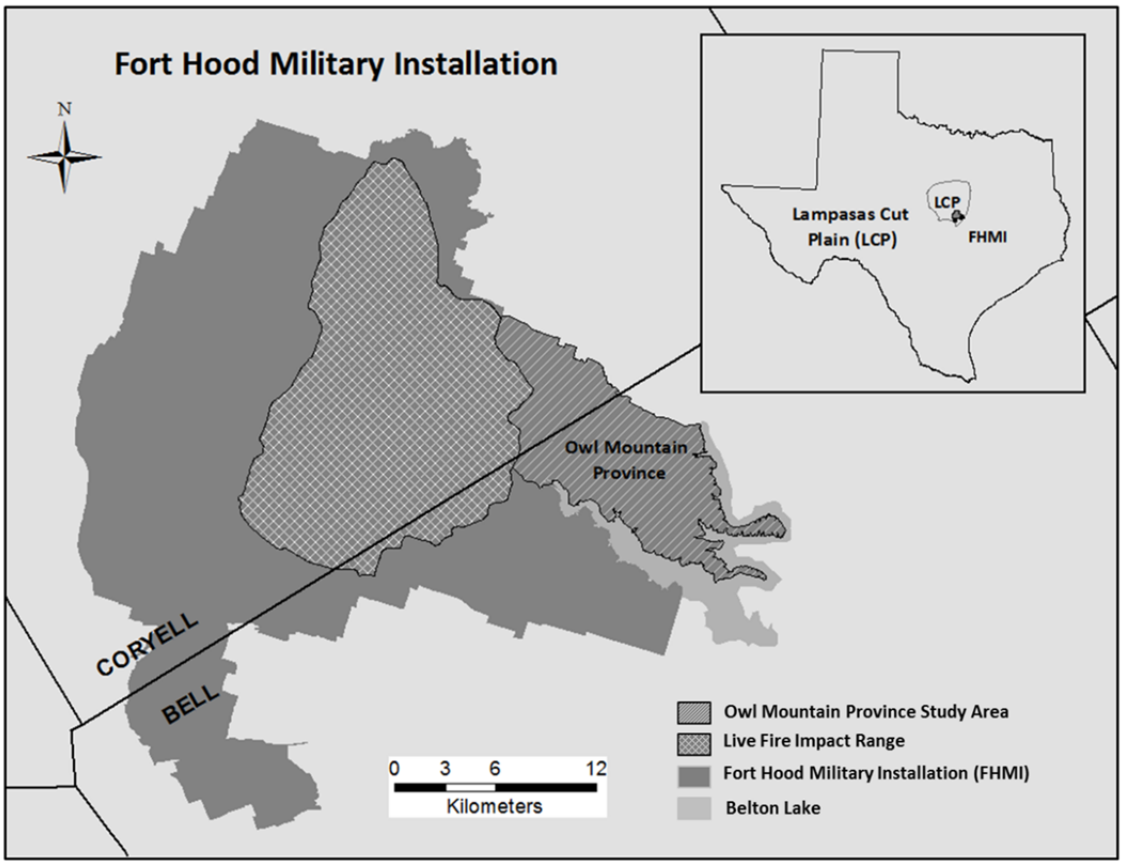

Figure V.3. The Owl Mountain Province is the northeastern peninsula of the Fort Hood Military Installation. The area is used for troop maneuvers and training, as well as endangered species habitat and grazing acreage.

through urbanization, infrastructure support for the burgeoning population, and agriculture.

The installation was established in 1942, with most of the land appropriated from rural land owners under authority of eminent domain after the United States entered World War II (Pugsley 1992). Today, the installation is the largest active duty armored post in the U.S. Armed Services. It is home to two full divisions, 1st Cavalry Division and 4th Infantry Division, supports 12 additional units, and is home to approximately 41,000 soldiers and their families (Hayden *et al.* 2001). The administrative section of the installation is located in the south-central portion, surrounded by training areas used by the U.S. Army for dismounted and wheeled exercises, and tracked vehicle training (Hammer 2011). Training lands on the installation are divided into three major areas; West Fort Hood is primarily used for heavy mechanical (tracked and wheeled) maneuver training; the terrain is rolling and isolated mesas are present. The Live Fire Impact Range is located in the center of the installation and is used for pyrotechnic training. East Fort Hood is used primarily for dismounted and wheeled exercises, and some small-scale tracked vehicle training. Here, the terrain is more rugged than other areas with steep scarps and canyons (Hammer 2011; Hayden *et al*. 2001).

Vegetation and soil disturbance resulting from military activities also maintains much of the vegetation in early succession, particularly evident in the training areas in West Fort Hood, the Live Fire Impact Range, and parts of East Fort Hood (Hammer 2011; Teague and Reemts 2007). More remote areas of the eastern side typically support

later successional vegetation, with disturbance in these areas associated with the cutting of vegetation, construction of individual fighting positions ("foxholes"), road maintenance, and other activities associated with dismounted training (Teague and Reemts 2007). Many of these training areas are multi-use facilities with areas are set aside as endangered species habitat and recreational areas for military families. The Army also allows other non-military uses of Fort Hood lands such as fishing, hunting, and grazing. These uses, together with military training, affect the soil, water, vegetation and animals that occur on the installation (Hayden *et al*. 2001).

Pre-settlement vegetation on Fort Hood was characterized by tallgrass and midgrass prairies dominated by little bluestem (*Schizachyrium scoparium*)and Texas wintergrass (*Nassella leucotricha*) among other grasses, and forests, woodlands and shrublands variously dominated by Texas red oak (*Quercus buckleyi*), shin oak (*Quercus sinuata* var. *breviloba*), Ashe juniper (*Juniperus ashei*), Texas live oak (*Quercus fusiformis*) and post oak (*Quercus stellate*) (Van Devender and Spaulding 1979). Historically, fire, climate, native grazing and edaphic factors all played a role in maintaining an open structure in flat to rolling uplands of the Fort Hood landscape (Fuhlendorf and Smeins 1996; Sullivan 1993; Smeins 1980). Denser forests of deciduous trees and Ashe juniper were likely restricted to side slopes and canyons (Diamond 1997). Succession after land-clearing and loss of these natural processes resulted in a shift toward a more closed canopy, with an increase in woody species such as *J. ashei,* and decrease in native grass cover (Smeins 1980).

Since the establishment of Fort Hood in the 1940s, the area has undergone extensive land use changes associated with military training (Freeman *et al*. 2001). Vegetation communities on the installation are heterogeneous and patchy, often intergrading abruptly amongst different types. Woody vegetation is characterized by contiguous, closed-canopy, Ashe juniper-oak (*J. ashei-Quercus* spp.) forests on mesa slopes, tops, and canyons, with some post oak/blackjack oak (*Q. stellata/Quercus marilandica*) forests (Teague and Reemts 2007). Shin oak (*Q. sinuata* var. *breviloba*) shrubland/grassland matrices are found where wildfire has occurred. Expansive, open grasslands occur on some valleys and rolling uplands, and in small patches near and amongst mesa forest/shrubland stands (Hammer 2011). Grassland/plateau live oak (*Q. fusiformis*) savannas occur on some rolling uplands. Riparian corridors are characterized by juniper-oak forests and forest belts of southern pecan (*Carya illinoinensis*), walnut (*Juglans* spp.), American sycamore (*Platanus occidentalis*), eastern cottonwood (*Populus deltoides*), bur oak (*Q. macrocarpa*), black willow (*Salix nigra*), and red elm (*Ulmus rubra*) trees (Teague and Reemts 2007; Figure V.4).

Training on Fort Hood is the primary cause of wildfires on the installation, particularly in the Live Fire Impact Range. Tracers, incendiary devices, smoke generators, and other pyrotechnic devices provide a year round source of ignition (Hayden *et al*. 2001). Under certain conditions, training related wildfires occur almost daily in the Live Fire area, which serves to maintain large expanses of grassland and fire-adapted vegetation in this area. In February 1996, three grass fires were ignited by

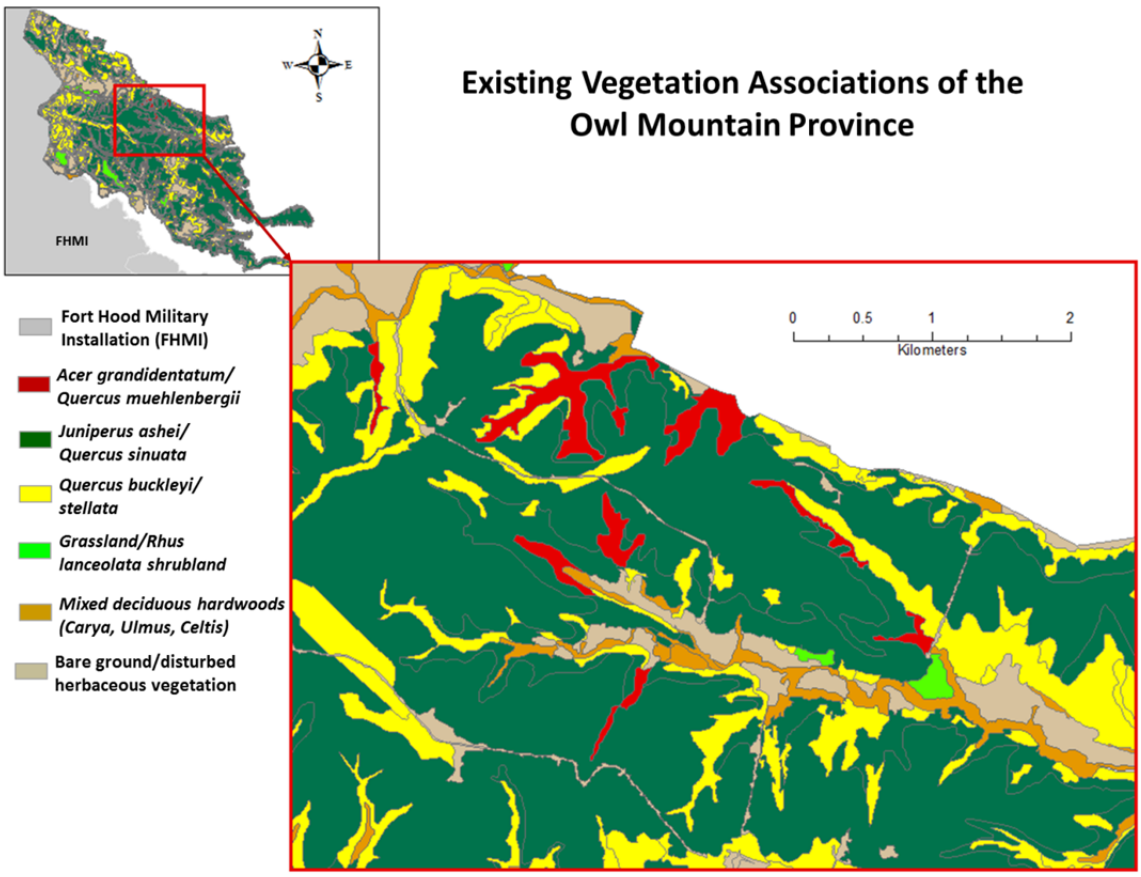

Figure V.4. Vegetation associations found in the Owl Mountain Province (modified from Hammer 2011 and Teague and Reemts 2007).

military training activities and spread into the adjacent oak-juniper woodlands as crown fires. The fires burned for over two weeks and consumed more than 4,000 hectares of woodland, eventually burning 2,728 hectares of endangered species habitat (Hammer 2011; Reemts and Hansen 2008; Hayden *et al*. 2001). Areas historically dominated by grassland in the training areas of East and West Fort Hood have fewer, less intense fires because of the effects of vehicle traffic and grazing on reducing fuels (Hammer 2011). These areas either remain in early successional vegetation (annual forbs and grasses) due to frequent disturbance or are invaded by Ashe juniper in areas where disturbance is less frequent or intense (Teague and Reemts 2007).

Ecohydrology of *Acer grandidentatum*

A. grandidentatum is a small, deciduous hardwood tree indigenous to North America; these trees exist as a continuous population from southern Idaho through the Wasatch Mountains of Utah (Tollefson 2006). Within the continuous range, its life form is dependent upon the moisture regime and varies greatly within elevation limits, occurring on both xeric and mesic sites. In canyon bottoms and along streams, trees with single or multiple trunks can grow up to 15m tall and 30cm in diameter (Phillips and Ehleringer 1995). On dry canyon slopes, it grows primarily as a shrub with two or more stems reaching 8m tall. It often grows with Gambel oak (*Quercus gambelii*) either as a co-dominant, or replacing Gambel oak in canyon bottoms and moister areas. In this environment, bigtooth maple is considered an early to late successional species in

riparian communities throughout Utah (Phillips and Ehleringer 1995). Bigtooth maple leafs and flowers earlier and grows faster in stem and crown diameter than Gambel oak, thus becoming more important in the canopy over time. On cooler sites, bigtooth maple may replace Gambel oak entirely, but further succession could lead to dominance by white fir (Tollefson 2006). Historically, the oak/maple cover type is believed to have had fire return intervals of about 40-60 years of primarily stand-replacing fires (Havlina 2003). Over the past 200 years, fire regimes have been suppressed by settlement and grazing removal of fine fuels (Bradley *et al*. 1991); as a result, oak/maple stands may be more extensive than they were 75 to 150 years ago (Corbin and Page, 2011). Bigtooth maple can also be found as isolated populations at lower latitudes throughout the southwestern United States and into northern Mexico, including incised canyons within the Fort Hood Military Installation (Tollefson 2006; Riskind and Diamond 1986; Gehlbach and Gardner 1983).

Bigtooth maple develops an extensive root system during the first growing season, with both lateral roots and a deep tap root (Alder *et al*. 1996). It is relatively tolerant of low soil water potentials, and can grow with oaks on drier, open slopes (Tollefson 2006; Correll and Johnston 1970). It is considered drought tolerant, with plants requiring 40-50cm of annual precipitation. Precipitation is the most important water source for small trees (<20cm dbh) located away from streams, while stream water is most important for small trees adjacent to the stream (Phillips and Ehleringer 1995). Larger trees (>20cm dbh) do not use stream water even if they are adjacent to the stream.

Roots are distributed throughout soil profiles, but active sites of water absorption are in the deeper soil horizons. Recent studies (Phillips and Ehleringer 1995; Flanagan *et al.* 1992; Ehleringer *et al.* 1991; Donovan and Ehleringer 1991;) indicate that a number of perennial plant species do not significantly utilize summer precipitation, rather these species, including bigtooth maple, rely on deep soil water that originates from winter recharge of soil profiles. Many species with large geographic ranges exhibit adaptations to local environments, including variations in morphology, gas exchange, and plant-water relations (Bsoul *et al.* 2006). Further south, where winter recharge from snowpack is non-existent, these trees may be relying on ascending fluids from deeper seated water tables and aquifers (Faulkner *et al.* 2016a).

Literature is somewhat lacking on the physiological attributes of these disjunct populations, but some parallels may be drawn between the stand dynamics of continuous and isolated populations. As they do in their continuous range, isolated populations of bigtooth maples within the Owl Mountain Province can exist on xeric and mesic sites as a shade tolerant, seral understory tree or shrub beneath Ashe juniper or a variety of oak species, and/or as co-dominant with other hardwoods such as pecan, sugarberry, elm, and oaks, particularly *Quercus muehlenbergii* and *Quercus buckleyi* (Hammer 2011; Teague and Reemts 2007).

Study Area

The Owl Mountain Province is located in the northeastern section of the Fort Hood Military Installation; the province is approximately 90 km^2 and is bounded by Owl Creek to the north, Belton Lake to the east, Cowhouse Creek to the south and the Live Fire Impact Range to the west (Figure V.3). The province is a multi-use facility and is utilized by the U.S. Army for troop maneuvers with the southern and western sections having been extensively modified by road construction and military training infrastructure. The terrain is rugged and dominated by xeric, plateaued drainage divides hosting thick, scattered clusters of Ashe juniper, Texas ash (*Fraxinus texensis*), and *Q. buckleyi* (Hammer 2011; Teague and Reemts 2007). Where the landscape has been partially denuded, cacti and shrubs such as prairie sumac (*Rhus lanceolate*) and false willow (*Baccharis neglecta*) grow in small sinks and fractures where meteoric water resources are focused. The northern and eastern sections are more remote with acreage set aside as grazing land and wildlife habitat (Pekins 2012; Hammer 2011; Hayden *et al*. 2001). This area is also home to several protected avian species such as Golden-cheeked Warbler (*Dendroica chrysoparia*) and Black-capped Vireo (*Vireo atricapilla*); and much of the eastern section of the province is left mostly undisturbed by military activities as endangered species habitat (Picinich 2011). The plateaus are bordered by steep scarps and incised canyons along the edges of the plateaus hosting mesic woodland species such as pecan (*C. illoinensis*), Texas cedar elm (*Ulmus crassifolia* Nutt.), Chinkapin oak (*Quercus muehlenbergii*), sugarberry (*Celtis laevigata*), Edwards Plateau Sedge (*Carex*

edwardsiana), and bigtooth maple (*A. grandidentatum*) (Hammer 2011; Teague and Reemts 2007; Figure V.4).

The soils of the study area were developed over Lower Cretaceous carbonate rocks from the Fredericksburg Group, namely the Walnut, Comanche Peak, and Edwards limestones and marls (Barnes 1970). The lower valleys along established drainage are covered by deeper, alluvial soils from the Topsey (BtC2) and Denton (DeB) soil series; these soils range from fine-silty to fine-loamy carbonatic, thermic, udic calciustolls and were derived over the Walnut and lower members of the Comanche Peak clays and marls (NRCS 2012; Picinich 2011). The incised canyons and steeper scarps contain rocky, alluvial soils from the Real-Rock outcrop complex (REF) formed over the upper members of the Comanche Peak, a loamy-skeletal carbonatic, thermic, shallow, typic calciustoll. The upland plateaus are mantled by shallow, residual soils (<30cm) from the Eckrant Series (ErB), a clayey-skeletal smectitic, thermic, lithic haplustoll formed over the resistant Edwards limestone (NRCS 2012; Fowler and Simmons 2008). The soils are dark colored, calcareous, and moderately alkaline with textures ranging from loamy to clayey, depending on the substrate and profile development. In established maple habitat, Real-Rock soils are characterized as gravelly, clay loam, forming on slopes ranging up to 40 degrees (NRCS 2012). The typical soil profile is less than 45cm deep with a low available water capacity (<3.5cm) (NRCS 2012; Picinich 2011).

Continuous geologic and hydrologic sampling has been on-going in the study area since September 2011. Water chemistry from surface springs atop the plateau document a

meteoric origin for much of the flowing water at the surface. These springs are flowing within the Edwards, and do not appear to be connected with soil moisture associated within established maple habitat (Faulkner *et al*. 2016a). Climate has varied greatly during the study period with lower than average precipitation over the past several years as Central Texas experienced a moderate to severe drought (United States Drought Monitor 2015; Figure V.5). Although no water was observed flowing within established maple habitat, there may be some instances where deeper seated phreatic or semi-confined hypogenic waters migrate upwards to augment soil moisture in these sites (Faulkner *et al*. 2016b)

Methodology

The Nature Conservancy and the Fort Hood Natural Resources Management Branch conducted vegetation surveys within the installation in 1996 and 2011, respectively (Hammer 2011; Teague and Reemts 2007; The Nature Conservancy 2003). These surveys were part of a larger monitoring and management action for threatened and endangered avian species habitat required as the result of several biological opinions issued to the U.S. Army by the U.S. Fish and Wildlife Service (Hayden *et al*. 2001). As a result of these surveys and aerial photograph interpretation, nine distinct areas of *A. grandidentatum* habitat were delineated within the Owl Mountain Province (Figure V.4), covering approximately 71 hectares (Hammer 2011; Teague and Reemts 2007; Table V.1). In order to determine the spatial distribution of *A. grandidentatum* within the

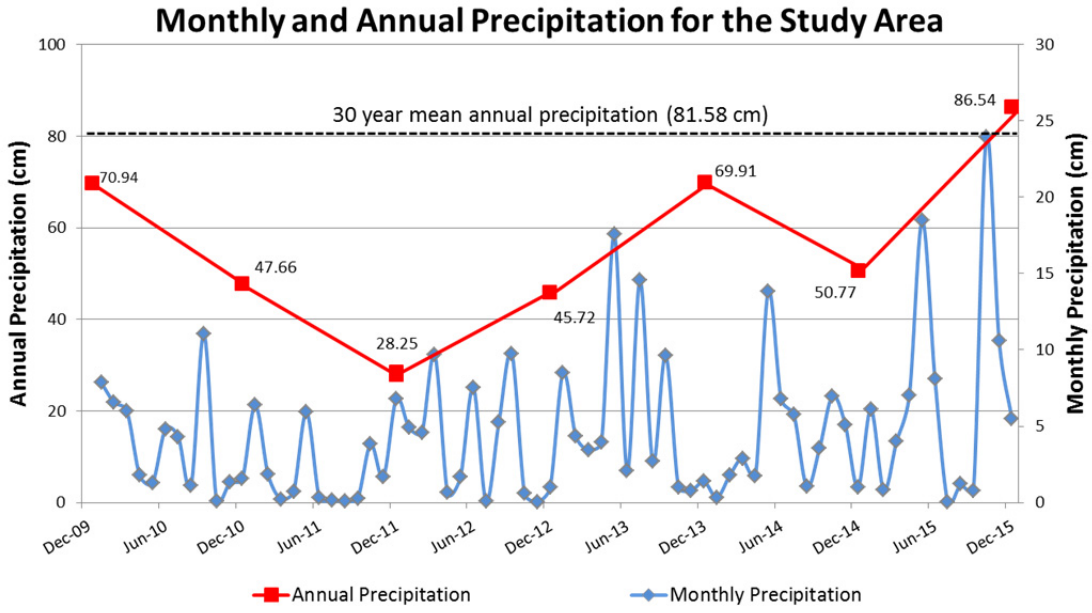

Figure V.5. Historical monthly and annual precipitation for the study area. Precipitation data sourced from Weather Underground for the cities of Belton, Gatesville, Temple, and Killeen, and Fort Hood airfield. Precipitation from these five weather stations was averaged to determine the mean precipitation for the study area. Data accessed on 12/30/2015.

designated habitat, fifty-four 78.5m^2 nested circular plots were established to inventory woody species and emergent vegetation. All woody species within a 5m radius plot greater than 6m in height were measured for diameter at breast height (dbh) and identified; all emergent woody vegetation were identified and counted within a 3m radius plot. Field data from the plots were used to determine the number of maple trees per hectare (TPH), basal area per hectare (BAPH), and the stems per hectare (SPH) for each designated maple habitat. In addition to the inventory, environmental parameters such as

Table V.1. Original bigtooth maple habitat as delineated by Fort Hood vegetation surveys (Hammer 2011; Teague and Reemts 2007)

Fort Hood Field ID	Vegetation Association	Source	Hectares	# of Plots	Plot Area (m^2)	Total Plot Area (m^2)
0	*Acer grandidentatum Quercus muehlenbergii Carex edwardsiana*	1996 transect 3	3.41	5	78.5	392.50
1	*Acer grandidentatum Quercus muehlenbergii Carex edwardsiana*	map validation 50; 1996 transect 45	7.39	5	78.5	392.50
46	*Acer grandidentatum Quercus muehlenbergii Carex edwardsiana*	map validation 262; 1996 transect 104	14.21	10	78.5	785.00
215	*Acer grandidentatum Quercus muehlenbergii Carex edwardsiana*	1996 transect 96	4.04	4	78.5	314.00
369	*Acer grandidentatum Quercus muehlenbergii Carex edwardsiana*	mvp 370; observation point ER74	5.79	4	78.5	314.00
389	*Acer grandidentatum Quercus muehlenbergii Carex edwardsiana*	1996 transect 38, 39, & 40	1.39	2	78.5	157.00
476	*Acer grandidentatum Quercus muehlenbergii Carex edwardsiana*	map validation 178; 1996 transect 38, 39, & 40	25.77	16	78.5	1,256.00
483	*Acer grandidentatum Quercus muehlenbergii Carex edwardsiana*	1996 transect 115	3.54	4	78.5	314.00
560	*Acer grandidentatum Quercus muehlenbergii Carex edwardsiana*	1996 transect 109	5.51	4	78.5	314.00
	Totals		**71.03**	**54**		**4,239.00**

elevation, aspect, canopy characteristics, geologic materials, snags, and other general site descriptions were recorded. Soil samples were collected from each plot and processed in the SFA Soil, Plant & Water Analysis Laboratory to determine soil pH, conductivity, and particle size analysis.

Once the initial data had been processed, new potential maple habitat was delineated using the remote sensing application ERDAS to isolate the spectral intensity of *A. grandidentatum*. A Landsat 8 short-wave infrared vegetation map (Figure V.6) was obtained from the U.S. Geological Survey and the spectral signatures for bigtooth maple were isolated (Figure V.7). Locations where the spectral intensity remained were used as a remote sensing model to locate existing but as yet undocumented *A. grandidentatum* habitat in the Owl and Bear Creek watersheds. Vegetation mapping in modeled habitat documented an additional 129 hectares of *A. grandidentatum* habitat located in ten distinct stands. Sixty-one additional 78.5m^2 nested plots were established in these new stands to inventory population dynamics of woody and emergent vegetation. Independent-samples T-tests were conducted to determine the differences between stand dynamics with regards to *A. grandidentatum, J. ashei,* and other hardwoods in established and modeled vegetation stands within the Owl Creek and Bear Creek watersheds at $\alpha = 0.05$.

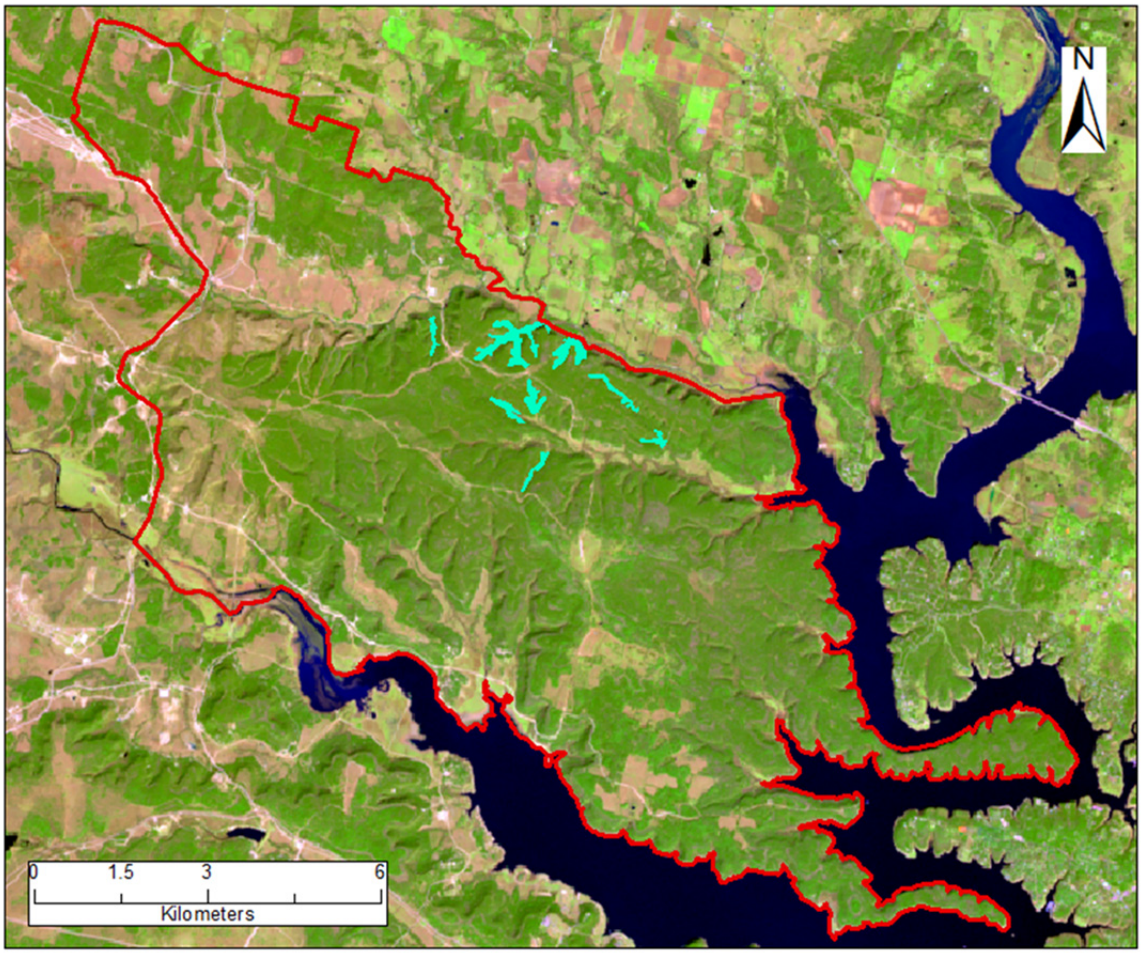

Figure V.6. Landsat 8 short-wave infrared image from U.S. Geological Survey database accessed on January 22, 2016; image captured on June 7, 2015. Designated maple habitat is highlighted.

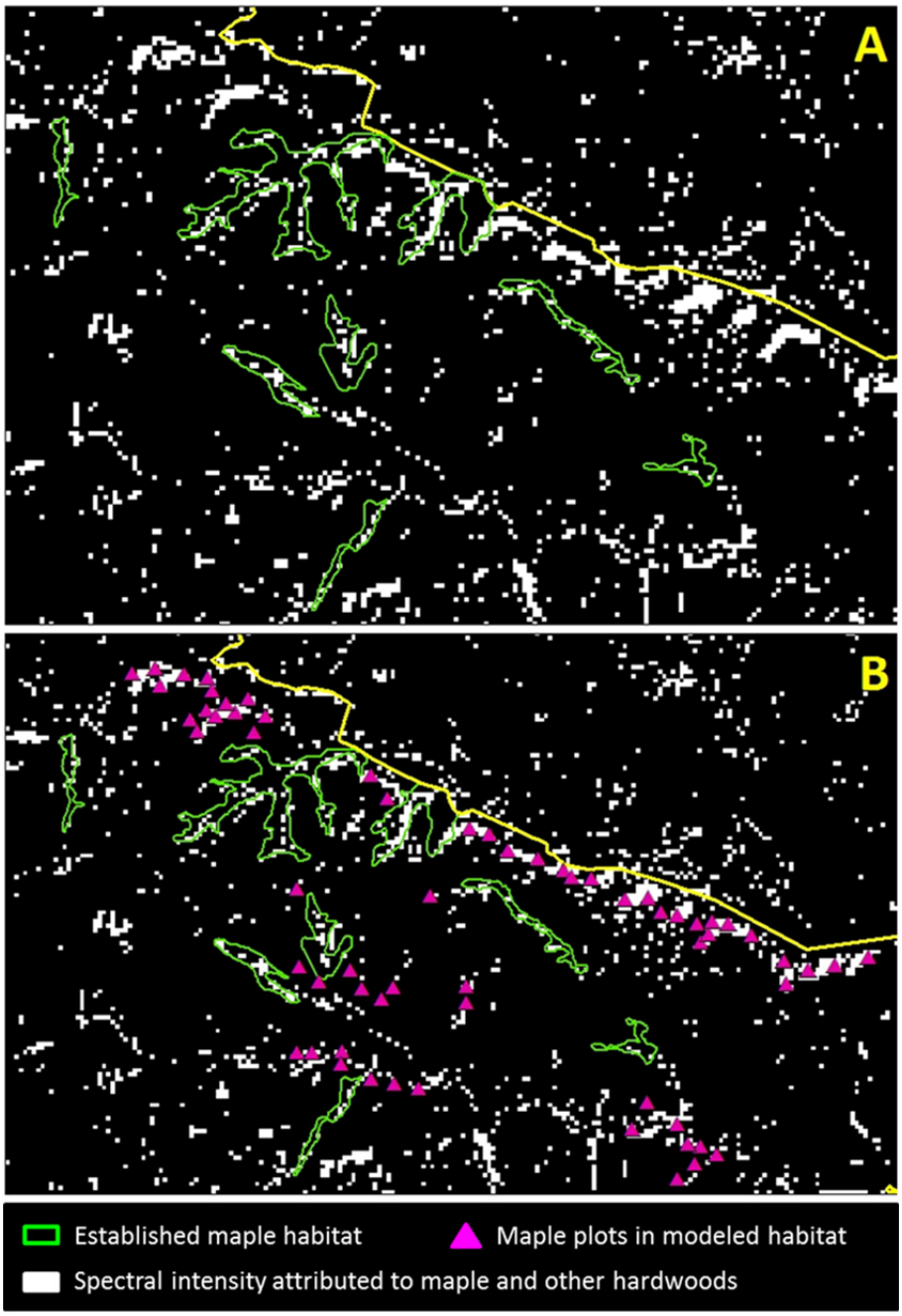

Figure V.7. ERDAS model used to delineate additional maple habitat. The shapefile for established maple habitat was used to isolate the spectral intensity attributed to bigtooth maple and other hardwoods (A). Mapping yielded 61 additional vegetation plots within newly defined maple habitat as well as 3 isolated occurrences (B).

Results and Discussion

Most of the originally established *A. grandidentatum* habitat was delineated within incised canyons along the scarps of the Owl and Bear Creek watersheds (Figure V.4) by transect surveys and aerial photography (Hammer 2011; Teague and Reemts 2007); vegetation associations were documented, but population dynamics were not recorded or described in the original vegetation surveys. Some of these canyons are located in remote areas of the installation, away from sections of the training areas utilized by the U.S. Army for troop maneuvers (Hammer 2011). Site conditions in these existing habitats can be described as mesic, narrow, slot canyons and/or semi-sheltered woodlands where *A. grandidentatum* can exist as co-dominant trees with a variety of oaks and elms or as part of the lower canopy. In some of the delineated maple habitat, *A. grandidentatum* is found with *J. ashei*, but in these areas, the maples are not dominant and only expressed in the understory. In areas where canopy openings have occurred as a result of snags and mortality, larger oaks (*Quercus spp.)* dominate the canopy with *A. grandidentatum* regenerating in the understory. Many of these sites also function as wildlife habitat, particularly for foraging species such as feral pigs (*Sus scrofa*), and soil disturbance is abundant. Unless the canopy opening has been recent, most of the canopies are closed with little cover by grasses and forbs.

These established sites exist today with a variety of aspects: north, northeast, south, and southeast (Figure V.8); and although these areas are associated with stream drainage, ephemeral water flows only after major precipitation events. Most meteoric

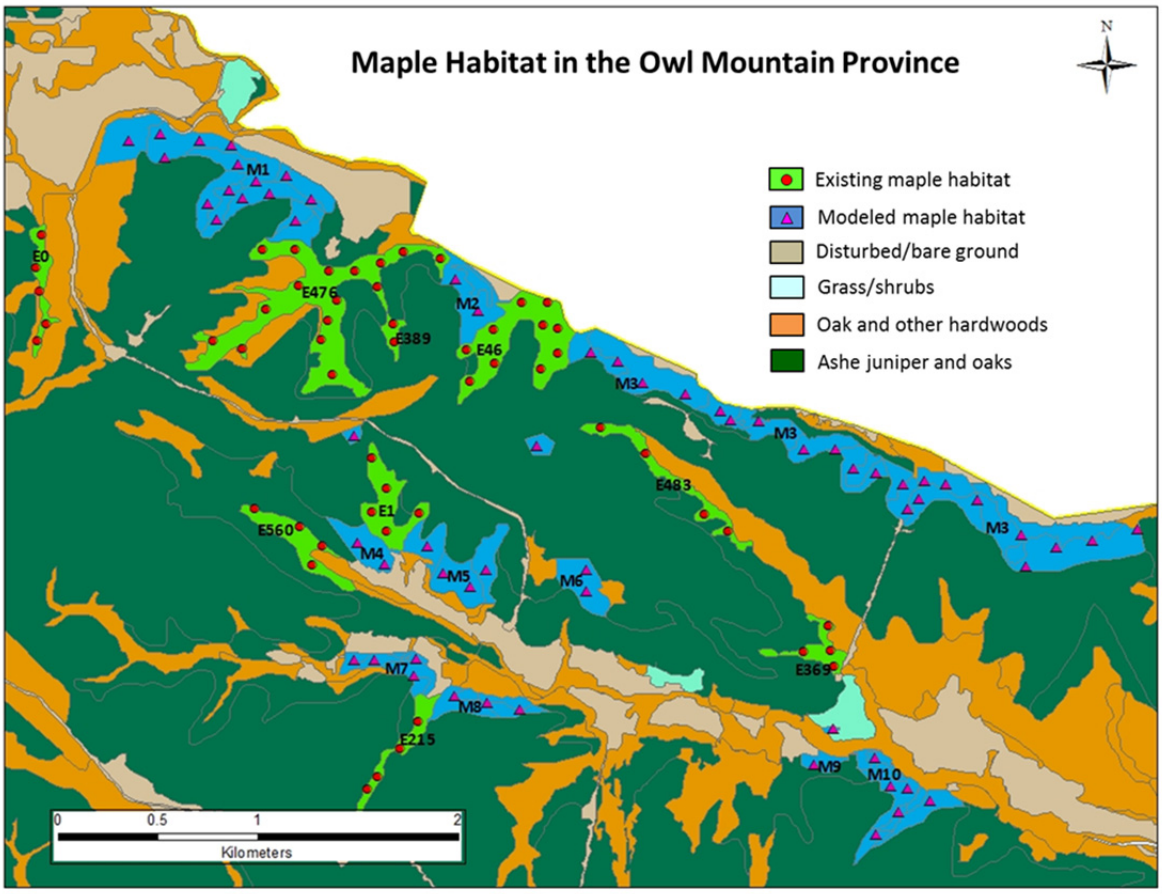

Figure V.8. Designated stands and plot locations in established and modeled maple habitat.

water is communicated directly into and discharges from the overlying Edwards; no existing springs or seeps have been documented in established or modeled maple habitat (Faulkner *et al*. 2016a). Slopes within these canyons range from less than 5° near stream channels to over 40° closer to the scarps (NRCS 2012). The terrain is rocky with shallow soils (<45 cm); rock falls are common as are snags and tree falls related to erosion of the over-steepened scarps. Soil samples collected during vegetation sampling were found to have a pH range from 7.7 to 8.3 with a mean pH of 8.2. Soil conductivity ranged from 181 to 565, with a mean of 304 μs/cm. Soil texture was analyzed using the Bouyoucos Method and the particle analyses are found in Figure V.9. These soils are well drained and found along rocky slopes associated the Comanche Peak limestone and marl.

Results from vegetation sampling in established *A. grandidentatum* habitat can be found in Table V.2. There was a significant difference in the stand dynamics with respect to maple and hardwood trees per hectare between the Owl Creek and Bear Creek watersheds; maples and hardwoods represent 80% of the trees per hectare in the Owl Creek watershed and only 61% of the TPH in the Bear Creek watershed. The Bear Creek watershed also contains more Ashe juniper (39%; M=212.31 TPH) than Owl Creek (20%; M=131.25 TPH). The Owl Creek habitat represents a more mature stand, with oaks and maples well represented in the canopy (80%) and understory (87%). The Bear Creek watershed is more fragmented by roads and heavily traveled by military and civilian vehicles; grasslands are grazed by cattle and other wildlife. In the Bear Creek plots, Ashe juniper represents over 34% of the basal area per hectare (M=4.07 m^2

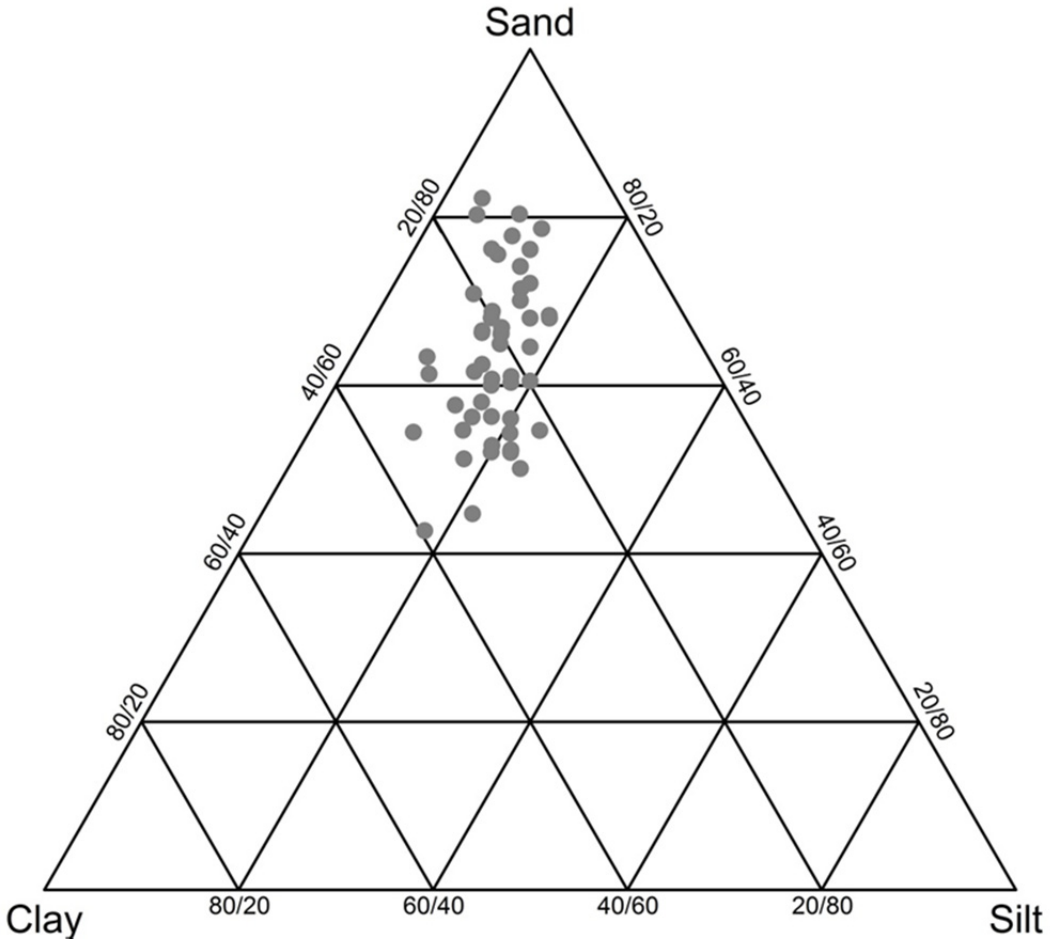

Figure V.9. Particle size analyses for soil samples from original 54 vegetation plots in established maple habitat.

Table V.2. Comparison of established vegetation plots within the Owl and Bear Creek watershed. Independent-samples T-tests were conducted at α=0.05.

Watershed Comparison between established plots	Mean		df	*P*
	Owl Creek (n=33)	Bear Creek (n=21)		
Bigtooth maple				
Trees per hectare	274.08	181.98	39	0.0613
Basal area per hectare (m^2)	4.37	3.18	32	0.1495
Stems per hectare	2808.42	2189.77	40	0.0513
Ashe juniper				
Trees per hectare	131.25	212.31	36	0.0330
Basal area per hectare (m^2)	1.88	4.07	27	0.0129
Stems per hectare	782.50	1482.31	33	0.0264
Other hardwoods				
Trees per hectare	247.06	151.65	41	0.0032
Basal area per hectare (m^2)	5.99	4.59	35	0.1438
Stems per hectare	2594.03	2240.30	29	0.4279

BAPH) *versus* 15% in the Owl Creek watershed (M=1.88 m^2 BAPH). These disturbances can increase competition between established vegetation communities with pioneer species such as *J. ashei* colonizing on recently opened sites. In the understory, maples and other hardwoods produce more emergent vegetation, but *J. ashei* may be more successful at establishing on marginal sites and would have an advantage when competing for resources and growing space on disturbed sites. Ashe juniper stems per hectare in the Owl Creek sites (M=782.50 SPH) represented 12% of the understory and 25% of the understory in the Bear Creek sites (M=1482.31). Statistical analyses of the established plots between watersheds revealed a significant difference between Ashe juniper populations regarding trees per hectare ($p<0.0330$), basal area per hectare ($p<0.0129$), and stems per hectare ($p<0.0264$). Other hardwoods trees per hectare also reported a significant difference ($p<0.0032$). All other parameters were not significantly different, ($p>0.05$).

Recent vegetation mapping in modeled maple habitat expands the range of *A. grandidentatum* well out of these sheltered canyons, along open scarps with a north, northeast and southwest aspect (Figures V.7 and V.8). Much of the newly delineated *A. grandidentatum* occurrences are along the northern border of the installation and exist as the southern scarp of the Owl Creek watershed. This scarp trends northwest/southeast and connects modeled *A. grandidentatum* habitat with previously established maple vegetation (Figure V.8). These newly delineated sites are more open, with *A. grandidentatum* existing as a dominant species in the canopy and understory (Table V.3).

Table V.3. Comparison of modeled vegetation plots within the Owl and Bear Creek watershed. Independent-samples T-tests were conducted at α=0.05.

Watershed Comparison between modeled plots	Mean		df	*P*
	Owl Creek (n=39)	Bear Creek (n=22)		
Bigtooth maple				
Trees per hectare	460.56	347.42	53	0.0001
Basal area per hectare (m^2)	5.78	5.75	47	0.9583
Stems per hectare	3473.83	2765.54	50	0.3764
Ashe juniper				
Trees per hectare	195.98	191.08	57	0.8407
Basal area per hectare (m^2)	2.81	3.03	52	0.6075
Stems per hectare	979.57	1816.90	42	0.0003
Other hardwoods				
Trees per hectare	58.79	104.23	49	0.1421
Basal area per hectare (m^2)	0.99	1.83	39	0.1076
Stems per hectare	943.29	1447.09	55	0.0004

J. ashei is present, but not dominant along the open scarps. *A. grandidentatum* habitats along these scarps are bordered by *J. ashei* and various hardwoods on the lowlands along the roads at the edges of open grasslands, as well as along the top of the plateaus. The Owl Creek watershed contains more area of newly delineated maple habitat (87 hectares) while the Bear Creek watershed only has 42 hectares; the new Bear Creek habitats are primarily associated with existing maple habitat, but are less extensive due to the isolated nature of the previously established and modeled habitats (Figure V.8).

Newly delineated maple plots associated with the Owl Creek and the Bear Creek watersheds were compared to determine if there was a significant difference in maple habitat between the two watersheds (Table V.3). Maple trees represented 64% of the trees per hectare in the Owl Creek watershed (M=460.56 TPH) and 60% of the basal area per hectare (5.78 m^2 BAPH); basal area per hectare of other hardwoods was not as prominent in modeled habitat, representing less than 11% in the Owl Creek watershed (M=0.99 m^2 BAPH). The Owl Creek sites may represent a later successional habitat with maples out-competing oaks in these more open sites just as they do in their continuous populations; maples are shade tolerant and can adapt to more xeric environments and lower soil water potentials, particularly during periodic droughts. Within the Bear Creek watershed, maples represented 54% of the trees per hectare (M=347.42 TPH) and basal area per hectare (5.76 m^2 BAPH); other hardwoods represented 17% of the basal area per hectare (M=1.84 m^2 BAPH). The Bear Creek sites experience greater disturbance and represent

habitat where competition between Ashe juniper (28%, M=3.03 m^2 BAPH) and hardwoods is still present; reflected in the basal area per hectare of Ashe juniper.

Understory dynamics within the newly delineated plots also support a later successional habitat for the Owl Creek watershed as maple stems represent 64% of the understory (M=3473.83 SPH). Other hardwoods represent 17% of the stems per hectare (M=943.29 SPH) and Ashe juniper represent 18% of the understory, (M=979.57 SPH). Understory dynamics for other hardwoods are not expressed in the canopy, supporting maples competitive edge when competing for resources on marginal sites. In the Bear Creek watershed, maple stems per hectare represent 45% of the understory (M=2765.54 SPH) and other hardwoods represent 24% (M=1447.09 SPH). Ashe juniper represents 30% of the stems per hectare (M=1816.90 SPH), reflecting the competition between species on these more fragmented and disturbed sites. Statistical analyses of the modeled plots between watersheds revealed a significant difference between maple trees per hectare ($p<0.0001$), Ashe juniper stems per hectare ($p<0.0003$), and other hardwoods stems per hectare ($p<0.0004$). All other parameters were not significantly different, ($p>0.05$).

Bigtooth maple provides browse for wildlife and livestock, but is generally consumed in small to moderate amounts. Its forage value is “fair” as its tall growth form limits forage availability (Tollefson 2006). Grazing acreage within the Owl Mountain Province supports cattle (Hayden *et al*. 2001), but these animals tend to remain within the Bear Creek watershed and on the plateaus where grasses are more abundant; many do not

forage along the more isolated scarps of the Owl Creek watershed, away from their supplemental feed sources provided by ranchers and as such, herbivory by cattle may affect maple populations within the Bear Creek watershed disproportionally with respect to the Owl Creek watershed.

Acer grandidentatum in the Owl Mountain Province

Long-term climatic changes in the region, including drought and warmer temperatures, have affected the fluctuating water table and moisture availability for these populations. Even though this area has experienced a drought over the past few years, these *A. grandidentatum* populations have been able to receive moisture from occasional precipitation and deeper seated fluids that rise due to porosity differences in underlying lithologies (Faulkner *et al*. 2016a). In karst regions, matrix porosity associated with lithofacies variation and solutional porosity associated with regional deformational events transmit deeper seated fluids to mesic sites to augment soil moisture. While established *A. grandidentatum* habitat was confined to narrow canyons, newly delineated habitat follows regional deformation trends along open scarps (Faulkner 2016b). Soils in established and new habitats are rocky and well drained, rock outcrops within these sites are common, and meteoric inputs are generally transmitted directly into the subsurface through karst conduits such as sinkholes, joints, and surface caves (Faulkner 2016b). The underlying geologic material derived from the Comanche Peak is interbedded with the overlying Edwards limestone along these scarps and can provide confining layers that

force ascending fluids to discharge along these scarps to provide moisture to support mesic vegetation communities. Meteoric inputs are most often received by and transmitted through the overlying Edwards; since the Edwards has a much greater porosity than the Comanche Peak, it may not provide additions to the water table to affect these communities (Faulkner 2016a; Figure V.10). Unless woody plants have access to a relatively large perched water table, all roots on karst may function as "shallow roots" allowing them to tolerate large variations in root zone water potential (Querejeta *et al*. 2007). Water relations on karst sites are quite complex; highly fractured rocks with solution to vuggy to cavernous permeability can enjoy wide fluctuations in water availability and woody plant growth in these regions must adapt to this highly variable water regime. Within the Owl and Bear Creek watersheds, the structural development of lineament trends controlling fluid transmission are expressed as cave development in the subsurface, joints in outcrop, stream segment orientation, and lithologic porosity differences that determine the general transmission of ascending fluids in the study area to augment soil moisture (Faulkner *et al*. 2016b). These trends are one of the primary controls on areas where maples exist, as well as anthropogenic and natural disturbance (Figure V.8).

Reproduction and regeneration is necessary to sustain maple habitat, and *A. grandidentatum* can reproduce sexually; flowers on the plant appear along with leaves every two to three years, generally after colder, wet winters. The flowers are either male or female and plants may bear male flowers only or produce both male and female

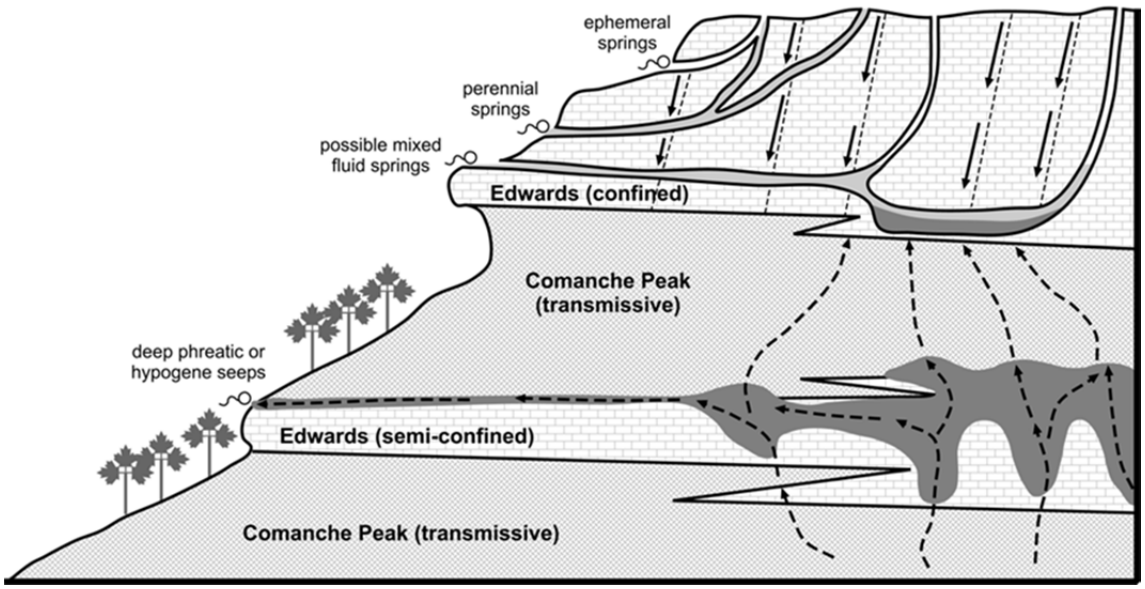

Figure V.10. Hydrogeologic model of maple habitat within the Owl Mountain Province. Many mesic vegetation sites exhibit no surface flow; these sites are maintained by phreatic and/or hypogenic water resources that augment soil moisture.

flowers on the same inflorescence. Flowers may be bisexual initially, with ultimate sexual expression linked to environmental factors such as moisture or temperature (Tollefson 2006). Flower sex ratios differ between mesic and xeric sites and also from year to year in response to climatic changes. Research in maple communities in northern Utah showed that plants produced more female flowers during wet years and on mesic sites and more male flowers during dry years and on dry sites (Tollefson 2006).

The fruit of *A. grandidentatum* is a double winged samara that typically contains only one seed. Maples in the mountain brush zone of Central Utah produce an estimated 235,000 samaras and their abundance varies by elevation (Tollefson 2006). Reproduction by seed is most important for establishment of *A. grandidentatum* in new areas and seeds germinate more readily when they have dispersed farther from parent trees. Sexual reproduction also increases genetic variability but may be suppressed by climate fluctuations and breeding population proximity (Donovan and Ehleringer 1994)). Seed dispersal within the Bear Creek watershed might not be as successful as many of these sites are quite fragmented and have experienced greater disturbance by wildlife, grazing, and military and civilian traffic. The Owl Creek watershed is more remote and the roads within it are significantly less traveled, providing a more optimum environment for maple regeneration and seed dispersal.

These trees also reproduce vegetatively, both by layering and sprouting from the root crown. Layering is considered to be a more effective means of stand replacement than seed dispersal and germination and occurs naturally in *A. grandidentatum* when the

lower branches come in contact with the soil and form new roots (Corbin and Page 2011). After the roots have formed the layer may grow independently of the parent plant, or may continue to be attached to it. Layering is common in older plants and is a more effective method of reproduction; studies in Pole Canyon, Utah on five-year old seedlings originating from germinated seeds numbered only 455 plants/hectare while stems originating from layering numbered 4,151 plants/hectare (Tollefson 2006). Sprouting from the root crown is common when the trees have been exposed to disturbance by fire, herbivory, flooding, or broken stems. Rooting behavior by *S. scrofa,* generally thought of as a destructive process, may actually help regenerate *A. grandidentatum* in the understory by encouraging sprouting from the root crown. While both of these asexual methods of reproduction are generally more successful, they reduce genetic variability in both continuous and isolated populations.

Original vegetation mapping had isolated populations confined to narrow canyons within the Owl and Bear Creek watersheds. Recent vegetation modeling and mapping has significantly increased the delineated area where maples exist (Figures V.6 and V.7), and has redefined the site description where these trees can and do thrive. In the newly delineated habitat, maples exist on open, rocky slopes as a dominant species in the canopy and are regenerating in the understory. Reproduction of the maples was thought to occur mostly through layering and sprouting, significantly decreasing their genetic diversity. As a result of this new vegetation model, it appears quite likely that seed

dispersal is responsible for some of the expansion of maple habitat, particularly along the exposed scarps in the Owl Creek watershed.

In addition to open scarps, three random occurrences of *A. grandidentatum* were found on top of the Owl Mountain plateau, in areas where disturbance is much greater and water resources are scarce. These trees were growing in proximity to the road in open areas surrounded by *J. ashei* and scrub oaks and were not associated with any of the established or modeled maple habitat (Figure V.8). It may be that the Fort Hood maples are more resilient than originally thought, as these trees were thriving in areas with shallow soils and in competition for limited water resources atop the plateau.

Recommendations

The spatial distribution of bigtooth maple habitat within the Owl Mountain Province is focused along scarps and incised canyons within the Owl and Bear Creek watersheds. These habitats provide the optimum hydrogeologic and morphologic setting for bigtooth maple to thrive, with the relatively low soil moisture augmented by ascending fluids (Figures V.8 and V.10). Future maple conservation and establishment efforts should be focused in areas where military and civilian traffic can be kept to a minimum, possibly with exclosures to control disturbance from herbivory and grazing. In areas where bigtooth maple is being introduced, some Ashe juniper control might be necessary as long as those controls are balanced with the acreage required to provide endangered species habitat for the golden-cheeked warbler in mature juniper-oak

woodlands. At present, Fort Hood has set aside 88,541 hectares of golden-cheek warbler habitat, some of the largest remaining patches of contiguous breeding habitat in the Lampasas Cut Plain, with the largest expanse in the Owl Mountain Province (Peak 2011; Hayden et al. 2001). Another avenue of future research might include the effects of rooting behavior of feral pigs and their influence on bigtooth maple regeneration as a result of disturbance.

Summary and Conclusions

A. grandidentatum exists as a disjunct, relict population in Central Texas. These isolated populations were presumed to be relicts from the most recent Pleistocene Ice Age; as temperatures warmed and water resources became focused along incising canyons, mesic vegetation communities, including *A. grandidentatum,* contracted to sheltered canyons and woodlands where water resources were focused. In Texas, original site descriptions of these relict vegetation communities were modeled after *A. grandidentatum* populations located in Bandera and Real counties in the Lost Maples State Natural Area. Within the study area, the spatial distribution of *A. grandidentatum* was once thought to be confined to mesic sites in narrow slot canyons within the Owl Mountain Province of the Fort Hood Military Installation.

Recent vegetation mapping in the Owl and Bear Creek watersheds has greatly expanded both the site description and locations where maples exist. Just as they do in continuous populations, within the study area *A. grandidentatum* can grow on open

slopes with oaks and other species that are able to equilibrate to lower soil water potentials. Soil moisture and available water resources for plant uptake are probably augmented by ascending fluids; these deeper phreatic and/or hypogene water resources are transmitted by matrix porosity along the northwest trend of the scarps in the Owl and Bear Creek watersheds, and by solutional porosity along north/south joint trends associated with Balcones deformation (Figures V.8 and V.10).

In the near future, the fire suppression in the Owl Mountain Province may favor the encroachment of pioneer species such as *J. ashei* into disturbed areas. The vegetation in areas designated as maple habitat consists of deciduous mixed-oak hardwood woodlands; in areas that have been disturbed by road building and vegetation removal, *J. ashei* has encroached and may initially out-compete other vegetation for resources. *J. ashei* can uptake, retain and use water very efficiently for a variety of reasons; extensive shallow root systems take advantage of soil waters and deeper tap roots are able to penetrate through fractured bedrock to perched water tables (Huxman *et al*. 2005). In addition, *J. ashei* has a much denser, closed canopy with more available surface area on which precipitation can adhere and eventually be lost to the atmosphere due to evapotranspiration (Thurow and Hester 1997). Since *J. ashei* borders existing maple habitat, it will compete for growing space and resources as disturbance provides encroachment opportunities. While disturbance may appear to favor pioneer species such as *J. ashei*, bigtooth maples are very shade tolerant and able to exist in varying moisture

regimes, allowing them to survive in the understory while patiently waiting for their day in the sun.

Acknowledgements

This research was partially funded by the Arthur Temple College of Forestry and Agriculture, the Division of Environmental Science, and the Department of Geology at Stephen F. Austin State University. Drs. Dean Coble and Yuhui Weng provided timely assistance with data organization and statistical analyses. Access to the Fort Hood Military Installation training areas, maps, and previous vegetation surveys was provided by Charles Pekins of the Fort Hood Natural Resources Management Branch. Field assistance was provided by Joel Faulkner and JaHoward Hutchins. Assistance with remote sensing analyses was provided by Kyle Altimore; Cassie Jay Barron assisted with soil sample processing; and Wayne Weatherford of the SFA Soil, Plant & Water Analysis Laboratory provided laboratory space and equipment.

CHAPTER VI:
CONCLUSIONS

The Fort Hood Military Installation is an 880km^2 U.S. Army base located in Lampasas Cut Plain within Bell and Coryell counties in north-central Texas. The installation provides resources and training facilities for active and reserve units in support of the Army's mission: to maintain a total force, trained and ready to fight, to serve our nation's interests both domestically and abroad, and to maintain a strategic force capable of decisive victory. The full range of mission-related training activities are conducted on Fort Hood, including maneuver exercises for units up to brigade level, firing of live weapons, and aviation training. In addition to military activities, the Army also allows a number of other non-military uses of the land, including fishing, hunting, grazing, and other types of recreational activities. These uses, together with the military training, affect the natural resources that occur on the installation (Hayden *et al.* 2001).

The purpose of this study was to employ a variety of analytical and spatial techniques to characterize the hydrogeologic and ecological features found in the Owl Mountain Province, the northeastern training area of the Fort Hood Military Installation. Baseline data, training area access, and a historical perspective were provided by Charles Pekins, Wildlife Biologist with the Fort Hood Natural Resources Management Branch. Since October of 2011, the Fort Hood Natural Resources Management Branch has been

responsible for implementing programs to catalogue and monitor natural resources on the installation.

Natural Resource Management at Fort Hood

Geologically, the installation is a karst landscape underlain by Lower Cretaceous carbonate rocks from the Trinity and Fredericksburg Group. The topographic expression of these units are characterized by mesa-like rolling uplands and incised canyons with rock outcrops, steep cliffs, and numerous karst features such as sinkholes, caves, rock shelters, springs, and seeps. In the subsurface, many of these caves and karst features follow regional deformation trends associated with the Balcones/Ouachita fault system and undulations across the Comanche Shelf associated with the Belton High. As surface denudation has occurred, many of these caves have been heavily overprinted by epigenic processes and impacted by anthropogenic surface modifications. Ongoing geologic mapping and spatial delineation of karst features on the surface and in the subsurface will help determine the speleogenetic evolution of this landscape, and continue to provide valuable information regarding environmentally sensitive features.

Hydrologically, the installation is underlain by the Trinity and Edwards aquifers and both receive meteoric input through a variety of surficial karst features. The poorly understood, complex interaction of these aquifers has potentially created a dynamic flow regime whereby ascending fluids could be partially responsible for the suite of features found in known caves and along the exposed scarps in the study area. Varying

permeabilities associated with interfingering lithologies have partially confined hypogene and/or phreatic waters creating potentiometric pathways for deep seated water to augment soil moisture in mesic canyons and scarps. Current geochemical data indicates that most meteoric water is discharged through a variety of springs and seeps associated with the Edwards and/or Edwards and Comanche Peak boundaries. The fluctuating water table and ongoing drought during spring sampling may have affected results.

Ecologically, the installation is near the intersection of the Cross Timbers and Prairies and Edwards Plateau vegetation regions, with floristic input from both regions creating a patchwork of contiguous, closed canopy *Juniperus ashei-Quercus* spp. forests interspersed with shrub and grasslands on the plateaus and riparian corridors in mesic canyons characterized by *Carya illinoinensis*, *Juglans* spp., *Platanus occidentalis*, *Populus deltoides*, *Salix nigra*, *Ulmus rubra* and *Acer grandidentatum*. The multi-use nature of the training lands of the installation maintains much of the vegetation in early succession, with less accessible areas typically supporting later successional vegetation.

Established populations of *A. grandidentatum* were delineated within the study area by previous vegetation inventories; and the spatial distribution of these populations were once thought to be confined to mesic canyons within the Owl and Bear Creek watersheds. In Texas, original site descriptions of these relict vegetation communities were modeled after *A. grandidentatum* populations located in Bandera and Real counties in the Lost Maples State Natural Area. Recent vegetation mapping has greatly expanded both the site description and locations where maples exist. Just as they do in continuous

populations, within the study area *A. grandidentatum* can grow on open slopes with oaks and other species that are able to equilibrate to lower soil water potentials. Soil moisture and available water resources for plant uptake are probably augmented by ascending fluids; these deeper phreatic and/or hypogene water resources are transmitted by matrix porosity along the northwest trend of the scarps in the Owl and Bear Creek watersheds, and by solutional porosity along north/south joint trends associated with Balcones deformation.

The installation also functions as an isolated island of high quality habitat for many threatened and endangered species and hosts populations of two federally listed migrant songbirds, the golden-cheeked warbler (*Dendroica chrysoparia*) and the black-capped vireo (*Vireo atricapilla*); the largest populations of both species under a single management authority, considered crucial for species recovery. Although recovery efforts such as habitat and population protection may appear to be at odds with the Army's previously stated mission, the Fort Hood Natural Resources Management Branch has implemented a number of adaptive ecosystem management techniques in order to provide training facilities for brigade combat teams to conduct realistic battlefield training while still providing contiguous, managed habitats to maintain viable population growth in both species.

Future Research

This work and the detailed study of the Nolan Creek Province by Bryant (2012) are some of the initial karst research associated with the Fort Hood Military Installation. Ongoing work by Reddell (2011) and others continue to try to unravel the complex speleogenetic evolution of this landscape and document the unique features and biota found within the installation. Karst studies, by their very nature, are interdisciplinary studies. Therefore, all future research would include components of geology, hydrogeology, geochemistry, and biology.

Some areas of future research on Fort Hood may include:

1) Stratigraphic mapping and correlation to better understand the nature and extent of the shoal facies within the Owl Mountain Province.
2) Depositional environment and diagenetic control on facies development on the northern part of the Comanche Shelf.
3) Quarterly spring sampling to provide continual baseline data to the Fort Hood Natural Resources Management Branch.
4) Geochemical studies (Chapter III) indicate that most of the spring samples had a meteoric origin. Dye tracing may help delineate infiltration areas and provide valuable information to resource managers.

5) Continued vegetation modeling of unique biotic associations to provide additional information for resource managers to determine best management practices with regards to environmentally sensitive vegetation.
6) Spatially delineate and quantify epigenic karst (sinkholes) density, providing valuable information regarding karst development and protection of these features.
7) Document the effect regional paleoclimate has exerted on Fort Hood vegetation patterns by using published speleothem studies (Musgrove et al. 2001) as a proxy for climate change.
8) *Acer grandidentatum* conservation and establishment on favorable sites within the Owl Mountain Province.
9) The effects of herbivory of feral pigs and their influence on *Acer grandidentatum* regeneration as a result of disturbance.
10) The structural control of relict karst features such as tafoni, grottos, niches, shelter caves, tufa cones, and scarp development (abstract submitted to the DeepKarst Conference, April 2016).
11) Karst density comparison of the Glen Rose in West Fort Hood to the Edwards in East Fort Hood (Owl Mountain and Nolan Creek provinces).
12) Determine the genetic isolation of the *Acer grandidentatum* populations on Fort Hood. Can and do these trees regenerate by seed dispersal?

Other possible avenues for future research include comparing the stand dynamics and structural control of other disjunct maple populations in southwestern Oklahoma, West Texas, and New Mexico with the populations on Fort Hood. Do regional deformation events play a role in the continued existence of these stands? Does the model presented in Chapter IV apply in varying lithologies?

In conclusion, this study investigated the lithologic, stratigraphic, and structural controls on the hydromorphic evolution of the Owl Mountain Province. Landscape evolution and the resulting vegetation patterns were examined via hydrogeologic principles and used as a foundation to analyze the unique mesic vegetation communities found in the Owl Creek and Bear Creek watersheds.

LITERATURE CITED

Adkins, W.S. and Arick, M.B. (1930). Geology of Bell County, Texas. The University of Texas Bulletin No. 3016, Austin: Bureau of Economic Geology.

Alder, N.N., Sperry, J.S., and Pockman, W.T. (1996). Root and stem xylem embolism, stomatal conductance, and leaf turgor in Acer grandidentatum populations along a soil moisture gradient. Oecologia Vol. (105), pp. 293-301.

Amsbury, D.L., Bay, Jr, T.A. and Lozo, F.E. (1984). A Field Guide to Lower Cretaceous Carbonate Strata in the Moffatt Mound Area near Lake Belton, Bell County, Texas, *in* Guidebook for SEPM Field Trip NO. 3. San Antonio: Gulf Coast Section of the Society of Economic Paleontologists and Mineralogists Foundation, pp. 1-19.

Anaya, R. and Jones, I. (2009). Groundwater Availability Model for the Edwards-Trinity (Plateau) and Pecos Valley Aquifers of Texas. Report 373, Austin: Texas Water Development Board, 103 pages.

Barnes, V. (1970). Geologic Atlas of Texas: Waco Sheet. Map and Lithology description, Austin: Bureau of Economic Geology, 8 pages.

Blome, C.D., Faith, J.R. and Ozuna, G.B. (2007). Geohydrologic framework of the Edwards and Trinity aquifers, south-central Texas: U.S. Geological Survey Fact Sheet 2006-3145, 6 pages.

Bloom, A.L. (1998). Geomorphology: A systematic analysis of late Cenozoic landforms. Upper Saddle River, NJ: Prentice Hall, 482 pages.

Bradley, A.F., Noste, N.V., and Fischer, W.C. (1991). *Fire ecology of forests and woodlands in Utah.* General Technical Report. INT-287. Ogden, UT: USDA Forest Service, Intermountain Research Station. 128 pages.

Bradley, R.G. and Malstaff, G. (2004). Dry Periods and Drought Events of the Edwards Plateau, Texas. Austin: Texas Water Development Board.

Brown, J.L. (1975). Paleoenvironment and Diagenetic History of the Moffat Mound, Edwards Formation, Central Texas. Master's Thesis, Baton Rouge: Louisiana State University.

Bryant, A.W. (2012). Geologic and Hydrogeologic Characterization of Groundwater Resources in the Fredericksburg Group, North Nolan Creek Province, Bell County, Texas. Master's Thesis, Nacogdoches: Stephen F. Austin State University.

Bryant, Y.M., Jr. and Shaffer, H.J. (1977). The late Quaternary paleoenvironment of Texas: A model for the archeologist. Volume 48, Austin: Bulletin of the Texas Archeological Society, pp. 1-25.

Bsoul, E., St. Hilaire, R., and VanLeeuwen, D.M. (2006). Bigtooth Maples exposed to asynchronous cyclic irrigation show provenance differences in drought adaptation mechanisms. Journal of American Horticultural Society Vol 131 (4): pp. 459-468.

Cannata, S.L. and Yelderman, J.C., Jr. (1987). Hydrogeology of the Edwards Aquifer in the Washita Prairie: Bosque, Coryell, Hamilton and McLennan counties, Texas, in Hydrogeology of the Edwards Aquifer: Northern Balcones and Washita Prairie segments. Austin: Austin Geological Society, pp. 47-60.

Caran, S.C., Woodruff, C.M., Jr., and Thompson, E.J. (1982). Lineament Analysis and Inference of Geologic Structure – Examples from the Balcones/Ouachita Trend of Texas. Gulf Coast Association of Geological Societies Transactions, Volume 31, pp. 59-69.

Collins, E.W. (2005). Geologic Map of the West Half of the Taylor, Texas, 30 x 60 Minute Quadrangle: Central Texas Urban Corridor, Encompassing Round Rock, Georgetown, Salado, Briggs, Liberty Hill, and Leander. Miscellaneous Map No. 43, Bureau of Economic Geology, 16 pages.

Corbin, B.L. and Page, D.H. (2011). Post-burn Resprouting in Bigtooth Maple (Acer grandidentatum): A Case Study. Natural Resources and Environmental Issues, Volume 16, Shrublands: Wildlands and Wildlife Habitats. Article 26.

Correll, D.S. and Johnston, M.C. (1970). Manual of the vascular plants of Texas. Renner, Texas Research Foundation.

Culotta, R., Latham, T., Sydow, M., Oliver, J., Brown, L. and Kaufman, S. (1992). Deep structure of the Texas Gulf Passive Margin and its Ouachita-Precambrian Basement: Results of the COCORP San Marcos Arch Survey. The American Association of Petroleum Geologists Bulletin, Volume 76, No. 2, pp. 270-283.

Desmarais, Y. (1952). Dynamics of leaf variation in the sugar maples. Brittonia, Volume 7, pp. 347-387.

Diamond, D.D. (1997). An Old-Growth Definition for Western Juniper Woodlands; Texas Ashe Juniper Dominated or Codominated Communities. U.S.D.A. Forest Service, Southern Research Station, General Technical Report SRS-15.

Dickinson, T.L.N. (2011). Abiotic and Biotic Factors Affecting First-Year Seedling Growth and Survival in Acer Grandidentatum, Bigtooth Maple. Master's Thesis, San Antonio: The University of Texas at San Antonio.

Diggs, G. M., Lipscomb, B.L. and O'Kennon, R.J. (1999). Introduction to north central Texas *in* Shiners & Mahler's illustrated flora of north central Texas. SIDA, Botanical Miscellany, Number 16, Botanical Research Institute of Texas, Fort Worth, Texas, USA, pp. 20-62.

Donavan, L.A. and Ehleringer, J.R. (1994). Water stress and use of summer precipitation in a Great Basin shrub community. Functional Ecology, Vol. 8: pp. 289-297.

Doughty, R.W. (1983). Wildlife and Man in Texas: Environmental Change and Conservation. Texas A&M University Press, College Station, TX, 246 pages.

Eckhardt, G. (2012). Hydrogeology of the Edwards Aquifer. http://www.edwardsaquifer.net/geology.html (accessed April 29, 2012).

Ehleringer, J.R., Phillips, S.L., Schuster, W.S.F, and Sandquist, D.R. (1991). Differential utilization of summer rains by desert plants. Oecologia, Vol 88: pp. 430-434.

Elliott, W.R. and Veni, G., eds., (1994). The Caves and Karst of Texas. Huntsville, Alabama, National Speleological Society and Texas Parks and Wildlife Department, 342 pages.

Faulkner, M.G., Stafford, K.W., and Bryant, A.W. (2013a). Delineation and Classification of Karst Depressions Using LiDAR: Fort Hood Military Installation, Texas, *in* Proceedings of the 13th Multidisciplinary Conference on Sinkholes and the Engineering and Environmental Impacts of Karst, Carlsbad, NM, pp. 459-467

Faulkner, M.G., Stafford, K.W., and Bryant, A.W. (2013b). Geoanalytical Analysis of Speleogenetic Development in the Owl Mountain Province: Fort Hood Military Installation, Texas. Geological Society of America Abstracts with Programs. Vol. 45, No. 3, page 29.

Faulkner, M.S. and Stafford, K.W. (2014). Preliminary Geochemical Analysis of Springs within the Owl Mountain and Nolan Creek Provinces, Fort Hood Military Installation, Bell and Coryell Counties, Texas. Geological Society of America Abstracts with Programs. Vol. 46, No. 1, page38.

Faulkner, M.S. and Bryant, A.W. (2015). Hypogene Karst of the Lampasas Cut Plain *in* Hypogene Karst of Texas. Texas Speleological Society, ed. Kevin Stafford (in press).

Faulkner, M.S., Stafford, K.W., and McBroom, M.W. (2015). Spatial Delineation of Subaqueous Karst Springs in Belton Lake along the Eastern Border of the Fort Hood Military Installation, Bell County, Texas. Geological Society of America *Abstracts with Programs.* Vol. 47, No. 1, page15.

Faulkner, M.S., Stafford, K.W., and McBroom, M.W. (2016a). The Hydromorphic Evolution of the Owl Mountain and Nolan Creek Provinces, Fort Hood Military Installation, Bell and Coryell counties, Texas. In Review.

Faulkner, M.S., Stafford, K.W., and McBroom, M.W. (2016b). Structural control of mesic vegetation communities within the Owl Creek and Bear Creek watersheds, Bell and Coryell counties, Texas. In Review.

Fenimore, C. (2015). United States Drought Monitor, National Drought Mitigation Center. http://droughtmonitor.unl.edu/Home/StateDroughtMonitor.aspx?TX. Accessed on 12/30/2015.

Ferrill, D.A. and Morris, A.P. (2008). Fault Zone Deformation Controlled by Carbonate Mechanical Stratigraphy, Balcones Fault System, Texas, *in* American Association of Petroleum Geologists Bulletin, pp.359-380.

Ferrill, D.A., Morris, A.P, Sims, D.W., Green, R., Franklin, N., and Waiting, D.J. (2008). Geologic Controls on Interactions between the Edwards and Trinity Aquifers, Balcones Fault System, Texas, *in* South Texas Geological Society Bulletin, pp. 21- 45.

Fisher, W.L. and Rodda, P.U. (1969). Edwards Formation (Lower Cretaceous), Texas: Dolomitization in a Carbonate Platform System, *in* American Association of Petroleum Geologists 53, no. 1, pp. 55-72.

Flanagan, L.B., Ehleringer, J.R., Marshall J.D. (1992). Differential uptake of summer precipitation among co-curring trees and shrubs in a pinyon-juniper woodland. Plant Cell and Environment, Vol. 15: pp. 831-836.

Flawn, P.T., Goldstein, A., Jr., King, P.B., and Weaver, C.E. (1961). The Ouachita System: The University of Texas Bureau of Economic Geology, Pub. 6120, 401 pages.

Flores, D. (1991). Bison ecology and bison diplomacy: the southern plains from 1800 to 1859. Journal of American History 78: pp. 465-485.

Fort Hood: The Great Place. (2013). History of the Great Place. http://www.hood.army.mil/history.aspx. Accessed on 12/29/2015.

Fowler, N.L. and Simmons, M.T. (2008). *Savanna dynamics in central Texas: just succession?* Applied Vegetation Science, pp. 23-31.

Freeman, M.D., Dase, A.E., and Blake, M.E. (2001). Agriculture and Rural Development on Fort Hood Lands, 1849-1942: National Register Assessments of 710 Historic Archaeological Properties. Prewitt and Associates, 252 pages.

Fuhlendorf, S.D. and Smeins, F.E. (1996). Long-term importance of grazing, fire, and weather patterns on Edwards Plateau vegetation change. 1997 Juniper Symposium Proceedings. College Station, TX, USA. Texas A & M University Research Station.

Garrison, M.R. (2005). Surface to Subsurface Correlations of Natural Fractures in Paleozoic Rocks in selected areas of Central and North-Central Texas. M.S. Thesis, Stillwater, OK. Oklahoma State University.

Gehlbach, F.R. and Gardner, R.C. (1983). *Relationships of Sugar Maples (Acer Saccharum and A. Grandidentatum) in Texas and Oklahoma with Special Reference to Relict Populations.* The Texas Journal of Science. Volume 35, Issue 3, pp. 231-239.

Geologic Data Base of Texas from Texas Natural Resources Information System. https://tnris.org/ Accessed January 2016.

George Veni and Associates. (2005). Report of findings, Fort Hood preliminary karst investigation. Austin.

Godfrey, C.L., G.S. McKee, and H. Oakes. (1973). General soils map of Texas. College Station: Texas Agricultural Experiment Station.

Griffith, G.E., Bryce, S.A., Omernik, J.M., Comstock, J.A., Rogers, A.C., Harrison, B., Hatch, S.L., and Bezanson, D. (2004). Ecoregions of Texas, U.S. Environmental Protection Agency, Corvallis, OR.

Hammer, M.L. (2011a). Introduction and site description, in Endangered Species Monitoring and Management at Fort Hood, Texas. Fort Hood: Fort Hood, Directorate of Public Works, Natural Resources Management Branch.

Hammer, M.L. (2011b). The U.S. Army, Fort Hood Garrison Annual Report CY 2011, U.S. Army, pp. 1-118.

Havlina, D. (2003). Fire Regime Conditions Class (FRCC) Interagency Handbook Reference Conditions for Interior Chaparral (CHAP5). http://www.frcc.gov/docs/PNVG/West?CHAP5_Descriptions.pdf. Accessed 2/19/2016.

Hayden, T.J., Cornelius, J.D., Weinberg, H.J., Jette, L.L., and Melton, R.H. (2001). Endangered Species Management Plan for Fort Hood, Texas FY01-05. US Army Corps of Engineers, Engineer Research and Development Center.

Hayward, O.T., Allen, P., and Amsbury, D. (1990). The Lampasas Cut Plain – Evidence for the Cyclic Evolution of a Regional Landscape, Central Texas, *in* Geological Society of America Field Trip #19 Guidebook, 104 pages.

Hester, T.R. (1986). Early human occupation along the Balcones Escarpment. (eds.) P.L. Abbott and C.M. Woodruff, *in* The Balcones Escarpment, Geological Society of America, San Antonio, pp. 55-62.

Hunt, C.B. (1974). Natural regions of the United States and Canada. W.H. Freeman & Co., San Francisco, CA.

Huxman, T.E., Wilcox, B.P., Breshears, D.D., Scott, R.L., Snyder, K.A., Small, E.E., Hultine, K., Pockman, W.T., and Jackson, R.B. (2005). Ecohydrological Implications of Woody Plant Encroachment. Ecology, Vol. 86(2), pp. 308-319.

Jones, I.C. (2003). Groundwater Availability Model: Northern Segment of the Edwards Aquifer, Texas. Report 358, Texas Water Development Board, 75 pages.

Jones, I.C. (2006). Defining Groundwater Flow Characteristics in the Northern Segment of the Edwards Aquifer Based on Groundwater Chemistry. Austin Geological Society Bulletin, v. 2, pp. 54-75.

Klimchouk, A. (2007). Hypogene Speleogenesis: Hydrogeological and Morphogenentic Perspective. Special Paper No. 1, National Cave and Karst Research Institute, Carlsbad, NM, 106 pages.

Klimchouk, A. (2009). Principal Characteristics of Hypogene Speleogenesis, *in* Advance in Hypogene Speleogenesis, Symposium 1, National Cave and Karst Research Institute, pp. 1-11.

Klimchouk, A., and Ford, D., eds. (2009). Hypogene Speleogenesis in the Piedmont Crimea Range, *in* Hypogene Speleogenesis and Karst Hydrogeology of Artesian Basins. Special Paper 1, pp. 159-172.

Klimchouk, A., Tymokhina, E.and Amelichev, G. (2012). Speleogenetic effects of interaction between deeply derived fracture-conduit flow and intrastratal matrix flow in hypogene karst settings. International Journal of Speleology, 41(2), pp. 37-55.

Larkin, T.J., and G.W. Bomar. (1983). *Climatic Atlas of Texas.* LP-192, Austin: Texas Department of Water Resouces, pp. 1-157.

Ludeke, K., German, D., and Scott, J. (2005). *Texas Vegetation Classification Project: Interpretive Booklet for Phase I.* Austin: Texas Parks and Wildlife and Texas Natural Resources Information System.

Lyons, R.K., M.K. Owens, R.V. Machen. (1998). Juniper Biology and Management in Texas. Texas Agricultural Extension Service, The Texas A & M University System. College Station, Texas

McCann, A.J. (2012). Surficial Fractures and Their Interferences on Fluid Movement in Hydrogeologic Reservoirs, Central Texas, M.S. Thesis, Stephen F. Austin State University, Nacogdoches, Texas, 234 pages.

McKenzie, D., and Reddell, J.R. (1964). Texas Speleological Survey: The Caves of Bell and Coryell Counties. Austin: Texas Speleological Survey

Mecke, M.B. (1996). Historical vegetation changes on the Edwards Plateau of Texas and the effects upon watersheds. Conference proceedings of CONSERV 96, Responsible Water Stewardship.

Musgrove, M., Banner, J.L., Mack, L.E., Combs, D.M., James E.W., Cheng, H., and Edwards, R.L. (2001). Geochronology of late Pleistocene to Holocene speleothems from central Texas: Implications for regional paleoclimate. Geological Society of America, pp. 1532-1543.

Natural Resources Conservation Service USDA. (2012). Custom Soil Resources Report for Bell and Coryell County, Texas. United States Department of Agriculture, Washington D.C., USA.

Nelle, S. (1997). Holistic perspective on juniper. *In*: C.A. Taylor, Jr. [ED.]. 1997 Juniper Symposium Proceedings. Chapter 4: Holistic Perspective, Rangeland Hydrology and Wildlife Considerations in Juniper Management. College Station, TX, USA. Texas A & M University Research Station.

Nelson, H.F. (1973). The Edwards Reef Complex and Associated Sedimentation." *The Geological Society of America.* Dallas: Bureau of Economic Geology, pp. 1-35.

Nordt, L.C., Boutton, T.W., Hallmark, C.T., and Waters, M.R. (1994). Late Quaternary climate changes in Central Texas based on the isotopic composition of organic carbon. *Quaternary Research* 41, pp.109-120.

Oterdoom, H.J. (1994). *Maples in Nature and in the Garden*. Maples of the World, Timber Press, Portland, OR.

Palmer, A.N. (1991). Origin and Morphology of Limestone Caves. Geological Society of America Bulletin, v. 103, pp. 1-21

Palmer, A.N. (2007). Cave Geology. Dayton, Ohio, Cave Books, 454 pages.

Palmer, E.C. (1986). Land Use and Cultural Change along the Balcones Escarpment, 1718-1986. Austin: Texas Geological Society.

Peak, R.G. (2011). Population trends of the Golden-checked Warbler on Fort Hood, Texas 1992-2011. In endangered species monitoring and management at Fort Hood, Texas: 2011 annual report.

Pekins, C. (2012). Fort Hood Natural Resources Management Branch, Fort Hood Military Installation. Personal communication regarding training area access, spring locations, and vegetation surveys.

Phillips, S.L. and Ehleringer, J.R. (1995). Limited uptake of summer precipitation by bigtooth maple (*Acer grandidentatum* Nutt) and Gambel's oak (*Quercus gambelii* Nutt). Trees. Vol 9, pp. 214-219.

Picinich, C. (2011). Land Group 3 and Land Group 4 Vegetation Sampling on Fort Hood, Texas in Endangered species monitoring and management at Fort Hood, Texas. Fort Hood: Fort Hood Directorate of Public Works, Natural Resources Management Branch.

Pugsley, W S. (1992). Imprint on the Land, Life Before Camp Hood, 1820-1942. Prewitt and Associates.

Querejeta, J.I., Estrada-Medina, H., Allen, M.F., and Jimenez-Osornio, J.J. (2007). Water source partitioning among trees growing on shallow karst soils in a seasonally dry tropical climate. Ecophysiology, Volume 152, pp. 26-36.

Reddell, J.R., Fant, J., Reyes, M., and Warton, M. (2011). Karst Research on Fort Hood, Bell and Coryell Counties, Texas. Unpublished Report prepared for U.S. Army, Fort Hood Natural Resources Management Branch, Fort Hood, Texas, USA. p. 1078.

Reddell, J.R. (2001). The caves of the Lampasas Cut Plain. Texas Speleological Survey, Austin, Texas. 64 pages.

Reemts, C.M. and Hansen, L.L. (2008). Slow recolonization of burned oak-juniper woodlands by Ashe juniper (*Juniperus ashei*): Ten years of succession after crown fire. Forest Ecology and Management 225, pp. 1057-1066.

Riskind, D.H., and Diamond, D.D. (1986). The Balcones Escarpment: Plant Communities of the Edwards Plateau of Texas. Geological Society of America, pp. 21-32.

Rose, P.R. (1972). Edwards Group, Surface and Subsurface, Central Texas, Report of Investigations. Bureau of Economic Geology, The University of Texas, Austin, 198 pages.

Senger, R.K., Collins, E.W., and Kreitler, C.W. (1990). Hydrogeology of the Northern Segment of the Edwards Aquifer, Austin Region. Report of Investigations No. 192, Bureau of Economic Geology, The University of Texas, Austin

Shaw, M.G. (2012). Carbonate Facies of the Owl Mountain Area, Fort Hood Military Installation, Bell and Coryell Counties, Texas. Geological Society of America Abstracts with Programs, Vol. 44, No. 1, p. 3.

Smeins, F.E. (1980). Natural role of fire on the Edwards Plateau. In Prescribed burning of the Edwards Plateau of Texas, pp. 4-16. Edited by L.D. White. Texas Agricultural Extension Service, College Station, TX.

Smeins, F.E. (1984). Origin of the brush problem: a geological and ecological perspective of contemporary distributions. In Proc. Brush Management Symposium. pp. 5-16. Edited by K.W. McDaniel. Texas Tech Press, Lubbock, TX.

Smeins, F.E. and Fuhlendorf, S.D. (1997). Biology and ecology of Ashe juniper. *In*: C.A. Taylor, Jr. [ED.]. 1997 Juniper Symposium Proceedings. Chapter 3: Biology, Ecology and Ecophysiology of Juniper. College Station, TX, USA. Texas A & M University Research Station.

Smeins, F.E., Fuhlendorf, S.D., and Taylor, C., Jr. (1997). Environmental and Land Use Changes: A Long Term Perspective. *In*: C.A. Taylor, Jr. [ED.]. 1997 Juniper Symposium Proceedings. Chapter 1: Environmental and Land Use Changes. College Station, TX, USA. Texas A & M University Research Station.

Sullivan, J. (1993). Juniperus ashei. In: Fire Effects Information System, U.S. Department of Agriculture, Forest Service, Rocky Mountain Research Station, Fire Sciences Laboratory. Accessed February 16, 2016.

Talbert, S.J. and Atchley, S.C. (2000). Sequence Stratigraphy of the Lower Cretaceous (Albian) Fredericksburg Group, Central and North Texas, *in* Gulf Coast Association of Geological Societies Transactions, Volume L, 2000, pp. 369-378.

Teague, J. and Reemts, C. (2007). Vegetation Classification and Mapping on Fort Hood Military Reservation, Texas, Final Report. The Nature Conservancy, San Antonio, TX, USA.

Texas Commission on Environmental Quality. (2015). Texas Surface Water Quality Standards. https://www.tceq.texas.gov/waterquality/standards. Accessed on 1/7/2015.

Texas Natural Resource Information System. (2016). Ecoregions of Texas https://tnris.org/ Accessed 1/25/2016.

Texas Speleological Survey. (2014). TSS Map CD. Austin: Texas Speleological Survey.

The Nature Conservancy. (2003). A biodiversity and conservation assessment for the Edwards Plateau Ecoregion. Edwards Plateau Ecoregional Planning Team, The Nature Conservancy, San Antonio, TX, USA.

The Nature Conservancy. (2004). Terrestrial and Marine Ecoregions of the United States, The Nature Conservancy, Global Priorities Group.

Thurow, T.L. and Hester, J.W. (1997). How an increase or reduction in juniper cover alters rangeland hydrology, *in*: C.A. Taylor, Jr. [ED.]. 1997 Juniper Symposium Proceedings. Chapter 4: Holistic Perspective, Rangeland Hydrology and Wildlife Considerations in Juniper Management. College Station, TX, USA. Texas A & M University Research Station.

Tollefson, J. (2006). *Acer grandidentatum.* U.S.D.A. Rocky Mountain Research Station, Fire Sciences Laboratory. http://www.fs.fed.us/database/feis/plants/tree/acegra/all.html Accessed on 4/14/2103.

U.S. Army Corps of Engineers, Fort Worth District. (2007). History of Belton Lake. http://www.swf-wc.usace.army.mil/belton/Information/History.asp. Accessed on 12/18/2015.

U.S. Department of Agriculture. (2007). Ecological Subregions: Sections and Subsections for the Conterminous United States. Vector Digital Data. USDA Forest Service ECOMAP Team, Washington, DC.

U.S. Environmental Protection Agency. (2015). Regulated Drinking Water Contaminants. http://www.epa.gov/your-drinking-water/. Accessed on 1/7/2016.

Van Devender, T.R. and Spaulding, W.G. (1979). Development of vegetation and climate in the southwestern United States. Science 204, pp. 701-710.

Walker, L.E. (1979). Occurrence, Availability, and Chemical Quality of Ground Water in the Edwards Plateau Region of Texas. Bureau of Economic Geology, The University of Texas, Austin, 336 pages.

Weather Underground, Historical Weather Data for Gatesville, Killeen, Fort Hood Airfield, Temple, and Belton. http://www.wunderground.com/. Accessed 12/30/2015.

Wells, P.V. (1970). Postglacial vegetation history of the Great Plains. Science 167, pp. 1574-1582

White, P. J. (1948). Caves of Central Texas. Bulletin of the National Speleological Society, 10, pp.46-64

Woodruff, C.M., Jr., and Abbott, P.L. (1979). Stream Piracy and Evolution of the Edwards Aquifer along the Balcones Escarpment, Central Texas, *in* Earth Surface Processes, by C.M., Jr. Woodruff and P.L. Abbott, Austin: Geological Society of America, pp. 77-90.

Yelderman, J.C., Jr., Slade, R.M., Jr., Sharp, J.M., Jr. and Woodruff, C.M., Jr. (1987). Hydrogeology of the Edwards Aquifer, northern Balcones and Washita Prairie segments: Austin Geological Society, Guidebook 11, 91 pages.

YSI (2009). 6-Series Multi-parameter Water Quality Sonde User Manual, YSI Incorporated.

APPENDICES

APPENDIX I:

Water Chemistry

Date	Field Data - Bear Springs 1							
	Orifice (cm)		Flow	Discharge	pH	Temp	DO	Cond
	Width	Depth	(cm sec^{-1})	(cm^3 sec^{-1})		(^0C)	(%)	(µs)
Dec-12	40.20	3.90	12.14	1903.31	7.13	19.30	74.30	678.80
Jan-13	40.00	4.00	15.30	2448.00	7.36	19.20	81.00	653.20
Feb-13	40.30	3.70	21.40	3190.95	6.79	19.20	84.60	372.40
Mar-13	40.00	4.00	14.68	2348.80	7.43	19.10	86.90	899.40
Apr-13	41.60	4.30	17.43	3117.88	7.35	19.50	80.60	709.30
May-13	41.20	3.80	21.42	3353.52	7.31	19.51	80.80	630.40
Jun-13	39.80	3.70	8.26	1216.37	7.35	19.53	78.60	644.40
Jul-13	37.40	3.80	7.90	1122.46	6.84	19.80	73.90	907.80
Aug-13	40.20	4.10	15.18	2501.97	7.36	19.56	71.90	660.50
Sep-13	36.00	3.80	16.12	2205.22	6.86	19.50	70.80	947.10
Oct-13	39.60	3.90	14.98	2340.85	7.18	19.42	78.30	710.30
Nov-13	32.00	3.60	12.69	1461.89	6.84	19.70	69.50	945.10
Dec-13	42.00	4.30	16.80	3034.08	5.62	19.30	72.80	630.70
Jan-14	42.80	4.30	22.88	4210.84	6.84	19.30	77.80	624.80
Feb-14	43.10	4.30	38.75	7181.54	6.40	19.30	81.50	624.10
Mar-14	42.90	4.20	33.46	6028.82	6.88	19.40	77.10	622.40
Apr-14	42.20	4.20	28.78	5100.97	7.31	19.40	74.80	623.80
May-14	41.20	4.10	16.28	2750.02	7.76	19.60	73.00	625.80
Jun-14	39.30	3.90	8.30	1272.14	7.72	19.40	67.00	626.60
Jul-14	39.10	3.90	6.65	1014.06	7.71	19.50	61.30	339.70
Aug-14	39.30	3.90	7.22	1106.61	7.26	19.40	57.30	512.50
Sep-14	39.40	4.00	9.84	1550.78	6.91	19.50	50.40	621.60
Oct-14	40.20	4.20	16.35	2760.53	6.73	19.30	57.60	629.20
Nov-14	40.10	4.10	9.58	1575.05	6.63	19.40	62.00	624.60
Dec-14	40.80	4.30	17.26	3028.09	6.34	19.20	70.60	336.90

Bear Springs 1		Anions (ppm)								
Date	LAB ID	Fluoride	Chloride	Sulfate	Phosphate	Nitrite	Nitrate	Carbonate	Bicarbonate	Total Carbonate
Dec-12	R31294	0.29	10.72	6.06	0.00	0.00	3.56	0.00	294.84	294.84
Jan-13	R31495	0.22	10.35	5.90	0.00	0.00	3.81	0.00	250.99	250.99
Feb-13	R31517	0.12	7.78	1.08	14.79	0.00	5.54	0.00	241.92	241.92
Mar-13	R31567	0.22	11.35	7.86	0.00	0.10	3.96	0.00	294.84	294.84
Apr-13	R32004	0.40	8.39	5.26	0.00	0.00	4.37	0.00	317.52	317.52
May-13	R32044	0.40	8.60	4.99	0.00	0.00	3.70	0.00	285.77	285.77
Jun-13	R32254	1.16	14.54	6.93	0.00	0.00	8.11	0.00	267.62	267.62
Jul-13	R32372	0.60	9.74	5.80	0.00	0.00	3.74	0.00	176.90	176.90
Aug-13	R32578	0.27	8.68	5.09	0.00	0.00	3.45	0.00	258.55	258.55
Sep-13	R32665	0.37	13.24	5.50	0.00	0.00	4.20	0.00	225.29	225.29
Oct-13	R32846	0.41	10.34	5.45	0.00	0.00	4.45	0.00	285.77	285.77
Nov-13	R33468	0.15	8.58	5.02	0.00	0.00	3.82	0.00	214.70	214.70
Dec-13	R33528	0.26	9.22	5.03	0.00	0.00	4.02	0.00	189.00	189.00
Jan-14	R33601	0.21	12.05	0.57	6.30	0.00	0.04	0.00	246.46	246.46
Feb-14	R33744	0.20	10.35	2.79	4.24	0.00	1.67	0.00	201.10	201.10
Mar-14	R31597	0.19	8.65	5.01	0.00	0.00	3.30	0.00	223.78	223.78
Apr-14	R35122	1.15	7.87	4.94	0.00	0.20	3.53	0.00	243.43	243.43
May-14	R35570	0.13	7.29	4.86	0.00	0.21	3.35	0.00	173.88	173.88
Jun-14	R36140	0.15	7.21	5.11	0.10	0.00	3.26	0.00	232.85	232.85
Jul-14	R36317	0.12	7.01	4.46	0.00	0.00	3.10	0.00	235.87	235.87
Aug-14	R36529	0.11	6.81	4.32	0.00	0.00	2.54	0.00	205.63	205.63
Sep-14	R36892	0.10	6.62	4.19	0.00	0.00	1.98	0.00	199.58	199.58
Oct-14	R36899	0.10	6.52	4.27	0.00	0.00	2.18	0.00	267.62	267.62
Nov-14	R36965	0.13	8.48	4.94	0.00	0.00	6.85	0.00	273.67	273.67
Dec-14	R37228	0.14	8.14	4.68	0.00	0.00	5.88	0.00	328.10	328.10

Bear Springs 1		Water Soluble Species (ppm)										
Date	LAB ID	As 189.042	Ca 315.887	Cu 324.754	Fe 259.940	K 766.490	Mg 279.553	Mn 257.610	Na 588.995	S 180.731	Zn 213.856	Pb 220.353
Dec-12	R31294	0.00	124.50	0.00	0.00	0.90	8.00	0.00	5.97	4.12	0.01	0.01
Jan-13	R31495	0.02	121.00	0.00	0.00	0.75	8.38	0.00	5.92	3.59	0.00	0.01
Feb-13	R31517	0.01	118.50	0.00	0.00	0.49	8.20	0.00	5.72	3.47	0.00	0.01
Mar-13	R31567	0.00	136.23	0.00	0.00	0.62	8.33	0.00	6.02	3.45	0.00	0.00
Apr-13	R32004	0.01	125.90	0.00	0.00	0.49	8.63	0.00	6.03	3.31	0.01	0.00
May-13	R32044	0.01	124.90	0.07	0.00	0.45	8.53	0.00	5.93	3.43	0.01	0.00
Jun-13	R32254	0.00	103.70	0.00	0.00	0.55	10.47	0.00	9.20	4.18	0.00	0.01
Jul-13	R32372	0.01	128.70	0.00	0.00	0.38	10.67	0.00	7.26	4.33	0.00	0.01
Aug-13	R32578	0.00	123.20	0.00	0.00	0.40	8.90	0.00	6.12	7.48	6.36	8.60
Sep-13	R32665	0.00	113.70	0.00	0.00	0.68	19.94	0.00	10.08	5.85	0.01	0.01
Oct-13	R32846	0.00	113.52	0.00	0.06	0.85	11.63	0.00	0.00	3.29	0.00	0.00
Nov-13	R33468	0.00	47.14	0.00	0.00	0.84	11.65	0.00	0.00	2.77	0.00	0.00
Dec-13	R33528	0.00	113.90	0.00	0.00	0.87	11.61	0.00	0.00	3.71	0.00	0.00
Jan-14	R33601	0.00	122.06	0.00	0.00	0.00	10.01	0.00	0.00	3.59	0.00	0.00
Feb-14	R33744	0.00	119.90	0.00	0.01	0.00	11.80	0.00	7.46	2.87	0.00	0.00
Mar-14	R31597	0.00	152.66	0.01	0.00	1.91	12.80	0.00	17.49	1.10	0.00	0.00
Apr-14	R35122	0.00	131.54	0.00	0.00	0.48	11.53	0.00	7.65	2.52	0.00	0.00
May-14	R35570	0.00	150.91	0.00	0.00	0.58	11.90	0.00	7.49	3.08	0.00	0.00
Jun-14	R36140	0.00	124.41	0.01	0.06	1.37	9.78	0.00	6.25	2.92	0.01	0.00
Jul-14	R36317	0.00	126.11	0.00	0.00	0.40	10.18	0.00	8.00	3.02	0.00	0.00
Aug-14	R36529	0.00	132.51	0.00	0.00	0.61	11.14	0.00	7.48	2.73	0.00	0.00
Sep-14	R36892	0.00	123.66	0.00	0.00	0.62	11.52	0.03	6.46	4.93	0.00	0.01
Oct-14	R36899	0.00	125.23	0.00	0.01	0.36	11.57	0.00	6.53	4.93	0.01	0.01
Nov-14	R36965	0.00	130.90	0.00	0.00	0.59	11.22	0.00	7.28	3.17	0.00	0.00
Dec-14	R37228	0.00	117.79	0.00	0.00	0.32	10.81	0.00	6.65	2.82	0.00	0.00

Bear Springs 1		Total Species (ppm)										
Date	LAB ID	As 189.042	Ca 315.887	Cu 324.754	Fe 259.940	K 766.490	Mg 279.553	Mn 257.610	Na 588.995	S 180.731	Zn 213.856	Pb 220.353
Dec-12	R31294	0.01	138.80	0.00	0.10	0.90	8.44	0.00	6.45	3.30	0.00	0.00
Jan-13	R31495	0.00	124.30	0.00	0.07	0.51	6.51	0.00	5.75	2.99	0.03	0.00
Feb-13	R31517	0.01	117.70	0.00	0.02	0.53	7.86	0.00	5.48	2.75	0.00	0.00
Mar-13	R31567	0.00	125.20	0.01	0.02	0.56	5.56	0.00	5.90	2.98	0.03	0.00
Apr-13	R32004	0.01	127.10	0.00	0.05	0.35	6.35	0.00	6.01	3.01	0.01	0.00
May-13	R32044	0.01	132.20	0.00	0.02	0.43	8.94	0.00	6.25	3.06	0.00	0.00
Jun-13	R32254	0.00	140.50	0.00	0.02	0.36	7.36	0.00	6.84	3.48	0.00	0.00
Jul-13	R32372	0.00	188.00	0.00	0.05	0.49	8.49	0.00	9.77	4.43	0.00	0.00
Aug-13	R32578	0.00	124.30	0.00	0.03	0.38	7.38	0.00	6.23	3.24	0.00	0.00
Sep-13	R32665	0.00	119.80	0.00	0.09	0.56	8.56	0.00	9.94	4.58	0.00	0.00
Oct-13	R32846	0.00	133.79	0.00	0.05	0.51	7.54	0.00	6.86	3.38	0.01	0.00
Nov-13	R33468	0.00	142.60	0.00	0.02	0.43	2.14	0.00	6.84	3.39	0.01	0.00
Dec-13	R33528	0.00	136.42	0.00	0.03	0.51	2.10	0.00	7.02	3.45	0.01	0.00
Jan-14	R33601	0.00	114.00	0.00	0.03	0.78	9.20	0.00	2.48	3.43	0.00	0.00
Feb-14	R33744	0.00	117.39	0.00	0.01	0.41	10.56	0.00	6.35	2.63	0.00	0.00
Mar-14	R31597	0.00	122.21	0.00	0.09	0.75	10.17	0.00	9.83	11.70	0.00	0.00
Apr-14	R35122	0.00	132.42	0.00	0.02	0.17	10.38	0.00	6.63	2.93	0.01	0.00
May-14	R35570	0.00	117.72	0.00	0.00	0.41	9.05	0.00	5.52	2.62	0.01	0.00
Jun-14	R36140	0.00	124.41	0.01	0.06	1.37	9.78	0.00	6.25	2.92	0.01	0.03
Jul-14	R36317	0.00	135.18	0.00	0.00	4.19	10.61	0.00	8.18	3.30	0.00	0.00
Aug-14	R36529	0.00	123.33	0.00	0.06	1.33	9.97	0.00	5.90	4.22	0.00	0.00
Sep-14	R36892	0.00	155.57	0.00	0.29	0.38	12.53	0.00	7.89	3.27	0.00	0.00
Oct-14	R36899	0.00	152.76	0.00	0.02	0.40	12.39	0.00	7.83	3.27	0.00	0.00
Nov-14	R36965	0.00	121.65	0.00	0.01	0.36	10.32	0.00	6.29	2.79	0.00	0.00
Dec-14	R37228	0.00	128.78	0.00	0.02	0.85	10.45	0.00	6.23	3.92	0.00	0.00

Date	Field Data - Bear Springs 2							
	Orifice (cm)		Flow	Discharge	pH	Temp	DO	Cond
	Width	Depth	(cm sec^{-1})	(cm^3 sec^{-1})		(^{0}C)	(%)	(µs)
Dec-12	20.00	3.80	19.13	1453.50	7.11	19.30	79.10	672.60
Jan-13	19.80	3.80	0.77	57.93	7.30	19.10	86.20	662.20
Feb-13	20.00	3.60	6.30	453.60	6.87	19.20	82.30	666.10
Mar-13	21.20	3.90	15.28	1263.35	7.39	18.80	83.90	894.00
Apr-13	18.80	2.60	3.08	150.40	7.24	18.82	55.30	686.20
May-13	17.90	2.10	0.46	17.18	7.15	18.72	47.00	625.00
Jun-13	18.20	2.10	0.64	24.46	7.26	19.76	48.10	630.50
Jul-13	19.20	3.40	5.89	384.24	7.04	19.80	74.60	968.50
Aug-13	18.40	2.40	0.49	21.53	7.27	20.65	54.10	680.20
Sep-13	20.20	3.90	14.72	1159.64	6.89	19.60	63.80	956.80
Oct-13	19.00	3.00	5.32	303.24	7.12	19.70	57.50	772.20
Nov-13	20.00	3.70	8.42	622.78	6.82	19.50	69.70	943.00
Dec-13	20.00	3.80	6.20	471.20	5.52	19.10	68.90	630.60
Jan-14	19.80	3.60	6.45	459.90	6.75	19.00	72.80	625.50
Feb-14	19.70	3.50	13.66	941.86	6.41	19.10	74.90	626.20
Mar-14	19.90	3.60	16.86	1207.85	6.86	19.20	70.50	624.30
Apr-14	19.90	3.60	10.79	773.00	6.39	19.10	71.80	626.70
May-14	19.80	3.60	15.80	1126.22	7.42	19.20	68.90	632.10
Jun-14	19.90	3.60	11.08	793.77	7.82	19.40	63.00	629.60
Jul-14	19.80	3.50	8.85	613.31	7.72	19.60	61.50	446.10
Aug-14	19.80	3.60	11.91	848.94	7.18	19.30	66.30	583.60
Sep-14	19.90	3.60	10.10	723.56	6.84	19.20	59.70	635.20
Oct-14	19.80	3.40	5.92	398.53	6.93	19.40	61.90	625.60
Nov-14	19.90	3.50	14.12	983.46	6.67	19.00	69.10	625.20
Dec-14	19.80	3.50	3.13	216.56	6.45	18.80	71.80	613.90

Bear Springs 2		Anions (ppm)								
Date	LAB ID	Fluoride	Chloride	Sulfate	Phosphate	Nitrite	Nitrate	Carbonate	Bicarbonate	Total Carbonate
Dec-12	R31295	0.63	16.30	16.73	0.00	0.00	10.14	0.00	247.97	247.97
Jan-13	R31496	0.14	8.25	4.82	0.00	0.00	3.62	0.00	294.84	294.84
Feb-13	R31518	0.12	7.61	1.05	14.69	0.00	5.58	0.00	226.80	226.80
Mar-13	R31568	0.23	10.60	6.15	0.00	0.00	4.01	0.00	267.62	267.62
Apr-13	R32003	0.38	8.56	5.59	0.00	0.00	4.26	0.00	284.26	284.26
May-13	R32043	0.38	8.78	5.30	0.00	0.00	3.61	0.00	246.46	246.46
Jun-13	R32253	1.10	14.83	7.37	0.00	0.00	7.91	0.00	255.53	255.53
Jul-13	R32374	0.57	9.94	6.16	0.00	0.00	3.65	0.00	340.20	340.20
Aug-13	R32577	0.26	8.85	5.41	0.00	0.00	3.37	0.00	270.65	270.65
Sep-13	R32670	0.36	13.50	5.84	0.00	0.00	4.10	0.00	261.58	261.58
Oct-13	R32847	0.29	11.46	5.59	0.00	0.00	4.17	0.00	240.41	240.41
Nov-13	R33469	0.25	8.42	5.05	0.00	0.00	3.74	0.00	237.38	237.38
Dec-13	R33529	0.34	9.60	5.03	0.00	0.00	3.98	0.00	196.56	196.56
Jan-14	R33620	0.31	9.43	0.73	5.95	0.00	0.04	0.00	261.58	261.58
Feb-14	R33745	0.22	9.14	2.85	0.00	0.00	1.67	0.00	204.12	204.12
Mar-14	R31598	0.12	8.86	4.98	0.00	0.00	3.30	0.00	204.12	204.12
Apr-14	R35123	0.22	7.93	4.91	0.00	0.00	3.55	0.00	228.31	228.31
May-14	R35571	0.13	7.33	4.75	0.00	0.00	3.32	0.00	219.24	219.24
Jun-14	R36141	0.23	6.86	4.36	0.00	0.00	0.03	0.00	229.82	229.82
Jul-14	R36318	0.24	7.33	4.57	0.00	0.00	3.09	0.00	241.92	241.92
Aug-14	R36529	0.17	6.84	4.27	0.00	0.00	2.60	0.00	244.94	244.94
Sep-14	R36893	0.10	6.35	3.97	0.00	0.00	2.12	0.00	237.38	237.38
Oct-14	R36900	0.41	6.94	4.29	0.00	0.00	2.23	0.00	291.82	291.82
Nov-14	R36966	0.15	9.98	5.17	0.00	0.00	7.20	0.00	170.86	170.86
Dec-14	R37229	0.14	8.20	4.67	0.00	0.00	7.15	0.00	312.98	312.98

Bear Springs 2		Water Soluble Species (ppm)										
Date	LAB ID	As 189.042	Ca 315.887	Cu 324.754	Fe 259.940	K 766.490	Mg 279.553	Mn 257.610	Na 588.995	S 180.731	Zn 213.856	Pb 220.353
Dec-12	R31295	0.00	125.10	0.00	0.00	1.27	8.00	0.00	5.87	4.02	0.01	0.00
Jan-13	R31496	0.00	121.00	0.00	0.00	0.49	8.15	0.00	5.76	3.51	0.01	0.00
Feb-13	R31518	0.00	128.54	0.00	0.05	0.03	8.46	0.00	5.85	3.28	0.00	0.00
Mar-13	R31568	0.00	136.70	0.00	0.01	0.77	8.74	0.00	6.66	4.02	0.00	0.00
Apr-13	R32003	0.00	125.90	0.00	0.01	0.49	8.63	0.00	6.03	3.31	0.01	0.00
May-13	R32043	0.00	126.90	0.00	0.03	0.30	9.28	0.00	8.58	3.63	0.00	0.01
Jun-13	R32253	0.00	128.40	0.00	0.05	0.36	8.74	0.00	6.51	4.96	0.00	0.00
Jul-13	R32374	0.00	131.70	0.00	0.01	0.48	10.34	0.00	7.09	4.28	0.00	0.00
Aug-13	R32577	0.00	123.20	0.00	0.01	0.40	8.90	0.00	6.12	7.48	6.36	8.60
Sep-13	R32670	0.00	113.70	0.00	0.01	0.68	19.94	0.00	10.08	5.85	0.01	0.01
Oct-13	R32847	0.00	126.40	0.00	0.01	0.53	9.92	0.00	6.85	4.43	0.64	0.86
Nov-13	R33469	0.00	137.62	0.00	0.05	8.61	11.85	0.00	5.20	3.06	0.00	0.00
Dec-13	R33529	0.00	107.78	0.00	0.05	8.73	11.59	0.00	5.87	3.61	0.00	0.00
Jan-14	R33620	0.00	121.43	0.00	0.01	0.03	9.80	0.00	1.85	3.58	0.00	0.00
Feb-14	R33745	0.00	136.70	0.00	0.01	0.67	11.60	0.00	8.58	4.42	0.00	0.01
Mar-14	R31598	0.00	152.33	0.01	0.04	2.28	12.78	0.00	17.22	1.07	0.00	0.00
Apr-14	R35123	0.00	156.80	0.00	0.00	0.36	11.46	0.00	6.33	4.87	0.00	0.01
May-14	R35571	0.00	162.10	0.00	0.03	0.49	12.62	0.00	7.89	3.28	0.00	0.00
Jun-14	R36141	0.00	126.03	0.00	0.03	1.00	9.86	0.00	6.16	2.94	0.01	0.00
Jul-14	R36318	0.00	127.26	0.00	0.05	0.46	10.29	0.00	8.58	3.08	0.00	0.00
Aug-14	R36529	0.00	126.70	0.00	0.01	0.67	11.60	0.00	8.58	3.44	0.00	0.01
Sep-14	R36893	0.00	124.95	0.00	0.00	0.30	11.56	0.01	6.51	4.96	0.00	0.01
Oct-14	R36900	0.00	123.85	0.00	0.00	0.36	11.46	0.00	6.33	4.87	0.00	0.01
Nov-14	R36966	0.00	115.48	0.01	0.00	1.99	10.33	0.00	7.55	2.86	0.00	0.00
Dec-14	R37229	0.00	111.81	0.01	0.01	-0.42	11.77	0.00	7.43	2.78	0.00	0.00

Bear Springs 2		Total Species (ppm)										
Date	LAB ID	As 189.042	Ca 315.887	Cu 324.754	Fe 259.940	K 766.490	Mg 279.553	Mn 257.610	Na 588.995	S 180.731	Zn 213.856	Pb 220.353
Dec-12	R31295	0.00	134.20	0.00	0.40	0.58	8.78	0.01	6.09	3.05	0.00	0.00
Jan-13	R31496	0.00	133.10	0.00	0.07	0.54	8.77	0.00	6.12	3.07	0.04	0.01
Feb-13	R31518	0.00	121.80	0.00	0.03	0.65	8.03	0.00	5.59	2.82	0.00	0.01
Mar-13	R31568	0.00	119.40	0.00	0.01	0.56	7.62	0.00	5.64	2.85	0.03	0.00
Apr-13	R32003	0.01	127.10	0.00	0.05	0.35	8.67	0.00	6.01	3.01	0.01	0.00
May-13	R32043	0.01	134.50	0.00	0.07	0.51	8.64	0.01	6.16	3.61	0.00	0.02
Jun-13	R32253	0.00	140.50	0.00	0.02	0.36	10.03	0.00	6.84	3.48	0.00	0.00
Jul-13	R32374	0.00	203.80	0.00	0.24	0.72	14.23	0.00	10.02	4.62	0.00	0.01
Aug-13	R32577	0.00	124.30	0.00	0.03	0.38	8.87	0.00	6.23	3.24	0.00	0.00
Sep-13	R32670	0.00	119.80	0.00	0.09	0.56	20.43	0.00	9.94	4.58	0.00	0.01
Oct-13	R32847	0.00	119.40	0.00	0.01	0.56	7.62	0.00	5.64	2.85	0.03	0.00
Nov-13	R33469	0.00	131.96	0.00	0.03	0.06	10.31	0.00	6.68	2.95	0.00	0.00
Dec-13	R33529	0.00	119.02	0.00	0.03	0.47	9.17	0.00	5.58	2.63	0.00	0.00
Jan-14	R33620	0.00	111.18	0.00	0.01	0.44	8.95	0.00	2.80	3.38	0.00	0.00
Feb-14	R33745	0.00	136.57	0.00	0.01	3.67	10.73	0.00	8.39	3.36	0.00	0.00
Mar-14	R31598	0.00	145.81	0.00	0.00	0.11	12.14	0.00	11.00	13.83	0.00	0.00
Apr-14	R35123	0.00	131.96	0.00	0.03	0.06	10.31	0.00	6.68	2.95	0.00	0.00
May-14	R35571	0.00	119.02	0.00	0.03	0.42	9.17	0.00	5.58	2.63	0.00	0.00
Jun-14	R36141	0.00	126.03	0.00	0.03	1.00	9.86	0.00	6.16	2.94	0.01	0.02
Jul-14	R36318	0.00	136.57	0.00	0.01	3.67	10.73	0.00	8.39	3.36	0.00	0.00
Aug-14	R36529	0.00	111.18	0.00	0.01	0.44	8.95	0.00	2.64	3.38	0.00	0.00
Sep-14	R36893	0.00	159.85	0.00	0.06	0.33	12.67	0.00	8.19	3.43	0.00	0.00
Oct-14	R36900	0.00	156.28	0.00	0.00	0.55	12.79	0.00	8.04	3.37	0.01	0.00
Nov-14	R36966	0.00	120.35	0.00	0.01	0.60	10.21	0.00	6.20	2.75	0.00	0.00
Dec-14	R37229	0.00	115.33	0.00	0.03	0.23	10.38	0.00	6.28	2.62	0.00	0.00

Date	Field Data - Crayfish Spring							
	Orifice (cm)		Flow	Discharge	pH	Temp	DO	Cond
	Width	Depth	(cm sec^{-1})	(cm^3 sec^{-1})		(^{0}C)	(%)	(µs)
Dec-12	23.20	8.40	1.21	236.39	7.10	19.50	90.50	768.20
Jan-13	23.00	8.00	5.10	938.40	7.74	18.80	90.20	751.00
Feb-13	23.40	8.60	12.23	2461.17	7.43	18.50	91.00	741.50
Mar-13	23.10	8.20	3.41	645.92	6.93	18.50	98.70	1048.00
Apr-13	22.90	8.20	3.16	593.38	7.03	18.80	94.30	949.20
May-13	22.90	8.10	1.46	271.29	7.16	19.24	81.60	736.20
Jun-13	23.10	8.00	2.25	416.68	7.17	19.53	82.40	801.40
Jul-13	23.00	8.20	3.11	586.55	6.73	19.60	72.20	1175.20
Aug-13	23.10	7.60	0.76	133.73	7.16	20.33	75.30	617.40
Sep-13	22.90	6.40	0.65	94.82	6.61	20.20	68.20	621.30
Oct-13	14.90	3.40	7.22	365.77	6.82	20.10	71.30	649.30
Nov-13	14.80	3.60	6.43	342.38	6.77	19.90	86.30	754.40
Dec-13	14.60	3.90	12.85	731.68	5.22	19.30	70.40	598.50
Jan-14	14.70	3.90	12.90	739.56	6.95	18.60	82.10	716.20
Feb-14	14.70	3.80	9.10	508.33	6.39	18.00	85.70	623.20
Mar-14	14.60	3.70	4.84	261.46	6.57	18.10	81.60	384.40
Apr-14	14.60	3.80	6.10	338.43	7.82	17.60	85.50	696.90
May-14	14.90	3.90	18.83	1094.21	7.18	18.10	67.90	729.50
Jun-14	14.70	3.80	4.54	253.60	7.19	18.40	59.60	726.30
Jul-14	14.70	3.90	7.85	450.04	7.67	18.70	59.30	694.50
Aug-14	14.60	3.80	6.95	385.59	7.32	18.90	58.70	712.40
Sep-14	14.60	3.70	3.69	199.33	6.70	19.70	59.30	754.50
Oct-14	14.70	3.80	6.66	372.03	6.58	19.70	70.60	744.60
Nov-14	14.70	3.80	7.19	401.63	6.82	19.20	77.70	728.80
Dec-14	14.80	3.90	8.62	497.55	6.27	18.10	82.50	387.10

Crayfish Spring		Anions (ppm)								
Date	LAB ID	Fluoride	Chloride	Sulfate	Phosphate	Nitrite	Nitrate	Carbonate	Bicarbonate	Total Carbonate
Dec-12	R31299	0.61	19.99	11.17	0.00	0.00	3.50	0.00	264.60	264.60
Jan-13	R31498	0.61	15.34	16.08	0.00	0.00	10.63	0.00	257.04	257.04
Feb-13	R31519	0.33	12.12	2.09	39.39	0.00	9.55	0.00	297.86	297.86
Mar-13	R31569	0.73	16.03	18.30	0.00	0.00	11.08	0.00	182.95	182.95
Apr-13	no data	0.57	15.87	11.91	0.00	0.00	8.69	0.00	252.50	252.50
May-13	R32045	0.71	14.24	15.09	0.00	0.00	7.98	0.00	260.06	260.06
Jun-13	R32255	1.17	20.09	17.87	0.00	0.00	9.05	0.00	273.67	273.67
Jul-13	R32370	0.66	15.88	17.05	0.00	0.00	8.58	0.00	219.24	219.24
Aug-13	R32579	0.57	15.59	17.21	0.00	0.00	7.72	0.00	223.78	223.78
Sep-13	R32668	0.53	15.79	18.46	0.00	0.00	7.50	0.00	319.03	319.03
Oct-13	R32848	0.71	14.24	15.09	0.00	0.00	7.98	0.00	317.52	317.52
Nov-13	R33470	0.38	12.55	14.70	0.00	0.00	8.05	0.00	246.46	246.46
Dec-13	R33531	0.48	14.50	8.14	0.00	0.00	3.24	0.00	250.99	250.99
Jan-14	R35598	0.38	20.25	0.00	15.74	0.00	0.08	0.00	246.46	246.46
Feb-14	R33746	0.36	16.62	7.50	0.00	0.00	3.58	0.00	229.82	229.82
Mar-14	R31602	0.34	12.99	15.00	0.00	0.00	7.08	0.00	261.58	261.58
Apr-14	R35126	0.47	10.78	13.63	0.00	0.00	6.06	0.00	252.50	252.50
May-14	R35567	0.37	12.37	14.99	0.00	0.13	7.02	0.00	300.89	300.89
Jun-14	R36146	0.50	10.02	12.65	0.00	0.00	12.97	0.00	287.28	287.28
Jul-14	R36320	0.45	12.05	7.60	0.00	0.00	2.71	6.05	16.63	22.68
Aug-14	R36530	0.36	12.21	10.91	0.00	0.00	3.87	0.00	270.65	270.65
Sep-14	R36894	0.28	12.38	14.21	0.00	0.00	5.02	0.00	284.26	284.26
Oct-14	R36901	0.24	12.04	13.28	0.00	0.00	4.84	0.00	325.08	325.08
Nov-14	R36969	0.88	15.02	15.16	0.00	0.00	13.34	15.12	231.34	246.46
Dec-14	R37227	0.38	11.79	13.88	0.09	0.00	12.38	0.00	370.44	370.44

Crayfish Spring		Water Soluble Species (ppm)										
Date	LAB ID	As 189.042	Ca 315.887	Cu 324.754	Fe 259.940	K 766.490	Mg 279.553	Mn 257.610	Na 588.995	S 180.731	Zn 213.856	Pb 220.353
Dec-12	R31299	0.00	115.90	0.00	0.01	6.81	24.15	0.00	12.08	8.28	0.01	0.00
Jan-13	R31498	0.01	109.50	0.00	0.00	1.08	24.28	0.00	11.06	7.79	0.00	0.01
Feb-13	R31519	0.00	105.50	0.00	0.07	0.98	23.84	0.00	10.46	7.77	0.00	0.00
Mar-13	R31569	-0.01	117.36	0.00	0.01	1.40	26.62	0.00	12.54	9.24	0.00	0.00
Apr-13	no data	0.01	125.70	0.00	0.01	0.80	30.52	0.01	13.79	10.03	0.00	0.00
May-13	R32045	0.00	118.50	0.06	0.00	0.91	25.11	0.00	11.45	7.73	0.02	0.02
Jun-13	R32255	0.01	106.40	0.00	0.01	0.94	29.89	0.00	14.89	9.78	0.00	0.01
Jul-13	R32370	0.01	125.70	0.00	0.01	0.80	30.52	0.01	13.79	10.03	0.00	0.00
Aug-13	R32579	-0.01	127.60	0.00	0.01	0.74	25.60	0.03	11.94	8.36	0.02	0.01
Sep-13	R32668	0.01	123.60	0.00	0.01	0.70	26.66	0.00	12.27	9.60	0.00	0.01
Oct-13	R32848	0.00	105.50	0.00	0.07	0.98	23.84	0.00	10.46	7.77	0.00	0.00
Nov-13	R33470	0.00	113.85	0.00	0.05	8.17	27.07	0.00	0.82	7.18	0.00	0.00
Dec-13	R33531	0.00	106.44	0.00	0.05	7.47	32.45	0.00	0.79	5.04	0.00	0.00
Jan-14	R35598	0.00	115.77	0.00	0.00	0.17	23.55	0.00	3.23	6.68	0.00	0.00
Feb-14	R33746	0.00	110.62	0.01	0.00	2.93	23.26	0.00	12.26	4.69	0.00	0.00
Mar-14	R31602	0.00	148.22	0.00	0.04	1.90	33.82	0.01	26.59	1.79	0.00	0.01
Apr-14	R35126	0.00	130.41	0.00	0.05	0.63	23.09	0.00	12.71	4.95	0.00	0.00
May-14	R35567	0.00	151.60	0.00	0.03	1.09	32.01	0.00	14.30	5.30	0.01	0.00
Jun-14	R36146	0.00	126.82	0.00	0.03	1.17	21.49	0.00	9.76	4.70	0.01	0.00
Jul-14	R36320	0.00	130.41	0.00	0.05	0.63	23.09	0.00	12.71	4.95	0.00	0.00
Aug-14	R36530	0.00	106.44	0.00	0.05	7.43	32.45	0.00	0.79	5.04	0.00	0.00
Sep-14	R36894	0.00	132.46	0.00	0.00	0.72	29.79	0.00	12.46	9.60	0.00	0.01
Oct-14	R36901	0.00	122.04	0.00	0.01	0.66	28.02	0.00	11.66	8.91	0.01	0.02
Nov-14	R36969	0.00	110.62	0.01	0.00	2.93	23.26	0.00	12.26	4.69	0.00	0.00
Dec-14	R37227	0.00	115.39	0.00	0.07	1.13	24.82	0.00	12.32	5.24	0.00	0.00

Crayfish Spring		Total Species (ppm)										
Date	LAB ID	As 189.042	Ca 315.887	Cu 324.754	Fe 259.940	K 766.490	Mg 279.553	Mn 257.610	Na 588.995	S 180.731	Zn 213.856	Pb 220.353
Dec-12	R31299	0.00	127.60	0.00	0.07	1.01	29.41	0.00	12.83	7.52	0.00	0.00
Jan-13	R31498	0.00	121.00	0.00	0.10	1.17	26.31	0.00	11.74	7.11	0.04	0.01
Feb-13	R31519	0.00	110.60	0.00	0.24	1.29	23.25	0.01	10.20	6.35	0.00	0.00
Mar-13	R31569	0.00	123.30	0.01	0.15	1.22	22.66	0.00	10.44	6.82	0.03	0.00
Apr-13	no data	0.00	140.30	0.00	0.53	0.66	27.34	0.03	12.16	7.83	0.00	0.00
May-13	R32045	0.00	142.40	0.00	0.39	1.08	29.51	0.01	13.17	7.94	0.00	0.00
Jun-13	R32255	0.00	135.00	0.00	0.05	0.71	28.49	0.00	12.67	7.94	0.00	0.00
Jul-13	R32370	0.00	236.30	0.01	0.88	1.28	45.70	0.06	20.67	12.07	0.00	0.00
Aug-13	R32579	0.00	132.00	0.00	0.18	0.85	25.50	0.01	11.96	7.48	0.00	0.00
Sep-13	R32668	0.00	140.30	0.00	0.53	0.66	27.34	0.03	12.16	7.83	0.00	0.00
Oct-13	R32848	0.00	127.60	0.00	0.07	1.01	29.41	0.00	12.83	7.52	0.00	0.00
Nov-13	R33470	0.00	117.89	0.00	0.05	0.17	23.72	0.00	11.06	4.73	0.00	0.00
Dec-13	R33531	0.00	162.64	0.00	0.03	0.61	31.84	0.00	15.35	6.60	0.00	0.00
Jan-14	R35598	0.00	111.19	0.00	0.14	0.90	21.73	0.00	2.48	6.62	0.00	0.00
Feb-14	R33746	0.00	117.89	0.00	0.05	0.17	23.72	0.00	11.06	4.73	0.00	0.00
Mar-14	R31602	0.00	130.89	0.00	0.01	0.05	29.89	0.00	19.40	21.01	0.01	0.00
Apr-14	R35126	0.00	117.71	0.00	0.01	0.57	26.65	0.00	0.00	4.91	0.00	0.00
May-14	R35567	0.00	117.88	0.00	0.49	0.24	23.91	0.01	10.44	4.67	0.01	0.00
Jun-14	R36146	0.00	126.82	0.00	0.03	1.17	21.49	0.00	9.76	4.70	0.01	0.03
Jul-14	R36320	0.00	144.83	0.01	0.04	3.38	25.02	0.00	13.67	5.44	0.00	0.00
Aug-14	R36530	0.00	117.88	0.00	0.49	0.24	23.91	0.01	10.44	4.67	0.01	0.00
Sep-14	R36894	0.00	162.64	0.00	0.03	0.61	31.84	0.00	15.35	6.60	0.00	0.00
Oct-14	R36901	0.00	151.60	0.00	0.15	0.91	30.30	0.01	14.37	6.15	0.00	0.00
Nov-14	R36969	0.00	117.89	0.00	0.05	0.17	23.72	0.00	11.06	4.73	0.00	0.00
Dec-14	R37227	0.00	121.40	0.00	0.17	1.32	22.24	0.00	10.63	4.94	0.00	0.00

Date	Field Data - East Range Road							
	Orifice (cm)		Flow	Discharge	pH	Temp	DO	Cond
	Width	Depth	(cm sec^{-1})	(cm^3 sec^{-1})		(^{0}C)	(%)	(µs)
Dec-12	7.40	1.90	2.27	31.92	7.10	18.50	57.60	644.80
Jan-13	7.30	1.80	3.01	39.55	7.20	18.40	62.10	632.90
Feb-13	7.40	2.00	2.96	43.81	7.03	18.50	66.30	649.50
Mar-13	7.60	1.90	2.76	39.85	7.10	18.60	76.80	749.50
Apr-13	7.60	2.10	3.08	49.12	7.24	18.82	55.30	686.20
May-13	7.60	1.20	0.46	4.17	7.15	18.72	47.90	625.40
Jun-13	7.80	1.50	0.64	7.49	7.26	19.76	48.10	630.50
Jul-13	7.60	1.90	1.91	27.55	6.70	22.50	85.40	989.10
Aug-13	7.50	1.70	0.49	6.22	7.27	20.65	54.10	680.70
Sep-13	7.40	1.80	3.28	43.68	7.10	22.80	84.10	847.20
Oct-13	7.60	1.70	1.58	21.23	7.10	21.40	67.90	786.90
Nov-13	7.50	1.90	2.17	30.91	7.27	22.10	91.70	531.20
Dec-13	7.50	1.90	3.34	47.60	5.93	19.30	79.90	527.40
Jan-14	7.50	1.80	6.17	83.30	6.84	18.10	85.10	635.50
Feb-14	7.50	1.80	6.32	85.32	6.17	18.10	84.90	624.80
Mar-14	7.40	1.90	1.45	20.39	6.86	18.50	81.10	627.30
Apr-14	7.50	1.90	4.46	63.56	6.50	18.50	82.80	603.08
May-14	7.60	1.90	7.52	108.59	6.90	20.10	76.60	458.80
Jun-14	7.50	2.00	6.53	97.95	7.79	20.60	70.40	495.80
Jul-14	7.60	1.80	6.02	82.35	7.77	21.00	70.60	342.00
Aug-14	7.40	1.80	3.26	43.42	7.43	21.20	69.40	378.50
Sep-14	7.30	1.80	0.23	3.02	6.84	22.60	69.10	597.00
Oct-14	7.50	1.90	7.95	113.29	6.81	21.70	74.90	640.80
Nov-14	7.50	1.80	4.13	55.76	6.53	20.60	75.00	624.90
Dec-14	7.40	1.90	4.32	60.74	6.44	18.10	79.00	604.00

East Range Road		Anions (ppm)								
Date	LAB ID	Fluoride	Chloride	Sulfate	Phosphate	Nitrite	Nitrate	Carbonate	Bicarbonate	Total Carbonate
Dec-12	R31300	0.04	11.26	4.09	0.00	0.00	3.45	0.00	291.82	291.82
Jan-13	R31499	0.38	8.56	5.90	0.00	0.00	1.52	0.00	250.99	250.99
Feb-13	R31520	0.36	14.65	8.16	0.65	0.00	6.43	0.00	296.35	296.35
Mar-13	R31570	0.22	18.69	8.04	0.17	0.00	8.12	0.00	216.22	216.22
Apr-13	R32003	0.43	8.17	5.99	0.00	0.00	1.61	0.00	232.85	232.85
May-13	R32043	0.38	8.56	5.90	0.00	0.00	1.52	0.00	254.02	254.02
Jun-13	R32253	0.62	11.48	6.46	0.00	0.00	1.74	0.00	246.46	246.46
Jul-13	R32369	0.16	16.43	4.89	0.00	0.00	5.18	0.00	328.10	328.10
Aug-13	R32577	0.30	8.22	5.86	0.00	0.00	1.57	0.00	210.17	210.17
Sep-13	R32666	0.18	14.28	6.18	0.00	0.00	3.38	0.00	237.38	237.38
Oct-13	R32849	0.22	18.69	8.04	0.17	0.00	8.12	0.00	275.18	275.18
Nov-13	R33471	0.16	14.07	4.92	0.00	0.00	4.29	0.00	264.60	264.60
Dec-13	R33526	0.10	15.64	4.80	0.00	0.00	4.58	0.00	163.30	163.30
Jan-14	R33595	0.37	14.05	0.69	6.76	0.00	0.06	0.00	309.96	309.96
Feb-14	R33474	0.22	14.40	2.68	0.00	0.00	1.96	0.00	166.32	166.32
Mar-14	R31599	0.07	14.75	4.66	0.00	0.00	3.87	0.00	219.24	219.24
Apr-14	R35125	0.06	13.09	3.80	0.00	0.00	3.69	0.00	246.46	246.46
May-14	R35568	0.06	12.13	4.48	0.00	0.10	3.66	0.00	192.02	192.02
Jun-14	R36143	0.04	11.26	4.09	0.00	0.00	3.45	0.00	216.22	216.22
Jul-14	R36316	0.09	11.52	4.31	0.00	0.00	3.56	0.00	207.14	207.14
Aug-14	R36531	0.12	11.23	4.12	0.00	0.00	3.07	0.00	254.02	254.02
Sep-14	R36895	0.15	10.95	3.94	0.00	0.00	2.57	0.00	241.92	241.92
Oct-14	R36902	0.05	11.34	3.85	0.00	0.00	2.91	0.00	235.87	235.87
Nov-14	R36968	0.52	15.22	4.85	0.00	0.00	8.66	0.00	249.48	249.48
Dec-14	R37233	0.10	13.28	4.53	0.00	0.00	6.54	0.00	246.46	246.46

East Range Road		Water Soluble Species (ppm)										
Date	LAB ID	As 189.042	Ca 315.887	Cu 324.754	Fe 259.940	K 766.490	Mg 279.553	Mn 257.610	Na 588.995	S 180.731	Zn 213.856	Pb 220.353
Dec-12	R31300	0.00	120.70	0.00	0.00	0.56	7.85	0.00	5.81	3.62	0.01	0.00
Jan-13	R31499	-0.01	118.30	0.00	0.01	0.44	8.36	0.02	5.77	4.08	0.02	0.00
Feb-13	R31520	0.02	100.40	0.01	0.01	0.56	9.40	0.00	8.67	4.43	0.02	0.01
Mar-13	R31570	0.00	62.48	0.00	0.00	0.49	2.77	0.00	9.91	3.31	0.00	0.01
Apr-13	R32003	0.00	120.70	0.00	0.00	0.56	7.85	0.00	5.81	3.62	0.01	0.00
May-13	R32043	0.00	122.20	0.16	0.00	0.45	7.98	0.00	5.64	3.75	0.03	0.01
Jun-13	R32253	0.02	100.40	0.01	0.01	0.56	9.40	0.00	8.67	4.43	0.00	0.01
Jul-13	R32369	0.00	134.10	0.00	0.01	0.40	6.81	0.00	9.98	4.05	0.00	0.01
Aug-13	R32577	-0.01	118.30	0.00	0.01	0.44	8.36	0.02	5.77	4.08	0.02	0.00
Sep-13	R32666	-0.01	129.40	0.00	0.01	0.32	7.10	0.00	8.53	4.08	0.01	0.00
Oct-13	R32849	0.02	100.40	0.01	0.01	0.56	9.40	0.00	8.67	4.43	0.01	0.01
Nov-13	R33471	0.00	59.28	0.00	0.05	8.88	2.86	0.00	1.86	2.89	0.00	0.00
Dec-13	R33526	0.00	80.02	0.00	0.05	8.48	2.62	0.00	2.94	3.01	0.00	0.00
Jan-14	R33595	0.00	128.15	0.00	0.00	0.36	2.47	0.00	0.58	3.51	0.00	0.00
Feb-14	R33474	0.00	139.61	0.00	0.00	0.34	2.59	0.01	8.65	5.22	0.00	0.01
Mar-14	R31599	0.00	168.71	0.02	0.03	2.60	3.25	0.00	24.67	1.12	0.01	0.00
Apr-14	R35125	0.00	78.32	-0.01	0.01	1.01	2.11	0.00	9.69	2.34	0.00	0.00
May-14	R35568	0.00	178.49	0.00	0.03	0.36	3.06	0.00	11.11	3.17	0.00	0.00
Jun-14	R36143	0.00	132.21	0.00	0.02	0.93	2.12	0.00	8.18	2.94	0.01	0.00
Jul-14	R36316	0.00	137.78	0.00	0.05	0.66	2.31	0.00	10.76	3.18	0.00	0.00
Aug-14	R36531	0.00	59.28	0.00	0.05	8.82	2.86	0.00	1.86	2.89	0.00	0.00
Sep-14	R36895	0.00	139.61	0.00	0.00	0.34	2.59	0.01	8.65	5.22	0.00	0.01
Oct-14	R36902	0.00	138.30	0.00	0.01	0.24	2.42	0.00	8.63	5.09	0.00	0.02
Nov-14	R36968	0.00	124.20	0.01	0.00	1.46	2.53	0.00	9.54	2.88	0.00	0.00
Dec-14	R37233	0.00	78.32	-0.01	0.01	1.01	2.11	0.00	9.69	2.34	0.00	0.00

East Range Road		Total Species (ppm)										
Date	LAB ID	As 189.042	Ca 315.887	Cu 324.754	Fe 259.940	K 766.490	Mg 279.553	Mn 257.610	Na 588.995	S 180.731	Zn 213.856	Pb 220.353
Dec-12	R31300	0.00	126.10	0.00	0.91	0.53	4.78	0.01	14.44	5.49	0.00	0.00
Jan-13	R31499	0.00	135.90	0.00	0.05	0.24	2.10	0.00	8.45	3.19	0.00	0.01
Feb-13	R31520	0.00	126.30	0.00	0.05	0.30	8.88	0.00	6.29	3.54	0.00	0.00
Mar-13	R31570	0.00	123.30	0.00	0.04	0.43	1.99	0.00	8.66	2.86	0.02	0.00
Apr-13	R32003	0.00	123.10	0.00	0.05	0.24	7.96	0.00	5.75	3.34	0.01	0.01
May-13	R32043	0.01	134.50	0.00	0.07	0.51	8.64	0.01	6.16	3.61	0.00	0.02
Jun-13	R32253	0.00	126.30	0.00	0.05	0.30	8.88	0.00	6.29	3.54	0.00	0.00
Jul-13	R32369	0.00	326.10	0.00	0.91	0.53	4.78	0.01	14.44	5.49	0.00	0.00
Aug-13	R32577	0.00	124.60	0.00	0.24	0.60	8.26	0.02	5.98	3.59	0.00	0.00
Sep-13	R32666	0.00	135.90	0.00	0.05	0.24	2.10	0.00	8.45	3.19	0.00	-0.01
Oct-13	R32849	0.00	126.30	0.00	0.05	0.30	8.88	0.00	6.29	3.54	0.00	0.00
Nov-13	R33471	0.00	149.62	0.00	0.01	0.28	2.63	0.00	14.93	13.46	0.00	0.00
Dec-13	R33526	0.00	174.34	0.00	0.01	0.26	2.79	0.00	10.95	3.51	0.00	0.00
Jan-14	R33595	0.00	113.92	0.00	0.05	0.77	2.01	0.00	0.54	3.36	0.00	0.00
Feb-14	R33474	0.00	107.98	0.00	0.03	0.38	2.26	0.00	8.43	2.51	0.00	0.00
Mar-14	R31599	0.00	149.62	0.00	0.01	0.27	2.63	0.00	14.93	13.46	0.00	0.00
Apr-14	R35125	0.00	138.26	0.00	0.01	0.27	2.42	0.00	9.15	3.01	0.00	0.00
May-14	R35568	0.00	127.62	0.00	0.01	0.51	2.47	0.00	7.60	2.70	0.00	0.00
Jun-14	R36143	0.00	132.21	0.00	0.02	0.93	2.12	0.00	8.18	2.94	0.01	0.03
Jul-14	R36316	0.00	151.18	0.00	0.09	4.58	3.45	0.00	10.58	3.41	0.00	0.00
Aug-14	R36531	0.00	174.34	0.00	0.01	0.26	2.79	0.00	10.95	3.51	0.00	0.00
Sep-14	R36895	0.00	170.26	0.00	0.01	0.24	2.69	0.00	10.59	3.44	0.00	0.00
Oct-14	R36902	0.00	174.34	0.00	0.01	0.26	2.79	0.00	10.95	3.51	0.00	0.00
Nov-14	R36968	0.00	128.00	0.00	0.01	0.79	2.14	0.00	8.30	2.81	0.00	0.00
Dec-14	R37233	0.00	107.98	0.00	0.02	0.38	2.26	0.00	8.43	2.51	0.00	0.00

Date	Field Data - Geocache Spring							
	Orifice (cm)		Flow	Discharge	pH	Temp	DO	Cond
	Width	Depth	(cm sec^{-1})	(cm^3 sec^{-1})		(^{0}C)	(%)	(µs)
Dec-12	9.00	4.00	2.22	79.81	6.88	19.40	74.60	794.10
Jan-13	8.90	4.10	6.50	237.19	7.40	18.70	85.70	763.40
Feb-13	9.10	3.80	2.35	81.26	6.96	18.60	96.60	662.70
Mar-13	8.90	3.60	1.72	55.11	6.60	18.70	79.80	1096.40
Apr-13	8.90	3.60	2.04	65.20	6.96	18.40	72.40	829.15
May-13	8.90	3.60	4.42	141.62	7.38	18.80	68.50	1003.27
Jun-13	8.90	3.60	2.95	94.54	6.92	19.10	65.90	963.14
Jul-13	8.90	3.40	1.79	54.10	6.78	19.70	94.90	1012.40
Aug-13	9.10	4.20	3.00	114.57	6.84	19.90	74.80	890.57
Sep-13	9.10	4.20	6.16	235.59	6.71	20.40	55.50	1206.90
Oct-13	8.90	4.10	4.67	170.44	6.82	20.10	58.60	1114.20
Nov-13	7.60	2.90	5.15	113.48	6.75	19.70	67.20	1056.30
Dec-13	9.40	4.20	8.87	350.35	5.15	19.10	63.40	650.70
Jan-14	8.80	4.20	5.75	212.56	7.14	18.50	80.80	743.20
Feb-14	8.90	4.10	10.10	368.55	6.24	18.20	73.40	684.10
Mar-14	9.10	3.90	8.53	302.69	6.57	18.40	79.50	614.30
Apr-14	9.40	3.40	14.51	463.74	7.36	17.60	76.80	668.10
May-14	8.40	2.20	3.47	64.18	7.25	18.50	68.40	514.90
Jun-14	8.80	4.20	13.60	502.66	7.27	19.20	64.40	764.70
Jul-14	8.80	3.80	3.30	110.35	7.69	20.20	74.60	767.20
Aug-14	8.70	3.80	2.16	71.41	7.23	20.30	72.80	799.50
Sep-14	8.60	3.70	0.33	10.50	7.03	20.40	68.50	804.80
Oct-14	8.70	3.70	2.28	73.39	6.65	19.80	58.60	726.50
Nov-14	8.70	3.80	1.84	60.83	6.87	19.10	69.60	597.10
Dec-14	8.70	3.70	0.45	14.45	6.37	18.20	74.50	229.30

Geocache Spring		Anions (ppm)								
Date	LAB ID	Fluoride	Chloride	Sulfate	Phosphate	Nitrite	Nitrate	Carbonate	Bicarbonate	Total Carbonate
Dec-12	R31297	0.62	9.19	4.22	0.00	0.00	7.17	0.00	261.58	261.58
Jan-13	R31499	0.67	18.64	10.49	0.00	0.00	3.57	0.00	294.84	294.84
Feb-13	R31514	0.25	15.64	1.45	26.15	0.00	2.78	0.00	326.59	326.59
Mar-13	R31564	0.64	23.75	14.97	12.66	0.00	3.41	0.00	317.52	317.52
Apr-13	R32004	0.61	22.32	14.07	0.00	0.00	3.21	0.00	264.60	264.60
May-13	R32044	0.63	23.22	14.63	0.00	0.00	3.34	0.00	260.06	260.06
Jun-13	R32254	0.57	18.79	9.97	0.00	0.00	3.91	0.00	234.36	234.36
Jul-13	R32371	1.22	21.91	10.64	0.00	0.00	1.86	0.00	322.06	322.06
Aug-13	R32578	0.65	19.18	10.05	0.00	0.00	3.66	0.00	232.85	232.85
Sep-13	R32667	0.43	20.86	11.47	0.00	0.00	0.72	0.00	261.58	261.58
Oct-13	R32850	0.40	14.44	7.58	0.00	0.00	2.87	0.00	263.09	263.09
Nov-13	R33467	0.36	8.02	3.69	0.00	0.00	5.01	0.00	252.50	252.50
Dec-13	R33532	0.42	19.53	9.72	0.00	0.00	1.92	0.00	266.11	266.11
Jan-14	R33597	0.37	21.88	0.93	1.73	0.00	0.07	0.00	294.84	294.84
Feb-14	R33475	0.35	20.16	5.47	0.00	0.00	0.80	0.00	311.47	311.47
Mar-14	R31603	0.33	18.44	10.00	0.00	0.00	1.53	0.00	314.50	314.50
Apr-14	R35124	0.50	17.59	9.93	0.00	0.00	1.74	0.00	291.82	291.82
May-14	R35572	0.46	17.19	9.83	0.00	0.12	1.78	0.00	222.26	222.26
Jun-14	R36142	0.54	16.08	8.72	0.00	0.00	0.00	0.00	328.10	328.10
Jul-14	R36322	0.56	17.54	9.35	0.00	0.00	1.53	0.00	337.18	337.18
Aug-14	R36532	0.39	17.80	9.25	0.00	0.00	1.21	0.00	343.22	343.22
Sep-14	R36896	0.22	18.05	9.16	0.00	0.00	0.88	0.00	355.32	355.32
Oct-14	R36903	0.22	16.55	8.59	0.00	0.00	0.32	0.00	353.81	353.81
Nov-14	R36967	0.90	21.85	10.26	0.00	0.00	3.17	0.00	379.51	379.51
Dec-14	R37232	0.43	18.41	9.30	0.00	0.00	2.58	0.00	382.54	382.54

Geocache Spring		Water Soluble Species (ppm)										
Date	LAB ID	As 189.042	Ca 315.887	Cu 324.754	Fe 259.940	K 766.490	Mg 279.553	Mn 257.610	Na 588.995	S 180.731	Zn 213.856	Pb 220.353
Dec-12	R31297	0.00	99.44	0.00	0.00	3.92	31.23	0.00	14.26	5.80	0.01	0.01
Jan-13	R31499	0.02	97.34	0.00	0.01	1.09	32.43	0.00	13.90	5.42	0.01	0.01
Feb-13	R31514	0.02	100.26	0.00	0.01	1.12	33.40	0.00	14.32	5.58	0.01	0.01
Mar-13	R31564	0.00	42.13	0.00	0.01	1.29	37.62	0.01	16.81	6.37	0.00	0.02
Apr-13	R32004	0.01	84.79	0.00	0.01	1.85	33.67	0.01	14.82	5.79	0.01	0.00
May-13	R32044	0.01	79.70	0.00	0.01	1.74	31.65	0.01	13.93	5.44	0.01	0.00
Jun-13	R32254	0.01	82.10	0.00	0.01	1.79	32.60	0.01	14.35	5.61	0.01	0.00
Jul-13	R32371	0.00	108.70	0.00	0.01	0.99	39.05	0.00	17.77	6.84	0.00	0.01
Aug-13	R32578	0.01	86.81	0.00	0.01	1.72	33.96	0.00	15.02	5.86	0.01	0.00
Sep-13	R32667	0.00	102.90	0.00	0.02	0.85	34.98	0.00	16.57	6.64	0.00	0.00
Oct-13	R32850	0.00	96.73	0.00	0.02	0.80	32.88	0.00	15.58	6.24	0.00	0.00
Nov-13	R33467	0.00	42.04	0.00	0.05	8.55	19.79	0.00	5.41	2.13	0.00	0.00
Dec-13	R33532	0.00	103.13	0.00	0.05	7.84	38.52	0.00	6.41	5.38	0.00	0.00
Jan-14	R33597	0.00	99.86	0.00	0.00	0.46	33.54	0.00	8.98	5.06	0.00	0.00
Feb-14	R33475	0.00	105.59	0.00	0.05	1.54	34.47	0.00	15.94	3.58	0.01	0.00
Mar-14	R31603	0.00	123.54	0.00	0.03	1.79	46.04	0.00	13.45	1.27	0.00	0.00
Apr-14	R35124	0.00	105.89	0.00	0.01	0.83	39.81	0.00	17.18	6.39	0.00	0.01
May-14	R35572	0.00	131.07	0.00	0.03	1.08	44.49	0.00	20.28	4.16	0.00	0.00
Jun-14	R36142	0.00	105.59	0.00	0.05	1.54	34.47	0.00	15.94	3.58	0.01	0.00
Jul-14	R36322	0.00	108.42	0.00	0.05	0.61	36.47	0.00	14.64	3.75	0.00	0.00
Aug-14	R36532	0.00	103.13	0.00	0.05	8.74	38.52	0.00	6.41	5.38	0.00	0.00
Sep-14	R36896	0.00	109.95	0.00	0.00	0.59	42.57	0.00	21.42	6.92	0.00	0.02
Oct-14	R36903	0.00	105.89	0.00	0.01	0.83	39.81	0.00	17.18	6.39	0.00	0.01
Nov-14	R36967	0.00	96.77	0.02	0.00	1.98	35.30	0.00	17.70	3.57	0.00	0.00
Dec-14	R37232	0.00	84.32	0.01	0.02	0.22	41.36	0.00	19.81	3.86	0.00	0.00

Geocache Spring		Total Species (ppm)										
Date	LAB ID	As 189.042	Ca 315.887	Cu 324.754	Fe 259.940	K 766.490	Mg 279.553	Mn 257.610	Na 588.995	S 180.731	Zn 213.856	Pb 220.353
Dec-12	R31297	0.01	111.60	0.00	0.05	1.08	37.82	0.00	16.24	5.20	0.00	0.01
Jan-13	R31499	0.01	110.40	0.00	0.03	1.24	36.26	0.00	15.49	5.11	0.04	0.00
Feb-13	R31514	0.00	109.30	0.00	0.04	1.24	36.04	0.00	15.80	5.09	0.03	0.00
Mar-13	R31564	0.01	108.20	0.01	0.05	1.23	35.81	0.00	16.11	5.08	0.03	0.00
Apr-13	R32004	0.00	109.30	0.00	0.04	1.24	36.04	0.00	15.80	5.09	0.03	0.00
May-13	R32044	0.00	95.09	0.00	0.03	1.08	31.35	0.00	13.75	4.43	0.03	0.00
Jun-13	R32254	0.00	98.89	0.00	0.03	1.12	32.60	0.00	14.30	4.61	0.03	0.00
Jul-13	R32371	0.00	155.00	0.01	0.06	1.35	51.80	0.00	23.79	7.14	0.01	0.00
Aug-13	R32578	0.00	113.30	0.00	0.04	1.20	37.52	0.00	16.75	5.27	0.03	0.00
Sep-13	R32667	0.00	107.30	0.00	0.02	0.84	36.59	0.00	17.27	5.30	0.00	0.00
Oct-13	R32850	0.00	93.35	0.00	0.02	0.73	31.83	0.00	15.02	4.61	0.00	0.00
Nov-13	R33467	0.01	110.40	0.00	0.03	1.24	36.26	0.00	15.49	5.11	0.04	0.00
Dec-13	R33532	0.00	155.00	0.01	0.06	1.35	51.80	0.00	23.79	7.14	0.01	0.00
Jan-14	R33597	0.00	93.72	0.00	0.09	1.15	30.94	0.00	7.69	4.89	0.00	0.00
Feb-14	R33475	0.00	100.70	0.00	0.01	0.02	33.50	0.00	15.38	3.33	0.00	0.00
Mar-14	R31603	0.00	116.25	0.00	0.04	1.63	42.54	0.00	22.16	15.09	0.00	0.00
Apr-14	R35124	0.00	109.31	0.00	0.02	1.47	36.66	0.00	17.46	3.72	0.00	0.00
May-14	R35572	0.00	100.70	0.00	0.01	0.02	33.50	0.00	15.38	3.33	0.00	0.00
Jun-14	R36142	0.00	105.59	0.00	0.05	1.54	34.47	0.00	15.94	3.58	0.01	0.01
Jul-14	R36322	0.00	118.77	0.00	0.04	3.14	39.57	0.00	18.43	4.17	0.00	0.00
Aug-14	R36532	0.00	109.31	0.00	0.02	1.47	36.66	0.00	17.46	3.72	0.00	0.00
Sep-14	R36896	0.00	136.11	0.00	0.05	0.67	46.37	0.00	24.86	4.83	0.00	0.00
Oct-14	R36903	0.00	131.32	0.00	0.04	1.04	44.03	0.00	21.78	4.47	0.00	0.00
Nov-14	R36967	0.00	100.22	0.00	0.05	0.12	35.06	0.00	16.62	3.56	0.00	0.00
Dec-14	R37232	0.00	93.84	0.00	0.03	0.79	33.12	0.00	15.34	3.44	0.00	0.00

Date	Field Data - Gnarly Root							
	Orifice (cm)		Flow	Discharge	pH	Temp	DO	Cond
	Width	Depth	(cm sec^{-1})	(cm^3 sec^{-1})		(^{0}C)	(%)	(µs)
Dec-12	50.40	10.20	0.44	225.68	7.31	18.90	74.20	650.50
Jan-13	52.00	9.40	0.70	342.16	7.77	17.80	73.10	641.10
Feb-13	51.60	10.60	5.90	3227.06	7.22	17.90	73.10	626.40
Mar-13	54.30	11.40	17.12	10597.62	6.98	16.70	77.30	896.20
Apr-13	51.40	9.10	3.35	1567.72	7.57	18.91	78.90	681.40
May-13	50.20	6.10	1.71	522.51	7.56	19.71	75.60	240.80
Jun-13	50.40	7.40	7.80	2909.21	7.68	20.20	86.70	675.90
Jul-13	50.10	10.40	13.26	6908.99	7.28	21.30	82.80	931.30
Aug-13	49.60	8.80	5.24	2287.51	7.65	20.45	84.10	658.70
Sep-13	51.60	11.40	20.62	12129.51	7.16	20.40	76.30	930.90
Oct-13	50.30	11.10	18.65	10412.85	7.14	20.10	72.40	933.70
Nov-13	50.30	10.10	12.58	6391.02	7.17	19.10	67.40	924.40
Dec-13	52.40	11.80	25.57	15810.44	5.34	17.30	65.80	579.40
Jan-14	52.30	12.40	35.75	23184.59	6.86	16.70	89.20	604.10
Feb-14	55.60	12.30	32.80	22431.26	6.46	16.90	73.10	597.00
Mar-14	52.70	11.90	19.13	11997.00	7.23	17.50	69.20	312.30
Apr-14	51.30	11.10	22.67	12908.98	6.96	17.80	98.40	544.80
May-14	55.40	11.40	23.92	15106.92	6.68	19.90	69.80	603.30
Jun-14	54.10	11.30	19.00	11615.27	7.07	19.70	68.10	604.20
Jul-14	53.40	10.90	14.98	8719.26	7.64	20.10	64.50	330.60
Aug-14	51.80	10.80	16.76	9376.21	7.71	20.30	66.70	326.80
Sep-14	52.20	10.70	14.95	8350.17	7.34	20.60	67.70	480.40
Oct-14	53.60	10.90	20.80	12152.19	6.74	18.90	68.80	619.90
Nov-14	54.40	10.80	14.85	8724.67	7.05	17.40	66.30	623.30
Dec-14	56.60	11.10	21.83	13714.92	6.42	16.80	70.80	552.60

Gnarly Root		Anions (ppm)								
Date	LAB ID	Fluoride	Chloride	Sulfate	Phosphate	Nitrite	Nitrate	Carbonate	Bicarbonate	Total Carbonate
Dec-12	R31296	0.28	10.84	5.91	0.00	0.00	3.59	0.00	269.14	269.14
Jan-13	R31500	0.34	9.60	5.07	0.00	0.00	7.14	0.00	276.70	276.70
Feb-13	R31516	0.31	10.22	5.49	0.00	0.00	5.37	0.00	267.62	267.62
Mar-13	R31566	0.90	12.72	8.90	0.17	0.00	7.66	0.00	297.86	297.86
Apr-13	R32002	0.67	8.37	4.02	1.22	0.00	6.75	0.00	284.26	284.26
May-13	R32042	0.64	8.04	3.74	0.00	0.00	5.34	0.00	276.70	276.70
Jun-13	R32252	1.05	17.44	5.07	0.00	0.00	6.25	0.00	244.94	244.94
Jul-13	R32368	1.17	9.94	4.04	0.00	0.00	5.70	0.00	189.00	189.00
Aug-13	R32576	0.58	8.35	3.62	0.00	0.00	4.95	0.00	266.11	266.11
Sep-13	R32664	0.58	8.66	4.68	0.00	0.00	4.28	0.00	341.71	341.71
Oct-13	R32851	0.65	10.42	5.05	0.00	0.00	5.70	0.00	264.60	264.60
Nov-13	R33467	0.36	8.02	3.69	0.00	0.00	5.01	0.00	261.58	261.58
Dec-13	R33527	0.50	9.86	3.96	0.00	0.00	5.14	0.00	204.12	204.12
Jan-14	R33596	0.36	8.86	0.75	8.34	0.00	0.04	0.00	311.47	311.47
Feb-14	R33476	0.32	8.44	2.42	0.00	0.00	2.25	9.07	232.85	241.92
Mar-14	R31600	0.28	8.02	4.08	0.00	0.00	4.46	0.00	220.75	220.75
Apr-14	R35127	0.51	7.52	3.58	0.00	0.00	4.74	0.00	219.24	219.24
May-14	R35573	0.30	7.05	3.50	0.00	0.12	3.40	0.00	235.87	235.87
Jun-14	R36145	0.37	6.57	3.19	0.00	0.00	9.14	0.00	252.50	252.50
Jul-14	R36321	0.41	6.82	3.31	0.00	0.00	4.19	0.00	184.46	184.46
Aug-14	R36533	0.33	6.55	3.28	0.00	0.00	3.72	0.00	260.06	260.06
Sep-14	R36897	0.24	6.28	3.25	0.00	0.00	3.26	0.00	267.62	267.62
Oct-14	R36904	0.24	6.38	3.00	0.00	0.00	2.96	0.00	269.14	269.14
Nov-14	R36964	0.32	8.72	3.97	0.00	0.00	8.94	0.00	322.06	322.06
Dec-14	R37231	0.31	8.51	4.06	0.00	0.00	8.19	0.00	319.03	319.03

Gnarly Root		Water Soluble Species (ppm)										
Date	LAB ID	As 189.042	Ca 315.887	Cu 324.754	Fe 259.940	K 766.490	Mg 279.553	Mn 257.610	Na 588.995	S 180.731	Zn 213.856	Pb 220.353
Dec-12	R31296	-0.01	107.80	0.00	0.01	2.11	14.17	0.00	5.90	3.15	0.01	0.01
Jan-13	R31500	0.01	105.60	0.00	0.00	0.50	14.65	0.00	6.22	3.01	0.00	0.01
Feb-13	R31516	0.00	107.40	0.01	0.01	0.77	16.06	0.02	7.01	3.81	0.01	0.01
Mar-13	R31566	0.00	58.51	0.00	0.01	0.96	15.12	0.00	8.00	3.89	0.00	0.00
Apr-13	R32002	0.01	110.20	0.00	0.01	0.50	15.46	0.00	6.10	2.65	0.00	0.00
May-13	R32042	0.01	113.90	0.00	0.01	0.53	18.27	0.00	7.10	3.39	0.00	0.02
Jun-13	R32252	0.00	111.70	0.01	0.01	0.57	17.64	0.00	11.17	3.71	0.02	0.01
Jul-13	R32368	0.01	113.90	0.00	0.01	0.53	18.27	0.00	7.10	3.39	0.00	0.02
Aug-13	R32576	-0.01	107.00	0.00	0.01	0.44	15.55	0.00	6.24	3.28	0.01	0.01
Sep-13	R32664	0.00	107.40	0.01	0.01	0.77	16.06	0.02	7.01	3.81	0.01	0.01
Oct-13	R32851	0.01	105.60	0.00	0.00	0.50	14.65	0.00	6.22	3.01	0.00	0.01
Nov-13	R33467	0.00	42.04	0.00	0.05	8.55	19.79	0.00	5.41	2.13	0.00	0.00
Dec-13	R33527	0.00	98.32	0.00	0.05	8.46	18.78	0.00	5.04	3.02	0.00	0.00
Jan-14	R33596	0.00	99.89	0.00	0.00	0.06	16.23	0.00	1.96	2.92	0.00	0.00
Feb-14	R33476	0.00	101.86	0.00	0.00	0.37	17.23	0.00	6.91	2.43	0.00	0.00
Mar-14	R31600	0.00	131.03	0.01	0.04	1.13	21.29	0.02	16.63	0.97	0.00	0.00
Apr-14	R35127	0.00	98.32	0.00	0.05	8.41	18.78	0.00	5.02	3.02	0.00	0.00
May-14	R35573	0.00	141.60	0.00	0.03	0.37	21.94	0.00	8.14	2.62	0.00	0.00
Jun-14	R36145	0.00	104.17	0.01	0.03	0.77	16.15	0.00	5.83	2.32	0.01	0.00
Jul-14	R36321	0.00	111.77	0.00	0.05	0.33	17.66	0.00	8.16	2.60	0.00	0.00
Aug-14	R36533	0.00	131.03	0.01	0.04	1.13	21.29	0.02	16.63	0.97	0.00	0.00
Sep-14	R36897	0.00	114.19	0.00	0.00	0.35	20.23	0.00	6.99	4.29	0.00	0.02
Oct-14	R36904	0.00	111.43	0.00	0.00	0.21	19.58	0.00	6.50	4.14	0.00	0.01
Nov-14	R36964	0.00	101.86	0.00	0.00	0.37	17.23	0.00	6.91	2.43	0.00	0.00
Dec-14	R37231	0.00	81.79	0.01	0.03	1.15	19.89	-0.01	8.27	2.28	0.00	0.00

Gnarly Root		Total Species (ppm)										
Date	LAB ID	As 189.042	Ca 315.887	Cu 324.754	Fe 259.940	K 766.490	Mg 279.553	Mn 257.610	Na 588.995	S 180.731	Zn 213.856	Pb 220.353
Dec-12	R31296	0.00	114.40	0.00	0.10	0.38	15.42	0.00	5.95	2.32	0.00	0.01
Jan-13	R31500	0.00	114.40	0.00	0.07	0.52	15.18	0.00	6.38	2.57	0.03	0.01
Feb-13	R31516	0.00	111.80	0.00	0.02	0.23	15.70	0.00	6.07	2.36	0.01	0.00
Mar-13	R31566	0.01	112.00	0.00	0.01	0.61	13.80	0.00	6.83	3.17	0.02	0.00
Apr-13	R32002	0.00	111.80	0.00	0.02	0.23	15.70	0.00	6.07	2.36	0.01	0.00
May-13	R32042	0.01	113.90	0.00	0.11	0.87	15.97	0.00	6.49	2.68	0.01	0.00
Jun-13	R32252	0.01	117.30	0.00	0.20	0.25	16.56	0.01	6.27	2.46	0.00	0.01
Jul-13	R32368	0.01	188.70	0.01	0.34	0.55	25.62	0.01	10.19	3.74	0.00	0.01
Aug-13	R32576	0.01	113.90	0.00	0.11	0.87	15.97	0.00	6.49	2.68	0.01	0.00
Sep-13	R32664	0.00	112.30	0.00	0.17	0.32	15.94	0.00	6.03	2.59	0.00	0.01
Oct-13	R32851	0.01	188.70	0.01	0.34	0.55	25.62	0.01	10.19	3.74	0.00	0.01
Nov-13	R33467	0.00	104.17	0.01	0.03	0.77	16.15	0.00	5.83	2.32	0.01	0.01
Dec-13	R33527	0.00	124.40	0.00	0.01	2.67	19.07	0.00	8.37	2.91	0.00	0.00
Jan-14	R33596	0.00	96.47	0.00	0.07	0.46	14.91	0.00	2.52	2.79	0.00	0.00
Feb-14	R33476	0.00	102.08	0.00	0.01	0.27	16.46	0.00	7.05	2.32	0.00	0.00
Mar-14	R31600	0.00	116.30	0.00	0.00	0.56	19.46	0.00	10.81	9.29	0.00	0.00
Apr-14	R35127	0.00	112.24	0.00	0.01	0.05	17.65	0.00	6.68	2.39	0.00	0.00
May-14	R35573	0.00	102.53	0.00	0.08	0.51	15.37	0.00	5.56	2.15	0.00	0.00
Jun-14	R36145	0.00	104.17	0.01	0.03	0.77	16.15	0.00	5.83	2.32	0.01	0.01
Jul-14	R36321	0.00	124.40	0.00	0.01	2.67	19.07	0.00	8.37	2.91	0.00	0.00
Aug-14	R36533	0.00	109.71	0.00	0.03	0.46	17.15	0.00	6.73	2.42	0.00	0.00
Sep-14	R36897	0.00	139.91	0.00	0.02	0.24	21.44	0.00	8.21	2.78	0.00	0.00
Oct-14	R36904	0.00	138.53	0.00	0.10	0.39	21.05	0.00	8.03	2.80	0.00	0.00
Nov-14	R36964	0.00	109.71	0.00	0.03	0.41	17.15	0.00	6.73	2.42	0.00	0.00
Dec-14	R37231	0.00	102.08	0.00	0.01	0.27	16.46	0.00	7.05	2.32	0.00	0.00

Date	Field Data - Nolan Creek Spring							
	Orifice (cm)		Flow	Discharge	pH	Temp	DO	Cond
	Width	Depth	(cm sec^{-1})	(cm^3 sec^{-1})		(^{0}C)	(%)	(µs)
Dec-12	20.20	2.40	8.95	433.94	6.95	19.60	87.90	725.70
Jan-13	19.80	2.30	6.35	289.36	7.20	18.00	82.60	699.20
Feb-13	20.10	2.40	10.84	522.92	7.05	18.00	87.40	702.60
Mar-13	19.60	2.10	9.86	405.84	6.73	18.00	84.10	1008.40
Apr-13	21.10	2.20	9.35	434.23	7.19	18.38	79.60	771.50
May-13	20.60	2.50	17.40	896.02	7.12	18.53	71.60	657.30
Jun-13	19.40	2.10	9.96	405.92	7.13	19.30	71.80	484.70
Jul-13	19.80	1.90	3.46	130.08	6.81	19.70	76.60	1038.40
Aug-13	20.40	2.40	16.51	808.56	7.17	20.61	66.50	606.90
Sep-13	20.10	2.20	9.79	432.74	6.66	20.80	66.10	991.80
Oct-13	19.90	2.30	14.65	670.62	6.77	20.60	66.80	746.15
Nov-13	19.80	2.30	18.06	822.22	6.79	20.20	67.50	498.70
Dec-13	20.10	2.20	22.65	1001.54	5.19	19.00	65.10	651.10
Jan-14	19.60	2.20	18.33	790.22	6.96	18.10	73.30	357.80
Feb-14	20.10	2.40	17.45	841.88	6.30	17.30	79.20	657.30
Mar-14	19.80	2.30	9.37	426.85	6.43	17.20	71.20	684.20
Apr-14	20.60	2.30	6.92	327.63	5.69	17.10	83.80	364.50
May-14	20.40	2.40	5.28	258.31	7.46	18.50	62.10	661.20
Jun-14	18.40	1.80	4.23	139.97	7.14	18.70	57.20	682.20
Jul-14	19.60	2.20	9.47	408.26	7.76	19.20	56.20	687.20
Aug-14	19.20	2.10	6.47	260.87	7.03	19.70	57.50	688.40
Sep-14	19.90	2.30	12.92	591.39	6.71	20.60	55.20	698.00
Oct-14	19.70	2.10	7.80	322.69	6.48	20.50	60.20	687.90
Nov-14	22.40	2.30	16.95	873.42	6.66	19.70	70.10	685.70
Dec-14	20.10	2.20	7.75	342.71	7.01	17.40	71.60	362.30

Nolan Creek Spring		Anions (ppm)								
Date	LAB ID	Fluoride	Chloride	Sulfate	Phosphate	Nitrite	Nitrate	Carbonate	Bicarbonate	Total Carbonate
Dec-12	R31298	0.55	17.11	10.13	0.00	0.00	5.12	0.00	243.43	243.43
Jan-13	R31497	0.36	13.93	8.57	0.00	0.00	3.84	0.00	281.23	281.23
Feb-13	R31515	0.26	13.11	1.11	23.13	0.00	3.94	0.00	284.26	284.26
Mar-13	R31565	0.66	20.81	13.54	0.00	0.00	5.19	0.00	309.96	309.96
Apr-13	R32005	0.81	16.78	9.68	0.00	0.00	5.44	0.00	297.86	297.86
May-13	R32046	0.57	15.41	9.38	0.00	0.00	3.13	0.00	232.85	232.85
Jun-13	R32256	0.42	14.90	8.94	0.00	0.00	3.77	0.00	254.02	254.02
Jul-13	R32373	0.99	16.39	9.68	0.00	0.00	3.57	0.00	284.26	284.26
Aug-13	R32580	0.40	14.31	8.72	0.06	0.00	3.24	0.00	278.21	278.21
Sep-13	R32669	0.41	14.91	7.50	0.07	0.00	2.65	0.00	222.26	222.26
Oct-13	R32852	0.42	14.90	8.94	0.00	0.00	3.77	0.00	309.96	309.96
Nov-13	R33465	0.25	9.18	6.48	0.00	0.00	2.90	0.00	231.34	231.34
Dec-13	R33531	0.48	14.50	8.14	0.00	0.00	3.24	0.00	247.97	247.97
Jan-14	R33599	0.35	25.46	0.50	5.38	0.00	0.06	0.00	275.18	275.18
Feb-14	R33477	0.31	20.06	4.65	0.00	0.00	1.39	0.00	252.50	252.50
Mar-14	R31601	0.26	14.67	8.80	0.00	0.00	2.71	0.00	279.72	279.72
Apr-14	R35128	0.31	13.12	8.39	0.00	0.00	2.77	0.00	267.62	267.62
May-14	R35569	0.35	12.91	8.29	0.00	0.21	2.78	0.00	297.86	297.86
Jun-14	R36144	0.48	11.62	7.30	0.00	0.00	2.69	0.00	276.70	276.70
Jul-14	R36319	0.31	13.12	8.39	0.00	0.00	2.77	0.00	300.89	300.89
Aug-14	R36534	0.27	12.18	7.81	0.00	0.00	5.59	0.00	235.87	235.87
Sep-14	R36898	0.23	11.24	7.22	0.00	0.00	8.41	0.00	226.80	226.80
Oct-14	R36905	0.24	11.86	7.63	0.00	0.00	1.90	0.00	244.94	244.94
Nov-14	R36963	0.32	15.67	8.83	0.00	0.00	5.84	0.00	320.54	320.54
Dec-14	R37230	0.41	14.12	8.03	0.06	0.00	4.42	0.00	340.20	340.20

Nolan Creek Spring		Water Soluble Species (ppm)										
Date	LAB ID	As 189.042	Ca 315.887	Cu 324.754	Fe 259.940	K 766.490	Mg 279.553	Mn 257.610	Na 588.995	S 180.731	Zn 213.856	Pb 220.353
Dec-12	R31298	-0.01	94.87	0.00	0.01	6.12	27.29	0.00	12.08	5.25	0.02	0.00
Jan-13	R31497	0.01	92.03	0.00	0.00	1.28	27.01	0.00	10.82	4.81	0.01	0.00
Feb-13	R31515	0.00	93.46	0.00	0.04	1.11	28.68	0.00	11.25	4.09	0.00	0.00
Mar-13	R31565	-0.01	50.23	0.00	0.01	1.25	32.00	0.00	14.04	5.71	0.00	0.01
Apr-13	R32005	0.00	97.11	0.00	0.01	1.11	30.37	0.00	12.21	4.92	0.02	0.01
May-13	R32046	0.01	100.80	0.04	0.00	1.20	27.20	0.00	11.92	5.15	0.02	0.00
Jun-13	R32256	0.02	90.31	0.00	0.01	1.59	28.83	0.00	12.74	5.65	0.00	0.01
Jul-13	R32373	0.00	109.10	0.00	0.01	1.29	33.64	0.00	13.44	6.05	0.00	0.01
Aug-13	R32580	-0.03	100.60	0.00	0.01	1.33	28.09	0.00	11.10	4.93	0.01	0.01
Sep-13	R32669	-0.01	95.67	0.00	0.02	1.15	29.44	0.00	11.51	5.70	0.00	0.00
Oct-13	R32852	0.00	98.71	0.00	0.00	0.84	35.28	0.00	12.05	5.79	0.00	0.02
Nov-13	R33465	0.00	59.08	0.00	0.05	5.89	24.32	0.00	3.07	3.70	0.00	0.00
Dec-13	R33531	0.00	106.44	0.00	0.05	7.47	32.45	0.00	0.79	5.04	0.00	0.00
Jan-14	R33599	0.00	94.04	0.00	0.00	0.14	29.40	0.00	4.24	4.54	0.00	0.00
Feb-14	R33477	0.00	93.46	0.00	0.04	1.11	28.68	0.00	11.25	4.09	0.00	0.00
Mar-14	R31601	0.00	125.32	0.00	0.04	1.85	42.88	0.00	20.67	1.23	0.00	0.00
Apr-14	R35128	0.00	88.22	0.00	0.00	0.73	32.09	0.00	13.19	3.22	0.00	0.00
May-14	R35569	0.00	122.49	0.00	0.03	1.22	38.21	0.00	14.40	3.65	0.00	0.00
Jun-14	R36144	0.00	100.26	0.00	0.03	1.85	28.53	0.00	10.96	3.19	0.01	0.00
Jul-14	R36319	0.00	101.11	0.00	0.05	1.10	31.10	0.00	13.67	3.31	0.00	0.00
Aug-14	R36534	0.00	59.08	0.00	0.05	5.62	24.32	0.00	3.46	3.70	0.00	0.00
Sep-14	R36898	0.00	101.75	0.00	0.00	0.80	35.81	0.00	11.93	5.82	0.00	0.01
Oct-14	R36905	0.00	98.71	0.00	0.00	0.84	35.28	0.00	12.05	5.79	0.00	0.02
Nov-14	R36963	0.00	88.22	0.00	0.00	0.73	32.09	0.00	13.19	3.22	0.00	0.00
Dec-14	R37230	0.00	88.41	0.01	0.02	0.03	36.43	0.00	14.72	3.64	0.00	0.00

Nolan Creek Spring		Total Species (ppm)										
Date	LAB ID	As 189.042	Ca 315.887	Cu 324.754	Fe 259.940	K 766.490	Mg 279.553	Mn 257.610	Na 588.995	S 180.731	Zn 213.856	Pb 220.353
Dec-12	R31298	0.00	118.00	0.00	0.13	1.13	36.02	0.00	14.19	5.07	0.00	0.00
Jan-13	R31497	-0.01	102.90	0.00	0.05	1.38	29.83	0.00	11.81	4.38	0.04	0.00
Feb-13	R31515	0.00	118.00	0.00	0.13	1.13	36.02	0.00	14.19	5.07	0.00	0.00
Mar-13	R31565	0.00	99.54	0.01	0.03	1.16	29.92	0.00	12.92	4.43	0.02	0.00
Apr-13	R32005	0.00	115.20	0.00	0.23	1.09	33.69	0.00	13.35	4.83	0.01	0.00
May-13	R32046	0.01	105.80	0.00	0.20	1.53	27.64	0.01	10.93	4.37	0.00	0.00
Jun-13	R32256	0.00	113.50	0.00	0.03	1.55	30.14	0.00	11.99	4.76	0.00	0.00
Jul-13	R32373	0.00	145.70	0.00	0.08	1.61	44.34	0.00	17.67	6.18	0.00	0.00
Aug-13	R32580	0.01	105.80	0.00	0.20	1.53	27.64	0.01	10.93	4.37	0.00	0.00
Sep-13	R32669	0.01	96.04	0.00	0.05	1.05	28.97	0.00	11.07	4.33	0.00	0.01
Oct-13	R32852	0.00	123.61	0.00	0.03	1.14	38.98	0.00	15.44	4.08	0.00	0.00
Nov-13	R33465	0.00	100.26	0.00	0.03	1.85	28.53	0.00	10.96	3.19	0.01	0.01
Dec-13	R33531	0.00	93.74	0.00	0.05	0.16	31.77	0.00	13.19	3.29	0.00	0.00
Jan-14	R33599	0.00	88.85	0.00	0.02	1.03	27.70	0.00	3.51	4.35	0.00	0.00
Feb-14	R33477	0.00	97.81	0.00	0.05	3.81	0.00	0.00	12.67	2.67	0.00	0.00
Mar-14	R31601	0.00	98.21	0.00	0.01	0.18	34.34	0.00	18.96	12.13	0.00	0.00
Apr-14	R35128	0.00	105.15	0.00	0.01	0.70	32.49	0.00	11.49	3.35	0.00	0.00
May-14	R35569	0.00	97.81	0.00	0.05	0.18	30.10	0.00	11.22	3.12	0.01	0.00
Jun-14	R36144	0.00	100.26	0.00	0.03	1.85	28.53	0.00	10.96	3.19	0.01	0.01
Jul-14	R36319	0.00	112.14	0.00	0.01	4.19	33.67	0.00	15.30	3.71	0.01	0.00
Aug-14	R36534	0.00	105.15	0.00	0.02	1.03	27.70	0.00	3.51	4.35	0.00	0.00
Sep-14	R36898	0.00	125.14	0.00	0.02	1.08	39.08	0.00	14.97	4.00	0.00	0.00
Oct-14	R36905	0.00	123.61	0.00	0.03	1.14	38.98	0.00	15.44	4.08	0.00	0.00
Nov-14	R36963	0.00	97.15	0.00	0.05	0.16	31.77	0.00	13.19	3.29	0.00	0.00
Dec-14	R37230	0.00	93.74	0.00	0.03	0.88	31.75	0.00	12.26	3.36	0.00	0.00

APPENDIX II:

Piper Diagrams

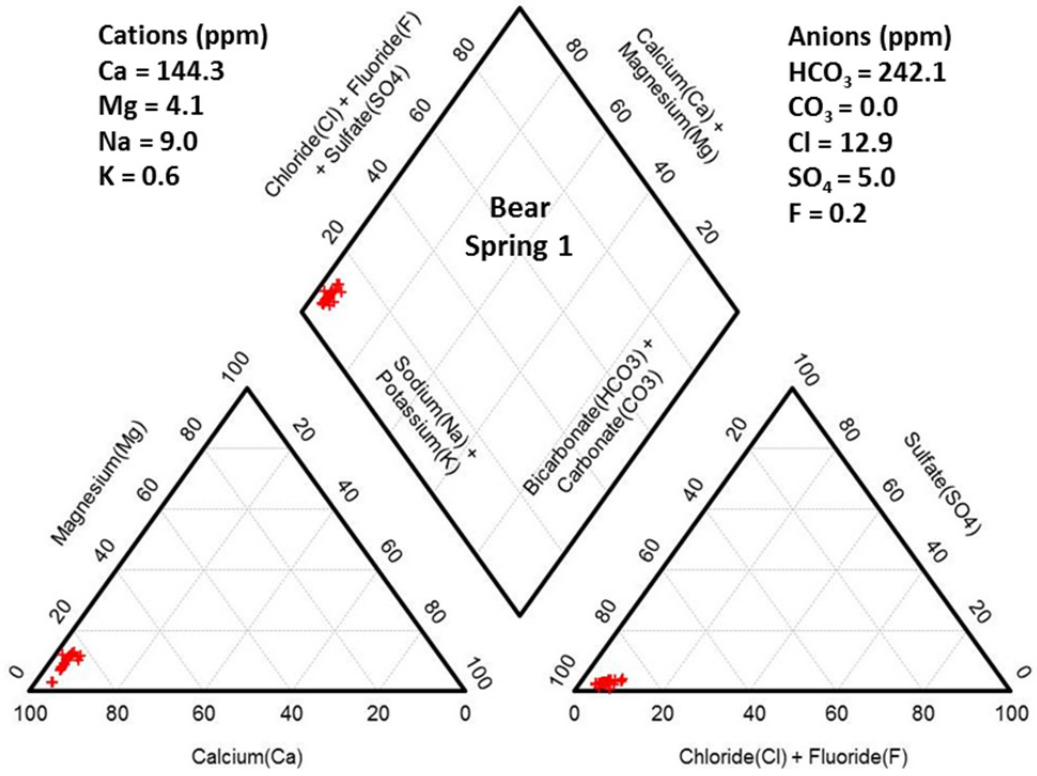
Cations (ppm)
Ca = 144.3
Mg = 4.1
Na = 9.0
K = 0.6
Anions (ppm)
HCO3 = 242.1
CO3 = 0.0
Cl = 12.9
SO4 = 5.0
F = 0.2
Bear
Spring 1
Chloride(Cl) + Fluoride(F) + Sulfate(SO4)
Calcium(Ca) + Magnesium(Mg)
Sodium(Na) + Potassium(K)
Bicarbonate(HCO3) + Carbonate(CO3)
Magnesium(Mg)
Calcium(Ca)
Sulfate(SO4)
Chloride(Cl) + Fluoride(F)

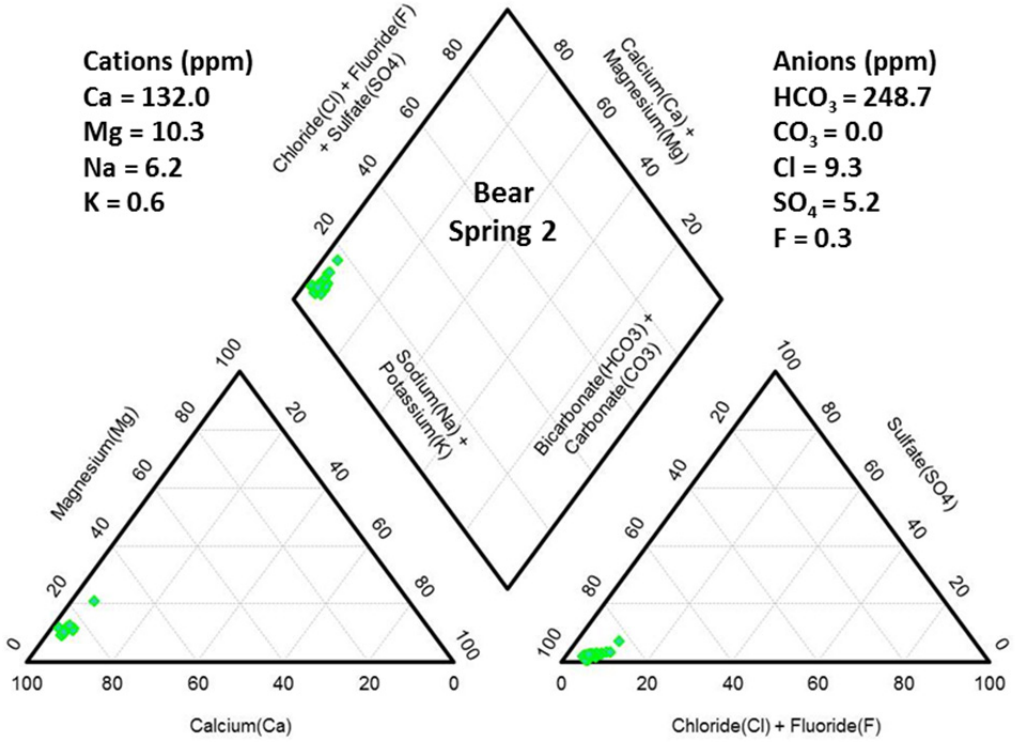
Cations (ppm)
Ca = 132.0
Mg = 10.3
Na = 6.2
K = 0.6
Anions (ppm)
HCO3 = 248.7
CO3 = 0.0
Cl = 9.3
SO4 = 5.2
F = 0.3
Bear Spring 2
Chloride(Cl) + Fluoride(F) + Sulfate(SO4)
Calcium(Ca) + Magnesium(Mg)
Sodium(Na) + Potassium(K)
Bicarbonate(HCO3) + Carbonate(CO3)
Magnesium(Mg)
Calcium(Ca)
Sulfate(SO4)
Chloride(Cl) + Fluoride(F)

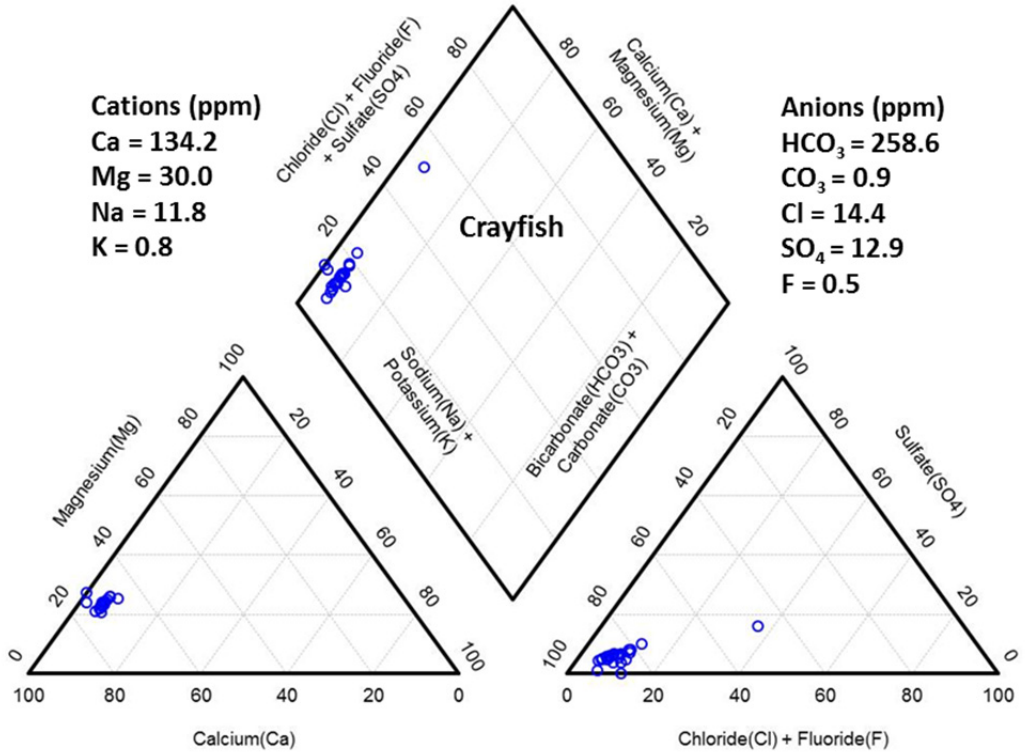
Cations (ppm)
Ca = 134.2
Mg = 30.0
Na = 11.8
K = 0.8
Anions (ppm)
HCO3 = 258.6
CO3 = 0.9
Cl = 14.4
SO4 = 12.9
F = 0.5
Crayfish
Chloride(Cl) + Fluoride(F) + Sulfate(SO4)
Calcium(Ca) + Magnesium(Mg)
Sodium(Na) + Potassium(K)
Bicarbonate(HCO3) + Carbonate(CO3)
Magnesium(Mg)
Calcium(Ca)
Sulfate(SO4)
Chloride(Cl) + Fluoride(F)

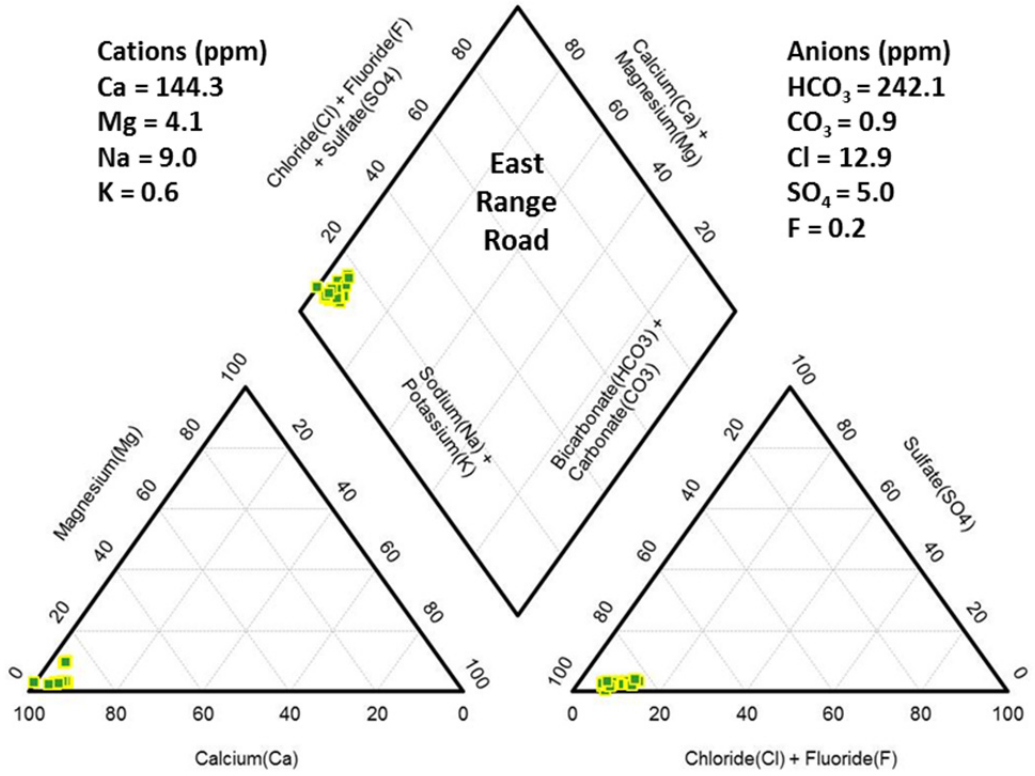
Cations (ppm)
Ca = 144.3
Mg = 4.1
Na = 9.0
K = 0.6
Anions (ppm)
HCO3 = 242.1
CO3 = 0.9
Cl = 12.9
SO4 = 5.0
F = 0.2
East
Range
Road
Chloride(Cl) + Fluoride(F) + Sulfate(SO4)
Calcium(Ca) + Magnesium(Mg)
Sodium(Na) + Potassium(K)
Bicarbonate(HCO3) + Carbonate(CO3)
Magnesium(Mg)
Calcium(Ca)
Sulfate(SO4)
Chloride(Cl) + Fluoride(F)

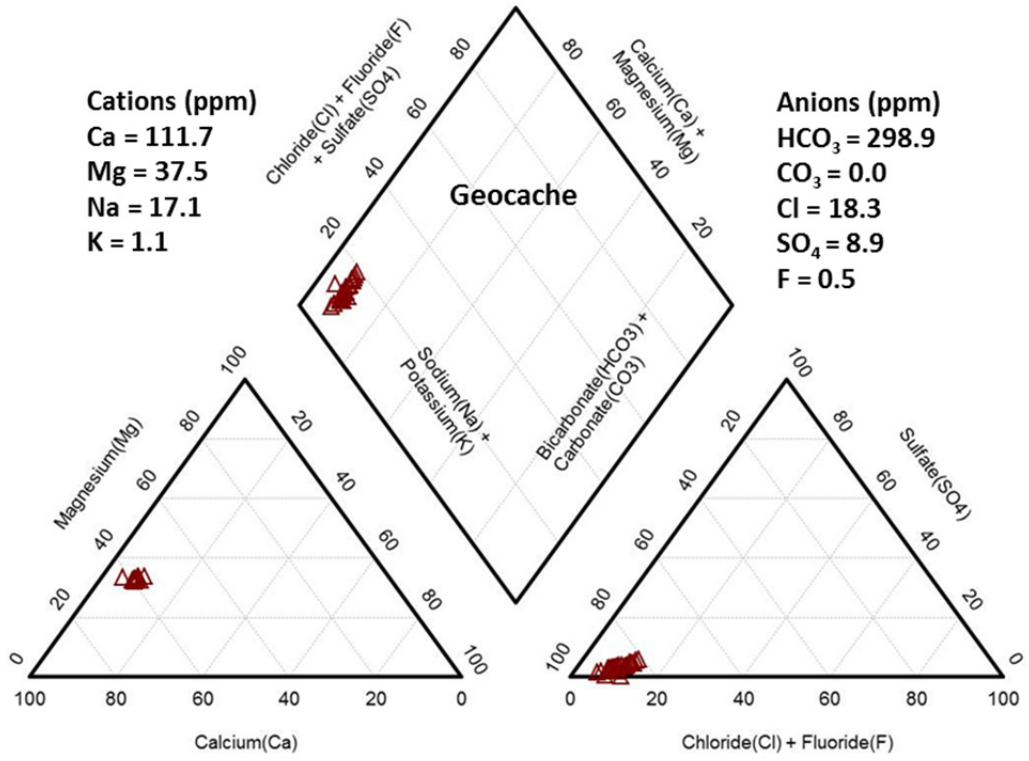
Cations (ppm)
Ca = 111.7
Mg = 37.5
Na = 17.1
K = 1.1
Anions (ppm)
HCO3 = 298.9
CO3 = 0.0
Cl = 18.3
SO4 = 8.9
F = 0.5
Geocache
Chloride(Cl) + Fluoride(F) + Sulfate(SO4)
Calcium(Ca) + Magnesium(Mg)
Sodium(Na) + Potassium(K)
Bicarbonate(HCO3) + Carbonate(CO3)
Magnesium(Mg)
Calcium(Ca)
Sulfate(SO4)
Chloride(Cl) + Fluoride(F)

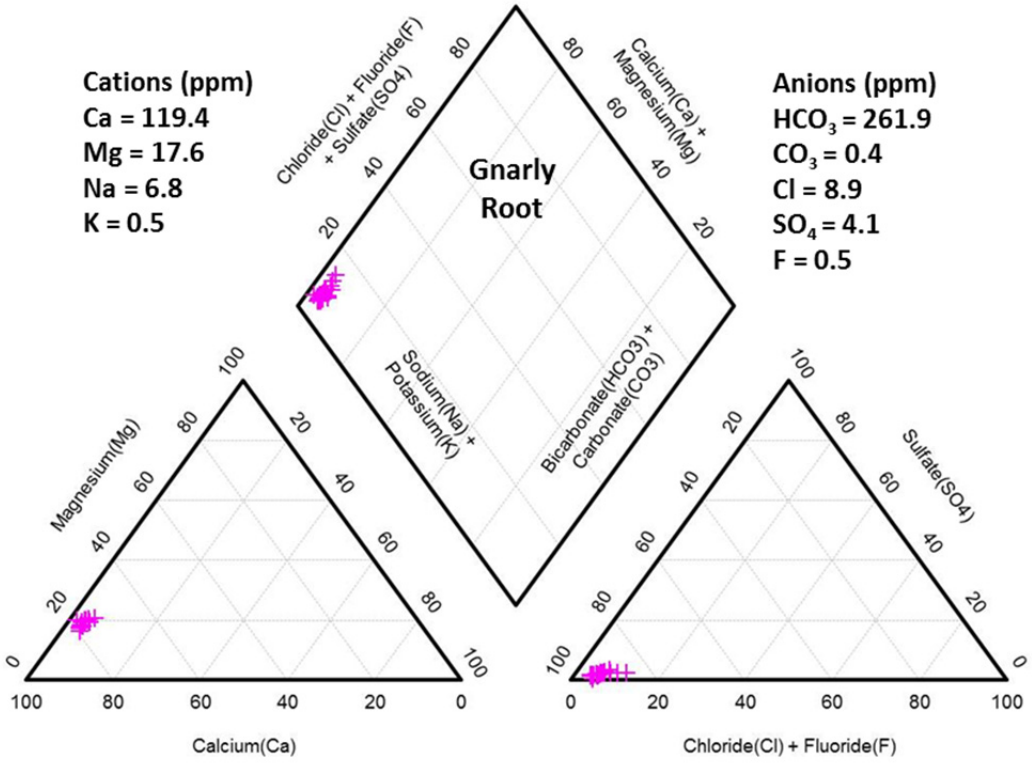
Cations (ppm)
Ca = 119.4
Mg = 17.6
Na = 6.8
K = 0.5
Anions (ppm)
HCO3 = 261.9
CO3 = 0.4
Cl = 8.9
SO4 = 4.1
F = 0.5
Gnarly Root
Chloride(Cl) + Fluoride(F) + Sulfate(SO4)
Calcium(Ca) + Magnesium(Mg)
Sodium(Na) + Potassium(K)
Bicarbonate(HCO3) + Carbonate(CO3)
Magnesium(Mg)
Calcium(Ca)
Sulfate(SO4)
Chloride(Cl) + Fluoride(F)

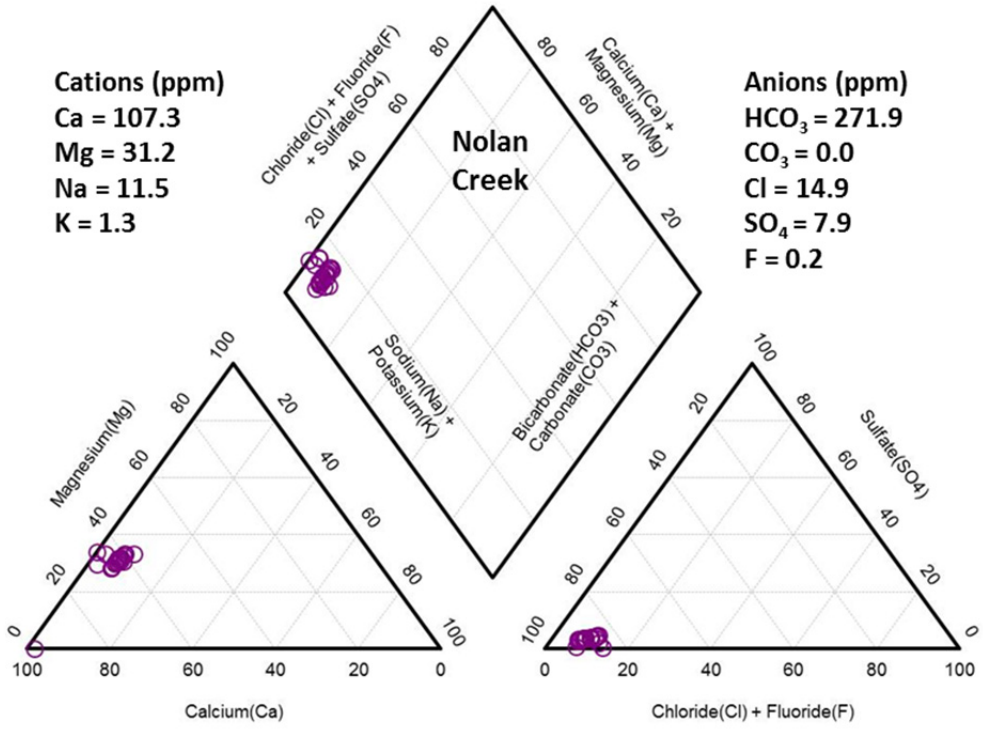
Cations (ppm)
Ca = 107.3
Mg = 31.2
Na = 11.5
K = 1.3
Anions (ppm)
HCO3 = 271.9
CO3 = 0.0
Cl = 14.9
SO4 = 7.9
F = 0.2
Nolan Creek
Chloride(Cl) + Fluoride(F) + Sulfate(SO4)
Calcium(Ca) + Magnesium(Mg)
Sodium(Na) + Potassium(K)
Bicarbonate(HCO3) + Carbonate(CO3)
Magnesium(Mg)
Calcium(Ca)
Sulfate(SO4)
Chloride(Cl) + Fluoride(F)

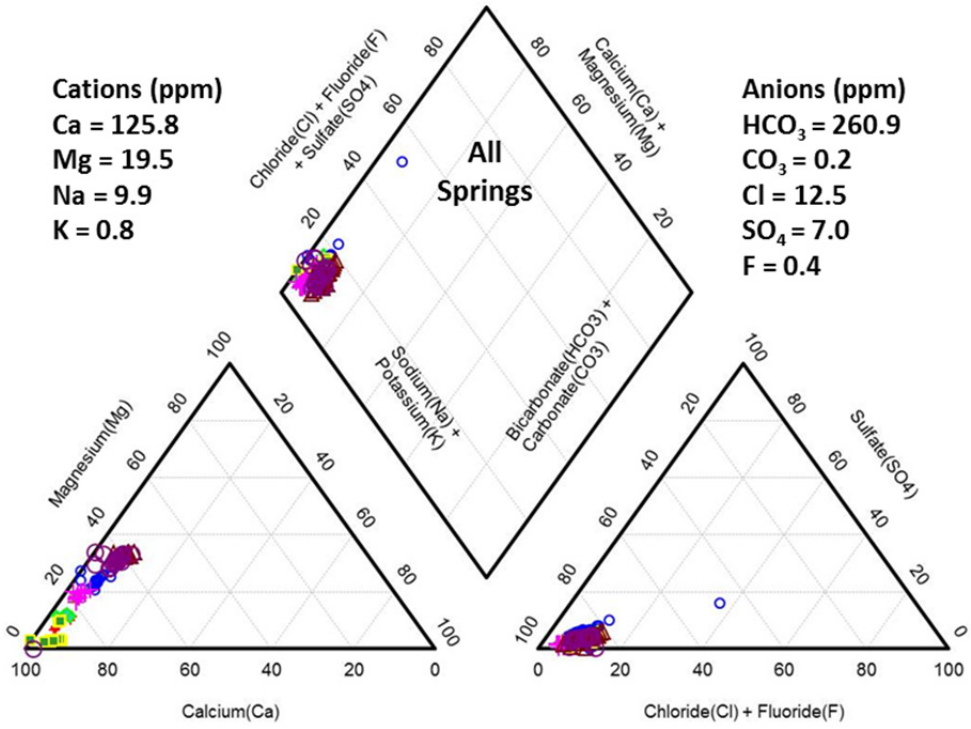
Cations (ppm)
Ca = 125.8
Mg = 19.5
Na = 9.9
K = 0.8
Anions (ppm)
HCO3 = 260.9
CO3 = 0.2
Cl = 12.5
SO4 = 7.0
F = 0.4
All Springs
Chloride(Cl) + Fluoride(F) + Sulfate(SO4)
Calcium(Ca) + Magnesium(Mg)
Sodium(Na) + Potassium(K)
Bicarbonate(HCO3) + Carbonate(CO3)
Magnesium(Mg)
Calcium(Ca)
Sulfate(SO4)
Chloride(Cl) + Fluoride(F)

APPENDIX III:

Sonde Parameters

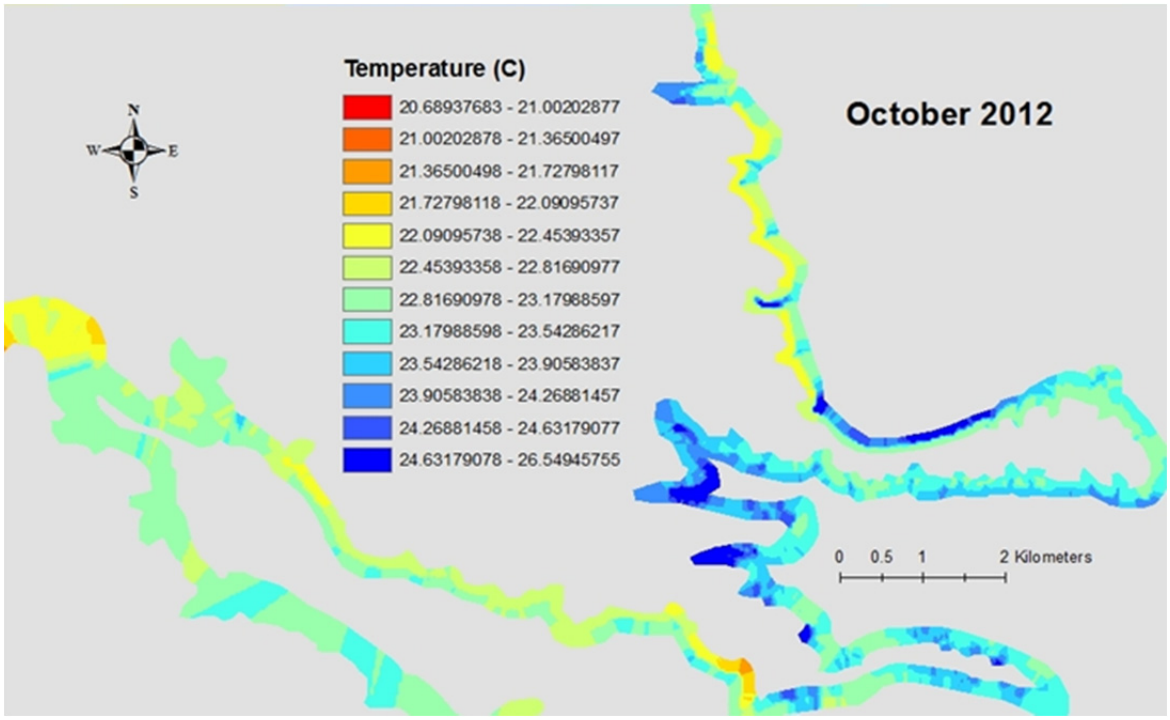
Temperature (C)
20.68937683 - 21.00202877
21.00202878 - 21.36500497
21.36500498 - 21.72798117
21.72798118 - 22.09095737
22.09095738 - 22.45393357
22.45393358 - 22.81690977
22.81690978 - 23.17988597
23.17988598 - 23.54286217
23.54286218 - 23.90583837
23.90583838 - 24.26881457
24.26881458 - 24.63179077
24.63179078 - 26.54945755
N
W
E
S
October 2012
0 0.5 1 2 Kilometers

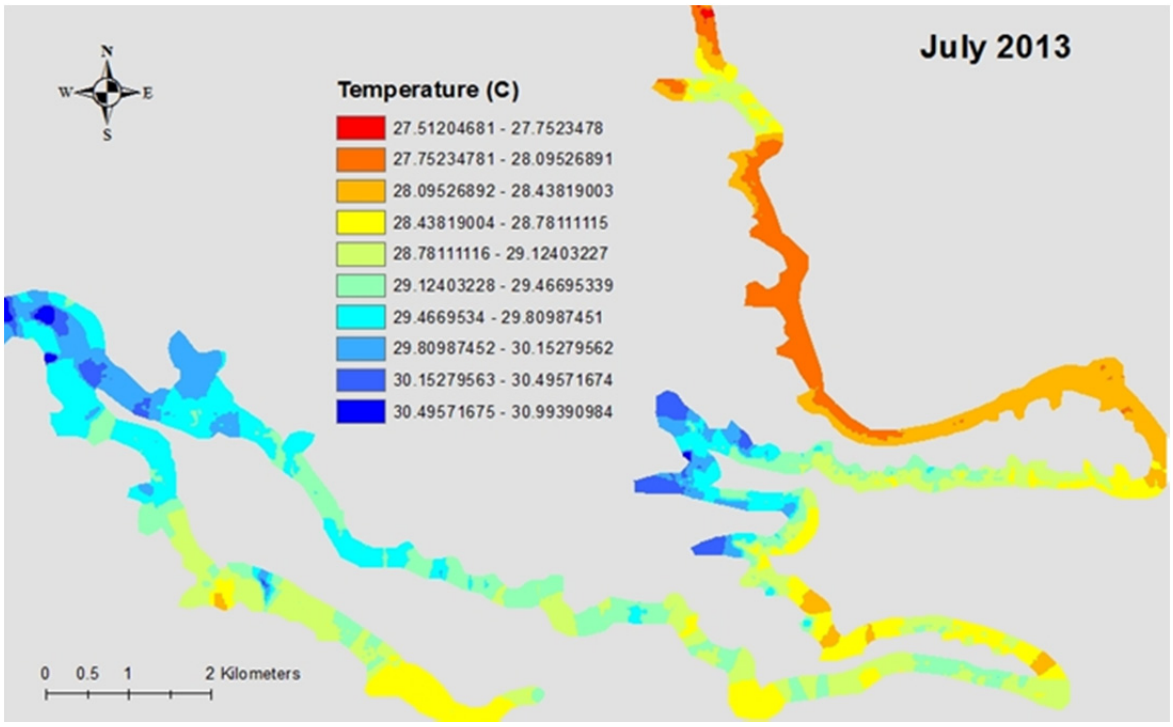
Temperature (C)
27.51204681 - 27.7523478
27.75234781 - 28.09526891
28.09526892 - 28.43819003
28.43819004 - 28.78111115
28.78111116 - 29.12403227
29.12403228 - 29.46695339
29.4669534 - 29.80987451
29.80987452 - 30.15279562
30.15279563 - 30.49571674
30.49571675 - 30.99390984
N
W
E
S
July 2013
0 0.5 1 2 Kilometers

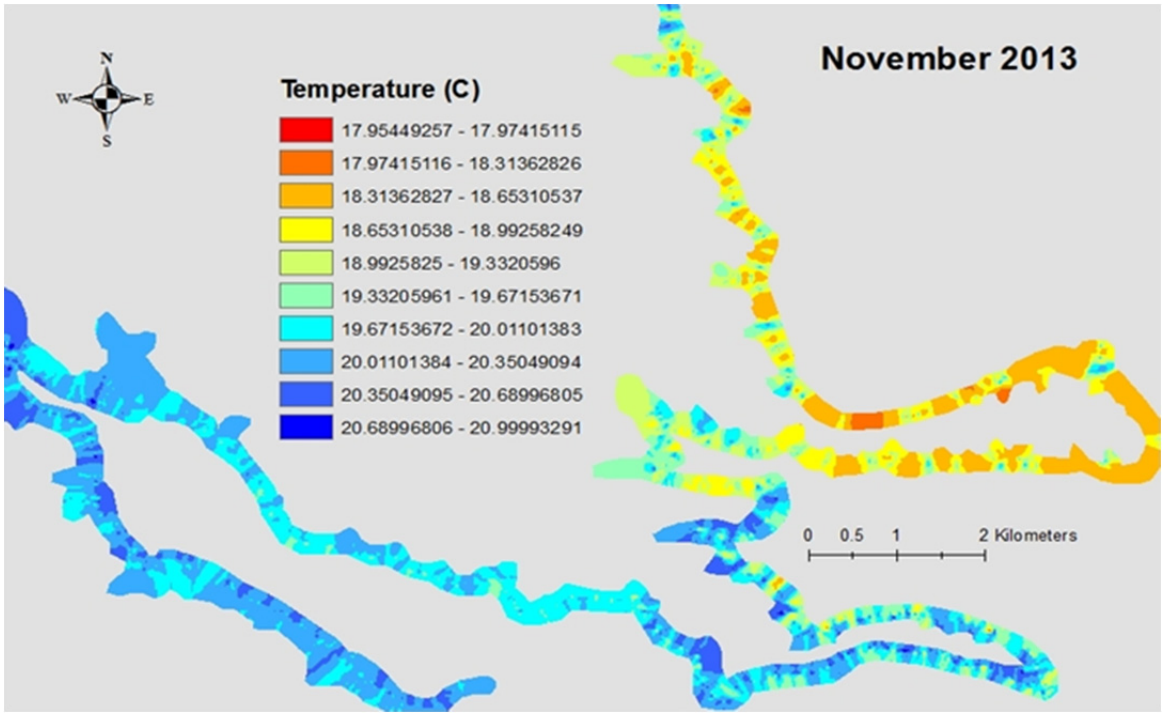
November 2013
N
W
E
S
Temperature (C)
17.95449257 - 17.97415115
17.97415116 - 18.31362826
18.31362827 - 18.65310537
18.65310538 - 18.99258249
18.9925825 - 19.3320596
19.33205961 - 19.67153671
19.67153672 - 20.01101383
20.01101384 - 20.35049094
20.35049095 - 20.68996805
20.68996806 - 20.99993291
0 0.5 1 2 Kilometers

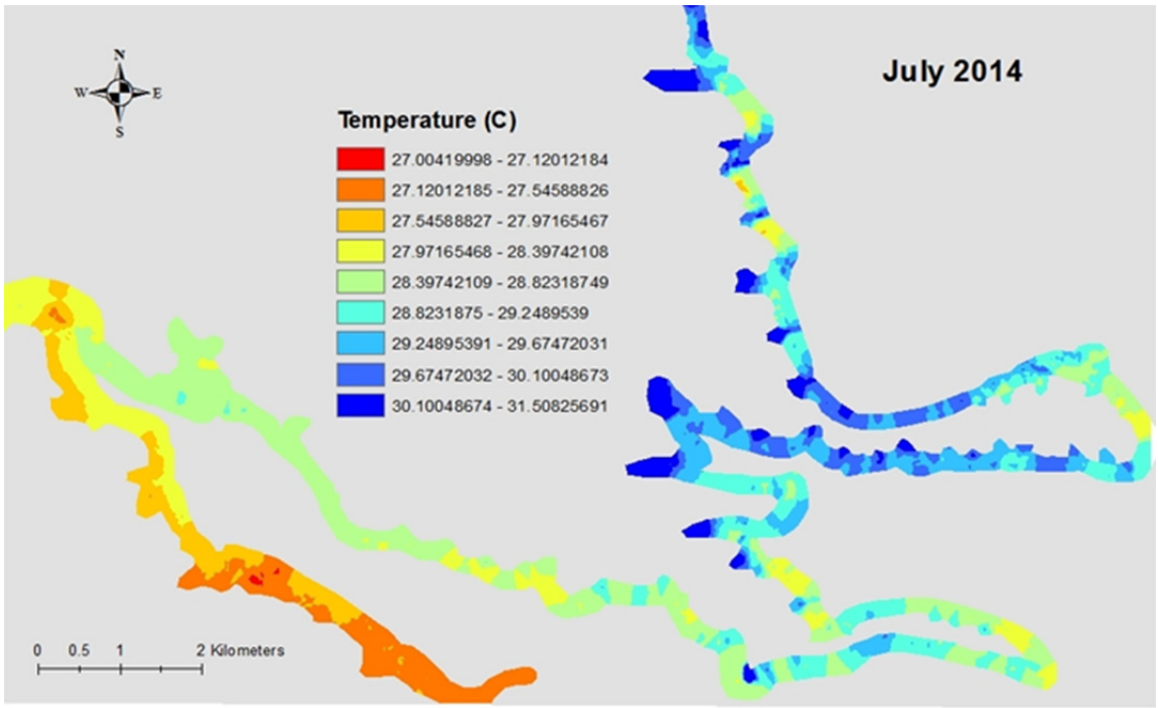
July 2014
N
W
E
S
Temperature (C)
27.00419998 - 27.12012184
27.12012185 - 27.54588826
27.54588827 - 27.97165467
27.97165468 - 28.39742108
28.39742109 - 28.82318749
28.8231875 - 29.2489539
29.24895391 - 29.67472031
29.67472032 - 30.10048673
30.10048674 - 31.50825691
0 0.5 1 2 Kilometers

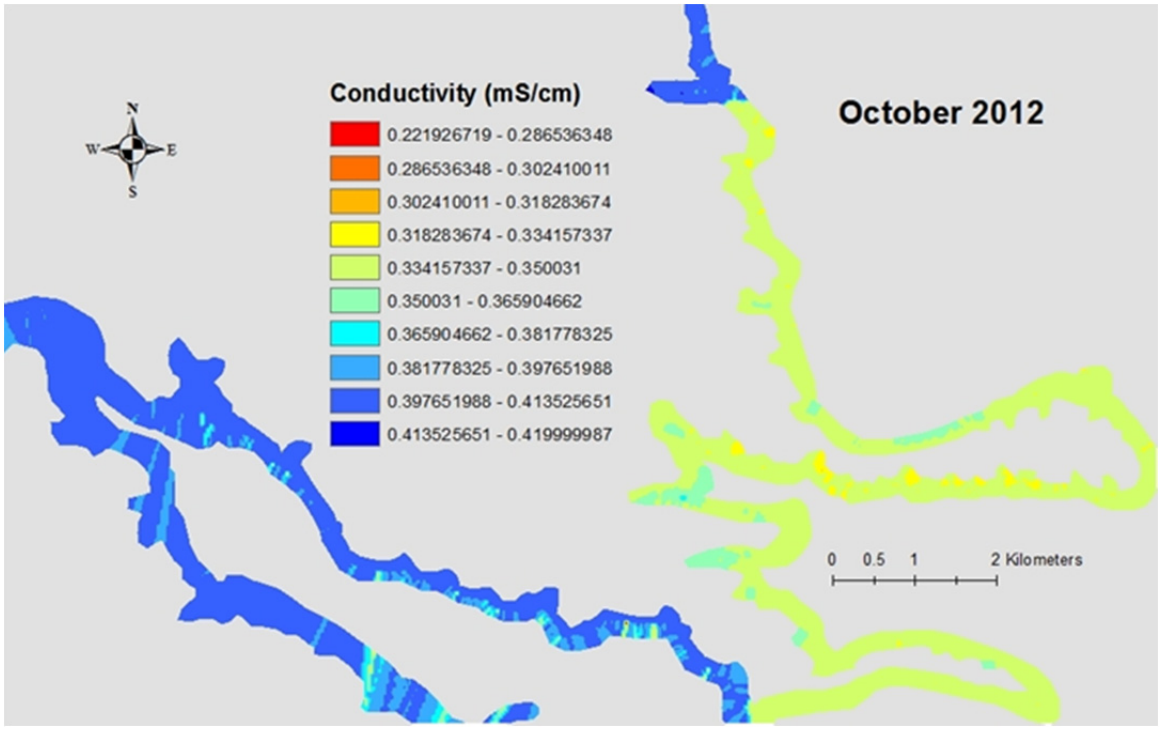
Conductivity (mS/cm)
0.221926719 - 0.286536348
0.286536348 - 0.302410011
0.302410011 - 0.318283674
0.318283674 - 0.334157337
0.334157337 - 0.350031
0.350031 - 0.365904662
0.365904662 - 0.381778325
0.381778325 - 0.397651988
0.397651988 - 0.413525651
0.413525651 - 0.419999987
N
W
E
S
October 2012
0 0.5 1 2 Kilometers

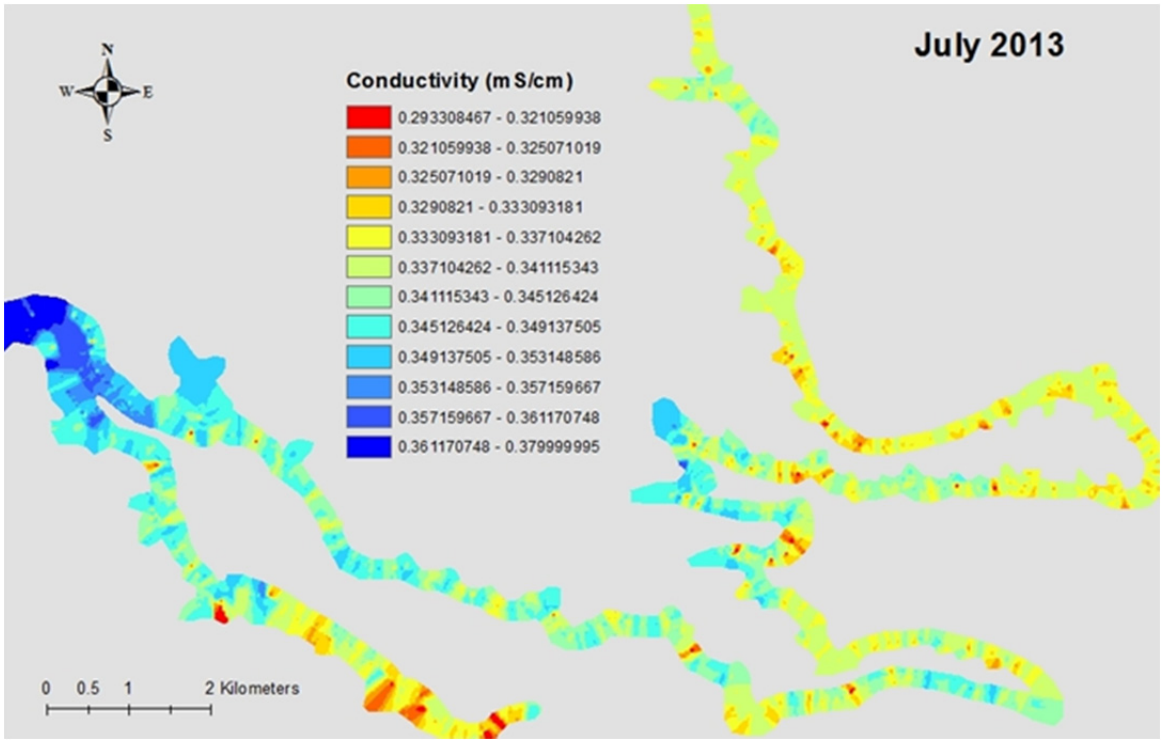
Conductivity (mS/cm)
0.293308467 - 0.321059938
0.321059938 - 0.325071019
0.325071019 - 0.3290821
0.3290821 - 0.333093181
0.333093181 - 0.337104262
0.337104262 - 0.341115343
0.341115343 - 0.345126424
0.345126424 - 0.349137505
0.349137505 - 0.353148586
0.353148586 - 0.357159667
0.357159667 - 0.361170748
0.361170748 - 0.379999995
N
W
E
S
July 2013
0 0.5 1 2 Kilometers

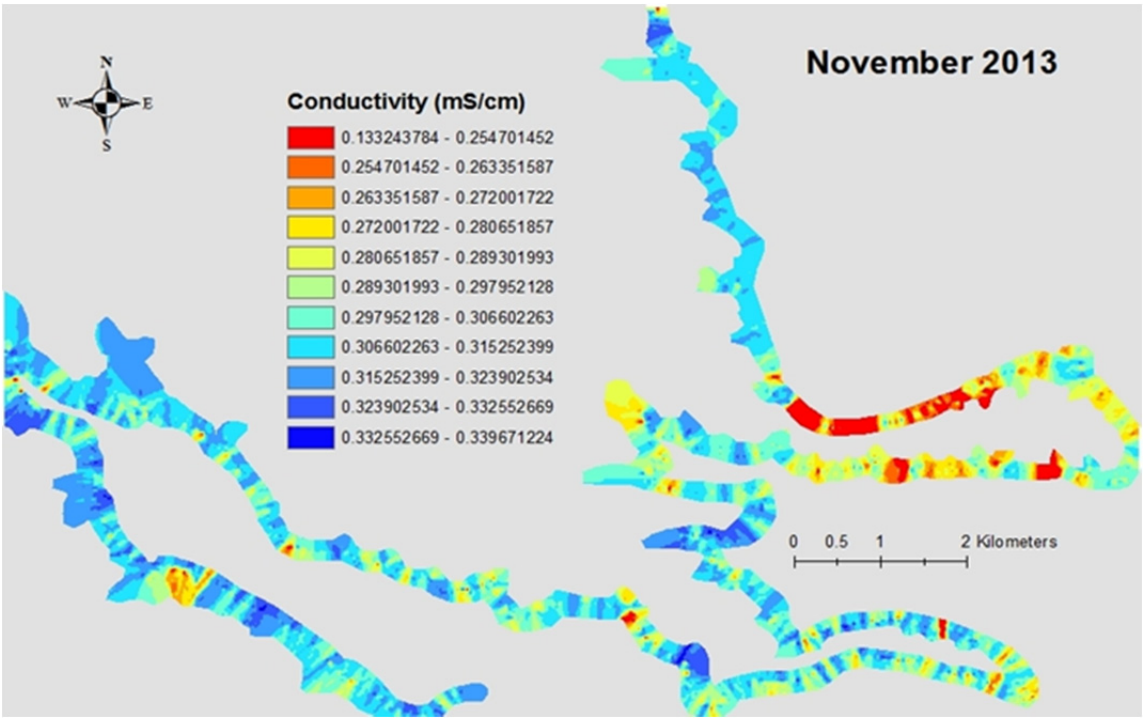
November 2013
N
W
E
S
Conductivity (mS/cm)
0.133243784 - 0.254701452
0.254701452 - 0.263351587
0.263351587 - 0.272001722
0.272001722 - 0.280651857
0.280651857 - 0.289301993
0.289301993 - 0.297952128
0.297952128 - 0.306602263
0.306602263 - 0.315252399
0.315252399 - 0.323902534
0.323902534 - 0.332552669
0.332552669 - 0.339671224
0 0.5 1 2 Kilometers

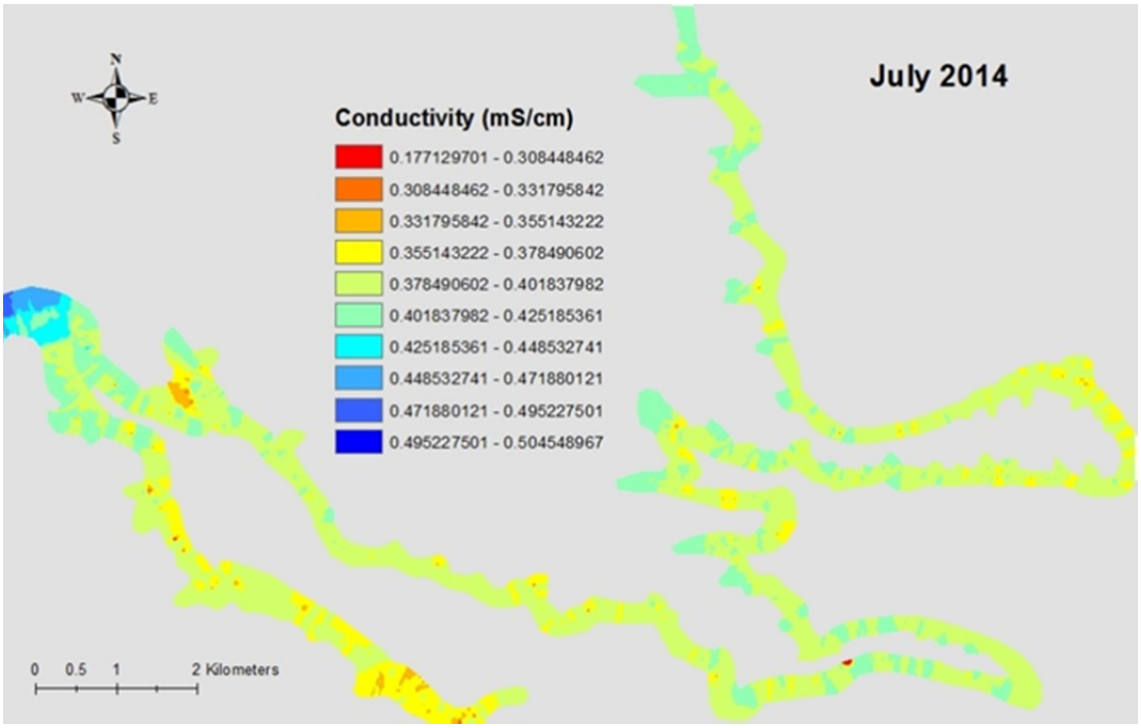
July 2014
N
W
E
S
Conductivity (mS/cm)
0.177129701 - 0.308448462
0.308448462 - 0.331795842
0.331795842 - 0.355143222
0.355143222 - 0.378490602
0.378490602 - 0.401837982
0.401837982 - 0.425185361
0.425185361 - 0.448532741
0.448532741 - 0.471880121
0.471880121 - 0.495227501
0.495227501 - 0.504548967
0 0.5 1 2 Kilometers

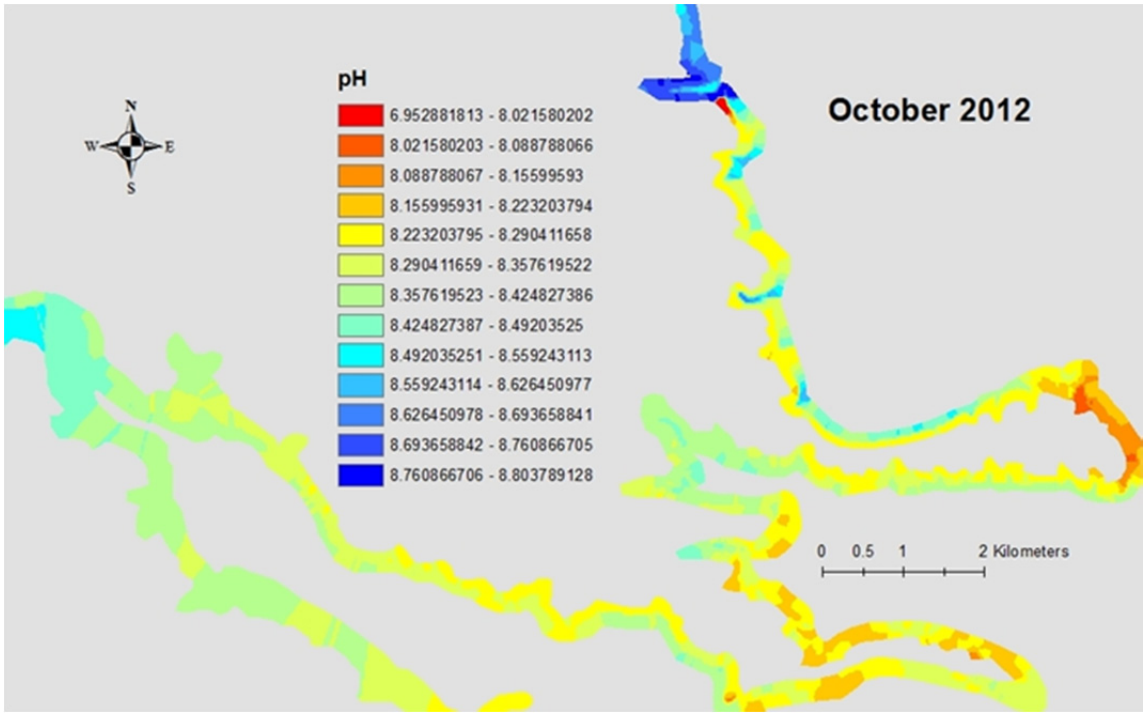
pH
6.952881813 - 8.021580202
8.021580203 - 8.088788066
8.088788067 - 8.15599593
8.155995931 - 8.223203794
8.223203795 - 8.290411658
8.290411659 - 8.357619522
8.357619523 - 8.424827386
8.424827387 - 8.49203525
8.492035251 - 8.559243113
8.559243114 - 8.626450977
8.626450978 - 8.693658841
8.693658842 - 8.760866705
8.760866706 - 8.803789128
N
W
E
S
October 2012
0 0.5 1 2 Kilometers

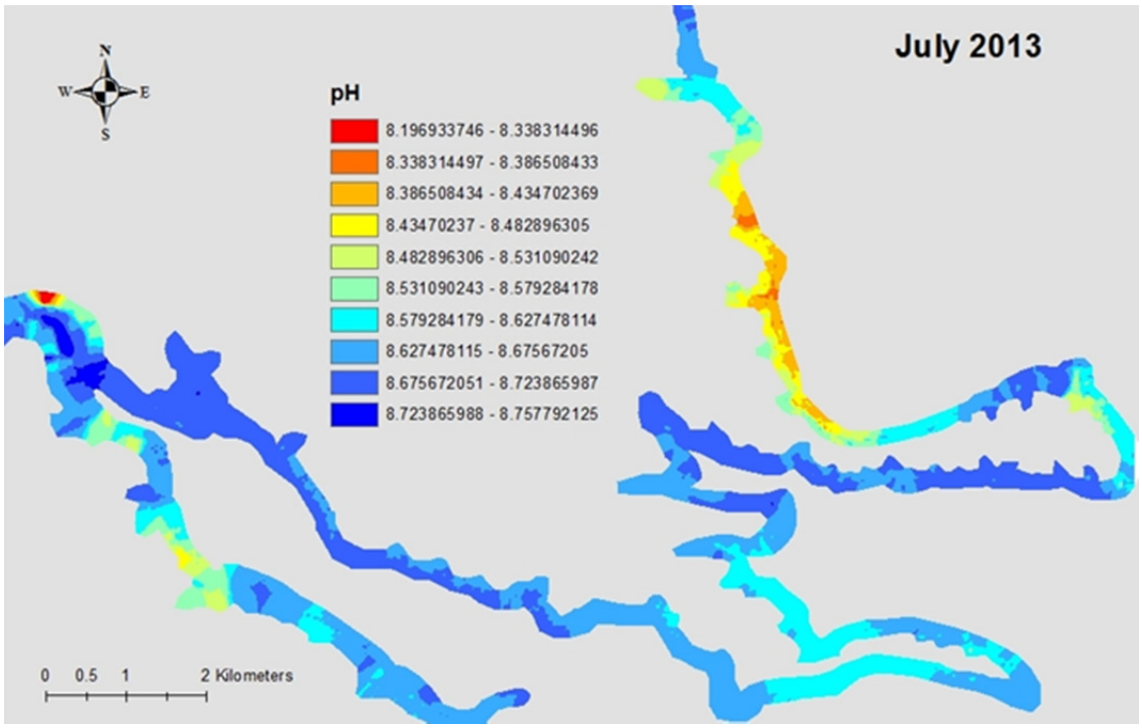
pH
8.196933746 - 8.338314496
8.338314497 - 8.386508433
8.386508434 - 8.434702369
8.43470237 - 8.482896305
8.482896306 - 8.531090242
8.531090243 - 8.579284178
8.579284179 - 8.627478114
8.627478115 - 8.67567205
8.675672051 - 8.723865987
8.723865988 - 8.757792125
N
W
E
S
July 2013
0 0.5 1 2 Kilometers

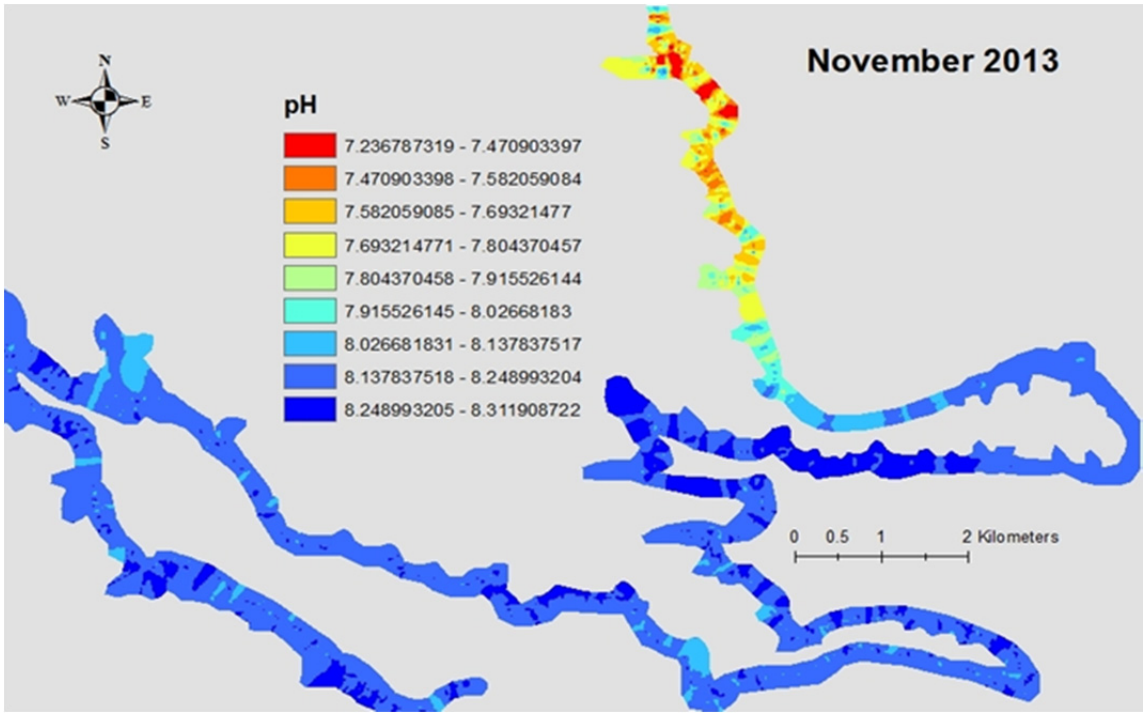
November 2013
N
W
E
S
pH
7.236787319 - 7.470903397
7.470903398 - 7.582059084
7.582059085 - 7.69321477
7.693214771 - 7.804370457
7.804370458 - 7.915526144
7.915526145 - 8.02668183
8.026681831 - 8.137837517
8.137837518 - 8.248993204
8.248993205 - 8.311908722
0 0.5 1 2 Kilometers

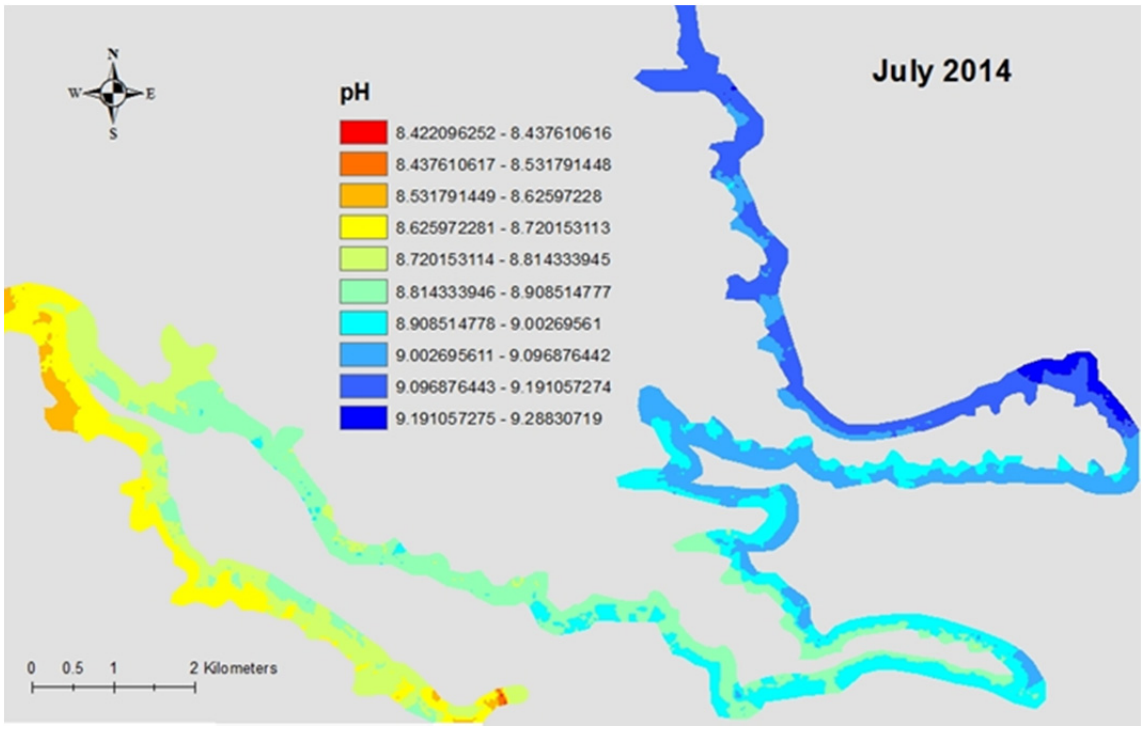
July 2014
N
W
E
S
pH
8.422096252 - 8.437610616
8.437610617 - 8.531791448
8.531791449 - 8.62597228
8.625972281 - 8.720153113
8.720153114 - 8.814333945
8.814333946 - 8.908514777
8.908514778 - 9.00269561
9.002695611 - 9.096876442
9.096876443 - 9.191057274
9.191057275 - 9.28830719
0 0.5 1 2 Kilometers

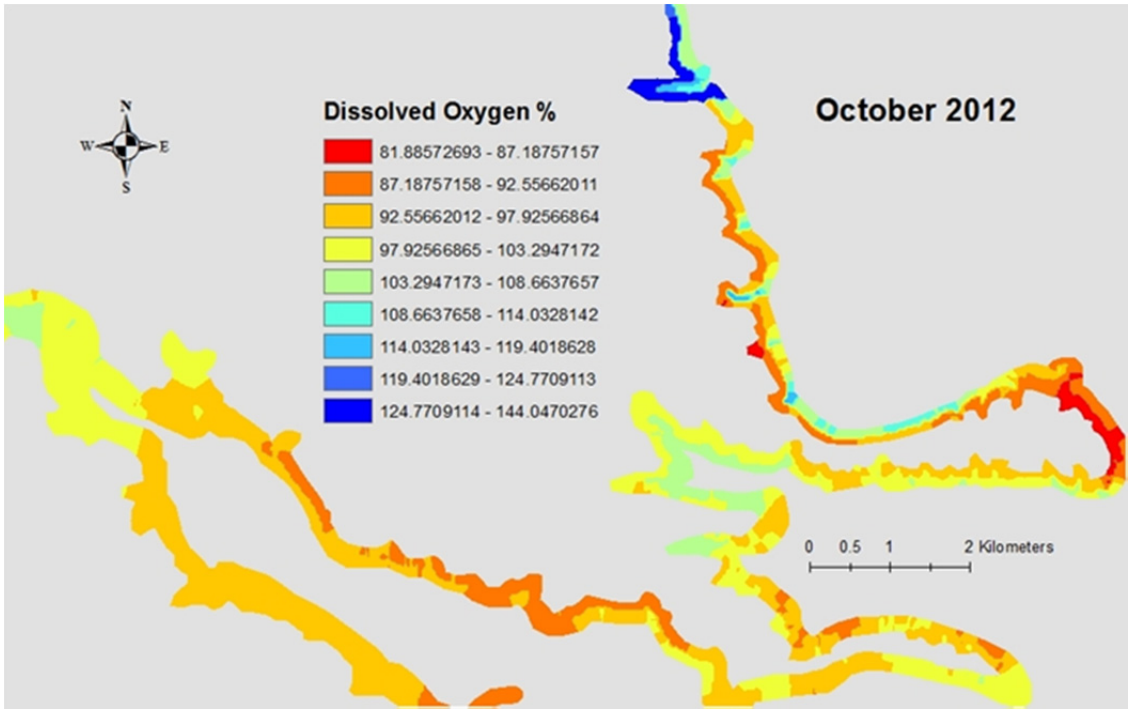
N
W
E
S
Dissolved Oxygen %
81.88572693 - 87.18757157
87.18757158 - 92.55662011
92.55662012 - 97.92566864
97.92566865 - 103.2947172
103.2947173 - 108.6637657
108.6637658 - 114.0328142
114.0328143 - 119.4018628
119.4018629 - 124.7709113
124.7709114 - 144.0470276
October 2012
0 0.5 1 2 Kilometers

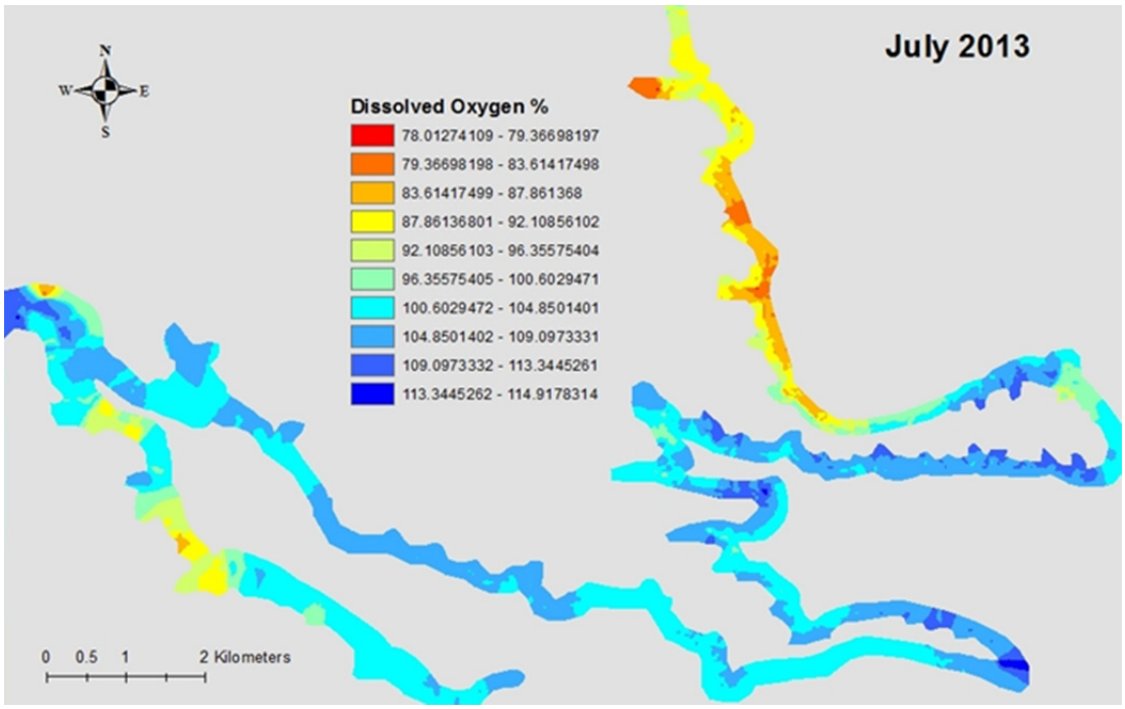
N
W
E
S
Dissolved Oxygen %
78.01274109 - 79.36698197
79.36698198 - 83.61417498
83.61417499 - 87.861368
87.86136801 - 92.10856102
92.10856103 - 96.35575404
96.35575405 - 100.6029471
100.6029472 - 104.8501401
104.8501402 - 109.0973331
109.0973332 - 113.3445261
113.3445262 - 114.9178314
July 2013
0 0.5 1 2 Kilometers

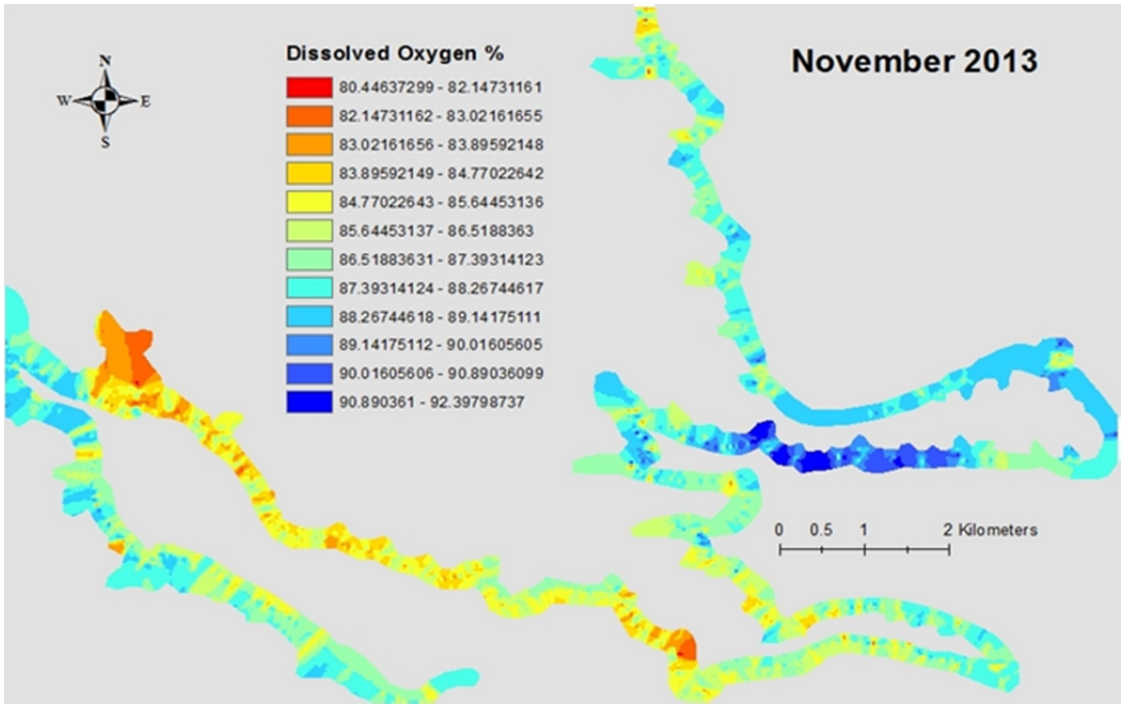
November 2013
Dissolved Oxygen %
80.44637299 - 82.14731161
82.14731162 - 83.02161655
83.02161656 - 83.89592148
83.89592149 - 84.77022642
84.77022643 - 85.64453136
85.64453137 - 86.5188363
86.51883631 - 87.39314123
87.39314124 - 88.26744617
88.26744618 - 89.14175111
89.14175112 - 90.01605605
90.01605606 - 90.89036099
90.890361 - 92.39798737
N
W
E
S
0 0.5 1 2 Kilometers

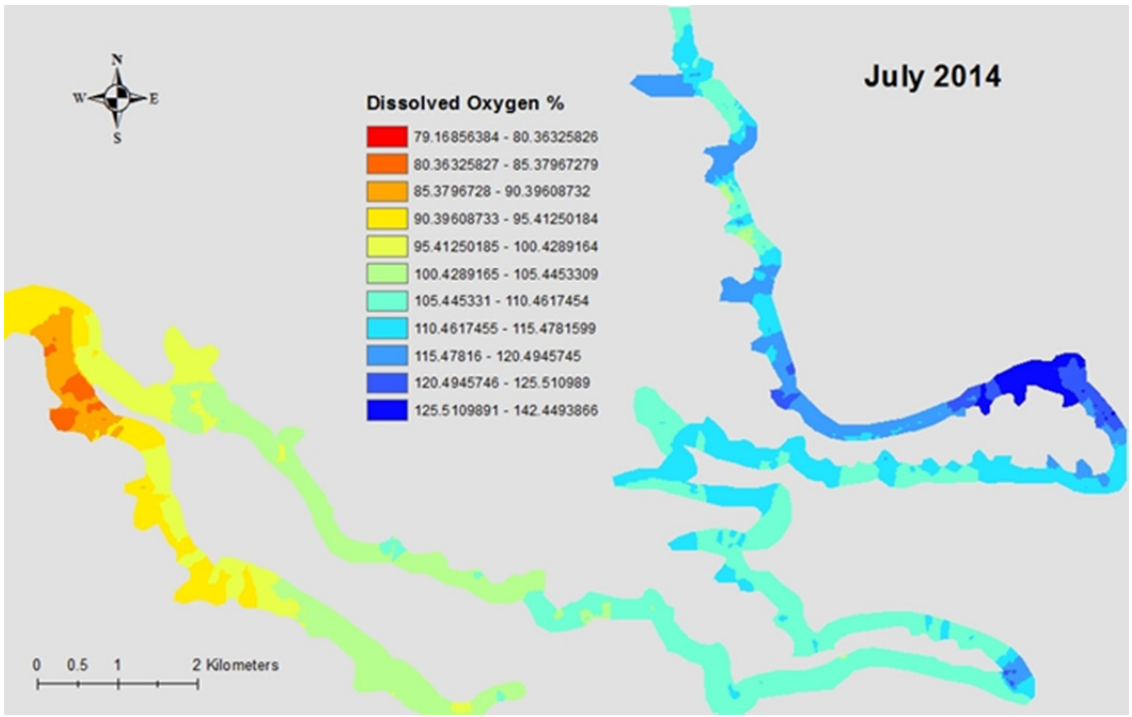
July 2014
Dissolved Oxygen %
79.16856384 - 80.36325826
80.36325827 - 85.37967279
85.3796728 - 90.39608732
90.39608733 - 95.41250184
95.41250185 - 100.4289164
100.4289165 - 105.4453309
105.445331 - 110.4617454
110.4617455 - 115.4781599
115.47816 - 120.4945745
120.4945746 - 125.510989
125.5109891 - 142.4493866
N
W
E
S
0 0.5 1 2 Kilometers

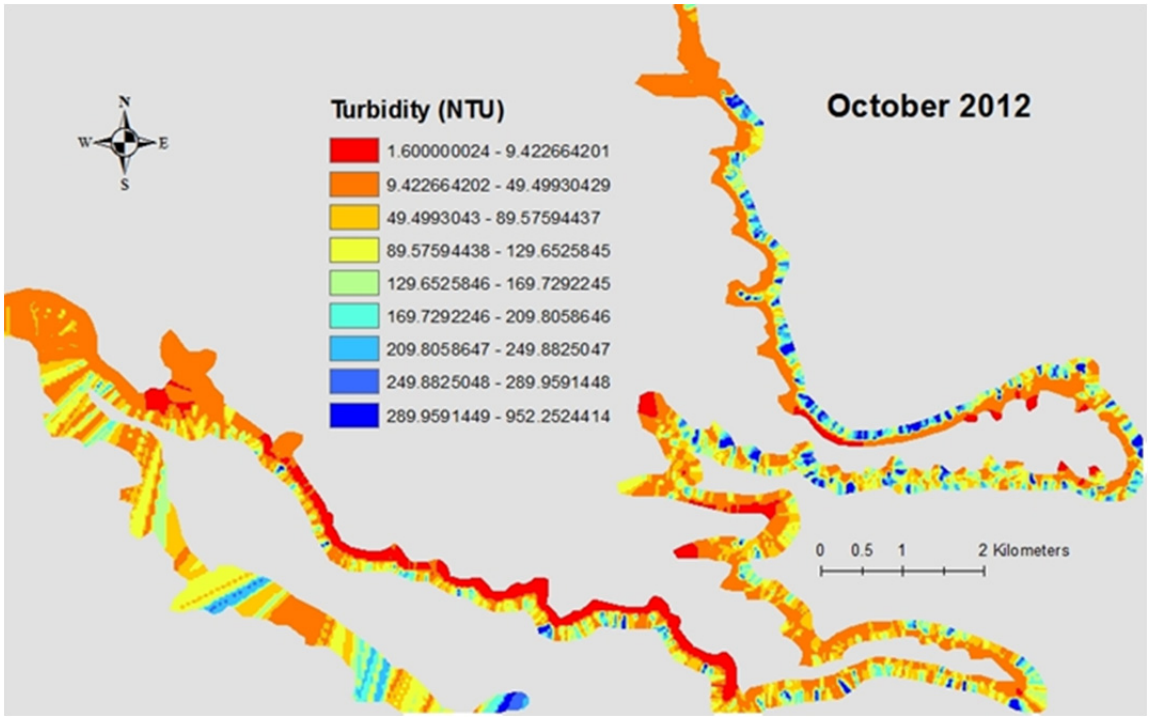
October 2012
Turbidity (NTU)
1.600000024 - 9.422664201
9.422664202 - 49.49930429
49.4993043 - 89.57594437
89.57594438 - 129.6525845
129.6525846 - 169.7292245
169.7292246 - 209.8058646
209.8058647 - 249.8825047
249.8825048 - 289.9591448
289.9591449 - 952.2524414
N
W
E
S
0 0.5 1 2 Kilometers

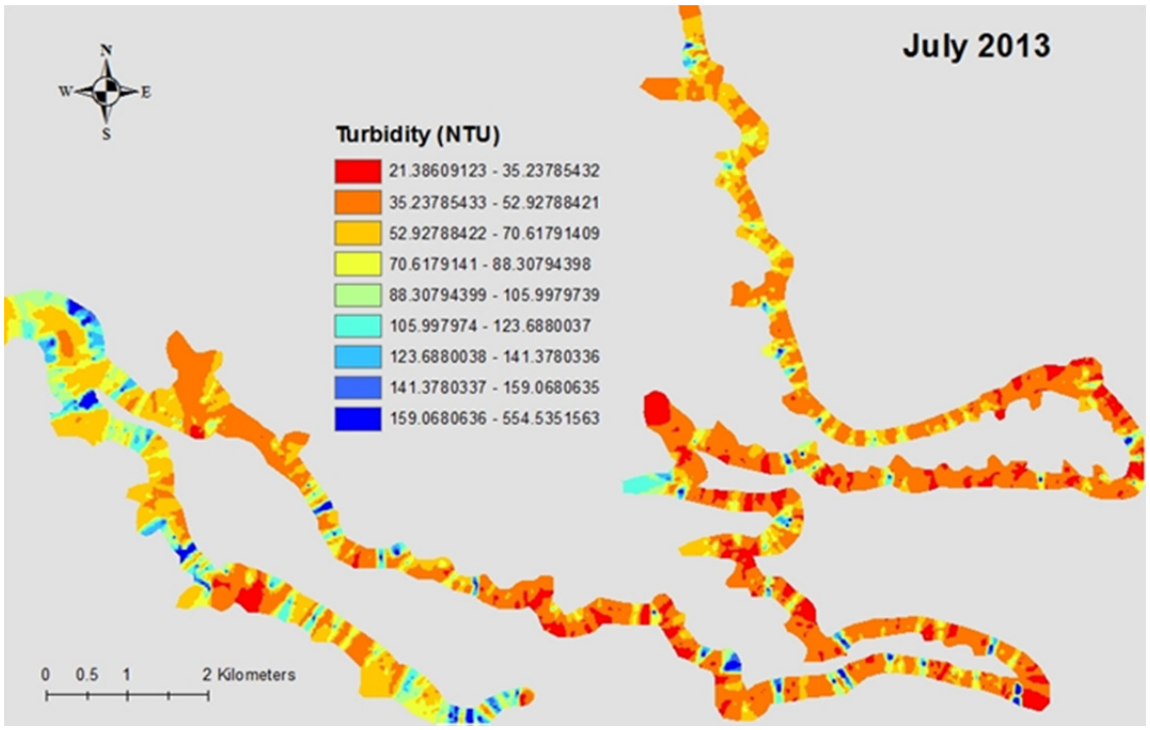
July 2013
Turbidity (NTU)
21.38609123 - 35.23785432
35.23785433 - 52.92788421
52.92788422 - 70.61791409
70.6179141 - 88.30794398
88.30794399 - 105.9979739
105.997974 - 123.6880037
123.6880038 - 141.3780336
141.3780337 - 159.0680635
159.0680636 - 554.5351563
N
W
E
S
0 0.5 1 2 Kilometers

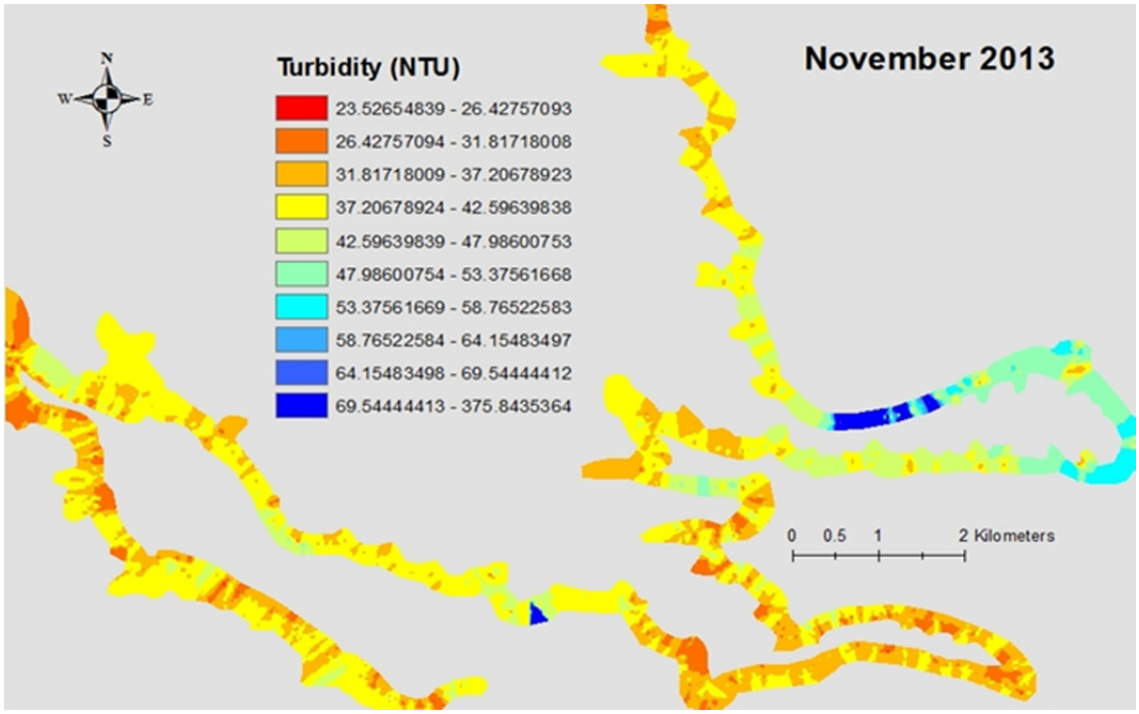
November 2013
Turbidity (NTU)
23.52654839 - 26.42757093
26.42757094 - 31.81718008
31.81718009 - 37.20678923
37.20678924 - 42.59639838
42.59639839 - 47.98600753
47.98600754 - 53.37561668
53.37561669 - 58.76522583
58.76522584 - 64.15483497
64.15483498 - 69.54444412
69.54444413 - 375.8435364
N
W
E
S
0 0.5 1 2 Kilometers

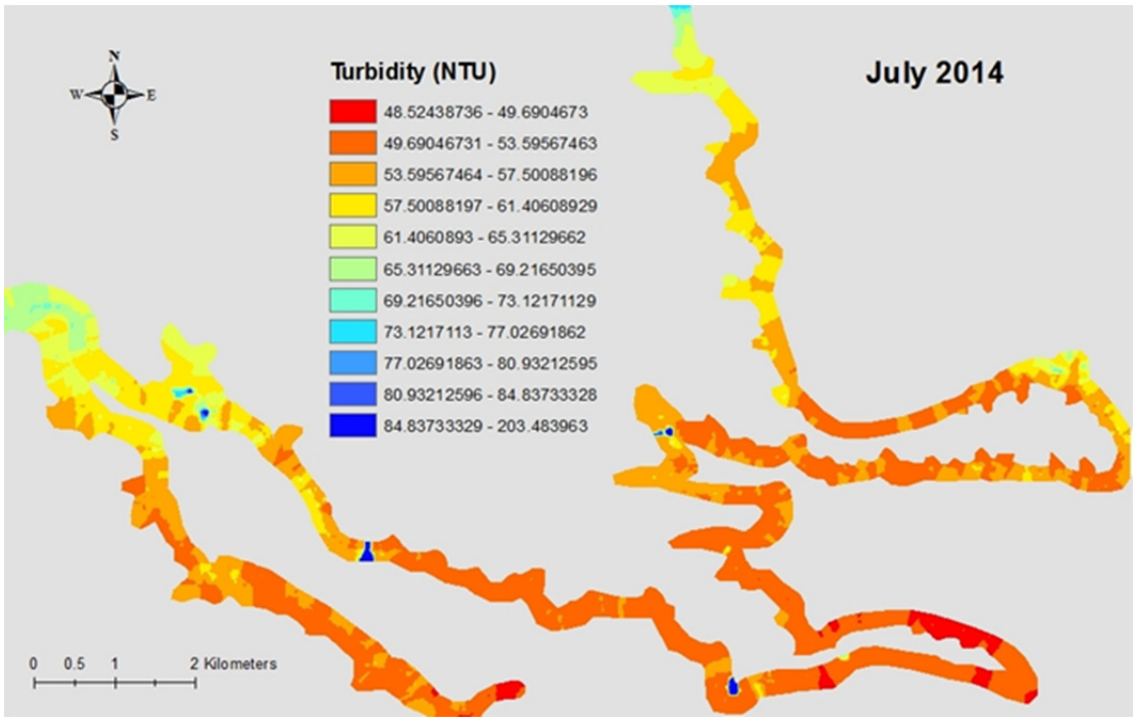
July 2014
Turbidity (NTU)
48.52438736 - 49.6904673
49.69046731 - 53.59567463
53.59567464 - 57.50088196
57.50088197 - 61.40608929
61.4060893 - 65.31129662
65.31129663 - 69.21650395
69.21650396 - 73.12171129
73.1217113 - 77.02691862
77.02691863 - 80.93212595
80.93212596 - 84.83733328
84.83733329 - 203.483963
N
W
E
S
0 0.5 1 2 Kilometers

APPENDIX IV:

Joint Measurements

Joints		Joints		Joints		Joints	
TA	Azimuth	TA	Azimuth	TA	Azimuth	TA	Azimuth
8	6	11	280	12	16	12	330
8	8	11	280	12	17	13	13
8	10	11	282	12	17	13	15
8	11	11	284	12	17	13	17
8	12	11	288	12	18	13	19
8	13	11	290	12	21	20	3
8	14	11	290	12	22	20	3
8	15	11	295	12	22	20	4
8	16	11	305	12	24	20	4
8	17	11	316	12	44	20	5
8	17	11	317	12	45	20	5
8	18	11	318	12	264	20	6
8	18	11	318	12	264	20	6
8	19	11	318	12	265	20	6
8	20	11	320	12	272	20	6
8	23	11	325	12	276	20	7
8	24	11	325	12	276	20	7
8	24	11	326	12	277	20	7
8	26	11	350	12	277	20	7
8	47	12	1	12	278	20	7
8	278	12	2	12	281	20	7
8	279	12	2	12	284	20	8
8	280	12	3	12	284	20	8
8	286	12	4	12	284	20	9
8	287	12	5	12	285	20	9
8	288	12	6	12	285	20	10
8	289	12	6	12	285	20	10
8	290	12	6	12	285	20	10
8	293	12	7	12	286	20	10
8	294	12	8	12	286	20	11
11	5	12	8	12	286	20	11
11	11	12	8	12	287	20	11
11	15	12	9	12	287	20	12
11	16	12	9	12	288	20	12
11	20	12	10	12	288	20	12
11	25	12	10	12	291	20	12
11	50	12	11	12	291	20	13
11	70	12	11	12	292	20	13
11	75	12	11	12	292	20	13
11	80	12	12	12	294	20	13
11	261	12	12	12	304	20	14
11	267	12	12	12	309	20	14
11	267	12	13	12	310	20	14
11	269	12	13	12	311	20	14
11	275	12	14	12	312	20	17
11	276	12	14	12	315	20	18
11	276	12	15	12	315	20	18
11	276	12	15	12	322	20	18
11	278	12	15	12	324	20	18
11	279	12	16	12	325	20	20

Joints		Joints		Joints		Joints	
TA	Azimuth	TA	Azimuth	TA	Azimuth	TA	Azimuth
20	20	20	297	21	276	22	10
20	22	20	297	21	276	22	10
20	24	20	307	21	276	22	10
20	24	20	307	21	278	22	11
20	27	20	318	21	279	22	11
20	27	20	318	21	280	22	11
20	29	20	319	21	280	22	11
20	29	20	319	21	282	22	12
20	52	20	320	21	284	22	12
20	52	20	320	21	288	22	12
20	72	20	320	21	290	22	12
20	72	20	320	21	290	22	12
20	77	20	320	21	295	22	13
20	77	20	320	21	305	22	13
20	82	20	322	21	316	22	13
20	82	20	322	21	317	22	14
20	269	20	327	21	318	22	14
20	269	20	327	21	318	22	15
20	269	20	327	21	318	22	15
20	271	20	327	21	320	22	15
20	271	20	328	21	325	22	16
20	277	20	328	21	325	22	16
20	277	20	352	21	326	22	16
20	278	20	352	21	350	22	16
20	278	21	2	22	1	22	16
20	278	21	4	22	2	22	17
20	278	21	4	22	2	22	17
20	278	21	5	22	3	22	17
20	278	21	5	22	3	22	17
20	280	21	8	22	4	22	18
20	280	21	9	22	4	22	18
20	281	21	10	22	4	22	19
20	281	21	11	22	5	22	21
20	282	21	11	22	5	22	21
20	282	21	12	22	5	22	22
20	282	21	15	22	5	22	22
20	282	21	16	22	6	22	22
20	284	21	16	22	6	22	23
20	284	21	18	22	6	22	23
20	286	21	20	22	6	22	26
20	286	21	22	22	7	22	27
20	290	21	25	22	7	22	28
20	290	21	27	22	8	22	46
20	290	21	50	22	8	22	51
20	292	21	70	22	8	22	71
20	292	21	75	22	9	22	76
20	292	21	80	22	9	22	81
20	292	21	267	22	9	22	268
20	293	21	269	22	9	22	270
20	294	21	275	22	10	22	276

Joints		Joints		Joints		Joints	
TA	Azimuth	TA	Azimuth	TA	Azimuth	TA	Azimuth
22	277	23	6	23	278	23	326
22	277	23	7	23	279	23	326
22	277	23	8	23	279	23	326
22	277	23	8	23	280	23	327
22	278	23	9	23	281	23	327
22	279	23	9	23	281	23	332
22	279	23	10	23	283	115	3
22	280	23	10	23	283	115	3
22	281	23	10	23	285	115	4
22	281	23	11	23	285	115	5
22	283	23	11	23	286	115	7
22	284	23	12	23	286	115	7
22	285	23	12	23	286	115	9
22	285	23	12	23	286	115	9
22	285	23	13	23	287	115	10
22	286	23	13	23	287	115	11
22	286	23	14	23	287	115	12
22	287	23	14	23	287	115	13
22	287	23	16	23	287	115	13
22	288	23	16	23	288	115	13
22	288	23	16	23	288	115	15
22	289	23	17	23	288	115	15
22	289	23	17	23	288	115	16
22	291	23	17	23	289	115	17
22	291	23	17	23	289	115	17
22	291	23	18	23	289	115	18
22	292	23	19	23	290	115	18
22	292	23	19	23	291	115	19
22	293	23	22	23	291	115	19
22	296	23	22	23	292	115	21
22	306	23	23	23	293	115	23
22	317	23	23	23	293	115	24
22	318	23	23	23	294	115	25
22	319	23	28	23	296	115	26
22	319	23	46	23	296	115	45
22	319	23	51	23	306	115	262
22	321	23	71	23	306	115	265
22	326	23	76	23	311	115	265
22	326	23	81	23	312	115	266
22	327	23	263	23	313	115	268
22	351	23	266	23	314	115	273
23	2	23	266	23	317	115	277
23	3	23	267	23	317	115	278
23	4	23	268	23	317	115	282
23	4	23	270	23	318	115	285
23	4	23	274	23	319	115	285
23	5	23	276	23	319	115	286
23	5	23	277	23	319	115	286
23	6	23	277	23	321	115	286
23	6	23	277	23	324	115	287

Joints	
TA	Azimuth
115	287
115	288
115	289
115	289
115	292
115	293
115	295
115	305
115	310
115	311
115	312
115	313
115	316
115	316
115	323
115	325
115	326
115	331
115	351

APPENDIX V:

Cave Measurements

Caves			Caves			Caves		
County	Azimuth	L(m)	County	Azimuth	L(m)	County	Azimuth	L(m)
Bell	22	2.5	Bell	40	2.8	Bell	18	3.1
Bell	342	2.5	Bell	50	2.8	Bell	278	3.1
Bell	21	2.5	Bell	56	2.8	Bell	64	3.1
Bell	73	2.5	Bell	330	2.8	Bell	284	3.1
Bell	283	2.5	Bell	293	2.8	Coryell	120	3.1
Bell	303	2.5	Bell	31	2.8	Bell	20	3.1
Bell	303	2.5	Bell	22	2.8	Bell	18	3.1
Bell	330	2.5	Bell	20	2.8	Bell	282	3.2
Bell	322	2.5	Bell	282	2.9	Bell	0	3.2
Bell	33	2.6	Bell	263	2.9	Bell	22	3.2
Bell	21	2.6	Coryell	335	2.9	Bell	337	3.2
Bell	18	2.6	Bell	284	2.9	Bell	353	3.2
Bell	290	2.6	Bell	296	2.9	Bell	326	3.2
Bell	18	2.6	Bell	269	3.0	Coryell	42	3.2
Bell	125	2.6	Bell	72	3.0	Coryell	36	3.2
Bell	277	2.6	Bell	18	3.0	Bell	18	3.2
Bell	18	2.6	Bell	36	3.0	Bell	330	3.2
Bell	28	2.6	Bell	284	3.0	Bell	20	3.3
Bell	295	2.6	Bell	286	3.0	Bell	285	3.3
Bell	320	2.6	Bell	350	3.0	Bell	281	3.3
Bell	53	2.6	Bell	342	3.0	Coryell	10	3.3
Bell	62	2.6	Bell	50	3.0	Coryell	312	3.3
Bell	353	2.6	Bell	16	3.0	Bell	12	3.3
Bell	28	2.6	Bell	34	3.0	Bell	20	3.3
Bell	50	2.6	Bell	24	3.0	Bell	22	3.3
Bell	10	2.7	Coryell	42	3.0	Bell	280	3.3
Bell	33	2.7	Bell	285	3.0	Coryell	120	3.3
Bell	90	2.7	Bell	280	3.0	Bell	280	3.3
Bell	301	2.7	Bell	354	3.0	Coryell	51	3.3
Bell	22	2.7	Bell	140	3.0	Bell	318	3.4
Bell	24	2.7	Coryell	303	3.1	Bell	65	3.4
Bell	322	2.8	Bell	22	3.1	Bell	357	3.4
Bell	283	2.8	Bell	38	3.1	Bell	295	3.4
Bell	323	2.8	Bell	318	3.1	Bell	295	3.4
Bell	282	2.8	Bell	63	3.1	Bell	279	3.4

Caves		
County	Azimuth	L(m)
Bell	282	3.4
Bell	306	3.4
Bell	285	3.4
Bell	290	3.4
Bell	268	3.4
Bell	120	3.4
Bell	28	3.4
Bell	96	3.4
Bell	48	3.4
Bell	340	3.5
Bell	287	3.5
Bell	330	3.5
Bell	303	3.5
Bell	83	3.5
Bell	284	3.5
Bell	315	3.5
Bell	282	3.5
Bell	14	3.5
Bell	20	3.5
Bell	285	3.5
Bell	22	3.5
Bell	28	3.5
Bell	292	3.5
Bell	283	3.5
Bell	292	3.5
Bell	298	3.5
Bell	109	3.6
Coryell	220	3.6
Bell	32	3.6
Bell	330	3.6
Bell	310	3.6
Bell	22	3.6
Bell	5	3.6
Bell	0	3.6
Bell	43	3.6

Caves		
County	Azimuth	L(m)
Bell	285	3.6
Bell	18	3.6
Coryell	14	3.6
Bell	280	3.7
Bell	284	3.7
Bell	62	3.7
Bell	10	3.7
Bell	316	3.7
Bell	282	3.7
Bell	285	3.7
Bell	335	3.7
Bell	49	3.7
Bell	322	3.8
Bell	15	3.8
Bell	18	3.8
Bell	20	3.8
Bell	284	3.8
Bell	90	3.8
Bell	328	3.8
Bell	278	3.8
Bell	305	3.8
Coryell	320	3.8
Bell	296	3.8
Bell	342	3.8
Bell	280	3.8
Bell	220	3.9
Bell	306	3.9
Bell	30	3.9
Bell	278	4.0
Bell	293	4.0
Bell	295	4.0
Bell	295	4.0
Bell	97	4.0
Bell	3	4.0
Bell	50	4.0

Caves		
County	Azimuth	L(m)
Bell	20	4.0
Bell	22	4.0
Bell	285	4.0
Bell	96	4.0
Bell	290	4.0
Bell	281	4.0
Bell	22	4.0
Bell	270	4.0
Bell	286	4.0
Bell	22	4.0
Coryell	10	4.0
Coryell	22	4.0
Coryell	14	4.0
Coryell	120	4.0
Coryell	43	4.0
Coryell	22	4.0
Coryell	22	4.1
Bell	35	4.1
Bell	322	4.2
Bell	36	4.2
Bell	281	4.2
Bell	10	4.2
Bell	104	4.2
Bell	306	4.2
Bell	322	4.2
Bell	22	4.2
Bell	72	4.2
Bell	20	4.3
Bell	296	4.3
Bell	15	4.3
Coryell	295	4.3
Bell	48	4.3
Bell	19	4.3
Bell	98	4.3
Bell	94	4.3

Caves			Caves			Caves		
County	Azimuth	L(m)	County	Azimuth	L(m)	County	Azimuth	L(m)
Bell	32	4.3	Bell	267	4.7	Bell	97	5.1
Bell	294	4.3	Bell	97	4.7	Bell	307	5.1
Coryell	306	4.3	Bell	281	4.7	Bell	97	5.2
Coryell	352	4.3	Bell	280	4.7	Bell	295	5.2
Bell	285	4.3	Coryell	300	4.7	Coryell	287	5.2
Bell	68	4.3	Coryell	281	4.7	Bell	305	5.2
Bell	18	4.3	Bell	0	4.7	Bell	86	5.2
Bell	286	4.3	Bell	281	4.7	Bell	282	5.3
Bell	90	4.3	Bell	281	4.7	Bell	302	5.3
Bell	28	4.3	Bell	315	4.8	Bell	275	5.3
Bell	10	4.4	Coryell	272	4.8	Bell	330	5.3
Bell	292	4.4	Bell	65	4.8	Coryell	275	5.3
Bell	295	4.4	Bell	278	4.8	Bell	82	5.3
Bell	295	4.4	Bell	10	4.8	Coryell	285	5.3
Bell	15	4.4	Bell	284	4.8	Bell	295	5.3
Bell	312	4.4	Bell	75	4.8	Bell	311	5.3
Bell	350	4.4	Bell	293	4.8	Bell	0	5.3
Coryell	275	4.4	Bell	330	4.8	Bell	280	5.3
Bell	81	4.5	Coryell	282	4.8	Bell	290	5.4
Bell	292	4.5	Bell	290	4.9	Bell	278	5.4
Bell	282	4.5	Bell	292	4.9	Bell	278	5.4
Bell	18	4.5	Bell	300	4.9	Bell	312	5.4
Coryell	277	4.5	Bell	287	4.9	Bell	284	5.5
Bell	280	4.5	Coryell	120	4.9	Bell	10	5.5
Bell	303	4.5	Coryell	54	4.9	Bell	319	5.5
Bell	275	4.5	Bell	82	5.0	Bell	331	5.5
Coryell	282	4.5	Bell	287	5.0	Bell	20	5.5
Bell	42	4.6	Bell	285	5.0	Bell	281	5.5
Bell	22	4.6	Bell	307	5.0	Bell	28	5.5
Bell	295	4.6	Bell	265	5.0	Bell	330	5.5
Bell	12	4.6	Coryell	282	5.0	Bell	73	5.5
Bell	285	4.6	Bell	52	5.1	Bell	72	5.6
Bell	274	4.6	Bell	13	5.1	Bell	10	5.6
Bell	22	4.6	Bell	22	5.1	Bell	285	5.6
Bell	285	4.6	Bell	278	5.1	Bell	22	5.6

Caves		
County	Azimuth	L(m)
Bell	180	5.6
Coryell	304	5.6
Coryell	43	5.6
Coryell	41	5.6
Bell	337	5.6
Bell	294	5.6
Bell	262	5.7
Bell	330	5.7
Bell	26	5.7
Coryell	80	5.7
Bell	275	5.7
Bell	295	5.7
Bell	23	5.8
Bell	27	5.8
Bell	308	5.8
Bell	266	5.8
Bell	282	5.8
Bell	274	5.8
Bell	285	5.8
Bell	20	5.8
Bell	85	5.8
Bell	13	5.9
Bell	22	5.9
Bell	295	6.0
Bell	279	6.0
Bell	14	6.0
Coryell	292	6.0
Bell	300	6.0
Bell	240	6.0
Bell	0	6.0
Bell	290	6.0
Coryell	292	6.0
Coryell	281	6.0
Bell	290	6.0
Bell	25	6.0

Caves		
County	Azimuth	L(m)
Bell	16	6.0
Bell	275	6.1
Bell	283	6.1
Bell	6	6.2
Bell	0	6.3
Bell	312	6.3
Bell	14	6.3
Bell	280	6.3
Bell	18	6.3
Coryell	84	6.3
Bell	90	6.3
Bell	63	6.3
Bell	285	6.3
Bell	20	6.4
Bell	283	6.4
Coryell	85	6.4
Bell	280	6.4
Coryell	305	6.4
Coryell	282	6.4
Bell	276	6.4
Bell	306	6.4
Bell	42	6.5
Bell	285	6.5
Bell	90	6.5
Bell	295	6.5
Bell	275	6.5
Bell	330	6.5
Coryell	295	6.5
Coryell	24	6.5
Bell	58	6.5
Bell	281	6.5
Coryell	293	6.6
Bell	289	6.6
Coryell	70	6.6
Bell	291	6.6

Caves		
County	Azimuth	L(m)
Bell	289	6.6
Bell	302	6.6
Bell	5	6.6
Bell	338	6.6
Bell	11	6.7
Bell	22	6.7
Coryell	330	6.7
Bell	53	6.7
Bell	18	6.8
Bell	15	6.8
Bell	335	6.8
Bell	270	6.8
Bell	22	6.8
Coryell	282	6.8
Coryell	43	6.8
Bell	284	6.8
Bell	287	6.8
Bell	71	6.8
Coryell	287	6.8
Coryell	278	6.8
Bell	278	6.9
Bell	306	6.9
Bell	53	6.9
Bell	290	6.9
Bell	290	6.9
Bell	49	7.0
Bell	32	7.0
Bell	90	7.0
Bell	290	7.0
Bell	90	7.0
Bell	23	7.0
Bell	20	7.0
Coryell	278	7.0
Bell	300	7.0
Bell	278	7.0

Caves		
County	Azimuth	L(m)
Bell	330	7.0
Bell	41	7.0
Bell	280	7.0
Bell	18	7.0
Bell	283	7.0
Bell	26	7.0
Bell	305	7.0
Coryell	53	7.0
Coryell	28	7.1
Bell	280	7.1
Bell	298	7.1
Bell	285	7.1
Bell	275	7.2
Bell	22	7.2
Bell	280	7.3
Bell	81	7.3
Bell	41	7.3
Bell	62	7.3
Bell	308	7.3
Bell	265	7.3
Coryell	53	7.3
Bell	320	7.3
Bell	72	7.3
Bell	285	7.4
Bell	280	7.4
Coryell	74	7.4
Bell	350	7.4
Bell	292	7.4
Coryell	282	7.4
Bell	281	7.5
Bell	45	7.5
Bell	290	7.5
Bell	46	7.5
Coryell	120	7.5
Bell	328	7.6

Caves		
County	Azimuth	L(m)
Bell	18	7.6
Bell	350	7.6
Bell	20	7.6
Bell	76	7.6
Bell	311	7.7
Bell	295	7.7
Bell	24	7.7
Bell	336	7.7
Bell	350	7.7
Bell	18	7.7
Bell	18	7.7
Bell	295	7.8
Bell	282	7.8
Bell	26	7.8
Bell	47	7.8
Coryell	285	7.9
Coryell	303	7.9
Bell	18	8.0
Bell	75	8.0
Bell	311	8.0
Bell	280	8.0
Bell	63	8.0
Bell	71	8.0
Bell	68	8.0
Bell	341	8.0
Bell	302	8.0
Bell	265	8.0
Bell	18	8.0
Bell	22	8.0
Coryell	281	8.0
Bell	284	8.1
Bell	12	8.2
Bell	322	8.3
Bell	335	8.3
Bell	326	8.3

Caves		
County	Azimuth	L(m)
Bell	320	8.4
Bell	6	8.4
Bell	330	8.4
Bell	334	8.4
Bell	281	8.4
Bell	283	8.5
Bell	318	8.5
Bell	45	8.5
Bell	74	8.5
Bell	20	8.5
Coryell	292	8.5
Coryell	20	8.5
Coryell	306	8.6
Bell	310	8.6
Bell	276	8.6
Coryell	293	8.6
Bell	90	8.7
Bell	287	8.7
Coryell	22	8.7
Bell	40	8.7
Bell	90	8.8
Bell	338	8.8
Bell	335	8.9
Bell	275	8.9
Bell	282	9.0
Bell	215	9.0
Bell	18	9.0
Bell	85	9.0
Coryell	315	9.0
Coryell	281	9.0
Coryell	20	9.0
Bell	275	9.1
Bell	100	9.1
Bell	305	9.1
Bell	306	9.2

Caves		
County	Azimuth	L(m)
Bell	270	9.3
Bell	18	9.3
Coryell	282	9.3
Coryell	288	9.3
Bell	74	9.3
Bell	20	9.3
Bell	90	9.4
Bell	286	9.5
Bell	50	9.5
Bell	290	9.5
Bell	285	9.5
Bell	44	9.5
Bell	53	9.5
Bell	280	9.5
Bell	281	9.5
Bell	51	9.5
Bell	62	9.5
Bell	275	9.6
Coryell	285	9.7
Coryell	282	9.7
Bell	295	9.8
Bell	10	9.8
Bell	290	9.8
Bell	290	9.8
Coryell	22	9.9
Bell	65	10.0
Bell	282	10.0
Coryell	22	10.0
Coryell	22	10.0
Coryell	306	10.0
Coryell	53	10.0
Bell	284	10.1
Bell	318	10.2
Bell	280	10.2
Bell	78	10.2

Caves		
County	Azimuth	L(m)
Bell	14	10.3
Bell	286	10.3
Coryell	288	10.3
Bell	303	10.3
Bell	287	10.5
Bell	297	10.5
Bell	24	10.5
Coryell	22	10.6
Coryell	285	10.6
Bell	325	10.6
Bell	33	10.6
Bell	288	10.7
Bell	20	10.7
Bell	16	10.8
Coryell	282	10.8
Bell	290	10.8
Coryell	281	10.8
Coryell	22	10.8
Bell	323	10.8
Bell	390	10.9
Bell	22	10.9
Bell	293	10.9
Coryell	285	11.0
Bell	283	11.1
Bell	290	11.2
Bell	290	11.2
Coryell	28	11.4
Coryell	295	11.4
Bell	51	11.5
Bell	11	11.5
Coryell	53	11.5
Coryell	281	11.8
Coryell	285	11.8
Bell	330	12.0
Bell	278	12.0

Caves		
County	Azimuth	L(m)
Coryell	277	12.0
Coryell	288	12.0
Bell	305	12.0
Coryell	352	12.0
Bell	220	12.1
Coryell	88	12.3
Coryell	280	12.3
Bell	71	12.3
Bell	281	12.5
Bell	328	7.6
Bell	18	7.6
Bell	350	7.6
Bell	20	7.6
Bell	76	7.6
Bell	311	7.7
Bell	295	7.7
Bell	24	7.7
Bell	336	7.7
Bell	350	7.7
Bell	18	7.7
Bell	18	7.7
Bell	295	7.8
Bell	282	7.8
Bell	26	7.8
Bell	47	7.8
Coryell	285	7.9
Coryell	303	7.9
Bell	18	8.0
Bell	75	8.0
Bell	311	8.0
Bell	280	8.0
Bell	63	8.0
Bell	71	8.0
Bell	68	8.0
Bell	341	8.0

Caves			Caves			Caves		
County	Azimuth	L(m)	County	Azimuth	L(m)	County	Azimuth	L(m)
Bell	302	8.0	Bell	215	9.0	Bell	65	10.0
Bell	265	8.0	Bell	18	9.0	Bell	282	10.0
Bell	18	8.0	Bell	85	9.0	Coryell	22	10.0
Bell	22	8.0	Coryell	315	9.0	Coryell	22	10.0
Coryell	281	8.0	Coryell	281	9.0	Coryell	306	10.0
Bell	284	8.1	Coryell	20	9.0	Coryell	53	10.0
Bell	12	8.2	Bell	275	9.1	Bell	284	10.1
Bell	322	8.3	Bell	100	9.1	Bell	318	10.2
Bell	335	8.3	Bell	305	9.1	Bell	280	10.2
Bell	326	8.3	Bell	306	9.2	Bell	78	10.2
Bell	320	8.4	Bell	270	9.3	Bell	14	10.3
Bell	6	8.4	Bell	18	9.3	Bell	286	10.3
Bell	330	8.4	Coryell	282	9.3	Coryell	288	10.3
Bell	334	8.4	Coryell	288	9.3	Bell	303	10.3
Bell	281	8.4	Bell	74	9.3	Bell	287	10.5
Bell	283	8.5	Bell	20	9.3	Bell	297	10.5
Bell	318	8.5	Bell	90	9.4	Bell	24	10.5
Bell	45	8.5	Bell	286	9.5	Coryell	22	10.6
Bell	74	8.5	Bell	50	9.5	Coryell	285	10.6
Bell	20	8.5	Bell	290	9.5	Bell	325	10.6
Coryell	292	8.5	Bell	285	9.5	Bell	33	10.6
Coryell	20	8.5	Bell	44	9.5	Bell	288	10.7
Coryell	306	8.6	Bell	53	9.5	Bell	20	10.7
Bell	310	8.6	Bell	280	9.5	Bell	16	10.8
Bell	276	8.6	Bell	281	9.5	Coryell	282	10.8
Coryell	293	8.6	Bell	51	9.5	Bell	290	10.8
Bell	90	8.7	Bell	62	9.5	Coryell	281	10.8
Bell	287	8.7	Bell	275	9.6	Coryell	22	10.8
Coryell	22	8.7	Coryell	285	9.7	Bell	323	10.8
Bell	40	8.7	Coryell	282	9.7	Bell	390	10.9
Bell	90	8.8	Bell	295	9.8	Bell	22	10.9
Bell	338	8.8	Bell	10	9.8	Bell	293	10.9
Bell	335	8.9	Bell	290	9.8	Coryell	285	11.0
Bell	275	8.9	Bell	290	9.8	Bell	283	11.1
Bell	282	9.0	Coryell	22	9.9	Bell	290	11.2

Caves			Caves			Caves		
County	Azimuth	L(m)	County	Azimuth	L(m)	County	Azimuth	L(m)
Bell	290	11.2	Bell	287	14.2	Bell	332	14.1
Coryell	28	11.4	Bell	60	14.5	Coryell	303	14.2
Coryell	295	11.4	Bell	18	14.7	Bell	287	14.2
Bell	51	11.5	Bell	284	14.8	Bell	60	14.5
Bell	11	11.5	Coryell	285	15.0	Bell	18	14.7
Coryell	53	11.5	Bell	14	15.0	Bell	284	14.8
Coryell	281	11.8	Bell	285	15.1	Coryell	285	15.0
Coryell	285	11.8	Bell	278	15.2	Bell	14	15.0
Bell	330	12.0	Coryell	285	15.2	Bell	285	15.1
Bell	278	12.0	Coryell	285	15.2	Bell	278	15.2
Coryell	277	12.0	Coryell	300	15.3	Coryell	285	15.2
Coryell	288	12.0	Bell	285	15.4	Coryell	285	15.2
Bell	305	12.0	Bell	285	15.5	Coryell	300	15.3
Coryell	352	12.0	Bell	50	15.5	Bell	285	15.4
Bell	220	12.1	Bell	73	15.6	Bell	285	15.5
Coryell	88	12.3	Coryell	22	16.0	Bell	50	15.5
Coryell	280	12.3	Bell	281	16.0	Bell	73	15.6
Bell	71	12.3	Bell	305	16.1	Coryell	22	16.0
Bell	281	12.5	Coryell	22	16.2	Bell	281	16.0
Bell	28	12.6	Bell	282	16.4	Bell	305	16.1
Coryell	22	12.7	Bell	305	17.3	Coryell	22	16.2
Bell	282	12.9	Bell	28	12.6	Bell	282	16.4
Coryell	22	13.0	Coryell	22	12.7	Bell	305	17.3
Bell	73	13.2	Bell	282	12.9	Bell	28	12.6
Bell	284	13.3	Coryell	22	13.0	Coryell	22	12.7
Bell	285	13.3	Bell	73	13.2	Bell	282	12.9
Bell	72	13.4	Bell	284	13.3	Coryell	22	13.0
Bell	308	13.5	Bell	285	13.3	Bell	73	13.2
Bell	85	13.5	Bell	72	13.4	Bell	284	13.3
Bell	282	13.8	Bell	308	13.5	Bell	285	13.3
Bell	303	13.8	Bell	85	13.5	Bell	72	13.4
Bell	80	14.0	Bell	282	13.8	Bell	308	13.5
Bell	293	14.0	Bell	303	13.8	Bell	85	13.5
Bell	332	14.1	Bell	80	14.0	Bell	282	13.8
Coryell	303	14.2	Bell	293	14.0	Bell	303	13.8

Caves			Caves			Caves		
County	Azimuth	L(m)	County	Azimuth	L(m)	County	Azimuth	L(m)
Bell	80	14.0	Coryell	282	20.6	Bell	282	20.7
Bell	293	14.0	Bell	282	20.7	Coryell	288	21.2
Bell	332	14.1	Coryell	288	21.2	Bell	53	21.3
Coryell	303	14.2	Bell	53	21.3	Bell	280	21.7
Bell	287	14.2	Bell	280	21.7	Bell	0	22.0
Bell	60	14.5	Bell	0	22.0	Coryell	311	22.4
Bell	18	14.7	Coryell	311	22.4	Coryell	72	17.7
Bell	284	14.8	Coryell	72	17.7	Bell	281	17.8
Coryell	285	15.0	Bell	281	17.8	Bell	285	18.0
Bell	14	15.0	Bell	285	18.0	Bell	307	18.3
Bell	285	15.1	Bell	307	18.3	Coryell	28	18.6
Bell	278	15.2	Coryell	28	18.6	Bell	342	18.8
Coryell	285	15.2	Bell	342	18.8	Bell	38	18.9
Coryell	285	15.2	Bell	38	18.9	Coryell	275	19.3
Coryell	300	15.3	Coryell	275	19.3	Bell	53	19.6
Bell	285	15.4	Bell	53	19.6	Coryell	305	19.9
Bell	285	15.5	Coryell	305	19.9	Coryell	282	20.6
Bell	50	15.5	Coryell	282	20.6	Bell	282	20.7
Bell	73	15.6	Bell	282	20.7	Coryell	288	21.2
Coryell	22	16.0	Coryell	288	21.2	Bell	53	21.3
Bell	281	16.0	Bell	53	21.3	Bell	280	21.7
Bell	305	16.1	Bell	280	21.7	Bell	0	22.0
Coryell	22	16.2	Bell	0	22.0	Coryell	311	22.4
Bell	282	16.4	Coryell	311	22.4	Bell	289	22.9
Bell	305	17.3	Coryell	72	17.7	Coryell	285	22.9
Coryell	72	17.7	Bell	281	17.8	Bell	275	23.0
Bell	281	17.8	Bell	285	18.0	Bell	53	23.2
Bell	285	18.0	Bell	307	18.3	Bell	328	23.5
Bell	307	18.3	Coryell	28	18.6	Coryell	72	24.6
Coryell	28	18.6	Bell	342	18.8	Bell	41	25.0
Bell	342	18.8	Bell	38	18.9	Coryell	281	25.7
Bell	38	18.9	Coryell	275	19.3	Bell	292	26.3
Coryell	275	19.3	Bell	53	19.6	Coryell	335	26.3
Bell	53	19.6	Coryell	305	19.9	Bell	73	26.7
Coryell	305	19.9	Coryell	282	20.6	Bell	278	27.0

Caves			Caves			Caves		
County	Azimuth	L(m)	County	Azimuth	L(m)	County	Azimuth	L(m)
Bell	289	22.9	Bell	278	27.0	Bell	283	29.6
Coryell	285	22.9	Bell	289	22.9	Coryell	286	31.3
Bell	275	23.0	Coryell	285	22.9	Coryell	53	32.5
Bell	53	23.2	Bell	275	23.0	Coryell	300	28.0
Bell	328	23.5	Bell	53	23.2	Coryell	22	28.0
Coryell	72	24.6	Bell	328	23.5	Bell	283	29.6
Bell	41	25.0	Coryell	72	24.6	Coryell	286	31.3
Coryell	281	25.7	Bell	41	25.0	Coryell	53	32.5
Bell	292	26.3	Coryell	281	25.7	Coryell	281	32.9
Coryell	335	26.3	Bell	292	26.3	Coryell	285	35.1
Bell	73	26.7	Coryell	335	26.3	Bell	28	37.1
Bell	278	27.0	Bell	73	26.7	Coryell	281	32.9
Bell	289	22.9	Bell	278	27.0	Coryell	285	35.1
Coryell	285	22.9	Coryell	300	28.0	Bell	28	37.1
Bell	275	23.0	Coryell	22	28.0	Coryell	281	32.9
Bell	53	23.2	Bell	283	29.6	Coryell	285	35.1
Bell	328	23.5	Coryell	286	31.3	Bell	28	37.1
Coryell	72	24.6	Coryell	53	32.5	Coryell	281	32.9
Bell	41	25.0	Coryell	300	28.0	Coryell	285	35.1
Coryell	281	25.7	Coryell	22	28.0	Bell	28	37.1
Bell	292	26.3	Bell	283	29.6	Coryell	281	32.9
Coryell	335	26.3	Coryell	286	31.3	Coryell	285	35.1
Bell	73	26.7	Coryell	53	32.5	Bell	28	37.1
Bell	278	27.0	Coryell	300	28.0	Coryell	281	32.9
Bell	289	22.9	Coryell	22	28.0	Coryell	285	35.1
Coryell	285	22.9	Bell	283	29.6	Bell	28	37.1
Bell	275	23.0	Coryell	286	31.3	Coryell	281	32.9
Bell	53	23.2	Coryell	53	32.5	Coryell	285	35.1
Bell	328	23.5	Coryell	300	28.0	Bell	28	37.1
Coryell	72	24.6	Coryell	22	28.0	Coryell	292	37.9
Bell	41	25.0	Bell	283	29.6	Bell	280	38.6
Coryell	281	25.7	Coryell	286	31.3	Coryell	300	38.6
Bell	292	26.3	Coryell	53	32.5	Coryell	282	38.9
Coryell	335	26.3	Coryell	300	28.0	Coryell	292	37.9
Bell	73	26.7	Coryell	22	28.0	Bell	280	38.6

Caves			Caves			Caves		
County	Azimuth	L(m)	County	Azimuth	L(m)	County	Azimuth	L(m)
Coryell	300	38.6	Bell	287	44.7	Bell	35	53.0
Coryell	282	38.9	Bell	36	44.0	Bell	21	53.1
Coryell	292	37.9	Bell	287	44.7	Bell	41	54.0
Bell	280	38.6	Bell	36	44.0	Coryell	281	55.0
Coryell	300	38.6	Bell	287	44.7	Bell	35	53.0
Coryell	282	38.9	Bell	36	44.0	Bell	21	53.1
Coryell	292	37.9	Bell	287	44.7	Bell	41	54.0
Bell	280	38.6	Bell	36	44.0	Coryell	281	55.0
Coryell	300	38.6	Bell	287	44.7	Bell	35	53.0
Coryell	282	38.9	Bell	26	50.7	Bell	21	53.1
Coryell	292	37.9	Bell	26	50.7	Bell	41	54.0
Bell	280	38.6	Bell	26	50.7	Coryell	281	55.0
Coryell	300	38.6	Bell	26	50.7	Bell	35	53.0
Coryell	282	38.9	Bell	26	50.7	Bell	21	53.1
Coryell	292	37.9	Bell	26	50.7	Bell	41	54.0
Bell	280	38.6	Bell	26	50.7	Coryell	281	55.0
Coryell	300	38.6	Bell	26	50.7	Bell	35	53.0
Coryell	282	38.9	Bell	26	50.7	Bell	21	53.1
Coryell	292	37.9	Bell	26	50.7	Bell	41	54.0
Bell	280	38.6	Bell	35	53.0	Coryell	281	55.0
Coryell	300	38.6	Bell	21	53.1	Bell	35	53.0
Coryell	282	38.9	Bell	41	54.0	Bell	21	53.1
Coryell	292	37.9	Coryell	281	55.0	Bell	41	54.0
Bell	280	38.6	Bell	35	53.0	Coryell	281	55.0
Coryell	300	38.6	Bell	21	53.1	Bell	35	53.0
Coryell	282	38.9	Bell	41	54.0	Bell	21	53.1
Bell	36	44.0	Coryell	281	55.0	Bell	41	54.0
Bell	287	44.7	Bell	35	53.0	Coryell	281	55.0
Bell	36	44.0	Bell	21	53.1	Bell	280	58.0
Bell	287	44.7	Bell	41	54.0	Bell	280	58.0
Bell	36	44.0	Coryell	281	55.0	Bell	280	58.0
Bell	287	44.7	Bell	35	53.0	Bell	280	58.0
Bell	36	44.0	Bell	21	53.1	Bell	280	58.0
Bell	287	44.7	Bell	41	54.0	Bell	280	58.0
Bell	36	44.0	Coryell	281	55.0	Bell	280	58.0

Caves			Caves			Caves		
County	Azimuth	L(m)	County	Azimuth	L(m)	County	Azimuth	L(m)
Bell	35	53.0	Bell	280	58.0	Bell	18	91.4
Bell	21	53.1	Bell	280	58.0	Bell	18	91.4
Bell	41	54.0	Bell	280	58.0	Bell	18	91.4
Coryell	281	55.0	Bell	280	58.0	Bell	18	91.4
Bell	35	53.0	Bell	280	58.0	Bell	18	91.4
Bell	21	53.1	Coryell	282	75.2	Bell	18	91.4
Bell	41	54.0	Coryell	24	75.9	Bell	18	91.4
Coryell	281	55.0	Coryell	282	75.2	Bell	18	91.4
Bell	35	53.0	Coryell	24	75.9	Bell	18	91.4
Bell	21	53.1	Coryell	282	75.2	Bell	18	91.4
Bell	41	54.0	Coryell	24	75.9	Bell	18	91.4
Coryell	281	55.0	Coryell	282	75.2	Bell	18	91.4
Bell	35	53.0	Coryell	24	75.9	Bell	18	91.4
Bell	21	53.1	Coryell	282	75.2	Bell	18	91.4
Bell	41	54.0	Coryell	24	75.9	Bell	18	91.4
Coryell	281	55.0	Coryell	282	75.2	Bell	18	91.4
Bell	35	53.0	Coryell	24	75.9	Bell	18	91.4
Bell	21	53.1	Coryell	282	75.2	Bell	18	91.4
Bell	41	54.0	Coryell	24	75.9	Coryell	292	114.3
Coryell	281	55.0	Coryell	282	75.2	Coryell	292	114.3
Bell	35	53.0	Coryell	24	75.9	Coryell	292	114.3
Bell	21	53.1	Coryell	282	75.2	Coryell	292	114.3
Bell	41	54.0	Coryell	24	75.9	Coryell	292	114.3
Coryell	281	55.0	Coryell	282	75.2	Coryell	292	114.3
Bell	35	53.0	Coryell	24	75.9	Coryell	292	114.3
Bell	21	53.1	Coryell	282	75.2	Coryell	292	114.3
Bell	41	54.0	Coryell	24	75.9	Coryell	292	114.3
Coryell	281	55.0	Coryell	282	75.2	Coryell	292	114.3
Bell	280	58.0	Coryell	24	75.9	Coryell	292	114.3
Bell	280	58.0	Coryell	282	75.2	Coryell	292	114.3
Bell	280	58.0	Coryell	24	75.9	Coryell	292	114.3
Bell	280	58.0	Coryell	282	75.2	Coryell	292	114.3
Bell	280	58.0	Coryell	24	75.9	Coryell	292	114.3
Bell	280	58.0	Coryell	282	75.2	Coryell	292	114.3
Bell	280	58.0	Coryell	24	75.9	Coryell	292	114.3

Caves		
County	**Azimuth**	**L(m)**
Coryell	292	114.3
Coryell	292	114.3
Coryell	292	114.3
Coryell	292	114.3
Coryell	292	114.3
Coryell	292	114.3

APPENDIX VI:

Maple Habitat Orientation

Maple Habitat	
Stand	**Azimuth**
0	0
0	16
0	261
0	278
1	0
1	16
1	18
1	332
1	351
46	0
46	0
46	9
46	28
46	28
46	72
46	285
46	287
46	288
46	353
215	22
215	22
215	283
369	20
369	276
369	312
369	351
389	72
389	353
476	0
476	25
476	26
476	33
476	287
476	288
476	292
483	281
483	286
483	286
483	286
483	312
560	285
560	285
560	286

APPENDIX VII:

Stream Segment Orientation

Streams		Streams		Streams		Streams	
TA	Azimuth	TA	Azimuth	TA	Azimuth	TA	Azimuth
11	0	11	284	12	130	13	30
11	0	11	284	12	130	13	31
11	0	11	285	12	135	13	31
11	1	11	285	12	155	13	35
11	1	11	305	12	162	13	42
11	2	11	305	12	165	13	42
11	2	11	340	12	177	13	42
11	3	11	340	12	280	13	47
11	3	11	346	12	283	13	49
11	4	11	346	12	284	13	80
11	4	11	346	12	284	13	80
11	6	11	346	12	290	13	90
11	10	12	0	12	296	13	101
11	10	12	0	12	332	13	101
11	11	12	0	13	0	13	111
11	11	12	0	13	0	13	142
11	11	12	0	13	0	13	180
11	11	12	0	13	0	13	280
11	12	12	3	13	0	13	280
11	12	12	4	13	0	13	283
11	12	12	5	13	0	13	283
11	12	12	5	13	5	13	284
11	16	12	5	13	5	13	284
11	16	12	6	13	5	13	284
11	18	12	13	13	5	13	284
11	34	12	13	13	6	13	290
11	34	12	13	13	6	13	290
11	42	12	13	13	8	13	296
11	42	12	16	13	12	13	296
11	49	12	21	13	12	20	0
11	61	12	21	13	13	20	0
11	62	12	22	13	13	20	0
11	62	12	22	13	13	20	0
11	62	12	22	13	13	20	0
11	77	12	22	13	13	20	0
11	106	12	23	13	13	20	0
11	113	12	30	13	13	20	0
11	114	12	31	13	13	20	0
11	114	12	31	13	16	20	0
11	119	12	36	13	18	20	3
11	127	12	37	13	21	20	4
11	133	12	42	13	22	20	4
11	134	12	57	13	22	20	5
11	141	12	57	13	22	20	7
11	145	12	80	13	22	20	17
11	160	12	90	13	22	20	17
11	165	12	98	13	22	20	20
11	172	12	109	13	23	20	23
11	283	12	113	13	24	20	23
11	283	12	120	13	30	20	26

Streams		Streams		Streams		Streams	
TA	Azimuth	TA	Azimuth	TA	Azimuth	TA	Azimuth
20	27	21	12	23	22	115	1
20	31	21	12	23	22	115	2
20	36	21	14	23	22	115	2
20	40	21	16	23	4	115	2
20	41	21	16	23	6	115	3
20	41	21	16	23	7	115	3
20	66	21	21	23	7	115	3
20	77	21	21	23	24	115	3
20	80	21	22	23	25	115	4
20	87	21	26	23	25	115	4
20	88	21	42	23	25	115	4
20	88	21	44	23	26	115	4
20	90	21	48	23	10	115	6
20	90	21	48	23	30	115	6
20	90	21	358	23	23	115	6
20	93	21	358	23	32	115	6
20	97	23	0	23	24	115	6
20	101	23	0	23	33	115	6
20	105	23	0	23	34	115	6
20	105	23	3	23	42	115	8
20	109	23	4	23	17	115	8
20	116	23	4	23	45	115	10
20	122	23	3	23	80	115	10
20	125	23	3	23	17	115	12
20	135	23	3	23	83	115	12
20	138	23	5	23	281	115	14
20	138	23	6	23	19	115	14
20	143	23	6	23	283	115	14
20	145	23	12	23	284	115	14
20	153	23	13	23	23	115	14
20	154	23	13	23	285	115	14
20	155	23	8	23	285	115	22
20	159	23	8	23	5	115	22
20	160	23	9	23	7	115	42
20	162	23	9	23	286	115	65
20	166	23	22	23	287	115	67
20	171	23	22	23	287	115	68
20	174	23	23	23	291	115	80
20	178	23	27	23	26	115	271
21	0	23	43	23	293	115	271
21	2	23	16	23	297	115	272
21	3	23	16	23	298	115	272
21	3	23	16	23	31	115	278
21	3	23	16	23	24	115	278
21	4	23	16	23	299	115	281
21	4	23	16	23	352	115	281
21	5	23	16	23	34	115	281
21	6	23	18	115	0	115	281
21	6	23	4	115	0	115	281
21	11	23	22	115	1	115	283

Streams		Streams		Streams		Streams	
TA	Azimuth	TA	Azimuth	TA	Azimuth	TA	Azimuth
115	283	20/23	3	20/23	48	20/23	148
115	284	20/23	4	20/23	48	20/23	150
115	284	20/23	4	20/23	48	20/23	152
115	284	20/23	6	20/23	53	20/23	154
115	284	20/23	6	20/23	57	20/23	158
115	284	20/23	6	20/23	58	20/23	164
115	285	20/23	6	20/23	58	20/23	169
115	285	20/23	8	20/23	59	20/23	173
115	285	20/23	8	20/23	61	20/23	174
115	285	20/23	8	20/23	62	20/23	265
115	291	20/23	9	20/23	63	20/23	265
115	297	20/23	11	20/23	63	20/23	265
115	320	20/23	11	20/23	66	20/23	268
115	324	20/23	11	20/23	66	20/23	268
115	346	20/23	11	20/23	68	20/23	268
115	346	20/23	11	20/23	70	20/23	271
115	346	20/23	11	20/23	72	20/23	271
20/22	10	20/23	12	20/23	72	20/23	271
20/22	11	20/23	12	20/23	75	20/23	274
20/22	26	20/23	12	20/23	77	20/23	274
20/22	35	20/23	12	20/23	77	20/23	274
20/22	37	20/23	12	20/23	80	20/23	279
20/22	84	20/23	12	20/23	80	20/23	279
20/22	90	20/23	12	20/23	85	20/23	279
20/22	104	20/23	12	20/23	90	20/23	281
20/22	128	20/23	12	20/23	90	20/23	281
20/22	130	20/23	12	20/23	91	20/23	281
20/22	131	20/23	12	20/23	92	20/23	284
20/22	155	20/23	12	20/23	94	20/23	284
20/22	156	20/23	14	20/23	97	20/23	284
20/22	157	20/23	14	20/23	98	20/23	284
20/23	0	20/23	14	20/23	99	20/23	284
20/23	0	20/23	14	20/23	106	20/23	284
20/23	0	20/23	14	20/23	108	20/23	284
20/23	0	20/23	14	20/23	110	20/23	285
20/23	0	20/23	16	20/23	111	20/23	285
20/23	0	20/23	16	20/23	111	20/23	285
20/23	0	20/23	16	20/23	113	20/23	285
20/23	0	20/23	16	20/23	113	20/23	285
20/23	0	20/23	16	20/23	113	20/23	285
20/23	0	20/23	16	20/23	116	20/23	288
20/23	1	20/23	16	20/23	122	20/23	292
20/23	1	20/23	20	20/23	129	20/23	292
20/23	1	20/23	30	20/23	135	20/23	292
20/23	2	20/23	32	20/23	135	20/23	292
20/23	2	20/23	34	20/23	138	20/23	295
20/23	3	20/23	42	20/23	140	20/23	296
20/23	3	20/23	44	20/23	145	20/23	296
20/23	3	20/23	45	20/23	148	20/23	296
20/23	3	20/23	48	20/23	148	20/23	340

Streams	
TA	Azimuth
20/23	346
20/23	348
20/23	348
20/23	348
20/23	352
21/22	0
21/22	0
21/22	0
21/22	1
21/22	1
21/22	3
21/22	4
21/22	4
21/22	4
21/22	4
21/22	4
21/22	297
21/22	5
21/22	5
21/22	5
21/22	5
21/22	5
21/22	6
21/22	6
21/22	6
21/22	8
21/22	2
21/22	8
21/22	8
21/22	8
21/22	8
21/22	8
21/22	9
21/22	9
21/22	9
21/22	9
21/22	9
21/22	10
21/22	7
21/22	11
21/22	11
21/22	11
21/22	8
21/22	12
21/22	12
21/22	10
21/22	13
21/22	13
21/22	13

Streams	
TA	Azimuth
21/22	13
21/22	14
21/22	14
21/22	14
21/22	14
21/22	14
21/22	14
21/22	14
21/22	15
21/22	12
21/22	9
21/22	16
21/22	16
21/22	16
21/22	16
21/22	16
21/22	16
21/22	17
21/22	17
21/22	18
21/22	18
21/22	18
21/22	18
21/22	18
21/22	19
21/22	16
21/22	16
21/22	20
21/22	17
21/22	21
21/22	21
21/22	21
21/22	21
21/22	22
21/22	22
21/22	22
21/22	22
21/22	22
21/22	19
21/22	24
21/22	24
21/22	26
21/22	26
21/22	26
21/22	20
21/22	21
21/22	30
21/22	32
21/22	32

Streams	
TA	Azimuth
21/22	34
21/22	23
21/22	185
21/22	279
21/22	279
21/22	281
21/22	281
21/22	281
21/22	281
21/22	281
21/22	21
21/22	284
21/22	284
21/22	284
21/22	284
21/22	285
21/22	285
21/22	285
21/22	285
21/22	285
21/22	285
21/22	285
21/22	288
21/22	290
21/22	291
21/22	291
21/22	291
21/22	291
21/22	291
21/22	283
21/22	293
21/22	293
21/22	295
21/22	286
21/22	286
21/22	297
21/22	297
21/22	297
21/22	297
21/22	298
21/22	312
21/22	314
21/22	346
21/22	346
21/22	348
21/22	348
21/22	293
21/22	352
21/22	352

Streams	
TA	Azimuth
21/22	354
21/22	354
21/22	356
21/22	295
21/22	297

APPENDIX VIII:

Soil and Site Parameters For Vegetation Plots

Stand	Plot	Elevation (m)	Slope (degrees)	Aspect	Watershed	Soil pH	Soil Type *	Soil Cond (µs/cm)	% Sand	% Clay	% Silt	Canopy **
V0	1	215.85	22.70	N	Owl	7.73	REF	267	66.48	21.69	11.83	4
V0	2	212.80	8.20	N	Owl	8.22	REF	315	56.29	25.83	17.88	2
V0	3	218.29	7.30	N	Owl	8.01	REF	283	70.90	20.37	8.73	2
V0	4	221.34	9.10	N	Owl	8.09	REF	316	64.93	20.63	14.44	4
V0	5	225.91	25.50	N	Owl	8.21	REF	265	68.02	15.99	15.99	4
V1	1	246.04	30.90	SE	Bear	8.25	REF	312	70.10	15.95	13.95	4
V1	2	233.84	1.80	SE	Bear	7.88	REF	565	51.27	31.19	17.54	4
V1	3	237.50	4.60	SE	Bear	8	REF	424	82.27	13.79	3.94	4
V1	4	251.83	10.60	SE	Bear	8.15	REF	307	76.17	11.91	11.91	2
V1	5	228.05	9.90	SE	Bear	8.12	REF	352	60.51	19.74	19.74	3
V215	1	242.07	6.80	NNE	Bear	8.06	REF	356	68.02	13.99	17.99	1
V215	2	239.94	2.60	NNE	Bear	7.96	REF	388	71.50	15.20	13.30	2
V215	3	228.35	9.60	NNE	Bear	7.88	REF	359	68.03	19.98	11.99	1
V215	4	223.17	14.70	NNE	Bear	8.13	REF	243	66.89	19.48	13.63	1
V369	3	236.89	7.20	ESE	Bear	8.12	REF	308	52.23	25.88	21.89	2
V369	4	231.10	4.80	ESE	Bear	8.06	REF	351	54.32	24.92	20.76	2
V369	1	235.98	7.10	ESE	Bear	8.14	REF	428	60.01	24.00	16.00	2
V369	2	238.72	1.10	ESE	Bear	8.05	REF	343	57.66	28.87	13.47	2
V389	1	234.15	33.10	NNW	Owl	8.1	REF	408	62.52	23.67	13.81	3
V389	2	239.63	28.70	NNW	Owl	8.17	REF	371	52.86	27.50	19.64	3
V46	1	191.77	19.60	NNE	Owl	8.14	REF	280	56.05	23.97	19.98	2
V46	2	223.17	11.70	NNE	Owl	8.33	REF	243	61.07	21.41	17.52	2
V46	3	197.56	26.30	NNE	Owl	8.22	REF	274	68.33	13.86	17.81	2
V46	4	228.96	24.60	NNE	Owl	8.14	REF	266	60.76	23.54	15.70	2
V46	5	220.73	22.20	NNE	Owl	8.3	REF	209	58.03	25.98	15.99	2
V46	6	197.56	11.30	NNE	Owl	8.22	REF	229	78.64	9.49	11.87	2
V46	7	217.38	26.60	NNE	Owl	8.25	REF	226	80.37	10.91	8.72	2
V46	8	205.49	22.30	NNE	Owl	8.29	REF	194	64.57	17.72	17.72	2
V46	9	190.24	8.40	NNE	Owl	8.23	REF	256	52.34	25.81	21.84	2
V46	10	239.94	29.50	NNE	Owl	8.19	REF	263	52.08	27.96	19.97	2

*Soil Type (REF) = Real Rock outcrop complex, 12 to 40 % slopes

** Canopy description = Closed (4), partially closed (3), partially open (2), and open (1)

Stand	Plot	Elevation (m)	Slope (degrees)	Aspect	Watershed	Soil pH	Soil Type	Soil Cond (µs/cm)	%Sand	%Clay	%Silt	Canopy
V476	1	196.04	20.40	NE	Owl	8.18	REF	318	63.39	28.90	7.71	3
V476	2	213.72	36.90	NE	Owl	8.28	REF	310	54.66	29.57	15.77	3
V476	3	211.59	13.20	NE	Owl	8.19	REF	291	54.64	21.70	23.67	3
V476	4	216.77	4.20	NE	Owl	8.21	REF	261	68.00	14.00	18.00	3
V476	5	227.44	17.70	NE	Owl	8.24	REF	316	68.66	19.58	11.75	2
V476	6	232.62	3.80	NE	Owl	8.25	REF	438	42.73	39.49	17.77	2
V476	7	229.27	10.80	NE	Owl	8.26	REF	240	60.35	21.81	17.84	2
V476	8	239.02	7.90	NE	Owl	8.17	REF	254	54.45	34.78	10.77	2
V476	9	244.82	7.40	NE	Owl	8.13	REF	330	77.79	12.96	9.25	2
V476	10	220.73	16.10	NE	Owl	8.15	REF	349	74.16	13.92	11.93	2
V476	11	194.82	17.30	NE	Owl	8.36	REF	303	66.28	21.82	11.90	2
V476	12	222.87	20.80	NE	Owl	8.34	REF	294	76.22	15.85	7.93	2
V476	13	188.41	32.30	NE	Owl	8.24	REF	238	72.14	13.93	13.93	2
V476	14	230.49	31.20	NE	Owl	8.31	REF	224	75.58	15.54	8.88	2
V476	15	191.16	8.50	NE	Owl	8.24	REF	245	80.30	15.32	4.38	2
V476	16	232.62	4.80	NE	Owl	8.33	REF	194	66.30	19.82	13.88	2
V483	1	197.26	2.40	SE	Bear	8.34	REF	349	50.12	25.94	23.94	1
V483	2	201.52	5.20	SE	Bear	8.22	REF	292	56.25	27.84	15.91	2
V483	3	199.09	17.40	SE	Bear	8.21	REF	359	61.37	29.72	8.92	2
V483	4	207.01	5.80	SE	Bear	8.32	REF	279	44.74	33.55	21.71	2
V560	1	218.90	4.60	SE	Bear	8.1	REF	316	61.65	24.93	13.42	3
V560	2	222.87	15.50	SE	Bear	7.92	REF	264	52.04	25.98	21.98	3
V560	3	233.84	6.10	SE	Bear	8.28	REF	181	66.14	19.92	13.94	3
V560	4	239.02	7.70	SE	Bear	8.22	REF	393	68.83	19.48	11.69	3

*Soil Type (REF) = Real Rock outcrop complex, 12 to 40 % slopes

** Canopy description = Closed (4), partially closed (3), partially open (2), and open (1)

Stand	Plot	Elevation (m)	Slope (degrees)	Aspect	Watershed	Soil Type *	Canopy **
M1	1	228.05	15.50	NE	Owl	REF	3
M1	2	227.74	27.40	N	Owl	REF	2
M1	3	214.94	31.10	NE	Owl	REF	4
M1	4	210.67	20.80	NE	Owl	REF	2
M1	5	219.82	12.90	NE	Owl	REF	2
M1	6	228.05	19.50	NE	Owl	REF	2
M1	7	226.83	14.90	NE	Owl	REF	2
M1	8	223.78	23.10	NE	Owl	REF	3
M1	9	229.27	18.20	NE	Owl	REF	3
M1	10	231.71	25.50	NE	Owl	REF	3
M1	11	226.52	18.10	N	Owl	REF	2
M1	12	219.82	23.70	N	Owl	REF	2
M1	13	221.65	31.60	SE	Owl	REF	4
M1	14	225.61	4.10	SE	Owl	REF	3
M1	22	226.22	25.10	NE	Owl	REF	3
M2	21	234.45	17.80	SE	Owl	REF	2
M2	25	193.60	34.10	NE	Owl	REF	3
M3	15	207.62	38.50	NE	Owl	REF	2
M3	16	209.15	37.10	NE	Owl	REF	2
M3	17	215.24	25.30	NE	Owl	REF	2
M3	18	210.98	26.70	NE	Owl	REF	2
M3	19	222.56	25.40	NE	Owl	REF	3
M3	20	232.01	27.80	NE	Owl	REF	2
M3	26	228.05	30.20	NE	Owl	REF	2
M3	31	221.04	36.20	N	Owl	REF	2
M3	32	214.33	9.10	N	Owl	REF	4
M3	33	221.04	17.30	N	Owl	REF	2
M3	34	204.27	18.10	N	Owl	REF	3
M3	35	215.24	26.30	NE	Owl	REF	2
M3	36	213.72	19.50	NE	Owl	REF	2
M3	37	224.39	32.90	NE	Owl	REF	2
M3	38	223.48	8.30	N	Owl	REF	2
M3	39	230.79	27.50	NE	Owl	REF	2
M3	40	214.02	25.90	NE	Owl	REF	3
M3	41	203.96	20.80	NE	Owl	REF	2
M3	42	212.50	37.40	NE	Owl	REF	3
M3	43	228.35	36.40	NE	Owl	REF	2
M3	44	211.59	17.30	NE	Owl	REF	2
M3	45	219.82	33.90	NE	Owl	REF	2

*Soil Type (REF) = Real Rock outcrop complex, 12 to 40 % slopes

** Canopy description = Closed (4), partially closed (3), partially open (2), and open (1)

Stand	Plot	Elevation (m)	Slope (degrees)	Aspect	Watershed	Soil Type *	Canopy **
M4	57	219.51	5.10	SW	Bear	REF	3
M4	58	223.78	8.30	SW	Bear	REF	3
M5	60	221.95	5.50	SW	Bear	REF	3
M5	61	224.09	13.90	SW	Bear	REF	3
M5	81	220.12	8.20	SW	Bear	REF	2
M5	83	231.10	5.60	SW	Bear	REF	2
M6	62	229.88	1.90	SW	Bear	REF	3
M6	63	242.99	7.40	SW	Bear	REF	4
M7	51	218.90	2.00	N	Bear	REF	3
M7	52	221.95	8.40	N	Bear	REF	2
M7	53	217.07	1.20	N	Bear	REF	2
M7	59	236.59	6.50	NE	Bear	REF	3
M8	54	225.30	10.10	N	Bear	REF	2
M8	55	230.49	9.80	N	Bear	REF	4
M8	56	225.00	15.80	N	Bear	REF	2
M9	70	203.96	29.20	NE	Bear	REF	2
M10	73	194.82	14.70	NE	Bear	REF	3
M10	74	200.91	4.90	NE	Bear	REF	3
M10	75	207.01	6.20	NE	Bear	REF	4
M10	76	203.96	5.70	NE	Bear	REF	3
M10	77	215.85	32.10	NE	Bear	REF	4
M10	78	212.80	39.20	NE	Bear	REF	4

*Soil Type (REF) = Real Rock outcrop complex, 12 to 40 % slopes

** Canopy description = Closed (4), partially closed (3), partially open (2), and open (1)

APPENDIX IX:

Vegetation Plot Data

Established Habitat			Trees per plot (count)			Trees per Hectare (EF=127.3885)		
Stand	Plot	Water-shed	Maple	Ashe	Other	Maple	Ashe	Other
V0	1	Owl	0	0	3	0.00	0.00	382.17
V0	2	Owl	0	0	3	0.00	0.00	382.17
V0	3	Owl	5	2	1	636.94	254.78	127.39
V0	4	Owl	3	0	3	382.17	0.00	382.17
V0	5	Owl	3	0	3	382.17	0.00	382.17
V1	1	Bear	0	3	0	0.00	382.17	0.00
V1	2	Bear	4	0	0	509.55	0.00	0.00
V1	3	Bear	4	0	0	509.55	0.00	0.00
V1	4	Bear	1	0	2	127.39	0.00	254.78
V1	5	Bear	0	3	1	0.00	382.17	127.39
V215	1	Bear	0	3	2	0.00	382.17	254.78
V215	2	Bear	0	0	1	0.00	0.00	127.39
V215	3	Bear	0	3	1	0.00	382.17	127.39
V215	4	Bear	0	3	2	0.00	382.17	254.78
V369	3	Bear	2	2	0	254.78	254.78	0.00
V369	4	Bear	0	0	1	0.00	0.00	127.39
V369	1	Bear	0	2	0	0.00	254.78	0.00
V369	2	Bear	3	2	1	382.17	254.78	127.39
V389	1	Owl	3	2	2	382.17	254.78	254.78
V389	2	Owl	2	2	2	254.78	254.78	254.78
V46	1	Owl	2	0	4	254.78	0.00	509.55
V46	2	Owl	4	1	2	509.55	127.39	254.78
V46	3	Owl	4	1	3	509.55	127.39	382.17
V46	4	Owl	2	2	2	254.78	254.78	254.78
V46	5	Owl	1	2	2	127.39	254.78	254.78
V46	6	Owl	2	1	2	254.78	127.39	254.78
V46	7	Owl	1	2	3	127.39	254.78	382.17
V46	8	Owl	3	1	2	382.17	127.39	254.78
V46	9	Owl	2	2	1	254.78	254.78	127.39
V46	10	Owl	2	2	1	254.78	254.78	127.39

Established Habitat			Trees per plot (count)			Trees per Hectare (EF=127.3885)		
Stand	Plot	Water-shed	Maple	Ashe	Other	Maple	Ashe	Other
V476	1	Owl	0	0	3	0.00	0.00	382.17
V476	2	Owl	0	1	2	0.00	127.39	254.78
V476	3	Owl	1	1	1	127.39	127.39	127.39
V476	4	Owl	1	2	2	127.39	254.78	254.78
V476	5	Owl	4	1	1	509.55	127.39	127.39
V476	6	Owl	3	1	1	382.17	127.39	127.39
V476	7	Owl	2	3	1	254.78	382.17	127.39
V476	8	Owl	2	0	2	254.78	0.00	254.78
V476	9	Owl	3	1	1	382.17	127.39	127.39
V476	10	Owl	3	1	1	382.17	127.39	127.39
V476	11	Owl	3	0	2	382.17	0.00	254.78
V476	12	Owl	3	2	2	382.17	254.78	254.78
V476	13	Owl	1	1	1	127.39	127.39	127.39
V476	14	Owl	2	0	2	254.78	0.00	254.78
V476	15	Owl	2	0	1	254.78	0.00	127.39
V476	16	Owl	2	0	2	254.78	0.00	254.78
V483	1	Bear	2	2	1	254.78	254.78	127.39
V483	2	Bear	2	2	2	254.78	254.78	254.78
V483	3	Bear	3	1	1	382.17	127.39	127.39
V483	4	Bear	1	2	3	127.39	254.78	382.17
V560	1	Bear	1	2	2	127.39	254.78	254.78
V560	2	Bear	3	1	2	382.17	127.39	254.78
V560	3	Bear	2	2	2	254.78	254.78	254.78
V560	4	Bear	2	2	1	254.78	254.78	127.39

Established Habitat			Basal Area per Plot (m^2)			Basal Area per Hectare (m^2)		
Stand	**Plot**	**Water-shed**	**Maple**	**Ashe**	**Other**	**Maple**	**Ashe**	**Other**
V0	1	Owl	0.00	0.00	0.08	0.00	0.00	10.55
V0	2	Owl	0.00	0.00	0.07	0.00	0.00	8.74
V0	3	Owl	0.04	0.02	0.02	4.55	2.43	2.34
V0	4	Owl	0.05	0.00	0.03	6.50	0.00	3.61
V0	5	Owl	0.03	0.00	0.06	4.45	0.00	7.27
V1	1	Bear	0.00	0.08	0.00	0.00	10.24	0.00
V1	2	Bear	0.06	0.00	0.00	7.59	0.00	0.00
V1	3	Bear	0.07	0.00	0.00	8.38	0.00	0.00
V1	4	Bear	0.02	0.00	0.07	2.96	0.00	8.77
V1	5	Bear	0.00	0.06	0.03	0.00	7.83	4.02
V215	1	Bear	0.00	0.04	0.04	0.00	4.89	4.76
V215	2	Bear	0.00	0.00	0.09	0.00	0.00	11.82
V215	3	Bear	0.00	0.05	0.04	0.00	5.99	5.26
V215	4	Bear	0.00	0.05	0.05	0.00	6.75	6.18
V369	3	Bear	0.07	0.06	0.00	8.29	8.09	0.00
V369	4	Bear	0.00	0.00	0.08	0.00	0.00	10.55
V369	1	Bear	0.00	0.09	0.00	0.00	12.01	0.00
V369	2	Bear	0.05	0.02	0.04	6.90	3.12	4.55
V389	1	Owl	0.04	0.03	0.03	5.54	3.43	4.13
V389	2	Owl	0.06	0.04	0.03	7.29	4.77	3.70
V46	1	Owl	0.02	0.00	0.04	3.16	0.00	5.67
V46	2	Owl	0.04	0.01	0.05	5.44	1.04	6.01
V46	3	Owl	0.04	0.01	0.01	5.52	1.31	1.70
V46	4	Owl	0.06	0.02	0.03	7.33	2.43	3.69
V46	5	Owl	0.04	0.03	0.05	5.26	4.09	6.74
V46	6	Owl	0.04	0.02	0.04	4.99	2.24	5.07
V46	7	Owl	0.03	0.03	0.06	3.58	4.03	7.19
V46	8	Owl	0.05	0.02	0.03	6.02	2.05	3.35
V46	9	Owl	0.06	0.04	0.07	7.11	5.48	8.30
V46	10	Owl	0.07	0.04	0.04	8.40	5.23	5.40

Established Habitat			Basal Area per Plot (m^2)			Basal Area per Hectare (m^2)		
Stand	Plot	Water-shed	Maple	Ashe	Other	Maple	Ashe	Other
V476	1	Owl	0.00	0.00	0.09	0.00	0.00	11.12
V476	2	Owl	0.00	0.01	0.11	0.00	1.70	13.75
V476	3	Owl	0.04	0.01	0.06	4.55	0.85	7.67
V476	4	Owl	0.04	0.03	0.04	5.40	4.22	5.07
V476	5	Owl	0.04	0.01	0.03	5.50	1.87	3.90
V476	6	Owl	0.05	0.02	0.02	6.58	2.24	2.34
V476	7	Owl	0.02	0.03	0.09	2.30	4.21	11.18
V476	8	Owl	0.03	0.00	0.04	3.94	0.00	4.62
V476	9	Owl	0.05	0.02	0.02	6.38	2.34	2.85
V476	10	Owl	0.03	0.01	0.04	4.06	0.97	5.55
V476	11	Owl	0.04	0.00	0.05	4.97	0.00	6.76
V476	12	Owl	0.03	0.02	0.03	3.97	2.96	3.28
V476	13	Owl	0.03	0.02	0.05	4.02	2.24	6.98
V476	14	Owl	0.02	0.00	0.04	2.74	0.00	4.88
V476	15	Owl	0.02	0.00	0.06	2.22	0.00	7.67
V476	16	Owl	0.02	0.00	0.05	2.29	0.00	6.49
V483	1	Bear	0.03	0.02	0.02	4.11	2.22	2.74
V483	2	Bear	0.06	0.04	0.03	7.41	4.48	3.82
V483	3	Bear	0.05	0.02	0.03	7.00	2.24	3.90
V483	4	Bear	0.02	0.02	0.06	2.43	3.17	7.58
V560	1	Bear	0.01	0.01	0.07	1.79	1.71	9.28
V560	2	Bear	0.03	0.03	0.02	3.42	3.90	3.09
V560	3	Bear	0.03	0.03	0.06	4.11	3.27	7.31
V560	4	Bear	0.02	0.04	0.02	2.50	5.52	2.85

Established Habitat			Stem Count (3m plot)			Stems per Hectare (EF=353.7319)		
Stand	Plot	Water-shed	Maple	Ashe	Other	Maple	Ashe	Other
V0	1	Owl	5	0	8	1768.66	0.00	2829.86
V0	2	Owl	9	5	6	3183.59	1768.66	2122.39
V0	3	Owl	8	0	2	2829.86	0.00	707.46
V0	4	Owl	6	0	12	2122.39	0.00	4244.78
V0	5	Owl	4	0	11	1414.93	0.00	3891.05
V1	1	Bear	7	0	21	2476.12	0.00	7428.37
V1	2	Bear	9	0	1	3183.59	0.00	353.73
V1	3	Bear	7	0	2	2476.12	0.00	707.46
V1	4	Bear	8	0	3	2829.86	0.00	1061.20
V1	5	Bear	11	6	1	3891.05	2122.39	353.73
V215	1	Bear	13	7	16	4598.51	2476.12	5659.71
V215	2	Bear	3	8	7	1061.20	2829.86	2476.12
V215	3	Bear	1	0	6	353.73	0.00	2122.39
V215	4	Bear	7	8	5	2476.12	2829.86	1768.66
V369	3	Bear	2	4	0	707.46	1414.93	0.00
V369	4	Bear	11	2	3	3891.05	707.46	1061.20
V369	1	Bear	2	3	6	707.46	1061.20	2122.39
V369	2	Bear	8	2	3	2829.86	707.46	1061.20
V389	1	Owl	6	2	7	2122.39	707.46	2476.12
V389	2	Owl	9	2	3	3183.59	707.46	1061.20
V46	1	Owl	6	0	16	2122.39	0.00	5659.71
V46	2	Owl	6	3	8	2122.39	1061.20	2829.86
V46	3	Owl	7	1	11	2476.12	353.73	3891.05
V46	4	Owl	5	4	8	1768.66	1414.93	2829.86
V46	5	Owl	8	6	5	2829.86	2122.39	1768.66
V46	6	Owl	7	3	10	2476.12	1061.20	3537.32
V46	7	Owl	6	5	6	2122.39	1768.66	2122.39
V46	8	Owl	5	4	7	1768.66	1414.93	2476.12
V46	9	Owl	8	1	5	2829.86	353.73	1768.66
V46	10	Owl	6	4	8	2122.39	1414.93	2829.86

Established Habitat			Stem Count (3m plot)			Stems per Hectare (EF=353.7319)		
Stand	Plot	Water-shed	Maple	Ashe	Other	Maple	Ashe	Other
V476	1	Owl	3	0	1	1061.20	0.00	353.73
V476	2	Owl	8	0	10	2829.86	0.00	3537.32
V476	3	Owl	15	0	6	5305.98	0.00	2122.39
V476	4	Owl	8	3	4	2829.86	1061.20	1414.93
V476	5	Owl	3	0	9	1061.20	0.00	3183.59
V476	6	Owl	11	6	7	3891.05	2122.39	2476.12
V476	7	Owl	12	0	9	4244.78	0.00	3183.59
V476	8	Owl	10	2	6	3537.32	707.46	2122.39
V476	9	Owl	8	1	4	2829.86	353.73	1414.93
V476	10	Owl	12	3	7	4244.78	1061.20	2476.12
V476	11	Owl	7	2	4	2476.12	707.46	1414.93
V476	12	Owl	12	4	8	4244.78	1414.93	2829.86
V476	13	Owl	13	10	11	4598.51	3537.32	3891.05
V476	14	Owl	12	2	8	4244.78	707.46	2829.86
V476	15	Owl	9	0	8	3183.59	0.00	2829.86
V476	16	Owl	8	0	7	2829.86	0.00	2476.12
V483	1	Bear	5	7	6	1768.66	2476.12	2122.39
V483	2	Bear	6	5	5	2122.39	1768.66	1768.66
V483	3	Bear	6	3	5	2122.39	1061.20	1768.66
V483	4	Bear	4	7	4	1414.93	2476.12	1414.93
V560	1	Bear	3	2	9	1061.20	707.46	3183.59
V560	2	Bear	7	11	7	2476.12	3891.05	2476.12
V560	3	Bear	7	9	11	2476.12	3183.59	3891.05
V560	4	Bear	3	4	12	1061.20	1414.93	4244.78

Modeled Habitat			Trees per plot (count)			Trees per Hectare (EF=127.3885)		
Stand	Plot	Water-shed	Maple	Ashe	Other	Maple	Ashe	Other
M1	1	Owl	2	2	0	254.78	254.78	0.00
M1	2	Owl	3	2	1	382.17	254.78	127.39
M1	3	Owl	3	1	1	382.17	127.39	127.39
M1	4	Owl	3	1	0	382.17	127.39	0.00
M1	5	Owl	3	1	0	382.17	127.39	0.00
M1	6	Owl	4	1	0	509.55	127.39	0.00
M1	7	Owl	3	3	0	382.17	382.17	0.00
M1	8	Owl	2	2	0	254.78	254.78	0.00
M1	9	Owl	2	2	0	254.78	254.78	0.00
M1	10	Owl	4	2	0	509.55	254.78	0.00
M1	11	Owl	2	2	0	254.78	254.78	0.00
M1	12	Owl	2	2	0	254.78	254.78	0.00
M1	13	Owl	3	1	0	382.17	127.39	0.00
M1	14	Owl	2	1	1	254.78	127.39	127.39
M1	22	Owl	3	2	0	382.17	254.78	0.00
M2	21	Owl	3	2	0	382.17	254.78	0.00
M2	25	Owl	3	2	0	382.17	254.78	0.00
M3	15	Owl	3	2	0	382.17	254.78	0.00
M3	16	Owl	2	0	5	254.78	0.00	636.94
M3	17	Owl	6	2	0	764.33	254.78	0.00
M3	18	Owl	5	2	1	636.94	254.78	127.39
M3	19	Owl	4	2	1	509.55	254.78	127.39
M3	20	Owl	3	1	1	382.17	127.39	127.39
M3	26	Owl	2	4	0	254.78	509.55	0.00
M3	31	Owl	4	2	0	509.55	254.78	0.00
M3	32	Owl	3	0	3	382.17	0.00	382.17
M3	33	Owl	6	2	0	764.33	254.78	0.00
M3	34	Owl	5	2	1	636.94	254.78	127.39
M3	35	Owl	5	1	1	636.94	127.39	127.39
M3	36	Owl	4	1	0	509.55	127.39	0.00
M3	37	Owl	5	2	0	636.94	254.78	0.00
M3	38	Owl	5	1	0	636.94	127.39	0.00
M3	39	Owl	4	3	0	509.55	382.17	0.00
M3	40	Owl	4	2	0	509.55	254.78	0.00
M3	41	Owl	4	0	1	509.55	0.00	127.39
M3	42	Owl	5	0	1	636.94	0.00	127.39
M3	43	Owl	6	0	0	764.33	0.00	0.00
M3	44	Owl	4	1	0	509.55	127.39	0.00
M3	45	Owl	5	1	0	636.94	127.39	0.00

Modeled Habitat			Trees per plot (count)			Trees per Hectare (EF=127.3885)		
Stand	Plot	Water-shed	Maple	Ashe	Other	Maple	Ashe	Other
M4	57	Bear	3	2	1	382.17	254.78	127.39
M4	58	Bear	3	3	0	382.17	382.17	0.00
M5	60	Bear	3	2	0	382.17	254.78	0.00
M5	61	Bear	2	1	0	254.78	127.39	0.00
M5	81	Bear	3	2	0	382.17	254.78	0.00
M5	83	Bear	3	1	1	382.17	127.39	127.39
M6	62	Bear	3	1	1	382.17	127.39	127.39
M6	63	Bear	2	1	1	254.78	127.39	127.39
M7	51	Bear	3	2	0	382.17	254.78	0.00
M7	52	Bear	3	1	0	382.17	127.39	0.00
M7	53	Bear	2	1	0	254.78	127.39	0.00
M7	59	Bear	3	2	0	382.17	254.78	0.00
M8	54	Bear	3	1	0	382.17	127.39	0.00
M8	55	Bear	3	1	2	382.17	127.39	254.78
M8	56	Bear	3	2	0	382.17	254.78	0.00
M9	70	Bear	3	2	2	382.17	254.78	254.78
M10	73	Bear	3	2	1	382.17	254.78	127.39
M10	74	Bear	3	1	2	382.17	127.39	254.78
M10	75	Bear	2	1	2	254.78	127.39	254.78
M10	76	Bear	2	2	2	254.78	254.78	254.78
M10	77	Bear	2	1	2	254.78	127.39	254.78
M10	78	Bear	3	1	1	382.17	127.39	127.39

Modeled Habitat			Basal Area per Plot (m^2)			Basal Area per Hectare (m^2)		
Stand	Plot	Water-shed	Maple	Ashe	Other	Maple	Ashe	Other
M1	1	Owl	0.03	0.05	0.00	4.35	5.75	0.00
M1	2	Owl	0.03	0.01	0.04	3.43	1.77	5.40
M1	3	Owl	0.02	0.02	0.00	3.11	2.43	0.49
M1	4	Owl	0.04	0.01	0.00	5.41	1.17	0.00
M1	5	Owl	0.06	0.04	0.00	8.12	5.40	0.00
M1	6	Owl	0.05	0.01	0.00	6.32	1.46	0.00
M1	7	Owl	0.05	0.03	0.00	6.12	4.01	0.00
M1	8	Owl	0.09	0.03	0.00	11.98	3.85	0.00
M1	9	Owl	0.10	0.02	0.00	12.44	2.67	0.00
M1	10	Owl	0.03	0.05	0.00	4.06	5.92	0.00
M1	11	Owl	0.04	0.06	0.00	5.39	7.16	0.00
M1	12	Owl	0.08	0.03	0.00	10.31	4.02	0.00
M1	13	Owl	0.07	0.01	0.00	8.86	1.79	0.00
M1	14	Owl	0.06	0.02	0.03	7.96	2.64	3.29
M1	22	Owl	0.05	0.03	0.00	5.89	4.24	0.00
M2	21	Owl	0.05	0.03	0.00	6.21	4.02	0.00
M2	25	Owl	0.04	0.03	0.00	5.59	4.18	0.00
M3	15	Owl	0.05	0.03	0.00	6.39	4.13	0.00
M3	16	Owl	0.03	0.00	0.04	3.69	0.00	5.25
M3	17	Owl	0.03	0.03	0.00	4.02	3.53	0.00
M3	18	Owl	0.04	0.01	0.03	4.99	1.86	3.29
M3	19	Owl	0.04	0.02	0.02	5.03	3.18	2.15
M3	20	Owl	0.05	0.02	0.02	7.00	2.64	2.05
M3	26	Owl	0.02	0.04	0.00	2.23	5.56	0.00
M3	31	Owl	0.04	0.02	0.00	5.15	2.24	0.00
M3	32	Owl	0.03	0.00	0.04	4.25	0.00	4.55
M3	33	Owl	0.04	0.02	0.00	5.50	1.96	0.00
M3	34	Owl	0.03	0.01	0.04	3.94	1.42	5.26
M3	35	Owl	0.04	0.01	0.02	4.64	1.79	2.15
M3	36	Owl	0.04	0.02	0.00	5.39	2.64	0.00
M3	37	Owl	0.04	0.01	0.00	5.18	1.77	0.00
M3	38	Owl	0.05	0.03	0.00	5.76	3.29	0.00
M3	39	Owl	0.04	0.03	0.00	4.86	4.29	0.00
M3	40	Owl	0.04	0.03	0.00	4.53	3.19	0.00
M3	41	Owl	0.04	0.00	0.03	5.55	0.00	3.77
M3	42	Owl	0.04	0.00	0.01	4.74	0.00	1.04
M3	43	Owl	0.04	0.00	0.00	5.66	0.00	0.00
M3	44	Owl	0.05	0.02	0.00	6.27	2.24	0.00
M3	45	Owl	0.04	0.01	0.00	5.31	1.46	0.00

Modeled Habitat			Basal Area per Plot (m^2)			Basal Area per Hectare (m^2)		
Stand	Plot	Water-shed	Maple	Ashe	Other	Maple	Ashe	Other
M4	57	Bear	0.05	0.02	0.01	6.30	2.64	1.79
M4	58	Bear	0.03	0.04	0.00	3.37	4.78	0.00
M5	60	Bear	0.04	0.03	0.00	5.16	3.69	0.00
M5	61	Bear	0.06	0.05	0.00	7.09	6.65	0.00
M5	81	Bear	0.06	0.03	0.00	7.29	4.02	0.00
M5	83	Bear	0.04	0.02	0.04	4.66	2.96	5.40
M6	62	Bear	0.06	0.02	0.01	7.46	2.24	1.46
M6	63	Bear	0.05	0.01	0.03	5.94	1.39	4.02
M7	51	Bear	0.05	0.02	0.00	6.29	2.29	0.00
M7	52	Bear	0.05	0.02	0.00	6.91	2.64	0.00
M7	53	Bear	0.09	0.02	0.00	11.33	2.64	0.00
M7	59	Bear	0.05	0.04	0.00	6.24	5.18	0.00
M8	54	Bear	0.05	0.01	0.00	6.89	1.39	0.00
M8	55	Bear	0.03	0.01	0.04	4.25	1.46	5.40
M8	56	Bear	0.05	0.03	0.00	5.94	4.02	0.00
M9	70	Bear	0.02	0.02	0.03	3.02	2.43	3.81
M10	73	Bear	0.05	0.03	0.02	6.41	3.74	2.05
M10	74	Bear	0.03	0.02	0.02	4.11	2.34	2.64
M10	75	Bear	0.04	0.02	0.02	5.28	2.64	3.06
M10	76	Bear	0.01	0.04	0.04	1.50	4.69	5.33
M10	77	Bear	0.04	0.01	0.03	4.81	1.39	3.49
M10	78	Bear	0.05	0.01	0.02	6.35	1.39	1.96

Modeled Habitat			Stem Count (3m plot)			Stems per Hectare (EF=353.7319)		
Stand	Plot	Water-shed	Maple	Ashe	Other	Maple	Ashe	Other
M1	1	Owl	12	2	5	4244.78	707.46	1768.66
M1	2	Owl	11	7	4	3891.05	2476.12	1414.93
M1	3	Owl	12	9	5	4244.78	3183.59	1768.66
M1	4	Owl	16	4	6	5659.71	1414.93	2122.39
M1	5	Owl	8	0	0	2829.86	0.00	0.00
M1	6	Owl	4	6	0	1414.93	2122.39	0.00
M1	7	Owl	6	1	2	2122.39	353.73	707.46
M1	8	Owl	8	6	1	2829.86	2122.39	353.73
M1	9	Owl	7	4	2	2476.12	1414.93	707.46
M1	10	Owl	9	3	4	3183.59	1061.20	1414.93
M1	11	Owl	10	6	4	3537.32	2122.39	1414.93
M1	12	Owl	8	0	1	2829.86	0.00	353.73
M1	13	Owl	9	3	1	3183.59	1061.20	353.73
M1	14	Owl	7	2	5	2476.12	707.46	1768.66
M1	22	Owl	6	4	0	2122.39	1414.93	0.00
M2	21	Owl	12	7	4	4244.78	2476.12	1414.93
M2	25	Owl	11	2	3	3891.05	707.46	1061.20
M3	15	Owl	11	1	2	3891.05	353.73	707.46
M3	16	Owl	7	0	5	2476.12	0.00	1768.66
M3	17	Owl	9	0	3	3183.59	0.00	1061.20
M3	18	Owl	7	2	4	2476.12	707.46	1414.93
M3	19	Owl	11	0	0	3891.05	0.00	0.00
M3	20	Owl	8	3	4	2829.86	1061.20	1414.93
M3	26	Owl	14	2	4	4952.25	707.46	1414.93
M3	31	Owl	12	3	5	4244.78	1061.20	1768.66
M3	32	Owl	11	3	1	3891.05	1061.20	353.73
M3	33	Owl	9	0	4	3183.59	0.00	1414.93
M3	34	Owl	6	1	3	2122.39	353.73	1061.20
M3	35	Owl	9	1	2	3183.59	353.73	707.46
M3	36	Owl	12	3	2	4244.78	1061.20	707.46
M3	37	Owl	8	2	2	2829.86	707.46	707.46
M3	38	Owl	9	1	4	3183.59	353.73	1414.93
M3	39	Owl	11	4	2	3891.05	1414.93	707.46
M3	40	Owl	12	6	2	4244.78	2122.39	707.46
M3	41	Owl	13	2	1	4598.51	707.46	353.73
M3	42	Owl	11	2	3	3891.05	707.46	1061.20
M3	43	Owl	14	1	1	4952.25	353.73	353.73
M3	44	Owl	16	3	3	5659.71	1061.20	1061.20
M3	45	Owl	7	2	0	2476.12	707.46	0.00

Modeled Habitat			Stem Count (3m plot)			Stems per Hectare (EF=353.7319)		
Stand	**Plot**	**Water-shed**	**Maple**	**Ashe**	**Other**	**Maple**	**Ashe**	**Other**
M4	57	Bear	8	7	5	2829.86	2476.12	1768.66
M4	58	Bear	4	9	4	1414.93	3183.59	1414.93
M5	60	Bear	9	7	4	3183.59	2476.12	1414.93
M5	61	Bear	8	9	3	2829.86	3183.59	1061.20
M5	81	Bear	7	4	6	2476.12	1414.93	2122.39
M5	83	Bear	7	2	5	2476.12	707.46	1768.66
M6	62	Bear	9	3	4	3183.59	1061.20	1414.93
M6	63	Bear	6	6	3	2122.39	2122.39	1061.20
M7	51	Bear	5	6	5	1768.66	2122.39	1768.66
M7	52	Bear	12	2	6	4244.78	707.46	2122.39
M7	53	Bear	9	4	4	3183.59	1414.93	1414.93
M7	59	Bear	13	7	2	4598.51	2476.12	707.46
M8	54	Bear	10	3	5	3537.32	1061.20	1768.66
M8	55	Bear	8	6	2	2829.86	2122.39	707.46
M8	56	Bear	4	4	2	1414.93	1414.93	707.46
M9	70	Bear	9	3	5	3183.59	1061.20	1768.66
M10	73	Bear	8	2	5	2829.86	707.46	1768.66
M10	74	Bear	9	7	4	3183.59	2476.12	1414.93
M10	75	Bear	7	3	3	2476.12	1061.20	1061.20
M10	76	Bear	6	6	5	2122.39	2122.39	1768.66
M10	77	Bear	5	9	5	1768.66	3183.59	1768.66
M10	78	Bear	9	4	3	3183.59	1414.93	1061.20

APPENDIX X:

Independent-Samples T-tests Results

Established Habitat – Trees per Hectare

Bigtooth Maple TPH	*Owl Creek*	*Bear Creek*
Mean	274.08	181.98
Variance	25,478.92	31,760.18
Observations	33	21
Hypothesized Mean Difference	0	
df	39	
t Stat	1.93	
P(T<=t) one-tail	0.03	
t Critical one-tail	1.68	
P(T<=t) two-tail	0.06	
t Critical two-tail	2.02	

Ashe juniper TPH	*Owl Creek*	*Bear Creek*
Mean	131.25	212.31
Variance	12,662.62	20,014.32
Observations	33	21
Hypothesized Mean Difference	0	
df	36	
t Stat	-2.22	
P(T<=t) one-tail	0.02	
t Critical one-tail	1.69	
P(T<=t) two-tail	0.03	
t Critical two-tail	2.03	

Other Hardwoods TPH	*Owl Creek*	*Bear Creek*
Mean	247.06	151.65
Variance	11,095.16	12,364.06
Observations	33	21
Hypothesized Mean Difference	0	
df	41	
t Stat	3.14	
P(T<=t) one-tail	0.02	
t Critical one-tail	1.68	
P(T<=t) two-tail	0.03	
t Critical two-tail	2.02	

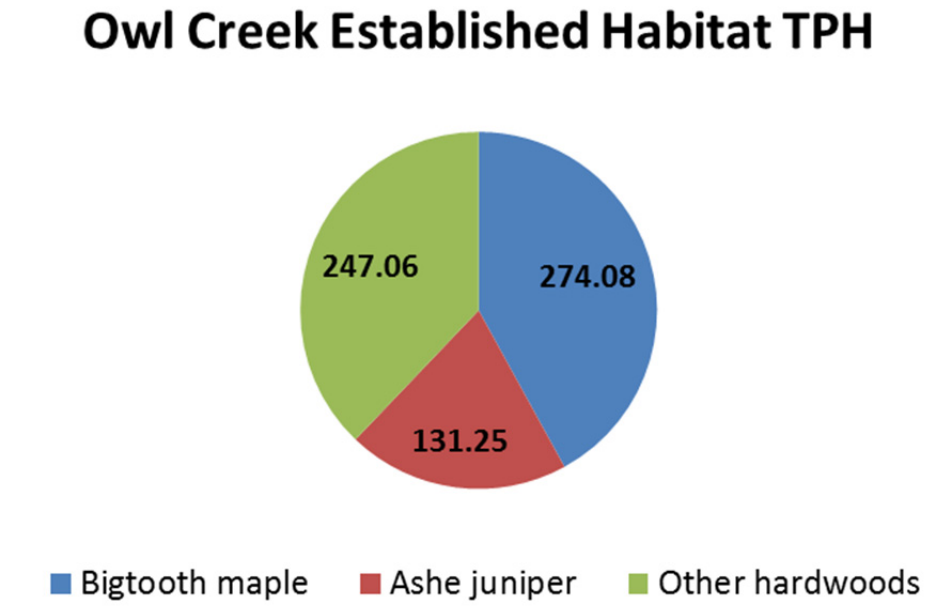
Owl Creek Established Habitat TPH
247.06
274.08
131.25
Bigtooth maple
Ashe juniper
Other hardwoods

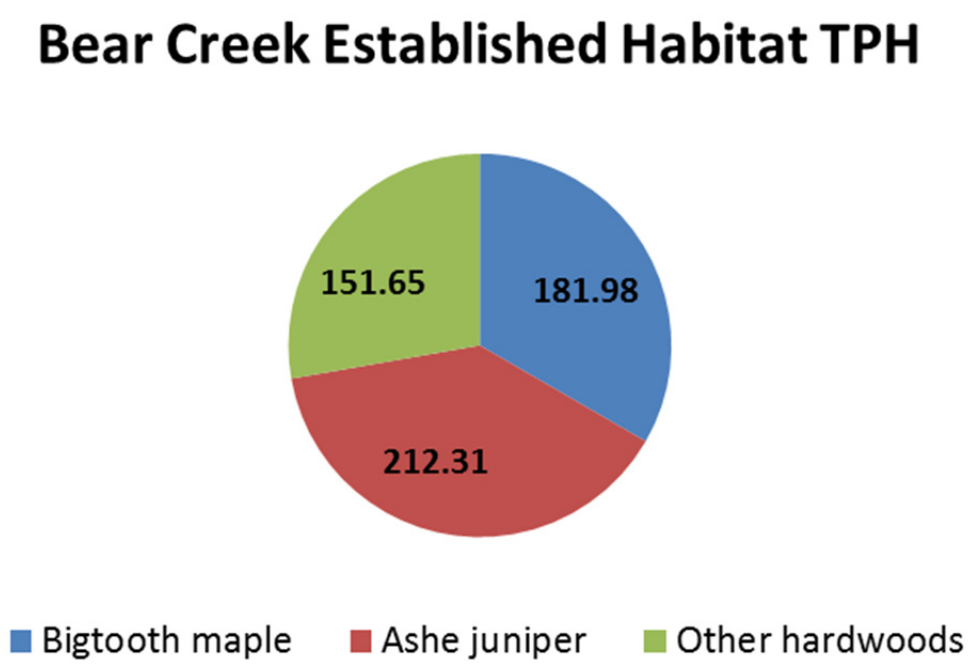
Bear Creek Established Habitat TPH
151.65
181.98
212.31
Bigtooth maple
Ashe juniper
Other hardwoods

Established Habitat – Basal Area per Hectare

Bigtooth Maple BAPH	*Owl Creek*	*Bear Creek*
Mean	4.37	3.18
Variance	5.05	10.23
Observations	33	21
Hypothesized Mean Difference	0	
df	32	
t Stat	1.48	
P(T<=t) one-tail	0.07	
t Critical one-tail	1.69	
P(T<=t) two-tail	0.15	
t Critical two-tail	2.04	

Ashe juniper BAPH	*Owl Creek*	*Bear Creek*
Mean	1.88	4.07
Variance	3.11	12.14
Observations	33	21
Hypothesized Mean Difference	0	
df	27	
t Stat	-2.66	
P(T<=t) one-tail	0.01	
t Critical one-tail	1.70	
P(T<=t) two-tail	0.01	
t Critical two-tail	2.05	

Other Hardwoods BAPH	*Owl Creek*	*Bear Creek*
Mean	5.99	4.59
Variance	8.03	13.10
Observations	33	21
Hypothesized Mean Difference	0	
df	35	
t Stat	1.49	
P(T<=t) one-tail	0.07	
t Critical one-tail	1.69	
P(T<=t) two-tail	0.14	
t Critical two-tail	2.03	

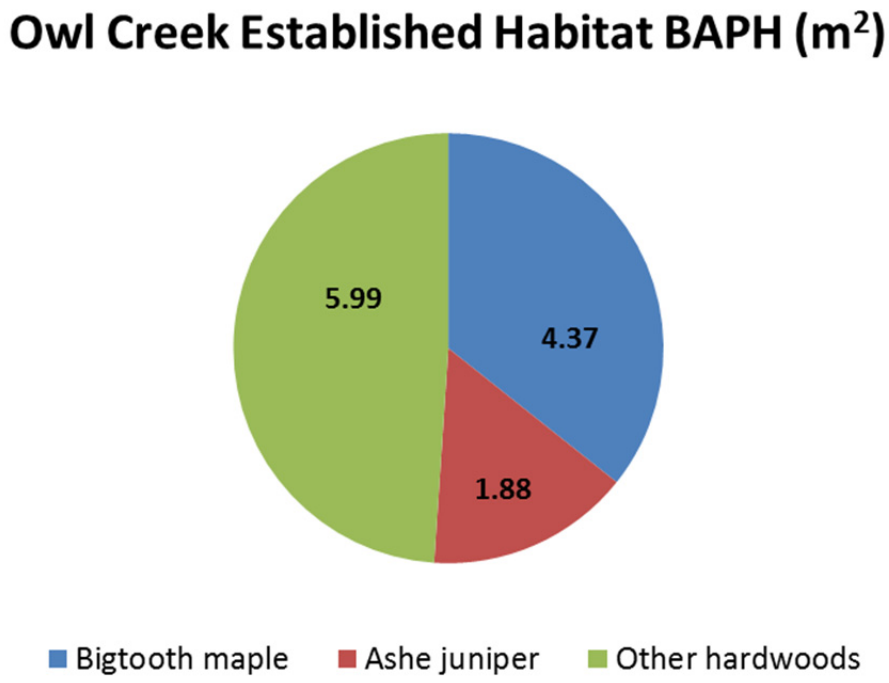
Owl Creek Established Habitat BAPH (m²)
5.99
4.37
1.88
Bigtooth maple
Ashe juniper
Other hardwoods

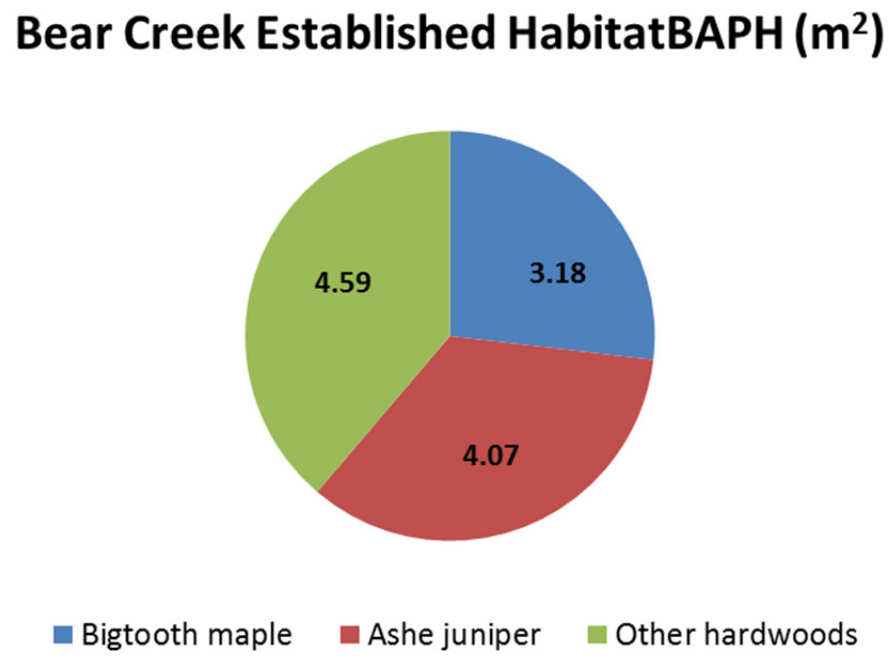
Bear Creek Established HabitatBAPH (m²)
4.59
3.18
4.07
Bigtooth maple
Ashe juniper
Other hardwoods

Established Habitat – Stems per Hectare

Bigtooth Maple SPH	***Owl Creek***	***Bear Creek***
Mean	2808.42	2189.77
Variance	1,070,919.61	1,309,058.99
Observations	33	21
Hypothesized Mean Difference	0	
df	40	
t Stat	2.01	
P(T<=t) one-tail	0.03	
t Critical one-tail	1.68	
P(T<=t) two-tail	0.05	
t Critical two-tail	2.02	

Ashe juniper SPH	***Owl Creek***	***Bear Creek***
Mean	782.50	1482.31
Variance	717,580.13	1,446,697.87
Observations	33	21
Hypothesized Mean Difference	0	
df	33	
t Stat	-2.32	
P(T<=t) one-tail	0.01	
t Critical one-tail	1.70	
P(T<=t) two-tail	0.03	
t Critical two-tail	2.03	

Other Hardwoods SPH	***Owl Creek***	***Bear Creek***
Mean	2594.03	2240.30
Variance	1,170,451.86	3,320,016.69
Observations	33	21
Hypothesized Mean Difference	0	
df	29	
t Stat	0.80	
P(T<=t) one-tail	0.21	
t Critical one-tail	1.70	
P(T<=t) two-tail	0.43	
t Critical two-tail	2.05	

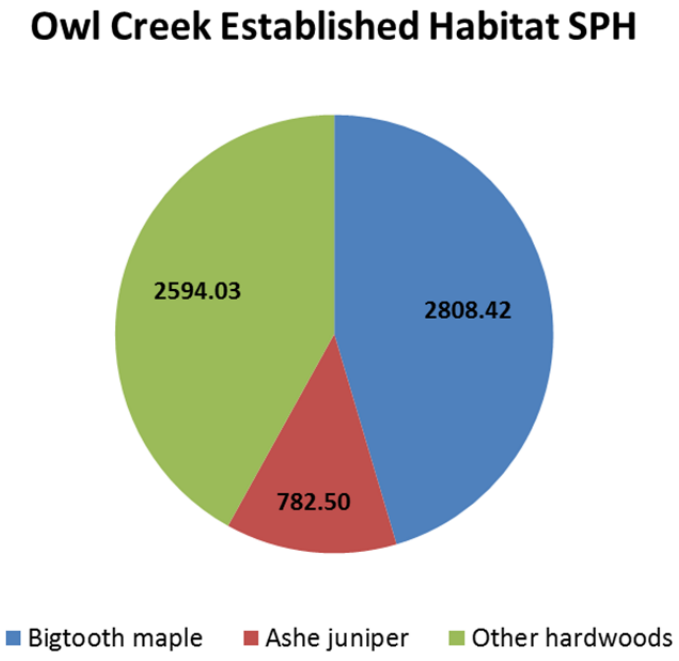
Owl Creek Established Habitat SPH
2594.03
2808.42
782.50
Bigtooth maple
Ashe juniper
Other hardwoods

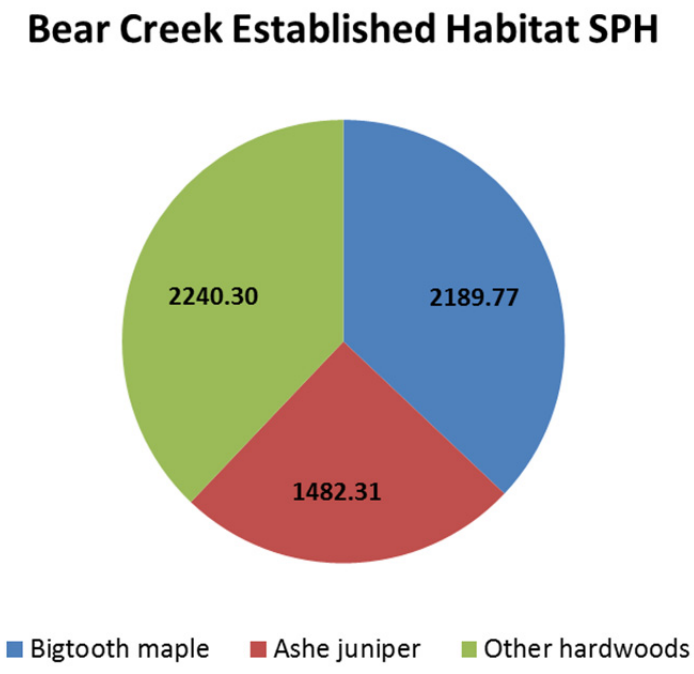
Bear Creek Established Habitat SPH
2240.30
2189.77
1482.31
Bigtooth maple
Ashe juniper
Other hardwoods

Modeled Habitat – Trees per Hectare

Bigtooth Maple TPH	***Owl Creek***	***Bear Creek***
Mean	460.57	347.43
Variance	24,440.30	3372.02
Observations	39	22
Hypothesized Mean Difference	0	
df	53	
t Stat	4.05	
P(T<=t) one-tail	8.37E-05	
t Critical one-tail	1.67	
P(T<=t) two-tail	2.00E-04	
t Critical two-tail	2.01	

Ashe juniper TPH	***Owl Creek***	***Bear Creek***
Mean	195.98	191.08
Variance	12,680.05	5795.65
Observations	39	22
Hypothesized Mean Difference	0	
df	57	
t Stat	0.20	
P(T<=t) one-tail	0.42	
t Critical one-tail	1.67	
P(T<=t) two-tail	0.84	
t Critical two-tail	2.00	

Other Hardwoods TPH	***Owl Creek***	***Bear Creek***
Mean	58.79	104.23
Variance	15,242.33	11,802.06
Observations	39	22
Hypothesized Mean Difference	0	
df	49	
t Stat	-1.49	
P(T<=t) one-tail	0.07	
t Critical one-tail	1.68	
P(T<=t) two-tail	0.14	
t Critical two-tail	2.01	

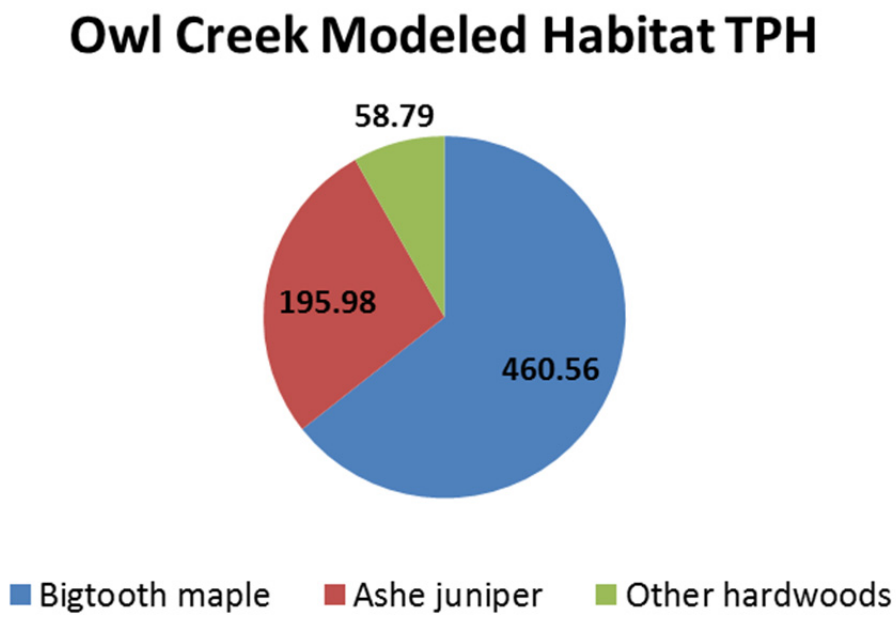
Owl Creek Modeled Habitat TPH
58.79
195.98
460.56
Bigtooth maple
Ashe juniper
Other hardwoods

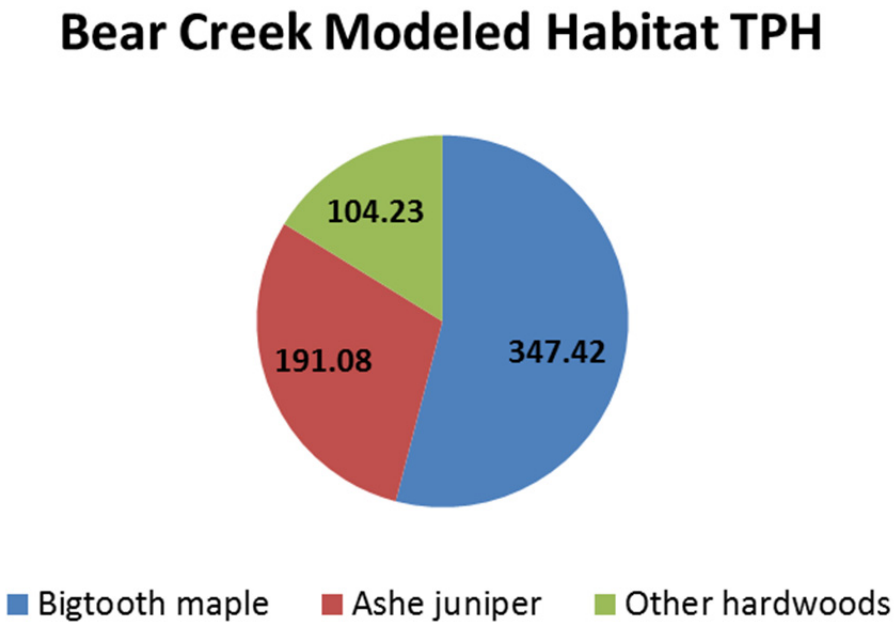
Bear Creek Modeled Habitat TPH
104.23
191.08
347.42
Bigtooth maple
Ashe juniper
Other hardwoods

Modeled Habitat – Basal Area per Hectare

Bigtooth Maple BAPH	***Owl Creek***	***Bear Creek***
Mean	5.78	5.75
Variance	4.65	3.87
Observations	39	22
Hypothesized Mean Difference	0	
df	47	
t Stat	0.05	
P(T<=t) one-tail	0.48	
t Critical one-tail	1.68	
P(T<=t) two-tail	0.96	
t Critical two-tail	2.01	

Ashe juniper BAPH	***Owl Creek***	***Bear Creek***
Mean	2.81	3.03
Variance	3.17	2.02
Observations	39	22
Hypothesized Mean Difference	0	
df	52	
t Stat	-0.52	
P(T<=t) one-tail	0.30	
t Critical one-tail	1.67	
P(T<=t) two-tail	0.61	
t Critical two-tail	2.01	

Other Hardwoods	***Owl Creek***	***Bear Creek***
Mean	0.99	1.84
Variance	3.09	4.05
Observations	39	22
Hypothesized Mean Difference	0	
df	39	
t Stat	-1.65	
P(T<=t) one-tail	0.05	
t Critical one-tail	1.68	
P(T<=t) two-tail	0.11	
t Critical two-tail	2.02	

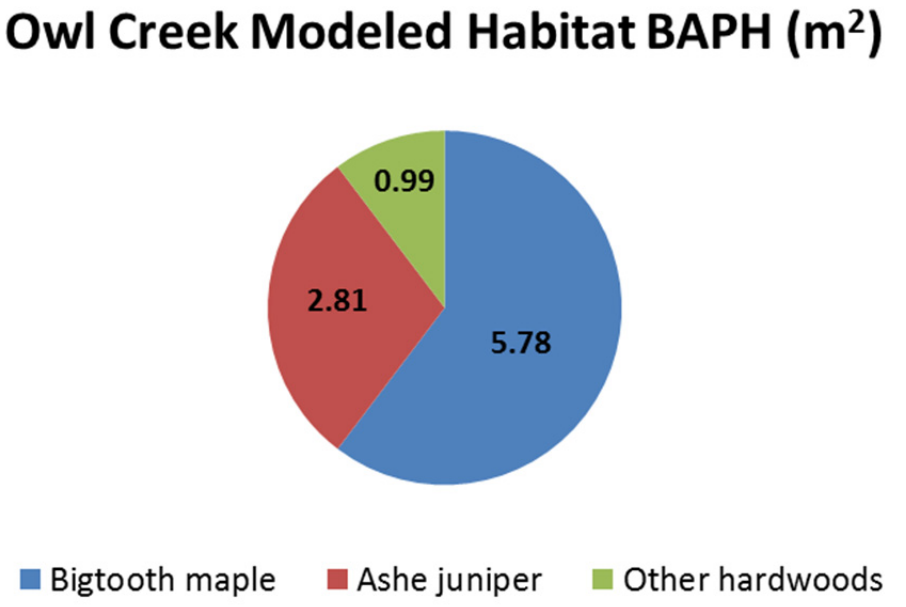
Owl Creek Modeled Habitat BAPH (m2)
0.99
2.81
5.78
Bigtooth maple
Ashe juniper
Other hardwoods

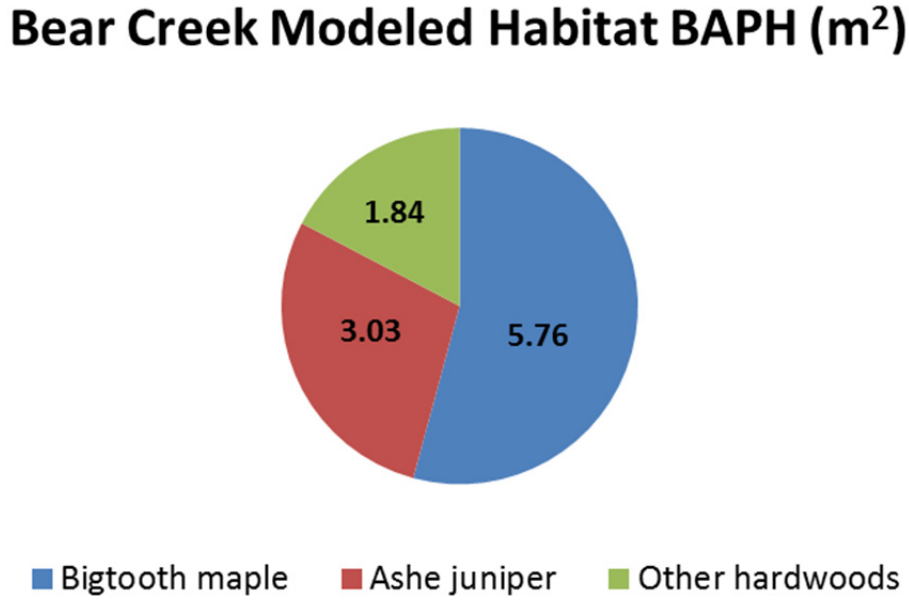
Bear Creek Modeled Habitat BAPH (m2)
1.84
3.03
5.76
Bigtooth maple
Ashe juniper
Other hardwoods

Modeled Habitat – Stems per Hectare

Bigtooth Maple SPH	*Owl Creek*	*Bear Creek*
Mean	3473.83	2765.54
Variance	980,408.97	663,006.66
Observations	39	22
Hypothesized Mean Difference	0	
df	51	
t Stat	3.01	
P(T<=t) one-tail	0.02	
t Critical one-tail	1.68	
P(T<=t) two-tail	0.04	
t Critical two-tail	2.01	

Ashe juniper SPH	*Owl Creek*	*Bear Creek*
Mean	979.57	1816.89
Variance	635,256.38	682,777.69
Observations	39	22
Hypothesized Mean Difference	0	
df	42	
t Stat	-3.85	
P(T<=t) one-tail	2.00E-04	
t Critical one-tail	1.68	
P(T<=t) two-tail	4.00E-04	
t Critical two-tail	2.02	

Other Hardwoods SPH	*Owl Creek*	*Bear Creek*
Mean	943.29	1447.09
Variance	364,402.78	189,585.24
Observations	39	22
Hypothesized Mean Difference	0	
df	55	
t Stat	-3.76	
P(T<=t) one-tail	2.00E-04	
t Critical one-tail	1.67	
P(T<=t) two-tail	4.00E-04	
t Critical two-tail	2.00	

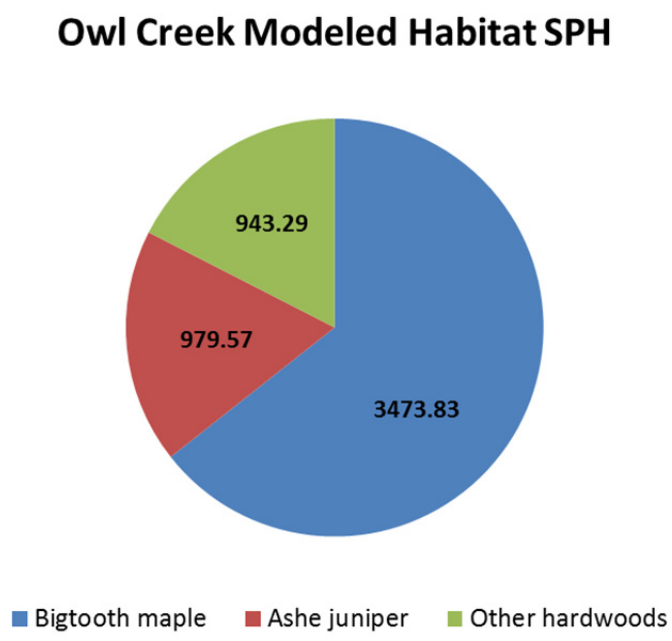
Owl Creek Modeled Habitat SPH
943.29
979.57
3473.83
Bigtooth maple
Ashe juniper
Other hardwoods

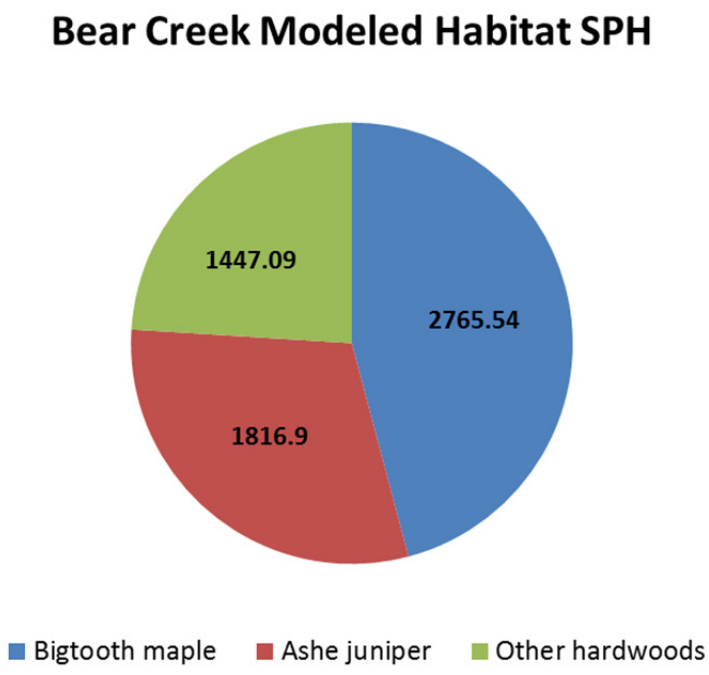
Bear Creek Modeled Habitat SPH
1447.09
2765.54
1816.9
Bigtooth maple
Ashe juniper
Other hardwoods

VITA

Melinda Shaw Faulkner graduated from Westbury High School in Houston, Texas in May of 1980. After a year of college, she went to work for Southwestern Bell and AT&T. She returned to school at Stephen F. Austin State University in August of 1999 to complete her degree and graduated Cum Laude with a Bachelor of Science Degree in Geology in May of 2002. She entered graduate school and received the degree of Master of Science in Geology in May of 2006. In January of 2008, Melinda entered the PhD. Program in the Arthur Temple College of Forestry and Agriculture at Stephen F. Austin State University. She will graduate with a terminal degree in Forestry May of 2016 and currently teaches geology courses at Stephen F. Austin State University.

Permanent Address: 1609 Redbud
Nacogdoches, TX 75965

Style manual designation: APA

This dissertation was typed by Melinda Shaw Faulkner